

**SYNTHESIS AND COMPUTATIONAL STUDIES OF  
FREE-BASE *meta*-BENZIPORPHODIMETHENES  
AND THEIR METAL COMPLEXES**

Thesis Submitted to the Delhi Technological University  
for the award of the degree of

**DOCTOR OF PHILOSOPHY  
IN  
CHEMISTRY**

*By*

**DEEPALI AHLUWALIA**  
(2k18/Ph.D/AC/03)



**DEPARTMENT OF APPLIED CHEMISTRY  
DELHI TECHNOLOGICAL UNIVERSITY  
Delhi-110042 (INDIA)**

2022

**©DELHI TECHNOLOGICAL UNIVERSITY-2022**  
**ALL RIGHTS RESERVED**

*Dedication*

*To my grandmother  
Mata*

*To my Parents  
Mr. & Mrs. Ahluwalia*

*To my siblings  
Chirag & Monika*

*To my lovely pets  
Richie & Bolt*

*Thanks for your endless sacrifices, love, support and prayers*



**DEPARTMENT OF APPLIED CHEMISTRY  
DELHI TECHNOLOGICAL UNIVERSITY  
Delhi-110042 (INDIA)**

**DECLARATION**

I declare that the research work reported in the thesis entitled "**Synthesis and computational studies of free base *meta*-benzoporphodimethenes and their metal complexes**" for the award of degree of ***Doctoral of Philosophy*** in Chemistry has been carried out by me under the supervision of **Prof. Sudhir Gopalrao Warkar** and **Prof. Anil Kumar**, Department of Applied Chemistry, Delhi Technological University, India.

The research work embodied in this thesis, except where otherwise indicate, is my original research. This thesis has not been submitted by me in part or full to any other University for the award of any degree or diploma. This thesis does not contain other person's data, graphs or other information, unless specifically acknowledged.

**Deepali Ahluwalia**  
Candidate  
2K18/Ph.D/AC/03

**Prof. Anil Kumar**  
Co-supervisor

**Prof. Sudhir G. Warkar**  
Supervisor

**Prof. Sudhir G. Warkar**  
Head of Department  
Applied Chemistry, DTU



**DEPARTMENT OF APPLIED CHEMISTRY  
DELHI TECHNOLOGICAL UNIVERSITY  
Delhi-110042 (INDIA)**

**CERTIFICATE**

This is to certify that the Ph.D. thesis entitled "**Synthesis and computational studies of free-base *meta*-benzoporphodimethenes and their metal complexes**" submitted to Delhi Technological University, Delhi, for the award of Doctoral of Philosophy in Chemistry, is based on original research work carried out by me, under the supervision of Prof. Sudhir G. Warkar and Prof. Anil Kumar, Department of Applied Chemistry, Delhi Technological University, Delhi, India. It is further certified that the work embodied in this thesis has neither partially or fully submitted to any other university or institution for the award of any degree or diploma.

**Deepali Ahluwalia**  
Candidate  
2K18/Ph.D/AC/03

This is to certify that the above statement made by the candidate is correct to the best of our knowledge.

**Prof. Anil Kumar**  
Co-supervisor

**Prof. Sudhir G. Warkar**  
Supervisor

**Prof. Sudhir G. Warkar**  
Head of Department  
Applied Chemistry, DTU

## **ACKNOWLEDGEMENTS**

This thesis is the compilation of my four years of hard work and dedication. The support of numerous people have led me here today. It gives me immense pleasure to present my gratitude to all of them.

Firstly, I would like to acknowledge my supervisor, Prof. S. G. Warkar. He has been no less than a pillar of strength throughout this journey. He has been my forever go to person whenever in trouble. Warkar Sir has always been this fatherly figure to me at the university who just encouraged me to spread my wings and fly higher each day. Next, I would like to thank my mentor, Prof. Anil Kumar for his proficient guidance and motivation. I always wondered where does he gets such positive approach towards every situation in life. If I have learnt something other than research from him is the patience. I am a person that readily gets bored doing the same kind of work. Prof. Kumar has always provided me the freedom to explore and learn new things, whenever I wished to. Both my supervisors play a major role in uplifting me and would always have an important role in my career.

I would also like to present my gratitude to the former Vice Chancellor of DTU, Prof. Yogesh Singh, and the current Vice-Chancellor Prof. J. P. Saini. I would also like to thank Prof. Archna Rani, Dr. Manish Jain, Prof. Ram Singh, Dr. Poonam, Dr. Raminder Kaur and other faculty and staff members of Department of Applied Chemistry, DTU, for their important contributions during my doctoral journey.

My sincerely thankful to my SRC committee members: Prof. Rajeev Gupta, University of Delhi, Prof. S. Nagendran, IIT Delhi, Prof. Roli Purwar and Dr. Vivek Aggarwal from DTU, for their meaningful suggestions.

I like to acknowledge Dr. Dinesh Udhari from Applied Mathematics who has also been my maths teacher back in school and a source of constant motivation here at DTU.

I would like to thank the administrative staff and other members of Chemistry Department. I am extremely thankful particularly to Mr. Raju and Mrs. Sharmila for being available when needed.

I am thankful to Dr. Milind M. Deshmukh from Dr. Harisingh Gour University, Madhya Pradesh, for teaching me Molecular Tailoring Approach. I would like to present my gratitude to him for all his lessons.

I am grateful to Dr. Arijit Bag from Maulana Abul Kalam Azad University of Technology, West Bengal, for helping me in the computational work done in two of my research articles.

I gratefully acknowledge the financial assistance provided by University Grant Commission in the form of Junior Research Fellowship and Senior Research Fellowship.

I am greatly thankful to Dr. Umesh Kumar and Dr. Namita Gandhi from Deshbandhu College, Delhi University, for their constant support and encouragement.

I am thankful to Prof. Reena Saxena from Kirori Mal College, Delhi University, for her support and guidance throughout.

I specially thank my labmate Ritika Kubba for being a great friend here at DTU. I wish to thank all my fellow Ph.D. scholars at the Department of Applied Chemistry, particularly Jyoti, Saurav, Shikha, Atul, Meenakshi, and others.

I would like to thank my best friends Amandeep Kaur, Shefali Saxena, Sanghamitra Sarkar and Sachin Kumar. Thank you for holding me tight and strong wherever I seek support. I am fortunate to have friends like them in my life.

I pay my sincere gratitude to my late daadi (*mata*) who believed in me when no one did. I wish I could make her and dadaji proud one fine day. I would also like to thank my *naani* for her blessings.

I wish to thank my *bhabhi* Monika for her love and support. My brother Chirag for his constant motivation. Dear brother, you're much more special to me than you would ever know.

I am also grateful to my pets Richie and Bolt. Though, I lost Richie last year but his place will always be intact in the happy days of my life. I am thankful to God for

blessing me with this love for animals. The selflessness that an animal teaches you is irreplaceable. I am thankful to my dogs Richie and Bolt for bringing immense joy to my life.

Last but not the least, my parents for their immense sacrifices, love and prayers. I am falling short of words while writing about them. I owe my existence to them. I love them with all my heart and soul. They've made numerous sacrifices for me. I thank them for raising me as a kind and humble human. It is their blessings that has made me who I am today and what I may become tomorrow.

Thank you God for being so kind.

**(Deepali Ahluwalia)**

## LIST OF CONTENTS

---

<i>Title</i>	<i>Page No.</i>
<i>Declaration</i>	
<i>Certificate</i>	
<i>Acknowledgements</i>	
<i>List of Contents</i>	
<i>List of Tables</i>	
<i>List of Figures</i>	
<i>List of Schemes</i>	
<i>List of Charts</i>	
<i>Abstract</i>	

---

### **CHAPTER 1: INTRODUCTION**

- 1.1. General Introduction
    - 1.1.1. Modifications in Porphyrin
    - 1.1.2. Carbaporphyrinoids- A turning point in porphyrin chemistry
    - 1.1.3. *meta*-benzoporphyrin
    - 1.1.4. *para*-benzoporphyrin
  - 1.2. *meta*-benzoporphodimethene analogues
    - 1.2.1. Synthetic route for *meta*-benzoporphodimethene analogues
    - 1.2.2. UV-Vis Spectroscopy
    - 1.2.3. Structural analysis
    - 1.2.4. NMR shifts in *meta*-benzoporphodimethenes
    - 1.2.5. Electronic structure studies
  - 1.3. Properties of metalated-*meta*-benzoporphodimethene complexes.
    - 1.3.1. Weak metal-arene interactions
    - 1.3.2. Fluorescence enhancement
    - 1.3.3. Fluorescence phenomena: structure co-relation
    - 1.3.4. Cell-imaging applications
- References*

### **CHAPTER 2: SCOPE OF THE WORK**

---

<i>Title</i>	<i>Page No.</i>
--------------	-----------------

---

## **CHAPTER 3: METHODOLOGY**

- 3.1. Introduction
- 3.2. Density functional theory
  - 3.2.1. Basics of DFT
  - 3.2.2. Principle of DFT
  - 3.2.3. Theorems of DFT
  - 3.2.4. Applications of DFT
  - 3.2.5. Basis functions and basis sets

*References*

## **CHAPTER 4: EFFECT OF *meso*-SUBSTITUTION**

- 4.1. Introduction
- 4.2. Models and methods
  - 4.2.1. Computational details
  - 4.2.2. Fragmentation method
- 4.3. Results and discussion
  - 4.3.1. Geometries of *meta*-benzoporphodimethenes
  - 4.3.2. Effect of substituents at  $sp^3$  *meso*-carbons
  - 4.3.3. Effect of substituents at  $sp^2$  *meso*-carbons
- 4.4. Concluding remarks

*References*

## **CHAPTER 5: SUBSTITUTIONS AT C3-POSITION**

- 5.1. Introduction
- 5.2. Methodology
  - 5.2.1. Computational details
  - 5.2.2. Fragmentation method for estimation of N-H $\cdots$ N hydrogen bond energy
- 5.3. Result and discussion
  - 5.3.1. Geometries of *meta*-benzoporphodimethene structures
  - 5.3.2. Non-covalent interactions

<i>Title</i>	<i>Page No.</i>
5.3.3. Effect of bulkiness at $sp^3$ <i>meso</i> -positions 5.3.4. Effect of substitutions at C3-positions 5.4. Concluding remarks <i>References</i>	119

## **CHAPTER 6: SYNTHESIS OF NEW STERICALLY HINDERED *m*-BPDM**

- 6.1. Introduction
- 6.2. Experimental section
  - 6.2.1. Reagents
  - 6.2.2. General information
  - 6.2.3. Synthetic procedure
- 6.3. Computational details
- 6.4. Results and discussion
  - 6.4.1. Synthesis and spectroscopy
  - 6.4.2. Frontier molecular orbitals
  - 6.4.3. Density-of-states
- 6.5. Concluding remarks

*References*

## **CHAPTER 7: CONFORMATIONAL ANALYSIS OF METALATED *m*-BPDM**

- 7.1. Introduction
- 7.2. Computational details
- 7.3. Results and discussion
  - 7.3.1. Lowest energy conformers
  - 7.3.2. Comparison of DFT optimized and X-ray geometries
  - 7.3.3. Geometrical studies
- 7.4. Concluding remarks

*References*

---

<i>Title</i>	<i>Page No.</i>
--------------	-----------------

---

## **CHAPTER 8: CONCLUSION AND FUTURE PROSPECTS**

- 8.1. Conclusion
- 8.2. Future prospects

## **LIST OF PUBLICATIONS/ CONFERENCES AND AWARDS**

## **ABOUT THE AUTHOR**

## **APPENDIX-I, II, III**

## LIST OF TABLES

<i>Table No.</i>	<i>Descriptions</i>	<i>Page No.</i>
1.1	Consolidated UV data for Scheme 1.10.	
1.2	Consolidated NMR data for Scheme 1.10.	
4.1	Non-bonded angles (in degrees) for structures in Charts 4.1, 4.2 and 4.3.	
4.2	Intramolecular hydrogen bond (H-Bond) energy (in $\text{kcal mol}^{-1}$ ) and distance (in Å). See charts 4.1-4.3 for the corresponding geometries of these molecules.	
5.1	Non-bonded angles in degrees for structures in Figure 4.1.	
5.2	Intramolecular Hydrogen Bond energy (in $\text{kcal mol}^{-1}$ ) and distances (in Å). See Chart 5.1 to 5.3 for corresponding geometries of these molecules	
6.1	Energy of frontier molecular orbitals and HOMO-LUMO energy gap.	
7.1	LANL2DZ total electronic energies ( $E_{\text{total}}$ ) and relative energies ( $E_{\text{rel}}$ ) for the DFT optimized structures. For all systems the values including the zero-point vibrational energies (ZPV) are also given; where a= Energy relative to the most stable conformer separately for R= H(1), CH <sub>3</sub> (2) and Ph(3)). ZPV= Zero-point vibrational energy.	
7.2	Relative Energies and Selected Geometrical Parameters of the X-ray and DFT Optimized Structures of the Zn, and Cd <i>m</i> -BPDMs (where R= H (1); CH <sub>3</sub> (2); Ph (3)).	

## LIST OF SCHEMES

<i>Scheme No.</i>	<i>Descriptions</i>	<i>Page No.</i>
1.1	Representation of modifications in the central core and the types of porphyrin analogues.	
1.2	Basic route for synthesis of Porphyrin and by-products	
1.3	Berlin <i>et. al.</i> synthesis of modified porphyrin system	
1.4	Synthesis of <i>meta</i> -benzoporphyrin analogue by Grazynski <i>et. al</i>	
1.5	Synthesis scheme for <i>para</i> -benzoporphyrins.	
1.6	Synthesis of <i>meta</i> -benzoporphodimethenes in 2004.	
1.7	Metalation of 6,6,21,21-tetraphenyl-11,16-bis(4-nitrophenyl)- <i>meta</i> -benzoporphodimethene reported in 2004	
1.8	Synthesis of 11,16-Bis(phenyl)-6,6,21,2-tetramethyl-m-benzi-6,21-porphodimethene by Hung <i>et. al.</i>	
1.9	Tetramethyl-m-benzoporphodimethene ( <b>1</b> ) molecule along with its O-Up ( <b>2</b> ) and O-Down ( <b>3</b> ) isomer, R= H, COOMe	
1.10	<i>meso</i> -substituted <i>meta</i> -benzoporphodimethene derivative by Kumar <i>et. al.</i>	
4.1	Fragmentation scheme for estimation of intramolecular N-H···N hydrogen bond in <b>1f</b> (parent molecule).	
4.2	<i>meta</i> -benzoporphodimethene systems under consideration.	
5.1	Fragmentation scheme for the estimation of N-H···N hydrogen bonds <b>HB1</b> and <b>HB2</b> in parent molecule <b>1a</b> ; see Figure 4.1 and text for details.	
6.1	Synthesis of 1,3-Bis(diphenylhydroxymethyl)benzene ( <b>1</b> ) precursor	
6.2	Synthesis of free base hexaaryl-m-benzoporphodimethene and its metal complexes	

## LIST OF FIGURES

<i>Figure No.</i>	<i>Descriptions</i>	<i>Page No.</i>
1.1	Porphyrin-like moiety in natural pigments	
1.2	Possible pathways for the delocalisation of $\pi$ -electrons in porphyrins	
1.3	Structure of porphyrin and the sites of modifications	
1.4	Inverted Porphyrin isomer by Arnoff and Calvin	
1.5	X-ray crystal structure of N-confused porphyrin reported by Furuta <i>et. al</i>	
1.6	Structure of N-confused porphyrin reported by Grazynski <i>et. al</i>	
1.7	Structure of freebase <i>m</i> -benzoporphodimethene.	
1.8	Colour change in <i>m</i> -benzoporphodimethene upon metalation using ZnCl <sub>2</sub> salt.	
1.9	UV-Vis Spectra for freebase <i>meta</i> -benzoporphodimethene analogues	
1.10	UV-Vis Spectra of <i>meta</i> -benzoporphodimethene, <b>1-8</b> (Scheme 1.10) zinc chloride complexes.	
1.11	Depiction of core geometry of porphyrin molecule, non-planar <i>meta</i> -benzoporphodimethene molecule and its metal complex (M=Zn, Cd, Hg)	
1.12	Molecular model of 11,16-Bis(phenyl)-6,6,21,21-tetramethyl- <i>m</i> -benzi-6,21-porphodimethene ( <b>1</b> ) along with its O-Up ( <b>2</b> ) and O-Down ( <b>3</b> ) isomers . Crystal structure coordinates were taken from ref. [82]	
1.13	Molecular model of 11,16-Bis(3,4,5-trimethoxy-phenyl)-6,6,21,21-tetramethyl- <i>meta</i> -benzoporphodimethene. Crystal structure coordinates were taken from [83]	
1.14	Crystal structure of Group 12 metal complexes of <i>meta</i> -benzoporphodimethene analogues.	
1.15	Representation of (i) <i>syn</i> - conformational, and (ii) <i>anti</i> -conformational isomers of <i>meta</i> -benzoporphodimethene	
1.16	The structures of dinuclear (2-Ag <sub>2</sub> TMBPDM, (a)) and tetranuclear (2-Ag <sub>4</sub> TMBPDM, (b)) complexes, with 11,16-bisphenyl groups ( <b>2</b> ), omitted for clarity purpose.	

<i>Figure No.</i>	<i>Descriptions</i>	<i>Page No.</i>
1.17	Overview of TMBPDM analogues studied by Kumar <i>et. al</i>	
1.18	Most Stable structures of all the tautomers discussed in Figure 1.17	
1.19	MDA-MB-468 cells incubated with different <i>meta</i> -benzoporphodimethenes and Zn <sup>2+</sup> ions for 30 min and respective bright field marked with A-D as well as fluorescence images (just down to its respective bright field image) were captured at 10X objective lens magnification	
3.1	Questions that can be solved by computational chemistry.	
3.2	All the possible molecular properties that can be determined by DFT.	
3.3	Key features of STOs and GTOs.	
4.1	Structure of H-bonded <i>meta</i> -benzoporphodimethene.	
4.2	Frontier Molecular Orbital (FMO) energy level diagram with energy gap when R'=H (1)	
4.3	Frontier Molecular Orbital (FMO) energy level diagram with energy gap when R'=Me (2)	
4.4	Frontier Molecular Orbital (FMO) energy level diagram with energy gap when R'=Ph (3)	
5.1	<i>meta</i> -benzoporphodimethene structures under study.	
5.2	Effect of substituents at C3-position on the phenylene ring.	
6.1	UV-Vis plots for compound <b>2</b> , <b>3</b> and <b>4</b> .	
6.2	<sup>1</sup> H-NMR of <b>1,3-Bis(diphenylhydroxymethyl)benzene (1)</b> precursor.	
6.3	<sup>1</sup> H-NMR of 11,16-Bis(phenyl)-6,6,21,21-tetraphenyl- <i>meta</i> -benzi-6,21-porphoodimethene (2) in CD <sub>3</sub> OCD <sub>3</sub> .	
6.4	<sup>1</sup> H-NMR of chlorozinc(II) 11,16-Bis(phenyl)-6,6,21,21-tetraphenyl- <i>meta</i> -benzi-6,21-porphoodimethene (3) in CD <sub>3</sub> OCD <sub>3</sub> .	
6.5	<sup>1</sup> H-NMR of chlorocadmium(II) 11,16-Bis(phenyl)-6,6,21,21-tetraphenyl- <i>meta</i> -benzi-6,21-porphoodimethene (4) in CD <sub>3</sub> OCD <sub>3</sub> .	
6.6	HRMS of 11,16-Bis(phenyl)-6,6,21,21-tetraphenyl- <i>meta</i> -benzi-6,21-porphoodimethene (2) in APCI positive mode.	

<i>Figure No.</i>	<i>Descriptions</i>	<i>Page No.</i>
6.7	HRMS of chlorozinc(II) 11,16-Bis(phenyl)-6,6,21,21-tetraphenyl- <i>meta</i> -benz-6,21-porphodimethene (3) in APCI positive mode.	
6.8	HRMS of chlorocadmium(II) 11,16-Bis(phenyl)-6,6,21,21-tetraphenyl- <i>meta</i> -benz-6,21-porphodimethene (4) in APCI positive mode	
6.9	Depiction of frontier molecular orbitals and their energy gap in 2, 3 and 4 <i>meta</i> -benzoporphodimethene systems (Isovalue = 0.02).	
6.10	TDOS plot for (a) free base <i>m</i> -BPDM (2) (b) Zn(II) <i>m</i> -BPDM complex (3) and (c) Cd(II) <i>m</i> -BPDM complex (4).	
6.11	TDOS/PDOS/OPDOS plot for (a) 2, (b) 3 and (c) 4.	
7.1	Geometries of <i>meta</i> -benzoporphodimethene structures under study.	
7.2	3D-representation of <i>anti</i> - and <i>syn</i> - conformers of <i>m</i> -BPDM metal complex.	

## LIST OF CHARTS

<i>Chart No.</i>	<i>Descriptions</i>	<i>Page No.</i>
4.1	Geometries of H-bonded molecules along with H-bonded distances (in Angstrom) when R'=H.	
4.2	Geometries of H-bonded molecules along with H-bonded distances (in Angstrom) when R'=CH <sub>3</sub>	
4.3	Geometries of H-bonded molecules along with H-bonded distances (in Angstrom) when R'=Ph.	
4.4	Comparison of inner geometry interms of Py <sub>0</sub> /17, Py <sub>1</sub> /17, and Py <sub>2</sub> /17 angles and the sum of intramolecular H-bond energy in different substituted <i>meta</i> -benzoporphodimethenes (BPDM)	
4.5	Frontier molecular orbital diagrams and their respective energies for R'=H ( <b>1</b> ).	
4.6	Frontier molecular orbital diagrams and their respective energies for R'=CH <sub>3</sub> ( <b>2</b> ).	
4.7	Frontier molecular orbital diagrams and their respective energies for R'=Ph ( <b>3</b> ).	
5.1	Geometries of molecules with H-bond distances (HB1, HB2; in Angstrom) when R'=H ( <b>1</b> )	
5.2	Geometries of molecules with H-bond distances (HB1, HB2; in Angstrom) when R'=CH <sub>3</sub> ( <b>2</b> )	
5.3	Geometries of molecules with H-bond distances (HB1, HB2; in Angstrom) when R'=Ph ( <b>3</b> )	
5.4	Non covalent interactions and RDG plots for R'=H. (Isovalue= 0.5)	
5.5	Non covalent interactions and RDG plots for R'=CH <sub>3</sub> . (Isovalue= 0.5)	
5.6	Non covalent interactions and RDG plots for R'=Ph. (Isovalue= 0.5)	
5.7	MESP surfaces of <i>m</i> -BPDM molecules when R'=H. The electron density isosurface of value 0.001 a.u. was chosen.	
4.8	MESP surfaces of <i>m</i> -BPDM molecules when R'=CH <sub>3</sub> . The electron density isosurface of value 0.001 a.u. was chosen.	

<i>Chart No.</i>	<i>Descriptions</i>	<i>Page No.</i>
5.9	MESP surfaces of <i>m</i> -BPDM molecules when R'=Ph. The electron density isosurface of value 0.001 a.u. was chosen.	
7.1	B3LYP/LANL2DZ optimized geometries for (a) Zinc <i>syn</i> conformer ; (b) Zinc <i>anti</i> conformer; (c) Cd <i>syn</i> conformer; (d) Cd <i>anti</i> -conformer; when R= H. at <i>sp</i> <sup>3</sup> <i>meso</i> carbons.	
7.2	B3LYP/LANL2DZ optimized geometries for (a) Zinc <i>syn</i> conformer; (b) Zinc <i>anti</i> conformer; (c) Cd <i>syn</i> conformer (d) Cd <i>anti</i> conformer; when R= CH <sub>3</sub> , at <i>sp</i> <sup>3</sup> <i>meso</i> carbons.	
7.3	B3LYP/LANL2DZ optimized geometries for (a) Zinc <i>syn</i> conformer ; (b) Zinc <i>anti</i> conformer; (c) Cd <i>syn</i> conformer; (d) Cd <i>anti</i> conformer; when R= Ph at <i>sp</i> <sup>3</sup> <i>meso</i> carbons.	
7.4	B3LYP/LANL2DZ optimized geometries for free base <i>m</i> -BPDM when (a) R= H; (b) R= methyl; (c) R = Phenyl at <i>sp</i> <sup>3</sup> <i>meso</i> carbons.	
7.5	X-Ray geometries for (a') Zinc <i>syn</i> conformer; (c') Cd <i>syn</i> conformer ; when R= CH <sub>3</sub> , at <i>sp</i> <sup>3</sup> <i>meso</i> carbons.	
7.6	Depiction of angles and bond distances measured in Table 7.2.	

## ABSTRACT

This thesis begins with presenting a thorough review of *m*-BPDM analogues and their metal complexes. The literature review led us to the foundation of research gap. The studies were then diverted towards finding out the factors that could enhance the stability of the free base analogues of *m*-BPDM systems. Hence, in the next two chapters (4 and 5) the effect of substitutions at *meso* and C3-positions, studied computationally, has been presented. Molecular tailoring approach has been incorporated in order to find out the intramolecular hydrogen bond energies. The energies so obtained have been correlated with other factors obtained from the optimized geometry's results, like the study of non-covalent interactions (NCI), frontier molecular orbital (FMO) visualization, molecular electrostatic surface potential (MESP) etc. We then moved to the synthesis of a new sterically hindered analogue of *m*-BPDM and its zinc and cadmium chloride complexes, *viz.* Chapter 6 of this thesis. The synthesis was confirmed by UV-Vis,  $^1\text{H-NMR}$  and mass spectrometry. The X-ray solid state structures stated the presence of two conformers of *m*-BPDM *viz.* *syn* and *anti*. It was found that crystal structures constituted varied conformers depending upon the group present at  $sp^3$  *meso* carbon atoms. Thus, through chapter 7, we intend to understand the effect of substitution at *meso*-carbon atoms on the metalated (Zn(II) and Cd(II)) *m*-BPDM conformer stability.

# CHAPTER 1

## INTRODUCTION

### **1.1. General Introduction**

Porphyrin is a tetra-pyrrolic moiety, very stable, aromatic and is one of the most important molecules in the biological system. Porphyrins are important because of its multiple biological functions and its ability to bind a number of metal ions.[1-4] The basic porphyrin-like moieties are found universally in natural pigments like heme, chlorophyll, bacteriochlorophyll, vitamin B<sub>12</sub> and cytochromes (**Figure 1.1**).[5-8]

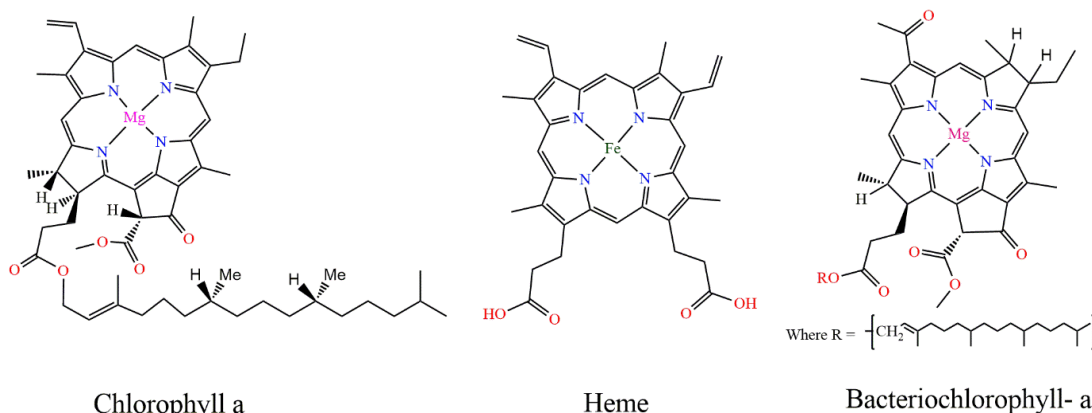


**Figure 1.1.** Porphyrin-like moiety in natural pigments

Simple porphyrin molecule is highly aromatic in nature. There are  $22\pi$ -electrons in a simple porphyrin molecule however only  $18\pi$ -electrons take part in complete conjugation in several possible delocalization pathways, as (represented by bold bonds) in **Figure 1.2.** [9,10]

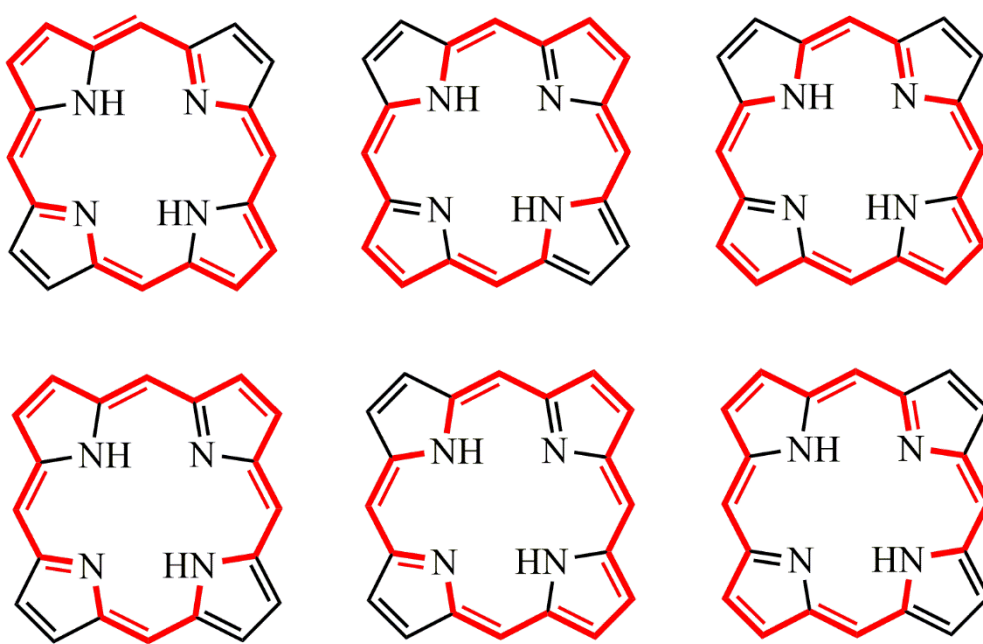


**Figure 1.2.** Possible pathways for the delocalisation of  $\pi$ -electrons in porphyrins. [5]

Over the years, researchers have showed great enthusiasm in exploring this prosthetic molecule employing modifications at several sites in the molecule (**Figure 1.3**).[9] The major objectives of these investigations is to find the applications parallel to that of natural porphyrins so as to mimic the natural phenomena in-vitro. The electronic structure of porphyrins play a significant role to decide the fate of the system. A vast variety of conjugated and non-conjugated porphyrinoid systems give us a choice for selecting moiety for different applications and investigations.[11,12]

The modification in porphyrin molecule can be done in many ways for various purposes. The central region of porphyrin molecule is NNNN core that is surrounded by four pyrrolic nitrogen atoms (**Figure 1.3**). The new synthetic analogues are classified according to their structure and the electronic current they possess, and are generally called modified class of porphyrins.[13] This chapter is divided into 3 major

topics. The first part is concerned with understanding the basic modifications that can be done in a porphyrin system. In the second section, a brief explanation about the carbaporphyrinoid family has been added. The major focus of the chapter is the third section, wherein *meta*-benzoporphodimethene systems have been discussed. In this part, discussions about the synthetic procedures, modifications, characterizations, computational studies and applications have been added.

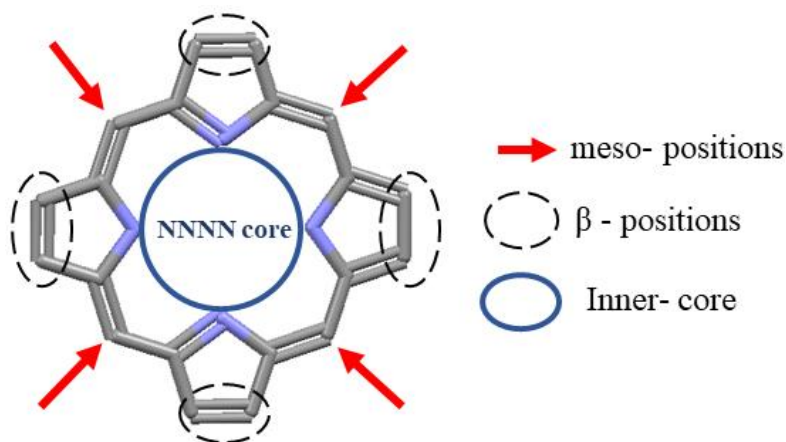
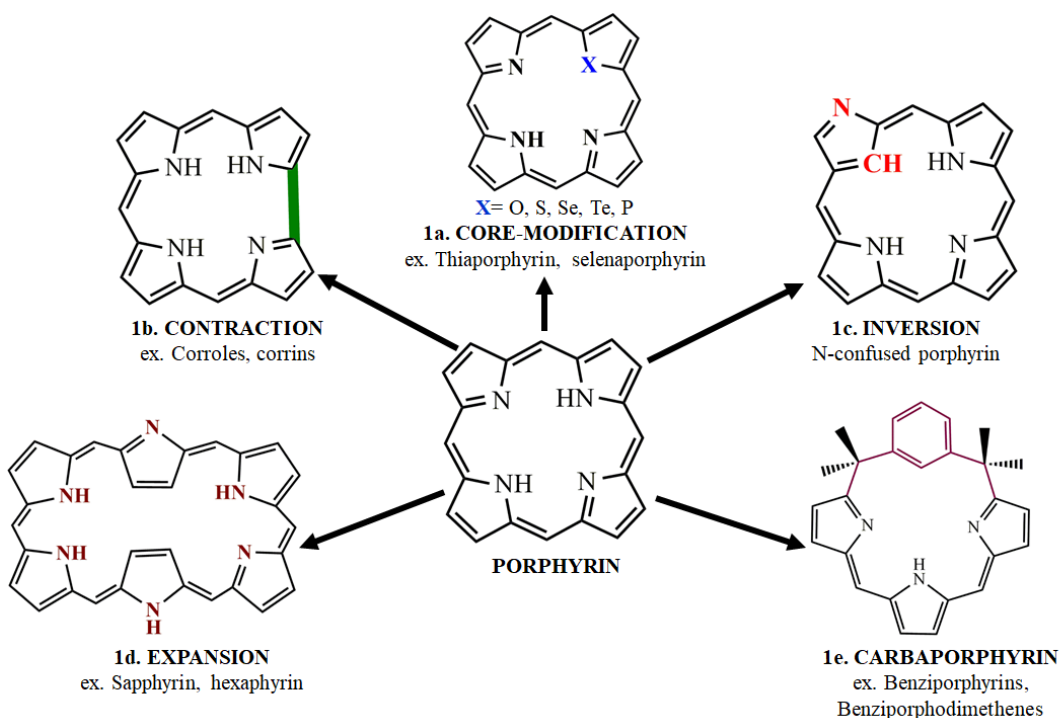


**Figure 1.3.** Structure of porphyrin and the sites of modifications.

### 1.1.1. Modifications in Porphyrin

Generalizations of these modified porphyrins are shown in **Scheme 1.1**. Periphery modified porphyrins, which includes modifications in the periphery of tetra-pyrrolic moiety *i.e.*, the  $\beta$ - and *meso*-positons (**Figure 1.3**).<sup>[14–18]</sup> Core-modified porphyrins,<sup>[19]</sup> where inner nitrogen atoms of the tetra-pyrrolic moiety are replaced by other elements (generally chalcogens), also called heteroporphyrins, *i.e.*, the NNNN core is replaced by XNNN core (**1a, Scheme 1.1**) The heteroatoms introduced other than nitrogen in the inner core modifies the inner core arrangement of macrocycle and hence changes the binding abilities of these molecules with different transition metal

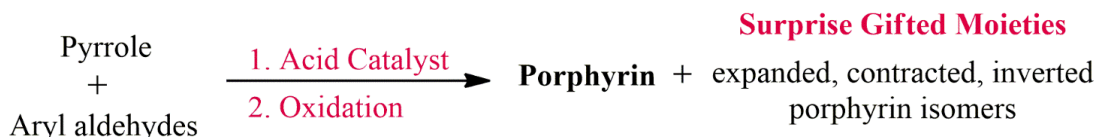
which results the shift in their absorption spectra.[12] Macrocycles containing oxygen,[13] sulphur,[19,20] tellurium,[21,22] selenium[23,24] and recently phosphorus[25–27] provide a platform to constitute a variety of macrocycles able to bind with different transition metals in their unusual oxidation states with excellent properties.[12][28] Contracted porphyrins,[29-41] wherein one lesser *meso* carbon is present than the regular porphyrin, for instance, corroles (**1b**, **Scheme 1.1**). In isomeric porphyrins,[42] similar structures and formula, i.e., C<sub>20</sub>H<sub>14</sub>N<sub>4</sub> by scrambling pyrrolic subunits and bridging carbon atoms. Inverted porphyrins,[28] porphyrin isomers having either N or C of pyrrolic units pointing out or inside of the ring, respectively, also called ‘N-confused porphyrins’ or ‘mutant porphyrins’ (**1c**, **Scheme 1.1**). Expanded porphyrins,[43] these are the synthetic analogue of porphyrin macrocycles with enlarge core comparative to the other members of the porphyrin family with a minimum of 17 atoms in the inner central core while retaining the extended conjugation of the system (**1d**, **Scheme 1.1**). The inner core atoms of macrocycle are generally greater than 17 atoms as of regular one and expand the  $\pi$ -electron conjugation. These expanded systems strongly absorb in the red region as compared to 17 atoms and 18 $\pi$  electrons porphyrins. Sapphyrins,[44] smaragdylins,[45] isosmaragdylins,[46] pentaphyrins, [47] hexaphyrins,[48,49] orangarins,[50] amethyrins,[51] octaphyrins, [52,53] rosarins,[54] rubyrins,[55] ozaphyrins,[56] bronzaphyrins,[57,58] heptaphyrins,[59] turcasarins,[60] dodecaphyrins[61] and hexadecaphyrins[61] are the few examples of expanded porphyrins. Lastly, carbaporphyrinoid systems, wherein one of the pyrrole rings is replaced by a carbon based aromatic ring, as in *meta*- and *para*- benzoporphyrins and *meta*-benzoporphodimethenes (**1e**, **Scheme 1.1**).



**Scheme 1.1.** Representation of modifications in the central core and the types of porphyrin analogues.

### 1.1.2. Carbaporphyrinoids- A turning point in Porphyrin Chemistry

The first porphyrin molecule was reported in the year 1867 by Thudichum J. L. W., as hematoporphyrin which was originally named as cruentine.[62]



**Scheme 1.2.** Basic route for synthesis of Porphyrin and by-products.

It is very common that the process not only give the desired product but other gifted compounds like expanded, contracted, inverted, and other categories of compounds as well (**Scheme 1.2**). It thus became necessary to optimize the conditions of reactions in a systematic way for obtaining the desired product only. Consequently, the one pot synthesis of porphyrins pioneered by Rothemund[63] had been optimized in the past

in a number of ways by using various modified catalysts to direct the synthesis towards a particular moiety and to reduce or eradicate the unwanted products.[64–69]

A revolutionary point arrived when in 1943, while revisiting Rothemund's synthesis of tetraphenylporphyrin Aronoff and Calvin reported six-porphyrin-like-compounds ( $R_4C_{20}H_{10}N_4$ ) which may be separated chromatographically. One of these isomers involved one inverted porphyrin ring (**Figure 1.4**).

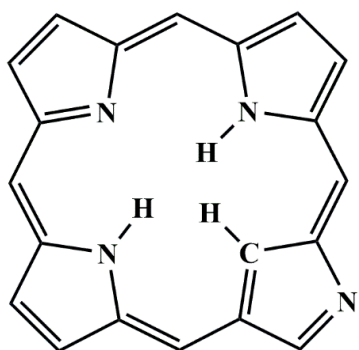
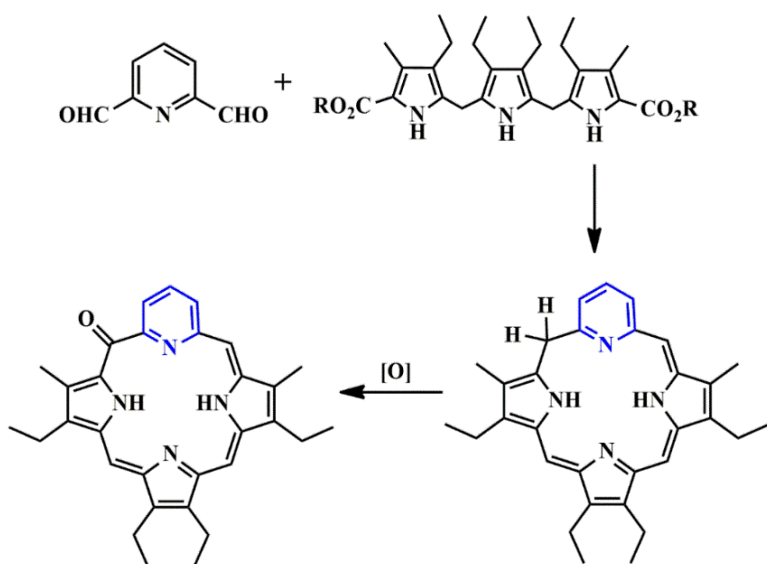


**Figure 1.4.** Inverted Porphyrin isomer by Arnoff and Calvin[63]

In this light, many reports were presented with variety of modifications on porphyrin moiety. In 1994, Berlin and Breitmeir replaced one five-membered ring in the macrocycle with a larger heteroarene (**Scheme 1.3**).[70]



**Scheme 1.3.** Berlin *et. al.* synthesis of modified porphyrin system.[70]

In the same year, two research groups independently reported the synthesis of N-confused porphyrins. Furuta and co-workers synthesized a phenyl-substituted derivative isomer of a porphyrin isomer, wherein they introduced slight change in the reacting species. The acid catalysed condensation of benzaldehyde and pyrrole was carried out. However, instead of using propanoic acid, t-BuOH/ CH<sub>2</sub>Cl<sub>2</sub> (1:1) and concentrated HBr was used. The reaction yielded 5% of N-confused porphyrin along with 20% tetraphenylporphyrin (TPP) (**Figure 1.5**).[71]

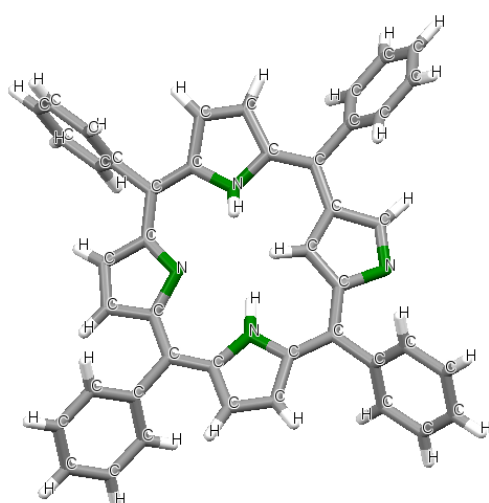


**Figure 1.5.** X-ray crystal structure of N-confused porphyrin reported by Furuta *et. al.* CCDC: 1300473[71].

At the same time, another group from Poland synthesized a newly core-modified 2-aza-21-carba-5,10,15,20-tetra-p-tolyporphyrin (CTTPH<sub>2</sub>) with 4% product yield (**Figure 1.6**). The centre of this macrocycle has remarkable ability as a tetradeятate ligand to form carbon-metal bond. The spectral properties highlighted its potential application as a photosensitizer in photodynamic therapy.[72]

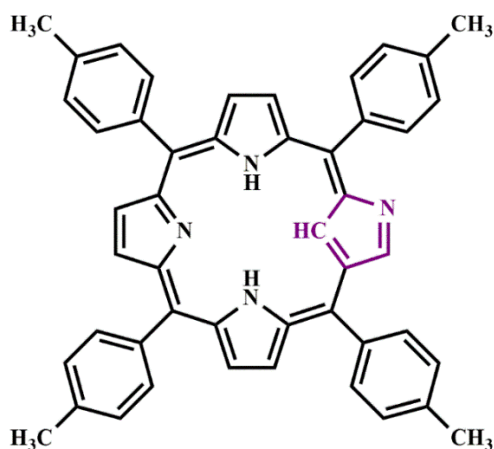


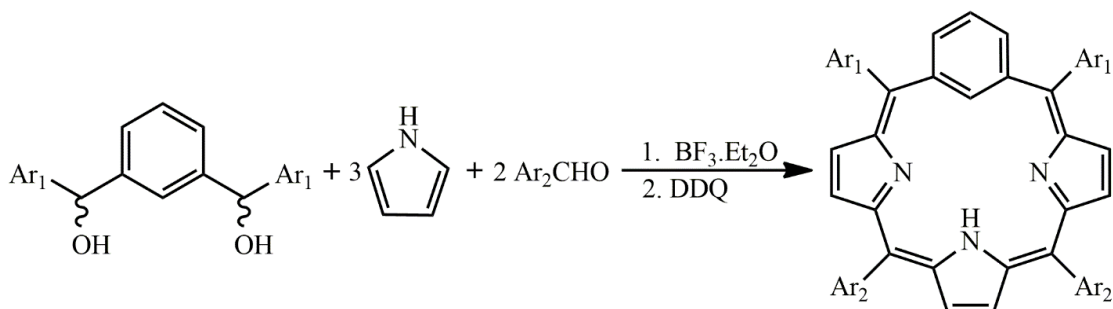
**Figure 1.6.** Structure of N-confused porphyrin reported by Grazynski *et. al.* [72]

These investigations opened a new platform for the scientists to explore the *meso*-,  $\beta$ - and inner-core of the porphyrin molecule.

### 1.1.3. *meta*-Benziporphyrin

The presence of C-H moiety in the inner core gives higher possibility for stabilization of rare metal carbon interaction.[73,74] It is important to note that in carbaporphyrinoids due to the C-H moiety in the inner core, the  $\pi$ -electrons delocalization is deeply affected and in some cases it ceases completely. The loss of electronic current can be detected by NMR spectroscopy.[75] When a pyrrole ring in porphyrin macrocycle is outplaced by phenylene ring then it creates a subclass called benziporphyrin. Carbaporphyrinoids consisting of atleast one all-carbon ring is often distinguished from N-confused porphyrins by using the prefix true in front of the name of carbaporphyrin. This class of true carbaporphyrins is important to us as it provides feasibility to study the behaviour of aromatic rings when surrounded by metal ions.[76]

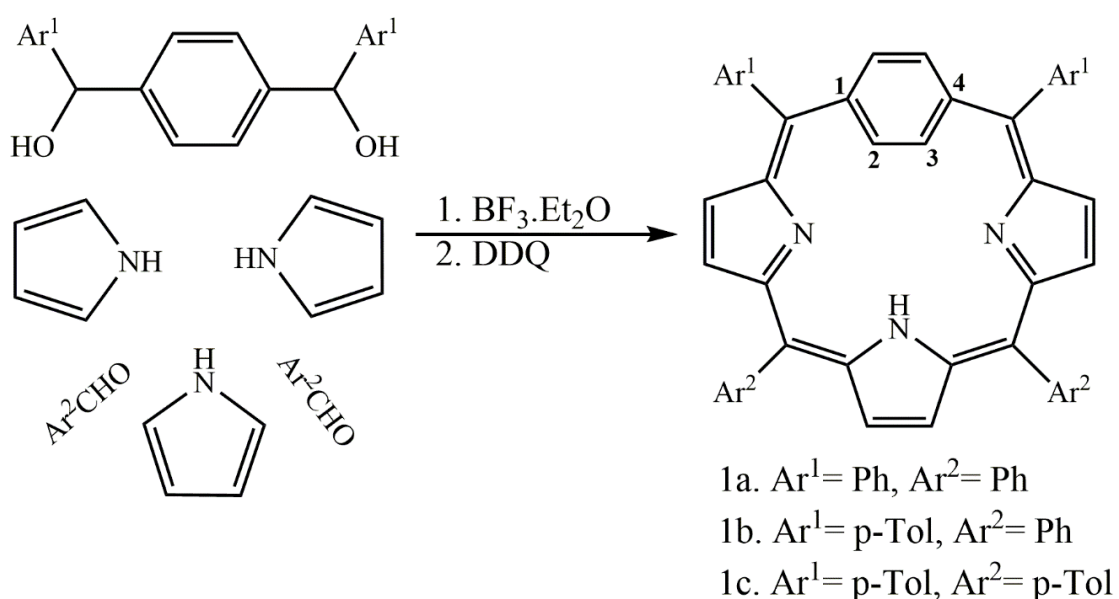
The idea of displacement of one of the pyrrole rings by another aromatic ring was first reported by Berlin *et. al.* as discussed prior in this section. Synthetic analogs like *meso*- substituted benziporphyrins were later prepared for obtaining a pure sample by Marcin Stepien, and Latos-Grazynski.[77] The synthesis involved condensation of a pyrrole, aromatic aldehyde and a precursor ( $\alpha,\alpha'$ -diol) followed by oxidation with DDQ, and further purification was done by chromatography, yielded 15% product (**Scheme 1.4**). The result of this experiment were satisfying considering the easy synthesis of diol precursor.



**Scheme 1.4.** Synthesis of *meta*-benziporphyrin analogue by Grazynski *et. al.*[77]

#### 1.1.4. *para*-benziporphyrin

The same was observed when the phenylene ring was incorporated in the system with 1 and 4 position of linkage, resulted in the new class of benziporphyrins, called ***para*-benziporphyrins**. *para*-Benziporphyrin was first reported by Marcin Stepien and Lechosław Latos-Grazynski in 2001 in synthesis similar to *meta*-benziporphyrin. The  $\alpha,\alpha'$ -dihydroxy-1,3-diisopropylbenzene in the synthesis was replaced by 1,4- isomer to obtain *para*-benziporphyrin. However, the yield was reduced drastically to 1-3% (**Scheme 1.5**).[78]



**Scheme 1.5.** Synthesis scheme for *para*-benziporphyrins. [78]

Later, Hung and co-workers synthesized the hetero- analogue of benziporphyrins by using  $\alpha$ ,  $\alpha'$ -dihydroxy-1, 4-diisopropylbenzene with 16-thiatripyrrane to give a 6% yield.[79] It is worth mentioning here that the *p*-phenylene ring in *para*-benziporphyrin was found out of the plane of three N atoms and is  $45^\circ$  tilted from the plane. A weak conjugation was also indicated by deviation in C-C bonds in *para*-phenylene from normal benzene ring. The NMR study reveals that the *para* phenylene ring protons face different magnetic field at low temperatures while the difference end up at high temperature clearly indicating the rotation of *para* phenylene ring in a *see-saw* motion at higher temperatures. While at low temperature the outer proton 2 and 3 comes at aromatic region, the inside proton 21 and 22 comes upfield due to inner shielding ring current. Further, molecular and spectral study indicates that *para*-benziporphyrin behaves like extended conjugated macromolecules having aromaticity

which differentiate it with *m*-benzoporphyrins. It is also different from oxybenzoporphyrin as that achieves aromaticity because of semiquinone arrangement.[80]

Several modifications in this molecule were then reported by various research groups. But, this chapter majorly focusses on the partially reduced form of *meta*-benzoporphyrin, i.e., *meta*-benzoporphodimethenes.

## 1.2. *meta*-benzoporphodimethene analogues

*meta*-Benzoporphodimethene (*m*-BPDM) systems was initially synthesized by Marcin Stępień during his Ph.D. thesis work.[78] These synthesized *m*-BPDM were alkoxy and hydroxy analogues which were obtained through reduction of *meta*-benzoporphyrins. *m*-BPDM are actually modified *m*-benzoporphyrins with two tetrahedral *meso* carbon atoms at 6- and 21- positions (**Figure 1.7**).[72]

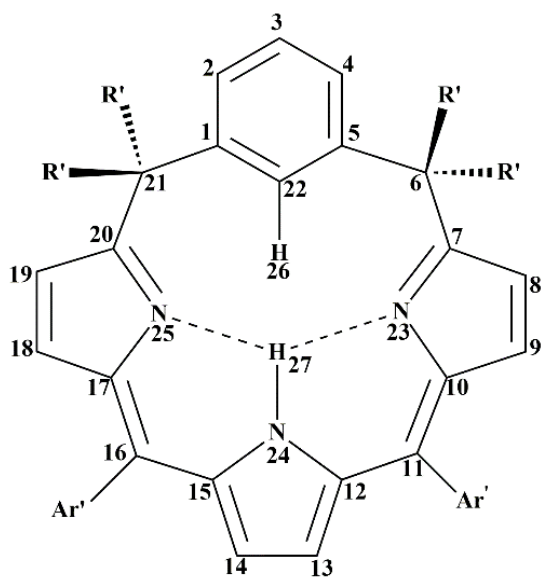
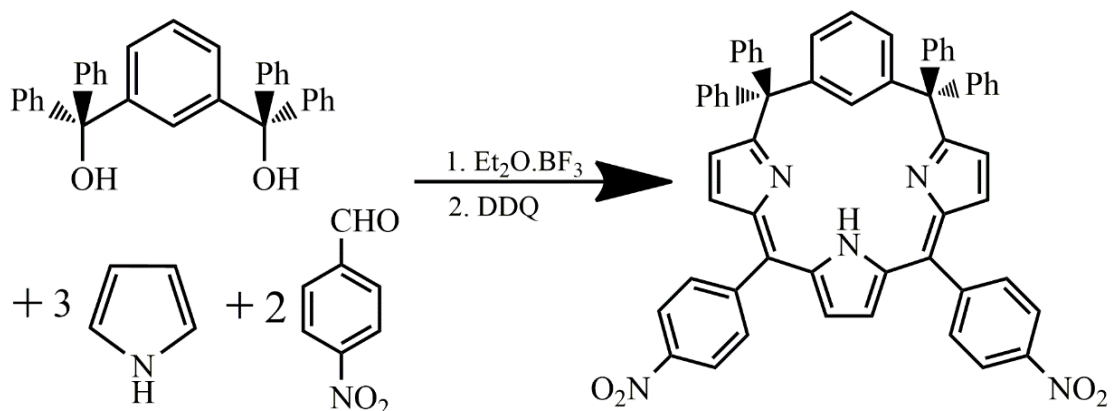


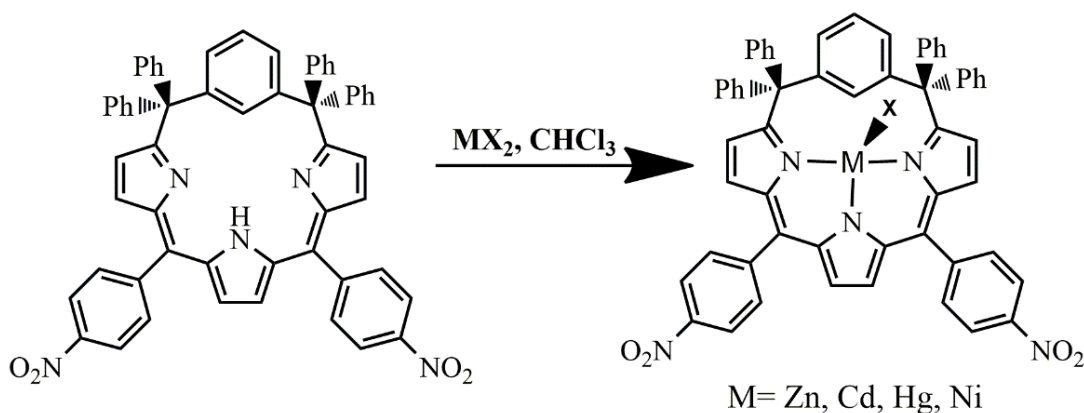
**Figure 1.7.** Structure of freebase *m*-benzoporphodimethene. [84]

### 1.2.1. Synthetic Route for *meta*-benziporphodimethene analogues

The prosthetic molecule *meta*-benziporphodimethene was first developed in serendipity by Grażyński and co-workers while spectroscopically manifesting the metal-arene interactions observed in the diamagnetic zinc(II), cadmium(II), and mercury(II) benzoporphyrin (both *meta* and *para* isomers) complexes and in the paramagnetic nickel(II) species. The synthesis of 6,6,21,21-tetraphenyl-11,16-bis(4-nitrophenyl)-*meta*-benziporphodimethene involved mixed condensation reaction between pyrrole, 4-nitrobenzaldehyde and  $\alpha,\alpha'$ -dihydroxy-1, 3-diphenylbenzene, in fixed ratios, in the presence of lewis acid and oxidants as shown in **Scheme 1.6**. The reaction yielded 14% of the product. They also reported metalation of the newly synthesized benzoporphodimethene analogue, by insertion of Zn(II), Cd(II), Hg(II) and Ni(II) ions, by boiling a mixture of the free base and an appropriate salt, usually anhydrous chloride, in a chloroform solution (**Scheme 1.7**).[78] The macrocycles designed in this study aimed to study different orientations of the arene with respect to the coordination center and different linkages between the arene fragment and the rest of the macrocycle, and to draw a comparison of benzoporphyrin isomers with the benzoporphodimethene molecules on the basis of NMR and UV-Vis analysis, which is discussed in the next section 1.2.2.

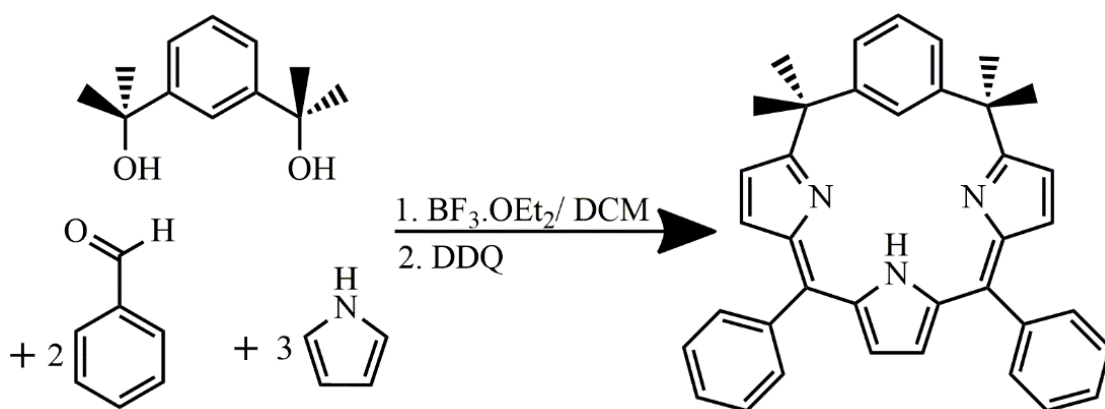


**Scheme 1.6.** Synthesis of *meta*-benziporphodimethenes in 2004.[72]



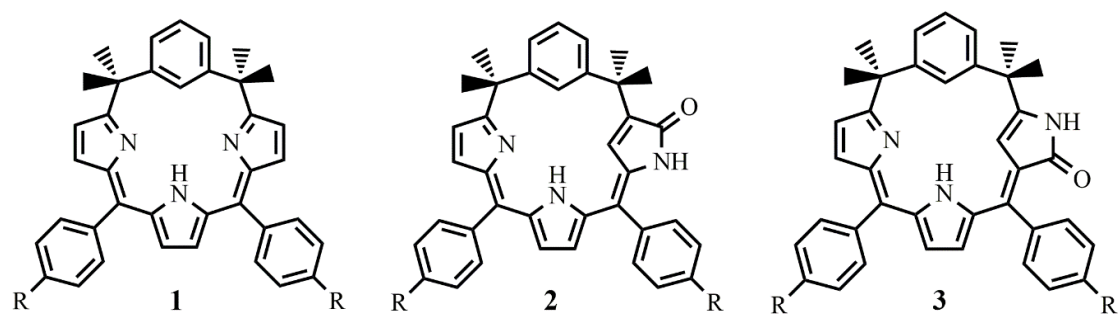
**Scheme 1.7.** Metalation of 6,6,21,21-tetraphenyl-11,16-bis(4-nitrophenyl)-*meta*-benzoporphodimethene reported in 2004.[72]

Later in 2008, Hung and co-workers developed a novel *meta*-benzoporphodimethene based molecule (**Scheme 1.8**), that was isolated as red solid with 27% product yield, that imparted no background emission and showed a turn-on probe for  $\text{Zn}^{2+}$  sensing.[81] This report aimed to traverse the applications of the newly synthesized analogue as a *chemosensor* (*vide infra*). The synthesis was confirmed by UV-Vis spectroscopy and other spectroscopic techniques. The same procedure as in **Scheme 1.12** has been followed for metalation.



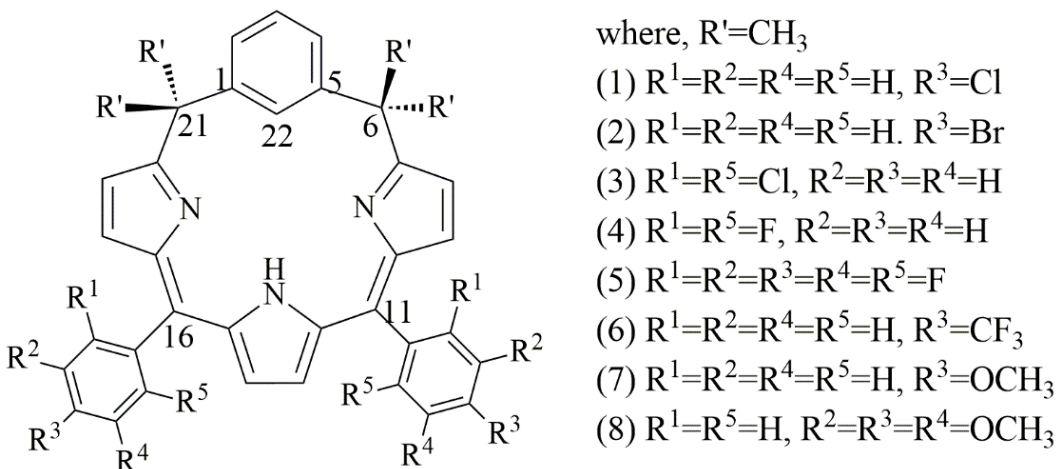
**Scheme 1.8.** Synthesis of 11,16-Bis(phenyl)-6,6,21,21-tetramethyl-m-benzi-6,21-porphodimethene by Hung *et. al.*[81]

Subsequently, this group also reported the formation of outer  $\alpha$ -pyrrolic carbon oxygenated N-confused tetramethyl-*m*-benzoporphodimethenes isomers containing a  $\gamma$ -lactam ring in the macrocycle in addition to the product (**1**, in **Scheme 1.9**) formed in **Scheme 1.8** [81]. Two isomeric (**Scheme 1.9**) carbonyl group of lactam ring either close to (O-Up, **2**) or away from (O-Down, **3**) the neighboring  $sp^3$  *meso* carbon with product yield of 27%, 4% and 0.8%, respectively.[82] The compounds were characterized using UV-Vis, NMR, X-ray crystallographic analysis and DFT methods, discussed in later sections in this chapter.



**Scheme 1.9.** Tetramethyl-*m*-benzoporphodimethene (**1**) molecule along with its O-Up (**2**) and O-Down (**3**) isomer, R= H, COOMe.[82]

The synthetic pathway for the *meta*-benzoporphodimethene remained the same but researchers attempted several modifications at *meso* carbon atoms (C11, C16 in **Scheme 1.10**) of this novel molecule and advancements in its applications were explored. A similar synthesis was intended by Kumar and co-workers from Delhi Technological University, in 2016, wherein they used substituted aldehydes, pyrrole and  $\alpha$ ,  $\alpha'$ -dihydroxy-1,3-diisopropylbenzene (**Scheme 1.10**) with 15-17% product yield.[83] The research group confirmed the product synthesized using UV-Vis, NMR, mass and X-ray crystallographic analysis. Quantum yield, fluorescence studies and bio-cell imaging applications were also explained in detail.



**Scheme 1.10.** Meso-substituted meta-benziporphodimethene derivative by Kumar *et. al.*[83]

### Spectroscopic Analysis

#### 1.2.2. UV-Vis Spectroscopy

*meta*-Benziporphodimethenes are generally red color compounds. Owing to its discrete conjugated system, compound shows a broad UV-Vis spectrum. In *m*-benziporphodimethenes (in **Scheme 1.8**), a high energy Soret band is detected at 349 nm and lower energy Q band is found at about 514 and 542 nm approximately.[81] This compound is non-fluorescent in freebase form and upon addition of  $\text{Zn}^{2+}$  (**Scheme 1.7**), an instant change in solution colour from pink to greenish blue was observed (**Figure 1.8**).[83]

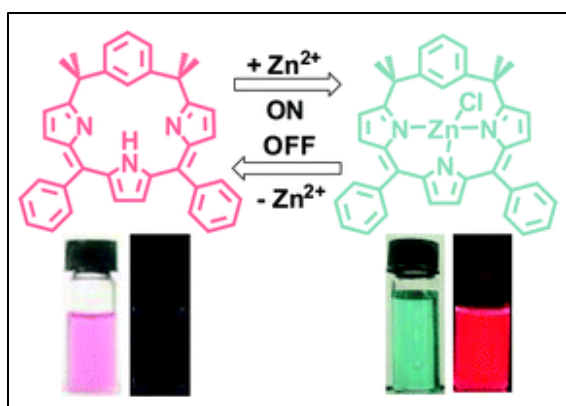


**Figure 1.8.** Colour change in *m*-benziporphodimethene upon metalation using  $\text{ZnCl}_2$  salt. [81]

The UV-Vis spectra is broad in nature due to the presence of  $sp^2$ - $sp^3$  mixed *meso* carbon atoms rendering non-conjugated system. In the report presented by Kumar and co-workers (**Figure 1.9**), the Soret like high energy band was observed around 342-378 nm for *para* and *ortho*- substituted *meso*-phenyl groups n freebase *meta*-benzoporphodimethenes, **1-8** in **Scheme 1.10**. The electron releasing substituent at *para* position showed considerable reduction in Soret like high energy band at 378 and 376 nm, **7,8** in **Scheme 1.10**. On the other hand, ortho-halogenation significantly enhance this high energy band emerging at 321, 320 and 319 nm for **3, 4, 5** in **Scheme 1.10** (**Table 1.1**).[83]

**Table 1.1.** Consolidated UV data for Scheme 1.10.[83]

Compound	Wavelength ( $\lambda_{\max}$ ) in nm			
	Freebase TMBPDM		$Zn^{2+}$ TMBPDM complex	
	Soret Band	Q-Band	Soret Band	Q-Band
<b>1</b>	353	517-548	351	594-639
<b>2</b>	351	513-542	350	594-638
<b>3</b>	321	508-538	348	602-649
<b>4</b>	320	507-533	346	598-642
<b>5</b>	319	508-531	346	600-642
<b>6</b>	342	509-539	347	594-641
<b>7</b>	378	513-545	343	592-643
<b>8</b>	376	513-546	346	598-642

Upon metalation of these freebase *meta*-benzoporphodimethene analogues **1-8** in **Scheme 1.10**, a significant red shift is observed which is due to the strong interactions

of d-orbital of zinc (II) with the macrocycle in the ground state absorption spectra of zinc complexes of these compounds with respect to their free-bases (**Figure 1.10**).

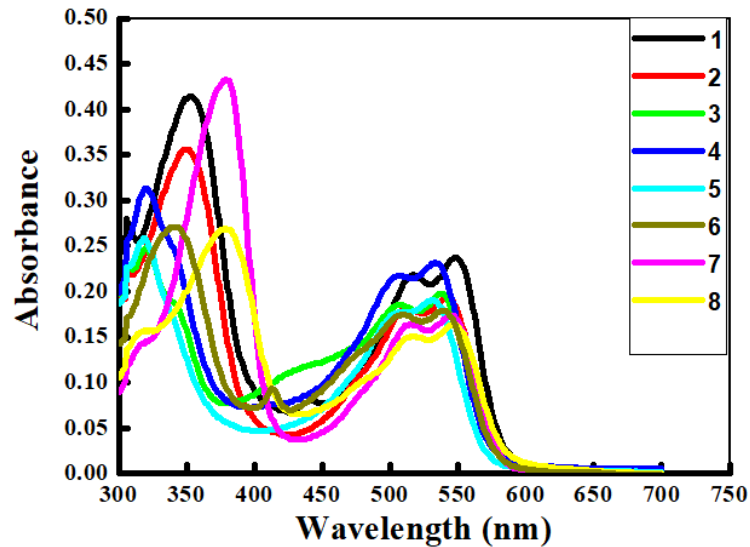


**Figure 1.9.** UV-Vis Spectra for freebase *meta*-benziporphodimethene analogues (Scheme 1.10).

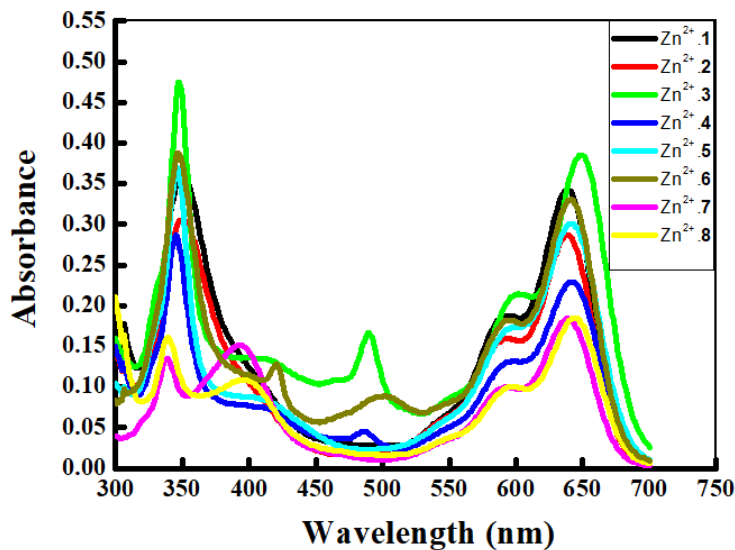


**Figure 1.10.** UV-Vis Spectra of *meta*-benziporphodimethene, **1-8** (Scheme 1.10) zinc chloride complexes.[83]

### 1.2.3. Structural Analysis

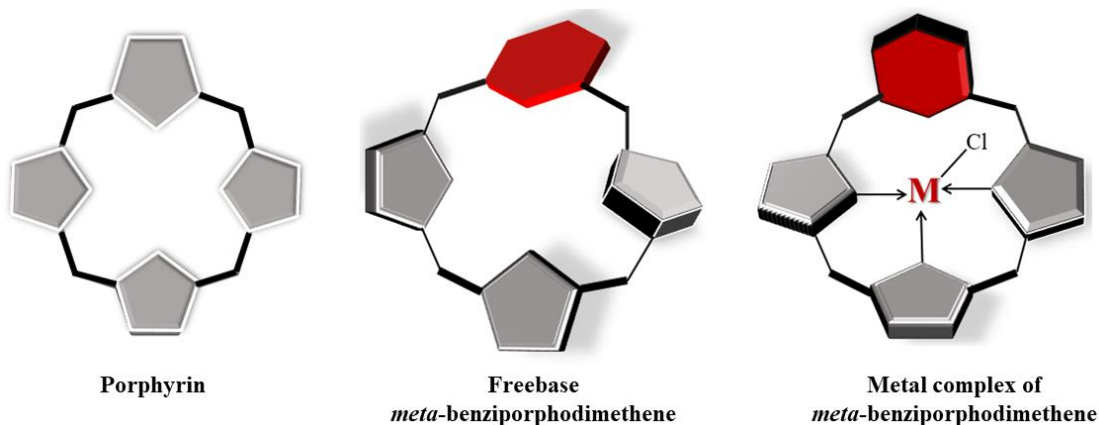


**Figure 1.11.** Depiction of core geometry of porphyrin molecule, non-planar *meta*-benziporphodimethene molecule and its metal complex ( $M = Zn, Cd, Hg$ )

The first ever crystal structure of *meta*-benziporphodimethene zinc complex was reported in 2008 by Hung *et. al.* The analysis mononymously confirmed the coordination of zinc ion with *meta*-benziporphodimethene through the three pyrrolic nitrogens and an axial chloride (**Figure 1.17**, 2-ZnCl).[81]

The same research group further then came up with crystal structures of freebase tetramethyl-*meta*-benziporphodimethene (TMBPDM) along with its two isomers (**Scheme 1.9**) as discussed in section 1.2.1. X-ray analysis shows that TMBPDM are more distorted than the other two isomers. The average deviation of 25 atoms on the macrocycle from a mean tripyrrin plane (plane through 17 atoms i.e. atoms of 3 pyrrole rings and two  $sp^2$  hybridised *meso*-carbon atoms) for **1** (TMBPDM) is 1.044 Å while the values for **2** (O-Up Isomer) and **3** (O-Down Isomer) are found to be 0.680 Å and 0.630 Å, respectively. The angle between the CNNN inner-core plane and the macrocyclic phenylene plane is  $70.35^\circ$  for **2** and  $69.76^\circ$  for **3**, but in case of **1**, the angle between phenylene plane and three pyrrolic nitrogen plane is only  $52.39^\circ$ .[82]

Another interesting feature in the crystal structure is that the angle between the vector along two  $sp^3$  *meso*-carbons and the plane, defined by the mean plane of 17 atoms on a tripyrrin moiety, is  $28.51^\circ$  for **1**, which is significantly larger than  $15.79^\circ$  and  $14.34^\circ$  for **2** and **3**, respectively. These data are in good agreement with the fact that **2** and **3** are less puckered than **1** with phenylene rings oriented vertical to the mean plane of the macrocycle (**Figure 1.12**).[82]

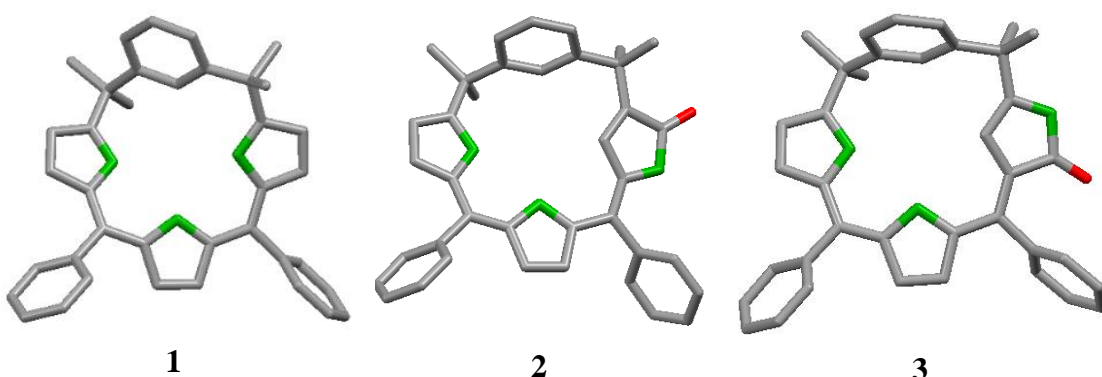


**Figure 1.12.** Molecular model of 11,16-Bis(phenyl)-6,6,21,21-tetramethyl-*m*-benzi-6,21-porphodimethene (**1**) along with its O-Up (**2**) and O-Down (**3**) isomers . Crystal structure coordinates were taken from ref. [82]

Later, Kumar *et. al.* determined the crystal structure of free base 11,16-Bis(3,4,5-trimethoxy-phenyl)-6,6,21,21-tetramethyl-*meta*-benzoporphodimethene (**8** in **Scheme 1.10**). The geometry of **8** was found lesser distorted than earlier reported structures of *meta*-benzoporphodimethenes (**Figure 1.13**). The average deviation of atoms which constitute the macrocycle was measured to be  $0.646\text{ \AA}$  which is sufficiently lesser as compared to  $1.044\text{ \AA}$  for free base *meta*-benzoporphodimethenes earlier reported by Hung and co-workers. The angle between the phenylene ring plane and three pyrrolic nitrogens of macrocycle is  $46.63^\circ$  which is remarkably lesser. Important and interesting observation in the crystal structure is that the angle between the plane formed by 17 tripyrrin atoms and the vector along the two  $sp^3$  *meso* carbons is only

15.45°. These observations confirm that the obtained structure of compound **8** is less pucker than the earlier reported structures of *meta*-benzoporphodimethenes.[83]

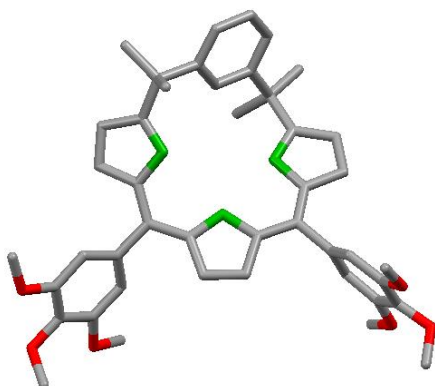


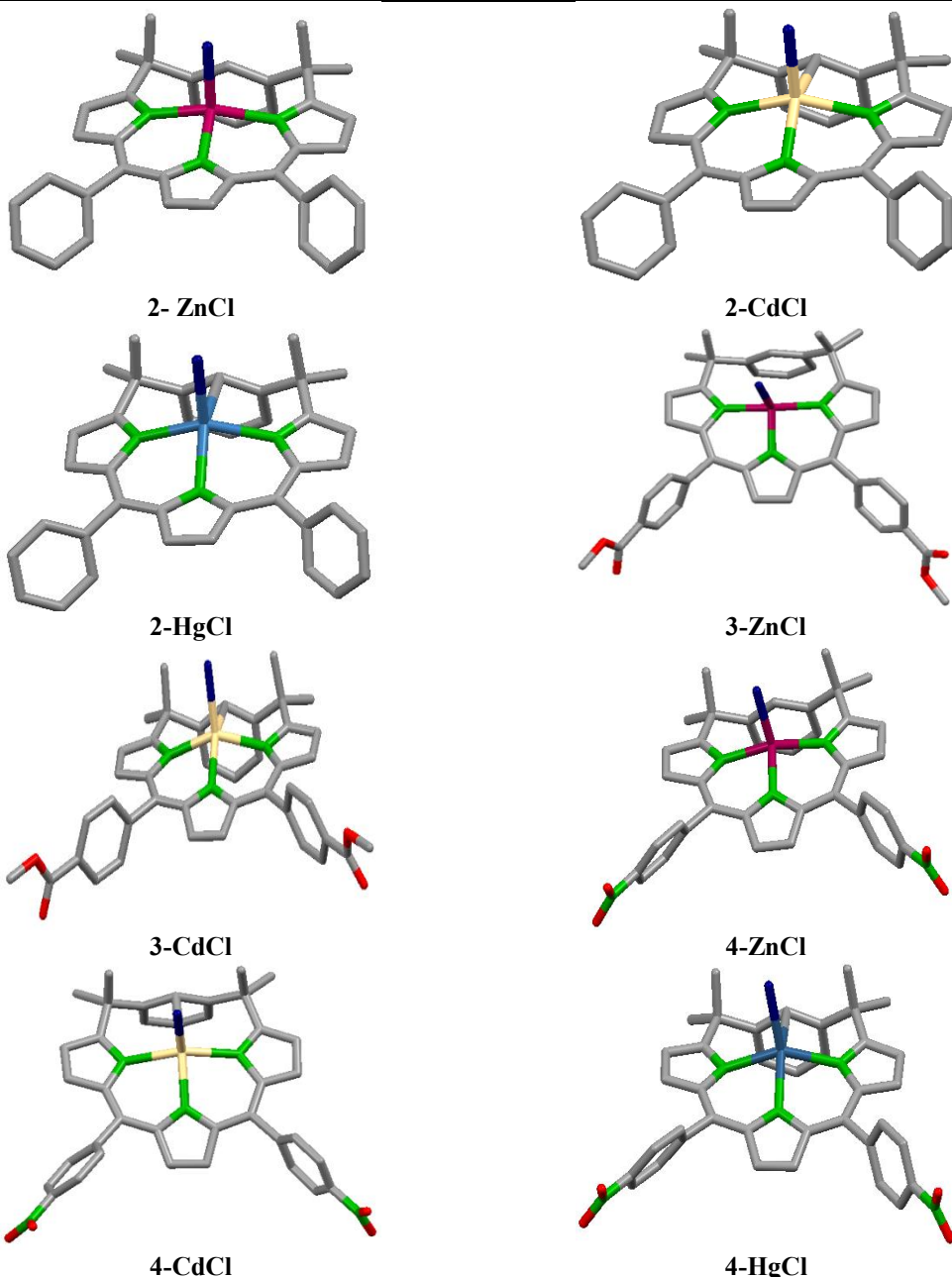
**Figure 1.13.** Molecular model of 11,16-Bis(3,4,5-trimethoxy-phenyl)-6,6,21,21-tetramethyl-*meta*-benzoporphodimethene. Crystal structure coordinates were taken from [83]

In the year 2011, Hung and co-workers reported crystal structures of group 12 metal complexes (Zn, Cd, Hg) of TMBPDM molecules (**Figure 1.14**).[76] The comparative studies suggested that the structure of freebase molecule is highly distorted while a flat pyrrin moiety with nearly coplanar pyrrolic nitrogen atoms is observed for all its metal chloride complexes. Further, the central metal ion was found to be tetra-coordinated with three coordinating pyrrolic nitrogen atoms and one chloride ion that sits at axial position of the TMBPDM metal chloride complexes as seen in the crystal structures below. They also reported that the apical deviation value for metal to the N<sub>3</sub> plane (plane consisting of 3 pyrrolic nitrogen atoms, i.e., N23, N24, N25) for TMBPDM core is remarkably lesser compared to benzoporphyrin complexes.[76] This in turn reflected the larger central core of TMBPDM relative to benzoporphyrins. The authors then studied the geometry of TMBPDM through calculating the angles between the plane passing through the phenylene ring (plane through C1, C2, C3, C4, C5, C22) and N<sub>3</sub> plane. Interestingly, for all the metal complexes, the phenylene ring was nearly perpendicular to the N<sub>3</sub> plane (approx. 81° to 92°) (**Figure 1.14**). The angle increased with the metal ion size. Although, as discussed earlier in this section, this

angle lies between 46° to 52° for freebase TMBPDM (**Figure 1.15**). Thus, it may be said that the geometry of freebase TMBPDM is highly distorted relative to its metal complex. The organometallic bond (M-C bond) distance in TMBPDM complexes is much larger than the direct M-C bond linkage, but significantly less than the sum of their Vander Waal radii. This hinted the presence of metal-arene interactions. The M-C bond distance is also affected by the electronic properties of TMBPDM systems. For example, when an electron withdrawing group is placed at 11,16- position, the organometallic bond distance was relatively lesser than electron donating substituent. Also, the metal-arene interaction was found to be weaker in TMBPDM compared to *m*-benzoporphyrins.[76] For instance, the organometallic M···C bond distance for TMBPDM Cd(II) complexes are nearly 2.831 Å which is longer than that for Cd(II) *m*-benzoporphyrin complexes viz. 2.716 Å. The authors also introduced the *syn*- and *anti*-conformation in TMBPDM complexes, which are expected to be present in some ratios depending upon the factors stabilizing the conformations. The *syn* form refers to the position of H26 atom (**Figure 1.7**) aligned parallel or in the same direction as axial chloride ion (**Figure 1.15, (i)**), while in *anti*-form H26 atom is aligned opposite to the axial chloride ion (**Figure 1.15, (ii)**).[76]

Besides Group 12, they also reported binuclear and tetranuclear silver (I) TMBPDM complexes. The use of silver nitrate salt for metalation purpose yielded novel dimer and tetramer of TMBPDM silver complexes (**Figure 1.16**). The dimeric TMBPDM-Ag binds together with a weak  $\eta^2$ - type  $\Pi$ -coordination from  $\beta$ -pyrrolic double bond C13=C14 to Ag ion. (**Figure 1.16, a**). In  $\text{Ag}_4$  complex, apart from Ag—Ag bond, the silver ion is reportedly coordinated by Ag-N (pyrrole), nitrate oxygen atoms and 2,6-lutidine to give this unconventional complex (**Figure 1.16, b**). It is noteworthy that the bond distance between Ag—C22 in 2-Ag<sub>2</sub> is significantly shorter relative to all

other metal chloride complexes of TMBPDM. The 2-Ag<sub>4</sub> fetches a usual triangular Ag–Ag–N moiety. The direct Ag–Ag linkage in this cluster is longest among all the crystal structures with Ag–Ag–N core.[76]



\*2: 11,16-bisphenyl-6,6,21,21-tetramethyl-m-benziporphodimethene

\*3: 11,16-bis(4-methylbenzoate)-6,6,21,21-tetramethyl-m-benziporphodimethene

\*4: 11,16-bis(4-nitrophenyl)-6,6,21,21-tetramethyl-m-benziporphodimethene

**Figure 1.14.** Crystal structure of Group 12 metal complexes of *meta*-benziporphodimethene analogues.[76]

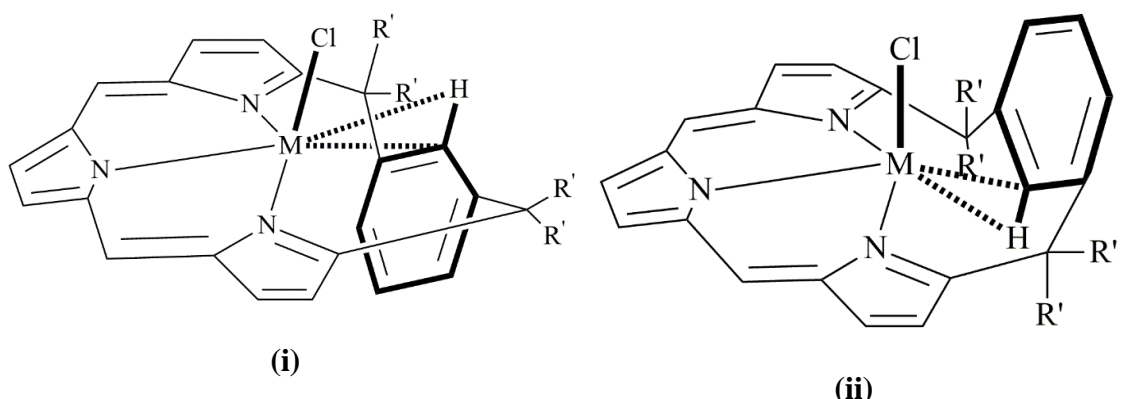


**Figure 1.15.** Representation of (i) *syn*- conformational, and (ii) *anti*- conformational isomers of *meta*-benziporphodimethene.[82]

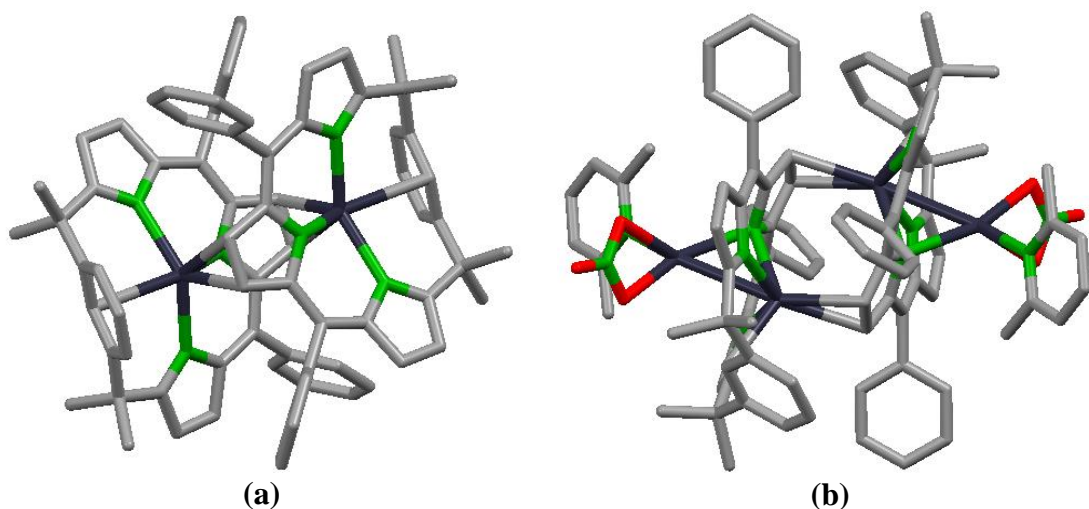


**Figure 1.16.** The structures of dinuclear ( $2\text{-Ag}_2$  TMBPDM, (a)) and tetranuclear ( $2\text{-Ag}_4$  TMBPDM, (b)) complexes, with 11,16- bisphenyl groups (2), omitted for clarity purpose.[76]

#### **1.2.4. NMR shifts in meta-benziporphodimethenes**

Interestingly, the two N-confused isomers exists as dimer forming intermolecular hydrogen bonding through lactam-amide bond. The dimerization was confirmed by taking the concentration dependent NMR spectra in  $\text{CDCl}_3$ . It was observed that with increasing concentration, the outer N-H proton comes more downfield as the extent of hydrogen bonding increases. The impact was observed more dominant in the O-Down isomer than in the O-Up isomer. This shows that O-Down isomers have more effective intermolecular hydrogen bonding than the O-Up isomer.[82]

*meta*-benziporphodimethenes are non-aromatic as the ring current attenuated due to tetrahedral *meso*-carbon atoms. The identical character is noticed in the NMR spectra of these compounds as the chemical shift of inner N-H proton appears at  $\delta \approx 12.0$ , signifying the absence of internal shielding by ring current. The methyl peaks of tetrahedral group appear at  $\approx 1.7$  ppm. The pyrrolic protons were observed at  $\delta \approx 6 - 7$  ppm. The pyrrolic protons 13 and 14 appear as singlets and come at  $\approx 6.0$  ppm, the other pyrrolic protons 9,18 and 8,19 come slightly downfield at around 6.5 ppm and give a ‘ab quartet’ pattern. The aromatic protons of *meso* aryl substituents and of *m*-phenylene ring appear in between  $\approx 7-8$  ppm as multiplet. The C(22)-H comes at around 8.0 ppm and also shows the absence of inner shielding ring current.[83]

**Table 1.2.** Consolidated NMR data for Scheme 1.10.[83]

Compound	N-H (H27,Py <sub>0</sub> )	Ar-H (H26)	Ar-H (C2, C3, C4, C11, C16)	$\beta$ -Py <sub>1</sub> , Py <sub>2</sub> -H (C8, C9, C18, C19)	$\beta$ -Py <sub>0</sub> -H (C13, C14)	OCH <sub>3</sub> (R <sup>2</sup> , R <sup>3</sup> , R <sup>4</sup> )	sp <sup>3</sup> -CH <sub>3</sub> (C6, C21)
1	12.32 (br, s)	7.93(s)	7.24-7.39 (m)	6.81 (ab quartet)	6.15 (s)	---	1.72 (s)
2	12.32 (br, s)	7.94(s)	7.31-7.57 (m)	6.83 (ab quartet)	6.16 (s)	---	1.74 (s)
3	12.16 (br, s)	8.06(s)	7.28-7.41 (m)	6.59 (d) -6.82 (d)	5.86 (s)	---	1.81 (s)
4	12.18 (br, s)	7.97(s)	6.91-7.45 (m)	6.70(d) -6.83 (d)	6.00 (s)	---	1.79 (s)
5	12.08 (br, s)	7.89(s)	7.25-7.34 (m)	6.65 (d)-6.90 (d)	5.98 (s)	---	1.78 (s)
6	12.00 (br, s)	7.92(s)	7.68 (d,4H-ArH), 7.56 (d,4H-ArH), 7.29 (m,3H-ArH)	6.75 (d)-6.85 (d)	6.07 (s)	---	1.75 (s)
7	12.38 (br, s)	7.93(s)	7.44 (d, 4 Ar-H), 7.27-7.32 (m, 3H,2,3,4 Ar-H), 6.95 (d, 4 Ar-H)	6.77 (d) -6.88 (d)	6.30 (s)	3.87 (s)	1.69 (s)
8	12.33 (br, s)	7.92(s)	7.30(q, 3H 2,3,4 Ar-H) + 6.74(s, 4Ar-H)	6.80 (d) -6.95 (d)	6.35 (s)	3.92 (s,6H, para OMe) + 3.83 (s,12H, meta OMe)	1.70 (s)

### 1.2.5. Electronic Structure study

Two major theoretical studies have been reported for *meta*-benzoporphodimethenes by Kumar and co-workers. In 2019, they presented a DFT overview of core-modified *m*-BPDM analogues and their N-confused derivatives consisting  $\gamma$ -lactam ring as discussed above. They primarily intended to study the effect on the geometries and relative energies of *m*-BPDM by varying the positions of N-confused ring and oxygenation at one of the pyrrole rings (**Figure 1.17**).[84] For clarity purpose, the phenyl ring at 11, 16- positions have not been shown in the figure below.

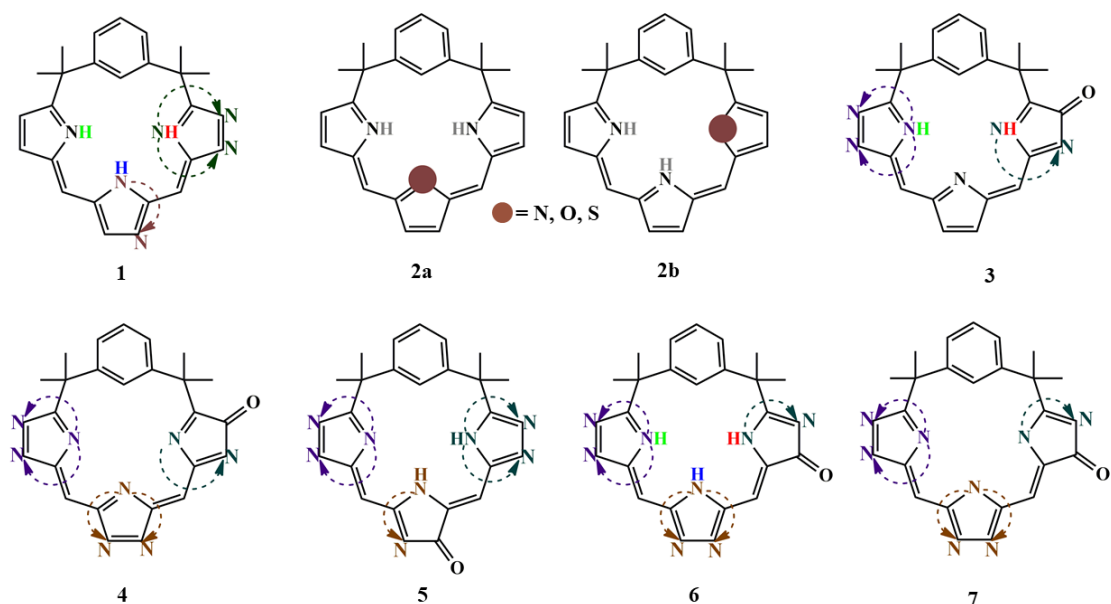


**Figure 1.17.** Overview of TMBPDM analogues studied by Kumar *et. al.*[84]

The tautomer of 1 (in **Scheme 1.9**) and its inverted compounds obtained via single pyrrolic  $\alpha,\alpha$ - to  $\alpha,\beta$ -linkage isomerization has been discussed. The parenthesis of this study has been shown as structure 1 in **Figure 1.17**. The dashed arrows signifies the changes in the position of N atoms, which basically is due to inversion of pyrrole ring. Varied colours of H-atoms in the core illustrates only one H is present in the molecule at a time. The position of H on N atoms (N23, N24, N25) have been jumbled relative

to N atoms. It has been found when H27 is bonded to N24, the molecule is energetically more favourable (**1a**, **Figure 1.18**) compared to when it is attached to N23 and N25 (see **Figure 1.7**). They, thus stated that the inner core H-bonding interactions plays a crucial role in stabilizing the tautomer. Although, the inversion of pyrrole ring leads to increment in relative energy of the molecule, when N23 or N25 are nearer to C11 or C16 centres respectively, the system are said to be more stable by 1.17 kcal/mol than when the respective N atoms are nearer to C6 or C21 centres (or  $sp^3$  hybridised carbon atoms). In other words, N-down configuration is more stable compared to N-up configuration (**1b**, **Figure 1.18**). It has also been stated, N-confused isomers denoted by green dashed arrows in 1, are more favourable than N-confused isomers denoted by brown dashed arrow. As per their results, the inverted pyrrole ring opposite to phenylene ring (pyrrole with N24 atom) either breaks the  $\pi$ -electron delocalisation or nullifies the H-bonding interactions. The comparison of furan and thiophene analogues placed in place of N24 pyrrole ring (**2a** and **2b**, **Figure 1.18**) has also been studied. These modified analogues are said to be more stable due to the presence of O $\cdots$ NH interactions that lowered the energy. The structure with thiophene ring having absence of hydrogen in the inner core are more symmetrical compared to their oxa and aza analogs (**2a**, **2b**, **Figure 1.18**). It has also been showed that thia and oxa analogues having unprotonated pyrrole rings have larger dipole moment than their corresponding aza analogue. Structure 3 in **Figure 1.17** represents isomers with or without inverted pyrrole ring in the presence of O-up oxygenated pyrrole ring in its reduced form, while structure 4, **Figure 1.17** depicts the oxidized form of the same. In the similar fashion, O-down isomers of *meta*-benzoporphodimethene analogues have been compared varying the linkages of

pyrrolic N- and H-atoms, denoted by dashed arrows and colours, respectively, in structure 6 and 7, **Figure 1.17**. As per their research, the O-up isomers are more favourable than O-down (see most stable forms of 3, 4, 6, 7 in **Figure 1.18**). This further explains the reported yield of O-up and O-down isomers discussed in prior section, as 4% and 0.8% yields, respectively. Also, isomers with inner-protonated pyrrole rings are more favourable and have minimum energy than the unprotonated forms. Another sequence of isomers is formed by oxygenation of N24 pyrrole ring in its oxidized and reduced form (Structure 5, **Figure 1.17**). the most stable configuration in this case was found when N24 atom is present adjacent to the oxygenated centre, in the oxidized form of Structure 5 (no inner H present, 5b, **Figure 1.18**). This was explained by the doubly CH $\cdots$ N interactions present in it. While the other tautomers undergo single CH $\cdots$ N interactions. The enhanced stability of these structures was due to the extended  $\pi$ -conjugate systems (12 $\pi$  electrons) and inner H-bonding network, in case of reduced form of structure 5, **Figure 1.17** (5a, **Figure 1.18**).[84]

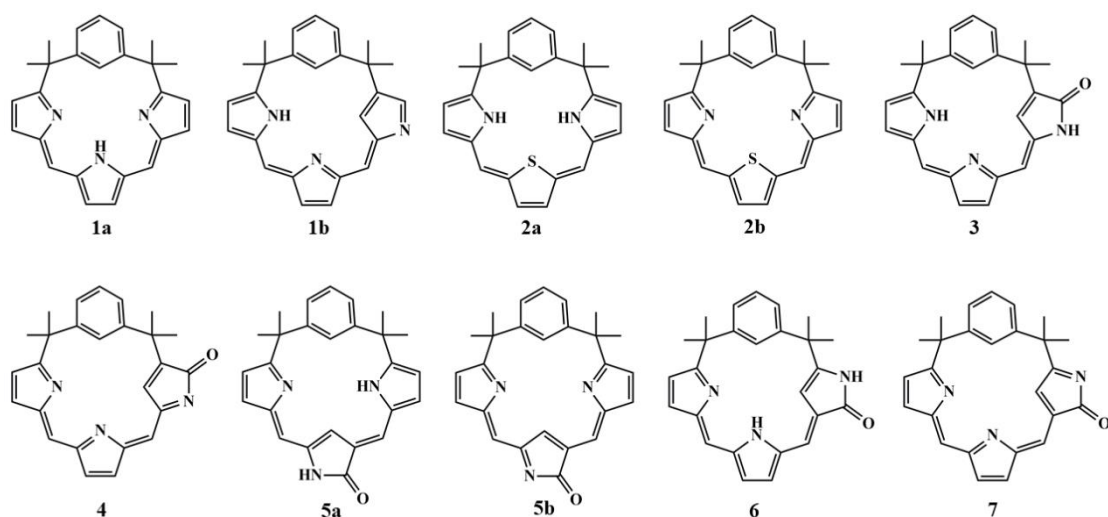


**Figure 1.17.** Most stable structures of all the tautomers discussed in Figure 1.16. [84]

### 1.3. Properties of metalated- *meta*- benziporphodimethene complexes.

#### 1.3.1. Weak Metal-Arene Interaction

One of the most important property of metalated complexes of tetramethyl-*meta*-benzene is the presence of metal-arene interaction in them. *m*-Benziporphodimethenes have the advantage to activate the C-H bond of *meta* phenylene ring in the vicinity of transition metal atoms and that gave it a new horizon to explore. X-ray structure analysis has confirmed the weak metal–arene interactions in cadmium and nickel complexes of *m*-benziporphyrin, with distances shorter than the sum of van der Waals radii.[72] The atypically large intramolecular through-space scalar couplings between the cadmium nucleus and the arene protons in *m*-benziporphyrin Cd(II) complexes as well as the downfield chemical shifts as a result of spin transfer from nickel center to an agostic proton in the paramagnetic *m*-benziporphyrin Ni(II) complexes provide solid supporting evidences for the presence of the metal-arene interaction. Fascinatingly, the strength of the metal-arene interaction is extremely dependent on the conformation of the arene moiety. As in the case of *meta*-benziporphyrins, this kind of interaction not only helps in the activation of phenylene ring but also in the stabilization of metal complexes.[72,76]

#### 1.3.2. Fluorescence enhancement

An important property of these compounds is that they are non-fluorescent in free-base form but turn on fluorescence upon zinc metalation with no background emission.[81,83] The most important part of this finding is that *meta*-benziporphodimethenes act as a specific sensor for zinc ions.[83,86] Very less fluorescence is observed for cadmium and mercury ions comparatively. Since the

fluorescence “switch on” upon zinc metalation and hence this kind of fluorescence comes under the category of “**chelation enhanced fluorescence**” (CHEF). CHEF sensors are mostly based on fluorophores, such as fluorescein,[87,88] dansyl and anthracene, that emits at wavelength shorter than 600 nm. Those sensors which are effective above 600 nm, where background emission is very little, minimizes light induced tissue damages, penetrates better and scatters less in optically diffuse samples. It is interesting to note that these kind of moieties do not form complexes with alkali, alkaline earth and other some transition metals which are physiologically important as shown by Hung and coworkers. They also proved that the stability constant for zinc complexation with *meta*-benzoporphodimethene is greater than the cadmium and mercury respectively and hence,  $Zn^{2+}$  have a tendency to replace  $Cd^{2+}$  and  $Hg^{2+}$  ions from their corresponding complexes.[81]

### **1.3.3. Fluorescence phenomena: Structure co-relation**

It is to be noted that m-benzoporphodimethene is a selective  $Zn^{2+}$  ion sensor and the intensity of fluorescence is comparatively higher than in case of cadmium or mercury. The most important reason for this phenomena is planarity of the macrocycle in the bind state. The free-base macrocycle exists as highly distorted non-planar molecule, but on metalation it has been observed that the tripyrrin moiety becomes planar. The average deviation of the three nitrogen atoms of the tripyrrin plane get reduced from 0.27 Å to 0.10 Å upon metalation. The metal ions in the complex occupy a tetrahedral coordination which involves three nitrogen of tripyrrin moiety and a chlorine which sits at the axial position. It has also been found that the zinc has the least apical deviation of 0.48-0.50 Å from the tripyrrine plane as compared to that of 0.62-0.67 Å for cadmium and 0.70-0.71 Å for mercury, and the orientation of m-phenylene ring in

metal-*m*-benzoporphodimethene changed from 81.4° in Zn-*m*-benzoporphodimethene to 89.3° for Cd and 92.1° for Hg. The data is highly in line with the efficient transfer of electron density from ligand to metal and plots a better resonance tendency in case of zinc as binding metal ion.[76]

#### **1.3.4. Cell-Imaging Applications**

Zinc ions in the human body are involved in various biological processes. Zinc in the human body can be found in bound state with protein as structural cofactors[88] and gene expression regulator.[89] Labile pool of zinc ions may also be developed in the vesicles of neurons. Besides, Zn<sup>2+</sup> is also a chief regulator of the cellular apoptosis,[90] and it is pertinent to severe diseases like Alzheimer's disease[91,92] and Parkinson's disease[93,94] when a disorder of zinc metabolism has occurred. Patients suffering from inflammatory diseases and tumors also show abnormal Zn<sup>2+</sup> concentration in sera and tissues.[65] As both vital roles and toxic influences of Zn<sup>2+</sup> are commonly observed, detection of Zn<sup>2+</sup> may help to reveal its physiological and pathological roles. Thus, a small-sized semiconductor optoelectronic device is needed for a real-time and indicator-free identification of Zn<sup>2+</sup> in liquid medium.

With such commercial application in mind, Hung and co-workers have designed an organic hydrogel film with micron-sized pillar array for real-time and indicator-free recognition of zinc ions in the solution by introducing a fluorescent indicator 11,16-bis(phenyl)-6,6,21,21-tetramethyl-*m*-benz-6,21-porphodimethene in a hydrogel host poly(2-hydroxyethyl methacrylate). High stability and selectivity to Zn<sup>2+</sup> ions is shown by the sensing film. The responsiveness of this film was increased by fabricating a micron-sized pillar array on the surface of the sensing film to increase

the surface area. For  $Zn^{2+}$  concentrations of  $10^{-4}$  M and  $10^{-3}$  M, the response time was estimated around 30s and 3s, respectively.[85]

Recently, Kumar and his coworkers explored these *meta*-benzoporphodimethenes for cellular imaging of zinc ions in MDA-MB-468 breast carcinoma cells and concluded that these molecules are lesser cytotoxic for longer time and can internalize successfully (**Figure 1.19**). The electron releasing and withdrawing group does not impact on internalization. Further, these molecules can be used for sensing intracellular zinc ions. Though, *meta*-benzoporphodimethenes respond to  $Cd^{2+}$  and  $Hg^{2+}$  ions but the concentration of these ions are rarely present in healthy cells so will not cause any interference in imaging of  $Zn^{2+}$  ions in healthy cells.[95] DFT studies were also carried out and suggested the symmetrical geometry of zinc complex of 11,16-bis(2,6 di-fluoro phenyl)-6,6,21,21-tetramethyl-*meta*-benzoporphodimethene and the values are comparable to the earlier reports.[67]

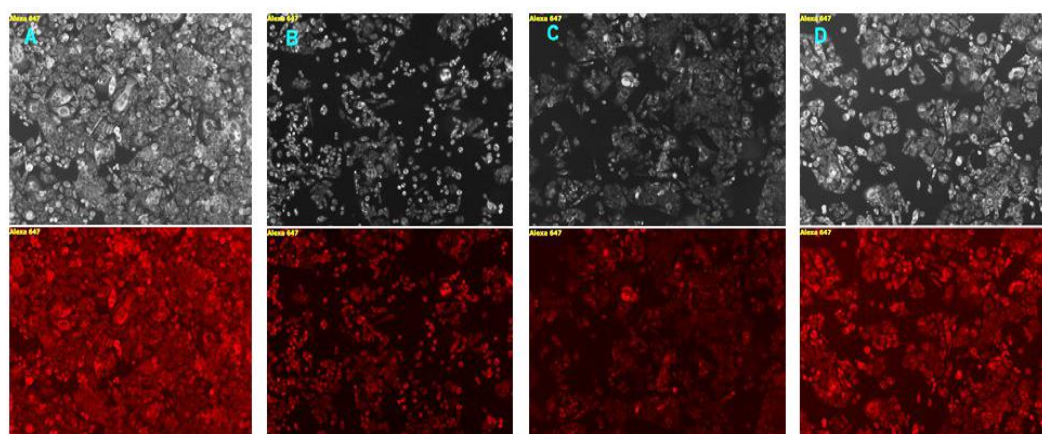


**Figure 1.19.** MDA-MB-468 cells incubated with different *meta*-benzoporphodimethenes and  $Zn^{2+}$  ions for 30 min and respective bright field marked with A-D as well as fluorescence images (just down to its respective bright field image) were captured at 10X objective lens magnification.[96]

## References

- [1] S.D. Straight, G. Kodis, Y. Terazono, M. Hambourger, T.A. Moore, A.L. Moore, D. Gust, Self-regulation of photoinduced electron transfer by a molecular nonlinear transducer, *Nature Nanotechnology.* 3 (2008) 280–283. <https://doi.org/10.1038/nnano.2008.97>.
- [2] S.D. Starnes, S. Arungundram, C.H. Saunders, Anion sensors based on  $\beta,\beta'$ -disubstituted porphyrin derivatives, *Tetrahedron Letters.* 43 (2002) 7785–7788. [https://doi.org/10.1016/S0040-4039\(02\)01828-2](https://doi.org/10.1016/S0040-4039(02)01828-2).
- [3] V.S.Y. Lin, S.G. DiMagno, M.J. Therien, Highly conjugated, acetylenyl bridged porphyrins: New models for light-harvesting antenna systems, *Science.* 264 (1994) 1105–1111. <https://doi.org/10.1126/science.8178169>.
- [4] J. Králová, Z. Kejík, T. Bříza, P. Poučková, A. Král, P. Martásek, V. Král, Porphyrin - Cyclodextrin conjugates as a nanosystem for versatile drug delivery and multimodal cancer therapy, *Journal of Medicinal Chemistry.* 53 (2010) 128–138. <https://doi.org/10.1021/jm9007278>.
- [5] G. Jori, C. Fabris, M. Soncin, S. Ferro, O. Coppelotti, D. Dei, L. Fantetti, G. Chiti, G. Roncucci, Photodynamic therapy in the treatment of microbial infections: Basic principles and perspective applications, *Lasers in Surgery and Medicine.* 38 (2006) 468–481. <https://doi.org/10.1002/lsm.20361>.
- [6] T. Ozawa, R.A. Santos, K.R. Lamborn, W.F. Bauer, M.S. Koo, S.B. Kahl, D.F. Deen, In vivo evaluation of the boronated porphyrin TABP-1 in U-87 MG intracerebral human glioblastoma xenografts., *Molecular Pharmaceutics.* 1 (2004) 368–374. <https://doi.org/10.1021/mp049933i>.
- [7] R.J. Hift, P.N. Meissner, M.R. Moore, *The Porphyrin Handbook,* 2000. <https://doi.org/10.1016/B978-0-08-092388-8.50018-2>.

- [8] R.G. Karl M. Kadish, Kevin M. Smith, *Handbook of Porphyrin Science with Applications to Chemistry, Physics, Materials Science, Engineering, Biology and Medicine*, Volume 6 N, World Scientific, London, 2010.
- [9] David Dolphin, *The Porphyrins*, Volume 6, Academic Press, New York, 1978.  
<https://doi.org/10.1016/b978-0-12-220103-5.50014-3>.
- [10] M. Yedukondalu, M. Ravikanth, Core-modified porphyrin based assemblies, *Coordination Chemistry Reviews*. 255 (2011) 547–573. <https://doi.org/10.1016/j.ccr.2010.10.039>.
- [11] R.G. Karl M. Kadish, Kevin M. Smith, *The Porphyrin Handbook*, Volume 6 A, Academic Press, 2000.
- [12] I. Gupta, M. Ravikanth, Recent developments in heteroporphyrins and their analogues, *Coordination Chemistry Reviews*. 250 (2006) 468–518.  
<https://doi.org/10.1016/j.ccr.2005.10.010>.
- [13] P.J. Chmielewski, L. Latos-graiynski, M.M. Olmstead, A.L. Balch, Nickel Complexes of 21-Oxaporphyrin and 21 , 23-Dioxaporphyrin, *Chemistry - A European Journal*. 3 (1997) 268–278. <https://doi.org/https://doi.org/10.1002/chem.19970030216>.
- [14] P.J. Chmielewski, Synthesis and Characterization of a Directly Linked N-Confused Porphyrin Dimer, *Angewandte Chemie*. 116 (2004) 5773–5776.  
<https://doi.org/10.1002/ange.200461361>.
- [15] M. Siczek, P.J. Chmielewski, Synthesis, Characterization, and Chirality of Dimeric N-Confused Porphyrin-Zinc Complexes: Toward the Enantioselective Synthesis of Bis(porphyrinoid) Systems, *Angewandte Chemie*. 119 (2007) 7576–7580. <https://doi.org/10.1002/ange.200701860>.

- [16] P.J. Chmielewski, Synthesis and Characterization of a Cyclic Bis-silver(I) Assembly of Four 2-Aza-21-carbaporphyrinatosilver(III) Subunits, *Angewandte Chemie.* 117 (2005) 6575–6578. <https://doi.org/10.1002/ange.200502208>.
- [17] T. Ishizuka, A. Osuka, H. Furuta, Inverted N-confused porphyrin dimer, *Angewandte Chemie - International Edition.* 43 (2004) 5077–5081. <https://doi.org/10.1002/anie.200460017>.
- [18] T. Ishizuka, S. Ikeda, M. Togano, I. Yoshida, Y. Ishikawa, A. Osuka, H. Furuta, Substitution, dimerization, metalation, and ring-opening reactions of N-fused porphyrins, *Tetrahedron.* 64 (2008) 4037–4050. <https://doi.org/10.1016/j.tet.2008.02.041>.
- [19] A. Ulman, J. Manassen, F. Frolow, D. Rabinovich, Synthesis of new tetraphenylporphyrin molecules containing heteroatoms other than nitrogen. III. Tetraphenyl-21-tellura-23-thiaporphyrin: an internally-bridged porphyrin, *Journal of American Chemical Society.* 97 (1975) 6540–6544. [https://doi.org/10.1016/S0040-4039\(01\)94699-4](https://doi.org/10.1016/S0040-4039(01)94699-4).
- [20] J. Latos-Grażyński, Lechosław, Lisowski, 21-Thiatetra-p -tolylporphyrin and Its Copper(I) Bicarbonate Complex. Structural Effects of Copper-Thiophehe Binding, *Journal of American Chemical Society.* 109 (1987) 4428–4429.
- [21] R.D. Ulman, Abraham, Manassen, J., Frolow, F., Synthesis of new tetraphenylporphyrin molecules containing heteroatoms other than nitrogen. iii. tetraphenyl-11-tellura-23-thiaporphyrin: an internally-bridged porphyrin, *Tetrahedron Letters.* 19 (1978) 1885–1886. [https://doi.org/10.1016/S0040-4039\(01\)94699-4](https://doi.org/10.1016/S0040-4039(01)94699-4).
- [22] L. Latos- Grażyński, E. Pacholska, P.J. Chmielewski, M.M. Olmstead, A.L. Balch, Alteration of the Reactivity of a Tellurophene Within a Core- Modified Porphyrin Environment: Synthesis and Oxidation of 21- Telluraporphyrin, *Angewandte Chemie International Edition in English.* 34 (1995) 2252–2254. <https://doi.org/10.1002/anie.199522521>.

- [23] R.D. Ulman, Abraham, Manassen, J., Frolow, F., Synthesis of new tetraphenylporphyrin molecules containing heteroatoms other than nitrogen: II. Tetraphenyl-21-selena-23-thiaporphyrin and tetraphenyl-21,23-diselenaporphyrin, *Tetrahedron Letters.* 19 (1978) 167–170. [https://doi.org/10.1016/S0040-4039\(01\)85074-7](https://doi.org/10.1016/S0040-4039(01)85074-7).
- [24] L. Latos-Grażyński, E. Pacholska, P.J. Chmielewski, M.M. Olmstead, A.L. Balch, 5,20-Diphenyl-10,15-bis(p-tolyl)-21-selenaporphyrin and Its Nickel(II) Complexes, *Inorganic Chemistry.* 35 (1996) 566–573. <https://doi.org/10.1021/ic950329z>.
- [25] Y. Matano, T. Nakabuchi, T. Miyajima, H. Imahori, Phosphole-containing hybrid calixpyrroles: New multifunctional macrocyclic ligands for platinum(II) ions, *Organometallics.* 25 (2006) 3105–3107. <https://doi.org/10.1021/om060300a>.
- [26] Y. Matano, T. Nakabuchi, T. Miyajima, H. Imahori, H. Nakano, Synthesis of a phosphorus-containing hybrid porphyrin, *Organic Letters.* 8 (2006) 5713–5716. <https://doi.org/10.1021/ol0622763>.
- [27] Y. Matano, M. Nakashima, T. Nakabuchi, H. Imahori, S. Fujishige, H. Nakano, Monophosphaporphyrins: Oxidative  $\pi$ -extension at the peripherally fused carbocycle of the phosphaporphyrin ring, *Organic Letters.* 10 (2008) 553–556. <https://doi.org/10.1021/ol7029118>.
- [28] Y. Matano, H. Imahori, Phosphole-containing calixpyrroles, calixphyrins, and porphyrins: Synthesis and coordination chemistry, *Accounts of Chemical Research.* 42 (2009) 1193–1204. <https://doi.org/10.1021/ar900075e>.
- [29] Z. Gross, I. Saltsman, R.P. Pandian, C.M. Barzilay, The first metal chelation by a neutral porphyrin analogue, *Tetrahedron Letters.* 38 (1997) 2383–2386. [https://doi.org/10.1016/S0040-4039\(97\)00357-2](https://doi.org/10.1016/S0040-4039(97)00357-2).

- [30] A. Kumar, I. Goldberg, M. Botoshansky, Y. Buchman, Z. Gross, Oxygen atom transfer reactions from isolated (Oxo)manganese(V) corroles to sulfides, *Journal of the American Chemical Society.* 132 (2010) 15233–15245. <https://doi.org/10.1021/ja1050296>.
- [31] J. Bendix, H.B. Gray, G. Golubkov, Z. Gross, High-field (high-frequency) EPR spectroscopy and structural characterization of a novel manganese(III) corrole, *Chemical Communications.* (2000) 1957–1958. <https://doi.org/10.1039/b006299p>.
- [32] J.H. Choy, S.Y. Kwak, Y.J. Jeong, J.S. Park, Epoxidation catalysis by a manganese corrole and isolation of an oxomanganese(V) corrole, *Angewandte Chemie - International Edition.* 39 (2000) 4045–4047. [https://doi.org/10.1002/1521-3773\(20001117\)39:22<4045::AID-ANIE4045>3.0.CO;2-P](https://doi.org/10.1002/1521-3773(20001117)39:22<4045::AID-ANIE4045>3.0.CO;2-P).
- [33] G. Golubkov, J. Bendix, H.B. Gray, A. Mahammed, I. Goldberg, A.J. DiBilio, Z. Gross, High-Valent Manganese Corroles and the First Perhalogenated Metallocorrole Catalyst, *Angewandte Chemie - International Edition.* 40 (2001) 2132–2134. [https://doi.org/10.1002/1521-3773\(20010601\)40:11<2132::AID-ANIE2132>3.0.CO;2-5](https://doi.org/10.1002/1521-3773(20010601)40:11<2132::AID-ANIE2132>3.0.CO;2-5).
- [34] Z. Gross, N. Galili, I. Saltsman, The first direct synthesis of corroles from pyrrole, *Angewandte Chemie - International Edition.* 38 (1999) 1427–1429. [https://doi.org/10.1002/\(SICI\)1521-3773\(19990517\)38:10<1427::AID-ANIE1427>3.0.CO;2-1](https://doi.org/10.1002/(SICI)1521-3773(19990517)38:10<1427::AID-ANIE1427>3.0.CO;2-1).
- [35] N. Galili, Z. Gross, N-Substituted Corroles : A Novel Class of Chiral Ligands\*, *Angewandte Chemie (International Ed. in English).* 38 (1999) 2366–2369.
- [36] Z. Gross, L. Simkhovich, N. Galili, T. Israel, First catalysis by corrole metal complexes : epoxidation , hydroxylation , and cyclopropanation The first ever application of corroles shows that their metal complexes are good catalysts , almost as potent as the corresponding metalloporphyrins in the oxy, *Tetrahedron.* (1999) 599–600.

- [37] L. Simkhovich, A. Mahammed, I. Goldberg, Z. Gross, Synthesis and characterization of germanium, tin, phosphorus, iron, and rhodium complexes of tris(pentafluorophenyl)corrole, and the utilization of the iron and rhodium corroles as cyclopropanation catalysts, *Chemistry - A European Journal.* 7 (2001) 1041–1055. [https://doi.org/10.1002/1521-3765\(20010302\)7:5<1041::AID-CHEM1041>3.0.CO;2-8](https://doi.org/10.1002/1521-3765(20010302)7:5<1041::AID-CHEM1041>3.0.CO;2-8).
- [38] L. Simkhovich, Z. Gross, Iron(IV) corroles are potent catalysts for aziridination of olefins by Chloramine-T, *Tetrahedron Letters.* 42 (2001) 8089–8092. [https://doi.org/10.1016/S0040-4039\(01\)01717-8](https://doi.org/10.1016/S0040-4039(01)01717-8).
- [39] A. Mahammed, Z. Gross, Iron and Manganese Corroles Are Potent Catalysts for the Decomposition of Peroxynitrite, *Angewandte Chemie.* 118 (2006) 6694–6697. <https://doi.org/10.1002/ange.200601399>.
- [40] I. Aviv, Z. Gross, Corrole-based applications, *Chemical Communications.* (2007) 1987–1999. <https://doi.org/10.1039/b618482k>.
- [41] A.H. Iris, Z. Gross, Aura of corroles, *Chemistry - A European Journal.* 15 (2009) 8382–8394. <https://doi.org/10.1002/chem.200900920>.
- [42] S.K. Pushpan, S. Venkatraman, V.G. Anand, J. Sankar, H. Rath, T.K. Chandrashekhar, Inverted porphyrins and expanded porphyrins: An overview, *Proceedings of the Indian Academy of Sciences: Chemical Sciences.* 114 (2002) 311–338. <https://doi.org/10.1007/BF02703823>.
- [43] J.L. Sessler, D. Seidel, Synthetic Expanded Porphyrin Chemistry, *Angewandte Chemie - International Edition.* 42 (2003) 5134–5175. <https://doi.org/10.1002/anie.200200561>.
- [44] V.J. Bauer, D.L.J. Clive, M.M. King, D. Dolphin, F.L. Harris, J. Loder, S.W.C. Wang, J.B. Paine, R.B. Woodward, Sapphyrins: Novel Aromatic Pentapyrrolic Macrocycles, *Journal of the American Chemical Society.* 105 (1983) 6429–6436. <https://doi.org/10.1021/ja00359a012>.

- [45] M. J. Broadhurst and R. Grigg, The Synthesis of 22 =-Electron Macrocycles. Sapphyrins and Related Compounds, Journal of the Chemical Society, Perkin Transactions 1. 1 (1972) 2111–2116. <https://doi.org/10.1039/P19720002111>.
- [46] J.L. Sessler, J.M. Davis, V. Lynch, Synthesis and characterization of a stable smaragdyrin isomer, Journal of Organic Chemistry. 63 (1998) 7062–7065. <https://doi.org/10.1021/jo981019b>.
- [47] Hans Rexhausen and Albert Gossauer, The Synthesis of a New 22 pi-Electron Macrocycle: Pentaphyrin, J. Chem. Soc., Chem. Commun. (1983) 275–275. <https://doi.org/10.1039/C39830000275>.
- [48] A. Gossauer, SYNTHESES OF SOME UNUSUAL POLYPYRROLE MACROCYCLES, Bull. SOC. Chim. Belg. 92 (1983) 793–795. <https://doi.org/10.1002/bscb.19830920905>.
- [49] A. Gossauer, N. Engel, Chlorophyll catabolism- structures , mechanisms , conversions, Journal of Photochemistry and Photobiology B: Biology. 32 (1996) 141–151. [https://doi.org/10.1016/1011-1344\(95\)07257-8](https://doi.org/10.1016/1011-1344(95)07257-8).
- [50] J.L. Sessler, S.J. Weghorn, Y. Hiseada, V. Lynch, Hexaalkyl Terpyrrole: A New Building Block for the Preparation of Expanded Porphyrins, Chemistry – A European Journal. 1 (1995) 56–67. <https://doi.org/10.1002/chem.19950 010110>.
- [51] E. Vogel, M. Broring, J. Fink, D. Rosen, H. Schmickler, J. Lex, K.W.K. Chan, Y. Wu, A. Dietmar, M. Nendel, K.N. Houk, From Porphyrin Isomers to octapyrrolic “Figure Eight” Macrocycles, Angewandte Chemie (International Ed. in English). 34 (1995) 2511–2514. <https://doi.org/10.1002/anie.199525111>.
- [52] M. Broring, J. Jendrny, L. Zander, H. Schmickler, J. Lex, Y. Wu, M. Nendel, J. Chen, D.A. Plattner, W.R. Roth, Octaphyrin-(1.0.1.0.1.0.1.0), Angewandte Chemie. 107 (1995) 2709–2711. <https://doi.org/10.1002/anie.199525151>.

- [53] A. Werner, M. Michels, L. Zander, J. Lex, E. Vogel, “Figure eight” cyclooctapyrroles: Enantiomeric separation and determination of the absolute configuration of a binuclear metal complex, *Angewandte Chemie - International Edition*. 38 (1999) 3650–3653. [https://doi.org/10.1002/\(SICI\)1521-3773\(19991216\)38:24<3650::AID-ANIE3650>3.0.CO;2-F](https://doi.org/10.1002/(SICI)1521-3773(19991216)38:24<3650::AID-ANIE3650>3.0.CO;2-F).
- [54] J.L. Sessler, S.J. Weghorn, T. Morishima, M. Rosingana, V. Lynch, V. Lee, Rosarin: A New, Easily Prepared Hexapyrrolic Expanded Porphyrin, *Journal of the American Chemical Society*. 114 (1992) 8306–8307. <https://doi.org/10.1021/ja00047a061>.
- [55] J.L. Sessler, T. Morishima, V. Lynch, Rubyrin: A New Hexapyrrolic Expanded Porphyrin, *Angewandte Chemie International Edition in English*. 30 (1991) 977–980. <https://doi.org/10.1002/anie.199109771>.
- [56] J.A.I. Douglas C. Miller, Martin R. Johnson, John J. Becker, Synthesis and Characterization of the new 22- $\pi$ -Aromatic Furan containing Macrocycle, “Ozaphyrin,” *Journal of Heterocyclic Chemistry*. 30 (1993) 1485–1490. <https://doi.org/https://doi.org/10.1002/jhet.5570300604>.
- [57] D.C. Miller, M.R. Johnson, J.A. Ibers, Synthesis and Characterization of New “Expanded” Thiophene- and Furan-Containing Macrocycles, *Journal of Organic Chemistry*. 59 (1994) 2877–2879. <https://doi.org/10.1021/jo00089a035>.
- [58] M.R. Johnson, D.C. Miller, K. Bush, J.J. Becker, J.A. Ibers, Synthesis and Characterization of a New 26 $\pi$ -Aromatic Thiophene-Containing Macroyclic Ligand, *Journal of Organic Chemistry*. 57 (1992) 4414–4417. <https://doi.org/10.1021/jo00042a019>.
- [59] J.L. Sessler, D. Seidel, V. Lynch, Synthesis of [28]heptaphyrin(1.0.0.1.0.0.0) and [32]Octaphyrin(1.0.0.0.1.0.0.0) via a directed oxidative ring closure: The first expanded porphyrins containing a quaterpyrrole subunit [18], *Journal of the American Chemical Society*. 121 (1999) 11257–11258. <https://doi.org/10.1021/ja992934x>.

- [60] J.L. Sessler, S.J. Weghorn, V. Lynch, M.R. Johnson, Turcasarin, the Largest Expanded Porphyrin to Date, *Angewandte Chemie International Edition in English*. 33 (1994) 1509–1512. <https://doi.org/10.1002/anie.199415091>.
- [61] J. Setsune, Y. Katakami, N. Iizuna, [48]Dodecaphyrin-(1.0.1.0.1.0.1.0.1.0.1.0) and [64]Hexadecaphyrin-(1.0.1.0.1.0.1.0.1.0.1.0.1.0): The Largest Cyclopolyprrols, *Journal of American Chemical Society*. 121 (1999) 8957–8958. <https://doi.org/10.1021/ja991669c>.
- [62] P.J. Chmielewski, L. Latos-grazynski, K. Rachlewicz, T. Glowiacz, Tetra-p-tolylporphyrin with an Inverted Pyrrole Ring: A Novel Isomer of Porphyrin, *Angewandte Chemie (International Ed. in English)*. 33 (1994) 779–781. <https://doi.org/https://doi.org/10.1002/anie.199407791>.
- [63] M.C. S. Arnoff, The Porphyrin-like products of the reaction of pyrrole with benzaldehyde, *Journal of Organic Chemistry*. 8 (1943) 205–223. <https://doi.org/https://doi.org/10.1021/jo01191a002>.
- [64] C.F. Koelsch, H.J. Richter, The Synthesis of Bis-2,2'-(1,3-diphenylindenol-3), *Journal of the American Chemical Society*. 57 (1935) 2010. <https://doi.org/10.1021/ja01313a509>.
- [65] P. Rothemund, A new porphyrin synthesis. The Synthesis of Porphin, *J. Am. Chem. Soc.* 157 (1936) 625–627.
- [66] A.D. Adler, F.R. Longo, W. Shergalis, Mechanistic Investigations of Porphyrin Syntheses. I. Preliminary Studies on ms-Tetraphenylporphin, *Journal of the American Chemical Society*. 86 (1964) 3145–3149. <https://doi.org/10.1021/ja01069a035>.
- [67] J.B. Kim, J.J. Leonard, F.R. Longo, A Mechanistic Study of the Synthesis and Spectral Properties of mero-Tetraarylporphyrins, *Journal of the American Chemical Society*. 94 (1972) 3986–3992. <https://doi.org/10.1021/ja00766a056>.

- [68] A.D. Adleb, F.R. Longo, J.D. Finarelli, J. Goldmacher, J. Assour, L. Korsakoff, A Simplified Synthesis for Meso-Tetraphenylporphine, *Journal of Organic Chemistry*. 32 (1967) 476. <https://doi.org/10.1021/jo01288a053>.
- [69] J.S. Lindsey, I.C. Schreiman, H.C. Hsu, P.C. Kearney, A.M. Marguerettaz, Rothemund and Adler-Longo Reactions Revisited: Synthesis of Tetraphenylporphyrins under Equilibrium Conditions, *Journal of Organic Chemistry*. 52 (1987) 827–836. <https://doi.org/10.1021/jo00381a022>.
- [70] K. Berlin, E. Breitmaier, Benziporphyrin, a Benzene- Containing, Nonaromatic Porphyrin Analogue, *Angewandte Chemie International Edition in English*. 33 (1994) 1246–1247. <https://doi.org/10.1002/anie.199412461>.
- [71] H. Furuta, T. Asano, T. Ogawa, “N-Confused Porphyrin”: A New Isomer of Tetraphenylporphyrin, *Journal of the American Chemical Society*. 116 (1994) 767–768. <https://doi.org/10.1021/ja00081a047>.
- [72] M. Stępień, L. Latos-Grażyński, L. Szterenberg, J. Panek, Z. Latajka, Cadmium(II) and Nickel(II) Complexes of Benziporphyrins. A Study of Weak Intramolecular Metal-Arene Interactions, *Journal of the American Chemical Society*. 126 (2004) 4566–4580. <https://doi.org/10.1021/ja039384u>.
- [73] G.P. Moss, Nomenclature of Tetrapyrroles, 1979. <https://doi.org/10.1351/pac199668101919>.
- [74] G.P. Moss, Nomenclature of tetrapyrroles: Recommendations 1986, *European Journal of Biochemistry*. 178 (1988) 277–328. <https://doi.org/10.1111/j.1432-1033.1988.tb14453.x>.
- [75] M. Stępień, L. Latos-Grażyński, Benziporphyrins: Exploring arene chemistry in a macrocyclic environment, *Accounts of Chemical Research*. 38 (2005) 88–98. <https://doi.org/10.1021/ar040189+>.

- [76] G.F. Chang, C.H. Wang, H.C. Lu, L.S. Kan, I. Chao, W.H. Chen, A. Kumar, L. Lo, M.A.C. Dela Rosa, C.H. Hung, Factors that regulate the conformation of m-benziporphodimethene complexes: Agostic metal-arene interaction, hydrogen bonding, and  $\tilde{\text{I}} \cdot 2\pi$  coordination, *Chemistry - A European Journal*. 17 (2011) 11332–11343. <https://doi.org/10.1002/chem.201100780>.
- [77] M. Stępień, L. Latos-Grażyński, Tetraphenylbenzoporphyrin - A ligand for organometallic chemistry, *Chemistry - A European Journal*. 7 (2001) 5113–5117. [https://doi.org/10.1002/1521-3765\(20011203\)7:23<5113::AID-CHEM5113>3.0.CO;2-V](https://doi.org/10.1002/1521-3765(20011203)7:23<5113::AID-CHEM5113>3.0.CO;2-V).
- [78] M. Stępień, L. Latos-Grażyński, Tetraphenyl-p-benzoporphyrin: A carbaporphyrinoid with two linked carbon atoms in the coordination core, *Journal of the American Chemical Society*. 124 (2002) 3838–3839. <https://doi.org/10.1021/ja017852z>.
- [79] C.H. Hung, C.Y. Lin, P.Y. Lin, Y.J. Chen, Synthesis and crystal structure of core-modified benzoporphyrin: Thia-p-benzoporphyrin, *Tetrahedron Letters*. 45 (2004) 129–132. <https://doi.org/10.1016/j.tetlet.2003.10.090>.
- [80] T.D. Lash, Oxybenzoporphyrin, a Fully Aromatic Semiquinone Porphyrin Analog with Pathways for  $18\pi$ - Electron Delocalization, *Angewandte Chemie International Edition in English*. 34 (1995) 2533–2535. <https://doi.org/10.1002/anie.199525331>.
- [81] C.H. Hung, G.F. Chang, A. Kumar, G.F. Lin, L.Y. Luo, W.M. Ching, E. Wei-Guang Diau, m-Benziporphodimethene: A new porphyrin analogue fluorescence zinc(II) sensor, *Chemical Communications*. (2008) 978–980. <https://doi.org/10.1039/b714412a>.
- [82] G.F. Chang, A. Kumar, W.M. Ching, H.W. Chu, C.H. Hung, Tetramethyl-m-benziporphodimethene and isomeric  $\alpha,\beta$ -unsaturated  $\gamma$ lactam embedded N-confused tetramethyl-m-benziporphodimethenes, *Chemistry - An Asian Journal*. 4 (2009) 164–173. <https://doi.org/10.1002/asia.200800279>.

- [83] R.K. Sharma, L.K. Gajanan, M.S. Mehata, F. Hussain, A. Kumar, Synthesis, characterization and fluorescence turn-on behavior of new porphyrin analogue: meta-benziporphodimethenes, *Spectrochimica Acta - Part A: Molecular and Biomolecular Spectroscopy.* 169 (2016) 58–65. <https://doi.org/10.1016/j.saa.2016.06.020>.
- [84] A. Kumar, C.H. Hung, S. Rana, M.M. Deshmukh, Study on the structure, stability and tautomerisms of meta-benziporphodimethene and N-Confused isomers containing  $\gamma$ -lactam ring, *Journal of Molecular Structure.* 1187 (2019) 138–150. <https://doi.org/10.1016/j.molstruc.2019.03.064>.
- [85] Y.C. Chao, Y.S. Huang, H.P. Wang, S.M. Fu, C.H. Huang, Y.C. Liang, W.C. Yang, Y.S. Huang, G.F. Chang, H.W. Zan, H.F. Meng, C.H. Hung, C.C. Fu, An organic hydrogel film with micron-sized pillar array for real-time and indicator-free detection of  $Zn^{2+}$ , *Organic Electronics.* 12 (2011) 1899–1902. <https://doi.org/10.1016/j.orgel.2011.07.001>.
- [86] P. Chavez-Crooker, N. Garrido, G.A. Ahearn, Copper transport by lobster hepatopancreatic epithelial cells separated by centrifugal elutriation: Measurements with the fluorescent dye Phen Green, *Journal of Experimental Biology.* 204 (2001) 1433–1444.
- [87] W. Breuer, S. Epsztejn, P. Millgram, I.Z. Cabantchik, Transport of iron and other transition metals into cells as revealed by a fluorescent probe, *American Journal of Physiology - Cell Physiology.* 268 (1995). <https://doi.org/10.1152/ajpcell.1995.268.6.c1354>.
- [88] E.H. Cox, G.L. McLendon, Zinc-dependent protein folding, *Current Opinion in Chemical Biology.* 4 (2000) 162–165. [https://doi.org/10.1016/S1367-5931\(99\)00070-8](https://doi.org/10.1016/S1367-5931(99)00070-8).
- [89] G.K. Andrews, Cellular zinc sensors: MTF-1 regulation of gene expression, *BioMetals.* 14 (2001) 223–237. <https://doi.org/10.1023/A:1012932712483>.

- [90] A.Q. Truong-Tran, J. Carter, R.E. Ruffin, P.D. Zalewski, The role of zinc in caspase activation and apoptotic cell death, *BioMetals.* 14 (2001) 315–330. <https://doi.org/10.1023/A:1012993017026>.
- [91] M.P. Cuajungco, G.J. Lees, Zinc and Alzheimer's disease: Is there a direct link?, *Brain Research Reviews.* 23 (1997) 219–236. [https://doi.org/10.1016/S0165-0173\(97\)00002-7](https://doi.org/10.1016/S0165-0173(97)00002-7).
- [92] C. Devirgiliis, P.D. Zalewski, G. Perozzi, C. Murgia, Zinc fluxes and zinc transporter genes in chronic diseases, *Mutation Research - Fundamental and Molecular Mechanisms of Mutagenesis.* 622 (2007) 84–93. <https://doi.org/10.1016/j.mrfmmm.2007.01.013>.
- [93] D.T. Dexter, A. Carayon, F. Javoy-agid, Y. Agid, F.R. Wells, S.E. Daniel, A.J. Lees, P. Jenner, C.D. Marsden, Alterations in the levels of iron, ferritin and other trace metals in parkinson's disease and other neurodegenerative diseases affecting the basal ganglia, *Brain.* 114 (1991) 1953–1975. <https://doi.org/10.1093/brain/114.4.1953>.
- [94] G.A. Qureshi, A.A. Qureshi, S.A. Memon, S.H. Parvez, Impact of selenium, iron, copper and zinc in on/off Parkinson's patients on L-dopa therapy, *Journal of Neural Transmission, Supplement.* (2006) 229–236. [https://doi.org/10.1007/978-3-211-33328-0\\_24](https://doi.org/10.1007/978-3-211-33328-0_24).
- [95] R.K. Sharma, A. Maurya, P. Rajamani, M.S. Mehata, A. Kumar, meta-Benziporphodimethenes: New Cell-Imaging Porphyrin Analogue Molecules, *ChemistrySelect.* 1 (2016) 3502–3509. <https://doi.org/10.1002/slct.201600812>.

## CHAPTER 2

### SCOPE OF THE WORK

---

The porphyrinoid family has extensively expanded over the years. The first ever report regarding computational studies of porphyrin systems was presented by G. M. Maggiora in the year 1964.[1] Several modifications on the porphyrin molecule leading to formation of new compounds, were also being discovered alongside. Corrole, first reported by Johnson and Kay in the year 1965, is a contracted porphyrin system.[2] The chemistry of corrole have been vastly investigated since then. Although, in terms of computational studies, corroles are less diverse than porphyrins.[3] Not only corroles, the expanded, hetero-atom substituted and various other analogues of porphyrins have been intensely investigated over time.[4,5] Computational chemistry acts as a bridge between the experimental and theoretical studies of any system. This bridging have been done for porphyrins and corroles majorly. Other analogues of porphyrinoid family still have a great scope for being investigated using various computational methods.

The new carbaporphyrinoid system- *meta*-benzoporphodimethene was introduced 18 years ago. The recent advancements in *meta*-benzoporphodimethenes (*m*-BPDM) have proved that the compound must gather great importance owing to its wide range of applications as a chemosensor.[6-12] After a thorough literature review, it was found that despite the outstanding properties exhibited by *m*-BPDM, the compound reached out only to a small audience.[13,14] This means, due to the low yield and rapid oxidation tendency the molecule fails to be meticulously investigated. For this reason, the current work focuses on finding out the possible factors that could enhance the stability and yield of this unique class of carbaporphyrinoid systems.

Sometimes, experimental methods are not sufficient to answer many crucial steps resulting in a number of chemical and biological processes. Also, computational chemistry is said to be a great tool to study the insights of a reaction even before one performs it in a laboratory. The advancements in technology has opened doors for theoretical chemists to analyse the systems under study, computationally and check the feasibility of the reactions beforehand.

The term 'hydrogen bond' (H-bond) seems to have surfaced around 1930 from the works of Pauling [15] and Huggins.[16,17] However, there are many studies before Pauling and Huggins which suggests the formation of weak interactions involving H-atom. For instance, the dimeric association of molecules with hydroxyl groups was suggested by Nernst in 1892.[18] The term "Nebenvalenz" by Werner [19] and "weak union" by Moore and Winmill [20] indicated the formation of this non-covalent interaction. Latimer and Rodebush[21] suggested that the hydrogen nucleus in an aqueous solution of amines is held jointly by two octets, constituting a weak bond. Although term H-bond gained popularity with Pauling's famous publication: *The nature of chemical bond*,[15] Huggins[22] claimed that he was the first to propose the term 'H-bond' in 1919. The definition by Pimentel and McClellan[23] is very similar to that by IUPAC[24] which states that "the H-bond is an attractive interaction between a H atom from a molecule or a molecular fragment X–H in which X is more electronegative than H, and an atom or a group of atoms in the same or a different molecule, in which there is an evidence of bond formation." [24] In general, the H-bond is denoted X-H $\cdots$ Y where X and Y are the two electronegative atoms such as N, O, F, Cl, etc. These type of interaction are termed as classical or conventional H-bonds. The strength and existence of this bond greatly depends on the Lewis acidity

of X-H and on the Lewis basicity of acceptor Y atom.[25-27] On the contrary, H-bonds having X = C as an unconventional donor also exists. These are denoted as C-H...Y bond and called as the non-conventional H-bonds. Here, Y atom is more electron rich than C atom. The most familiar H-bond acceptors (Y atom) in organic molecule are N, O and halogens, owing to their higher electronegativities.[28]

Typical energies of conventional intramolecular hydrogen bond (IHB) lies between 2 to 15 kcal/mol.[29] The H-bond interaction energy can go up to 40 kcal/mol, if the two subunits (X and Y here) are electrically charged.[30] The energy value for conventional IHB is much higher compared to its non-conventional counterpart.[29,30] As per the IUPAC H-bond definition, the comparison of electronegativity difference gives a firm idea of whether an IHB would exist or not.[31,32] For instance, the electronegativity on Pauling's scale for H (2.20), N (3.04), O (3.44) and F (3.98), leading to electronegativity difference as  $\Delta_{N-H} \approx 0.84$ ,  $\Delta_{O-H} \approx 1.24$ ,  $\Delta_{H-F} \approx 1.78$ . On the other hand, the electronegativity values for atoms like C (2.55), S (2.58), Se (2.55) etc. show electronegativity difference as  $\Delta_{C-H} \approx 0.35$ ,  $\Delta_{S-H} \approx 0.38$ ,  $\Delta_{Se-H} \approx 0.35$ , respectively.[33] Also, if the electronegativity difference between two atoms is below 0.5, then the bond is considered as covalent or non-polar.[34] This thus, distracted and discouraged the researchers to analyze the non-conventional H-bonds. Contrary to this, there are a number of reports about H-bond formed between the non-polar C-H and heteroatoms such as C-H...N, C-H...O, C-H...F, C-H...S, C-H...Se and C-H... $\pi$  bonds.[35-38] These non-conventional bonds (C-H...Y) falls in the category of weak interaction with energies varying between  $0 \leq \text{IHB} \leq 5$  kcal/mol.[39] An important geometrical aspect that need not be ruled out is that, for conventional IHB, the distance between the H atom and the proton acceptor (H...Y) is

much less than the sum of their van der Waals radii. Although, for the weaker C-H...Y bonds, the corresponding sum of van der Waals radii is slightly less or almost equal to it.[28,39,40]

Various methodologies have been utilized to find out the strength of these non-covalent interactions.[41-49] The theoretical estimation of intermolecular X-H $\cdots$ Y H-bond strength in a complex A...B is routinely done using a supermolecular approach, in which the H-bond energy is estimated as  $E_{HB} = E_{A...B} - (E_A + E_B)$ . Several methods for estimating the intermolecular interaction energies are reported in the literature.[50-53] On the other hand, quantifying the intramolecular hydrogen bond (IHB) strength is not as straightforward as the intermolecular one. The main difficulty lies in isolating the X-H $\cdots$ Y interaction present within a molecule than in a dimer or a complex. Many studies for gauging the strength of the IHB in the literature have applied the spectroscopic and electron density topographical approaches along with some empirical, semi-empirical, and *ab initio* procedures.[41-53] For excellent overview of these methods and their merits and demerits, see Ref. 55. In addition to these indirect approaches, Deshmukh and Gadre have proposed a direct and reliable method for the estimation of X-H $\cdots$ Y IHB energy in variety of systems based on the molecular tailoring approach (MTA).[55-64]

It is basically a fragmentation tool that allows us to calculate the intramolecular hydrogen bond strength in a molecule. The intramolecular hydrogen bond is very much famous for the inculcating stability in a molecule and allows it to stand individually. The details of these bonds shall be covered in the following chapters (4 and 5) of this thesis.

Our work is the very first attempt to club the computational chemistry with the experimental procedures *meta*-benzoporphodimethene analogues. Herein, we intend to explore all the possible factors that may or may not participate in intensifying the yield or stability of *m*-BPDM, computationally, based on the strength of bifurcated H-bond present in the inner core of free base *m*-BPDM. The work encompasses a variety of substitutions on the periphery of *m*-BPDM molecules. Fascinating results that were obtained through the theoretical analysis opens up a wide pathway for the research groups to overcome the low yield barrier and further study the applications of these prosthetic molecules.

The **objectives** of the present dissertation are as follows:

1. To study the effect of *meso*- substitutions on the geometry and intramolecular hydrogen bond strength on free base *meta*-benzoporphodimethene analogues.
2. To study the effect of C3-substitution on the geometry and intramolecular hydrogen bond strength in free base *meta*-benzoporphodimethenes analogues.
3. Synthesis and characterization of new sterically hindered *meta*-benzoporphodimethene and its metal complexes.
4. Conformational analysis of *syn*- and *anti*- isomers metalated *meta*-benzoporphodimethenes derivatives.

## References

- [1] G.M. Maggiora, Electronic Structure of Porphyrins. All Valence Electron Self-Consistent Field Molecular Orbital Calculations of Free Base, Magnesium, and Aquomagnesium Porphines, *J. Am. Chem. Soc.* 95 (1973) 6555–6559. <https://doi.org/10.1021/ja00801a005>.
- [2] A.W. Johnson, I.T. Kay, Synthesis, Corroles Part I, (1964). <https://doi.org/https://doi.org/10.1039/JR9650001620>.
- [3] H.L. Buckley, J. Arnold, Recent developments in out-of-plane metallocorrole chemistry across the periodic table, *Dalt. Trans.* 44 (2015) 30–36. <https://doi.org/10.1039/c4dt02277g>.
- [4] A. Ghosh, Electronic Structure of Corrole Derivatives: Insights from Molecular Structures, Spectroscopy, Electrochemistry, and Quantum Chemical Calculations, *Chem. Rev.* 117 (2017) 3798–3881. <https://doi.org/10.1021/acs.chemrev.6b00590>.
- [5] K.E. Thomas, A.B. Alemayehu, J. Conradie, C.M. Beavers, A. Ghosh, The structural chemistry of metallocorroles: Combined X-ray crystallography and quantum chemistry studies afford unique insights, *Acc. Chem. Res.* 45 (2012) 1203–1214. <https://doi.org/10.1021/ar200292d>.
- [6] M. Stępień, L. Latos-Grażyński, L. Szterenberg, J. Panek, Z. Latajka, Cadmium(II) and Nickel(II) Complexes of Benzoporphyrins. A Study of Weak Intramolecular Metal-Arene Interactions, *J. Am. Chem. Soc.* 126 (2004) 4566–4580. <https://doi.org/10.1021/ja039384u>
- [7] C.H. Hung, G.F. Chang, A. Kumar, G.F. Lin, L.Y. Luo, W.M. Ching, E. Wei-Guang Diau, m-Benzoporphodimethene: A new porphyrin analogue fluorescence zinc(II) sensor, *Chemical Communications.* (2008) 978–980. <https://doi.org/10.1039/b714412a>

- [8] R.K. Sharma, L.K. Gajanan, M.S. Mehata, F. Hussain, A. Kumar, Synthesis, characterization and fluorescence turn-on behavior of new porphyrin analogue: meta-benziporphodimethenes, *Spectrochimica Acta - Part A: Molecular and Biomolecular Spectroscopy.* 169 (2016) 58–65. <https://doi.org/10.1016/j.saa.2016.06.020>
- [9] R.K. Sharma, A. Maurya, P. Rajamani, M.S. Mehata, A. Kumar, meta - Benziporphodimethenes: New Cell-Imaging Porphyrin Analogue Molecules, *ChemistrySelect.* 1 (2016) 3502–3509. <https://doi.org/10.1002/slct.201600812>.
- [10] D. Chauhan, A. Kumar, S.G. Warkar, An efficient adsorbent for the removal of  $Zn^{2+}$   $Cd^{2+}$  and  $Hg^{2+}$  from the real industrial effluents. *Int. J. Environ. Sci. Technol.* (2021). <https://doi.org/10.1007/s13762-021-03615-5>
- [11] D. Chauhan, A. Kumar, S. G. Warkar, Modified polymeric hydrogels for the detection of  $Zn^{2+}$  in *E.coli* bacterial cells and  $Zn^{2+}$ ,  $Cd^{2+}$  and  $Hg^{2+}$  in industrial effluents (2021) *Environmental Technology*, DOI: 10.1080/0959330.2021.1928294
- [12] D. Chauhan, A. Kumar, S.G. Warkar, Synthesis, characterization and metal ions sensing applications of meta-benziporphodimethene-embedded polyacrylamide/ carboxymethyl guar gum polymeric hydrogels in water, *Environ. Tech.* (2020), DOI: 10.1080/0959330.2020.1812730
- [13] A. Kumar, C.H. Hung, S. Rana, M.M. Deshmukh, Study on the structure, stability and tautomerisms of meta-benziporphodimethene and N-Confused isomers containing  $\gamma$ -lactam ring, *J. Mol. Struct.* 1187 (2019) 138–150. <https://doi.org/10.1016/j.molstruc.2019.03.064>.
- [14] D. Ahluwalia, A. Kumar, S.G. Warkar, Recent developments in meta-benziporphodimethene: A new porphyrin analogue, *J. Mol. Struct.* 1228 (2021) 129672. <https://doi.org/10.1016/j.molstruc.2020.129672>.

- [15] Pauling, L. The nature of the chemical bond. Application of results obtained from the quantum mechanics and from a theory of paramagnetic susceptibility to the structure of molecules. *J. Am. Chem. Soc.* **1931**, *53*, 1367–1400.
- [16] Huggins, M. L. Hydrogen Bridges in Ice and Liquid Water. *J. Phys. Chem.* **1936**, *40*, 723-731.
- [17] Huggins, M. L. Hydrogen Bridges in Organic Compounds. *J. Org. Chem.* **1936**, *1*, 407-456.
- [18] Nernst, W. Über die Löslichkeit von Mischkristallen. *Z. Phys. Chem.* **1892**, *9*, 137-142.
- [19] Werner, A. Ueber Haupt und Nebenvalenzen und die Constitution der Ammoniumverbindungen. *Justus Liebigs Ann. Chem.* **1902**, *322*, 261-296.
- [20] Moore, T. S.; Winmill, T. F. The State of Amines in Aqueous Solution. *J. Chem. Soc.* **1912**, *101*, 1635-1676.
- [21] Latimer, W. M.; Rodebush, W. H. Polarity and Ionization from the Standpoint of the Lewis Theory of Valence. *J. Am. Chem. Soc.* **1920**, *42*, 1419-1443.
- [22] Huggins, M. L. 50 Years of Hydrogen Bond Theory. *Angew. Chem. Int. Ed. Engl.* **1971**, *10*, 147-152.
- [23] Pimentel, G. C.; McClellan, A. L. The Hydrogen Bond. *Freeman: San Francisco*, **1960**, *30*, 1-475.
- [24] Arunan, E.; Desiraju, G. R.; Klein, R. A.; Sadlej, J.; Scheiner, S.; Alkorta, I.; Clary, D. C.; Crabtree, R. H.; Dannenberg, J. J.; Hobza, P.; Kjaergaard, H. G.; Legon, A. C.; Mennucci, B.; Nesbitt, D. J. Defining the Hydrogen Bond: An Account (IUPAC Technical Report). *Pure Appl. Chem.* **2011**, *83*, 1619-1636.
- [25] Jeffery, G. A. An Introduction to Hydrogen Bonding; Oxford University Press, New York, **1997**.

- [26] Desiraju, G. R.; Steiner, T. The Weak Hydrogen Bond: In Structural Chemistry and Biology. *Oxford University Press, New York*. **1999**.
- [27] Scheiner, S. Hydrogen Bond: A Theoretical Perspective. *Oxford University Press, New York*. **1997**.
- [28] Alkorta, I.; Rozas, I. Non-conventional hydrogen bonds. *Chem. Soc. Rev.* **1998**, *27*, 163–170.
- [29] Grabowski, S. J. Theoretical studies of strong hydrogen bonds, *Annu. Rep. Prog. Chem. Sect. C*. **2006**, *102*, 131–165.
- [30] Afonin, A. V.; Vashchenko, A. V.; Sigalov, M. V. Estimating the energy of intramolecular hydrogen bonds from <sup>1</sup>H NMR and QTAIM calculations. *Org. Biomol. Chem.* **2016**, *14*, 11199–11211.
- [31] Juanes, M.; Saragi, R.T.; Caminati, W.; Lesarri, A. The Hydrogen Bond and Beyond: Perspectives for Rotational Investigations of Non-Covalent Interactions. *Chem. - A Eur. J.* **2019**, *25*, 11402–11411.
- [32] Arunan, E.; Desiraju, G.R.; Klein, R.A.; Sadlej, J.; Scheiner, S.; Alkorta, I.; Clary, D.C.; Crabtree, R.H.; Dannenber, J.J.; Hobza, P.; Kjaergaard, H.G.; Legon, A.C.; Mennucci, B.; Nesbitt, D.J. Definition of the hydrogen bond (IUPAC Recommendations 2011). *Pure Appl. Chem.* **2011**, *83*, 1637–1641.
- [33] Murphy, L.R.; Meek, T.L.; Louis Allred, A.; Alien, L.C. Evaluation and test of Pauling's electronegativity scale. *J. Phys. Chem. A*. **2000**, *104*, 5867–5871.
- [34] Hibbert, F.; Emsley, J. Hydrogen bonding and chemical reactivity. *Adv. Phys. Org. Chem.* **1990**, *26*, 255-379.
- [35] Jena, S.; Tulsyan, K.D.; Rana, A.; Choudhury, S.S.; Biswal, H.S. Non-conventional Hydrogen Bonding and Aromaticity: A Systematic Study on Model Nucleobases and Their Solvated Clusters. *ChemPhysChem.* **2020**, *21*, 1826-1835.

- [36] Scheiner, S. Comparison of CH $\cdots$ O, SH $\cdots$ O, Chalcogen, and Tetrel Bonds Formed by Neutral and Cationic Sulfur-Containing Compounds. *J. Phys. Chem. A.* **2015**, *119*, 9189–9199.
- [37] Biswal, H.S.; Wategaonkar, S. Sulfur, not too far behind O, N, and C: SH $\cdots$   $\pi$  hydrogen bond. *J. Phys. Chem. A.* **2009**, *113*, 12774–12782.
- [38] Grabowski, S.J. Ab initio calculations on conventional and unconventional hydrogen bonds-study of the hydrogen bond strength. *J. Phys. Chem. A.* **2001**, *105*, 10739–10746.y t r4 31
- [39] Kryachko, E.S.; Karpfen, A.; Remacle, F. Nonconventional hydrogen bonding between clusters of gold and hydrogen fluoride. *J. Phys. Chem. A.* **2005**, *109*, 7309–7318.
- [40] Alapour, S.; Farahani, M.D.; Silva, J.R.A.; Alves, C.N.; Friedrich, H.B.; Ramjugernath, D.; Koobanally, N.A. Investigation of conventional and non-conventional hydrogen bonds: a comparison of fluorine-substituted and non-fluorine substituted compounds. *Monatshefte Fur Chemie.* **2017**, *148*, 2061–2068.
- [41] Grabowski, S. J. Hydrogen Bonding Strength-Measures Based on Geometric and Topological Parameters. *J. Phys. Org. Chem.* **2004**, *17*, 18-31.
- [42] Hobza, P.; Havlas, Z. Blue-Shifting Hydrogen Bonds. *Chem. Rev.* **2000**, *100*, 4253-4264.
- [43] Fuster, F.; Silvi, B. Does the Topological Approach Characterize the Hydrogen Bond? *Theor. Chem. Acc.* **2000**, *104*, 13-21.
- [44] Espinosa, E.; Alkorta, I.; Elguero, J.; Molins, E. From Weak to Strong Interactions: A Comprehensive Analysis of the Topological and Energetic Properties of the Electron Density Distribution Involving X–H $\cdots$ F–Y Systems. *J. Chem. Phys.* **2002**, *117*, 5529-5542.

- [45] Klein, R. A. Hydrogen Bonding in Diols and Binary Diol-Water Systems Investigated using DFT Methods. II. Calculated Infrared OH- Stretch Frequencies, Force Constants, and NMR Chemical Shifts Correlate with Hydrogen Bond Geometry and Electron Density Topology. A Reevaluation of Geometrical Criteria for Hydrogen Bonding. *J. Comput. Chem.* **2003**, *24*, 1120-1131.
- [46] Deshmukh, M. M.; Sastry, N. V.; Gadre, S. R. Molecular Interpretation of Water Structuring and Destructuring Effects: Hydration of Alkanediols. *J. Chem. Phys.* **2004**, *121*, 12402-12410.
- [47] Lipkowski, P.; Koll, A.; Karpfen, A.; Wolschann, P. An Approach to Estimate the Energy of the Intramolecular Hydrogen Bond. *Chem. Phys. Lett.* **2002**, *360*, 256-263.
- [48] Buemi, G.; Zuccarello, F. Is the Intramolecular Hydrogen Bond Energy Valuable from Internal Rotation Barriers? *J. Mol. Struct. THEOCHEM.* **2002**, *581*, 71-85.
- [49] Kjaergaard, H. G.; Howard, D. L.; Schofield, D. P.; Robinson, T. W.; Ishiuchi, S.; Fujii, M. OH- and CH-Stretching Overtone Spectra of Catechol. *J. Phys. Chem. A.* **2002**, *106*, 258-266.
- [50] Keutsch, F. N.; Cruzan, D. J.; Saykally, R. J. The Water Trimer. *Chem. Rev.* **2003**, *103*, 2533-2578.
- [51] Sánchez-García, E.; George, L.; Montero, L. A.; Sander, W. 1:2 Formic Acid/Acetylene Complexes: Ab Initio and Matrix Isolation Studies of Weakly Interacting Systems. *J. Phys. Chem. A.* **2004**, *108*, 11846-11854.
- [52] Munshi, P.; Row, T. N. G. Exploring the Lower Limit in Hydrogen Bonds: Analysis of Weak C-H $\cdots$ O and C-H $\cdots$  $\pi$  Interactions in Substituted Coumarins from Charge Density Analysis. *J. Phys. Chem. A.* **2005**, *109*, 659-672.

- [53] Cockroft, S. L.; Hunter, C. A.; Lawso, K. R.; Perkins, J.; Urch, C. J. Electrostatic Control of Aromatic Stacking Interactions. *J. Am. Chem. Soc.* **2005**, *127*, 8594-8595.
- [54] Jabłoński, M. A. Critical Overview of Current Theoretical Methods of Estimating the Energy of Intramolecular Interactions. *Molecules*. **2020**, *25*, 5512-5549.
- [55] Deshmukh, M. M.; Gadre, S. R.; Bartolotti, L. J. *Estimation of Intramolecular Hydrogen Bond Energy via Molecular Tailoring Approach*. *J. Phys. Chem. A.* **2006**, *110*, 12519-12523.
- [56] Deshmukh, M. M.; Suresh, C. H.; Gadre, S. R. Intramolecular Hydrogen Bond Energy in Polyhydroxy Systems: A Critical Comparison of Molecular Tailoring and Isodesmic Approaches. *J. Phys. Chem. A.* **2007**, *111*, 6472-6480.
- [57] Deshmukh, M. M.; Bartolotti, L. J.; Gadre, S. R. Intramolecular Hydrogen Bonding and Cooperative Interactions in Carbohydrates via the Molecular Tailoring Approach. *J. Phys. Chem. A.* **2008**, *112*, 312-321.
- [58] Deshmukh, M. M.; Gadre, S. R. Estimation of N-H···O=C Intramolecular Hydrogen Bond Energy in Polypeptides. *J. Phys. Chem. A.* **2009**, *113*, 7927-7932.
- [59] Deshmukh, M. M.; Bartolotti, L. J.; Gadre, S. R. Intramolecular Hydrogen Bond Energy and Cooperative Interactions in  $\alpha$ -,  $\beta$ -, and  $\gamma$ -cyclodextrin Conformers. *J. Comput. Chem.* **2011**, *32*, 2996-3004.
- [60] Khedkar, J. K.; Deshmukh, M. M.; Gejji, S. P.; Gadre, S. R. Intramolecular Hydrogen Bonding and Cooperative Interactions in Calix[n]arenes (n=4,5). *J. Phys. Chem. A.* **2012**, *116*, 3739-3744.
- [61] Siddiqui, N.; Singh, V.; Deshmukh, M. M.; Gurunath, R. Structures, Stability and Hydrogen Bonding in Inositol Conformers. *Phys. Chem. Chem. Phys.* **2015**, *17*, 18514-18523.

- [62] Deshmukh, M. M.; Gadre, S. R.; Cocinero, E. M. Stability of Conformationally Locked Free Fructose: Theoretical and Computational Insights. *New J. Chem.* **2015**, *39*, 9006-9018.
- [63] Singh, V.; Ibnusaud, I.; Gadre, S. R.; Deshmukh, M. M. Fragmentation Method Reveals a Wide Spectrum of Intramolecular Hydrogen Bond Energies in Antioxidant Natural Products. *New J. Chem.* **2020**, *44*, 5841-5849.
- [64] Ahirwar, M. B.; Gadre, S. R.; Deshmukh, M. M. Direct and Reliable Method for Estimating the Hydrogen Bond Energies and Cooperativity in Water Clusters W<sub>n</sub>, n = 3 to 8. *J. Phys. Chem. A.* **2020**, *124*, 6699-6706.

## CHAPTER 3

### METHODOLOGY

---

#### 3.1. Introduction

Computational chemistry deals with calculating or examining or say investigating the chemical properties of certain system virtually. In other words, molecular modelling (also a term used for computational chemistry) helps us to find out the chemical properties of a molecular system on computer, without actually performing an experiment in laboratory. It is basically curating one's idea on computer, followed by checking the feasibility of that approach and then giving life to that vision in the laboratory. A number of problems that can be solved through computational chemistry have been shown in **Figure 3.1.**

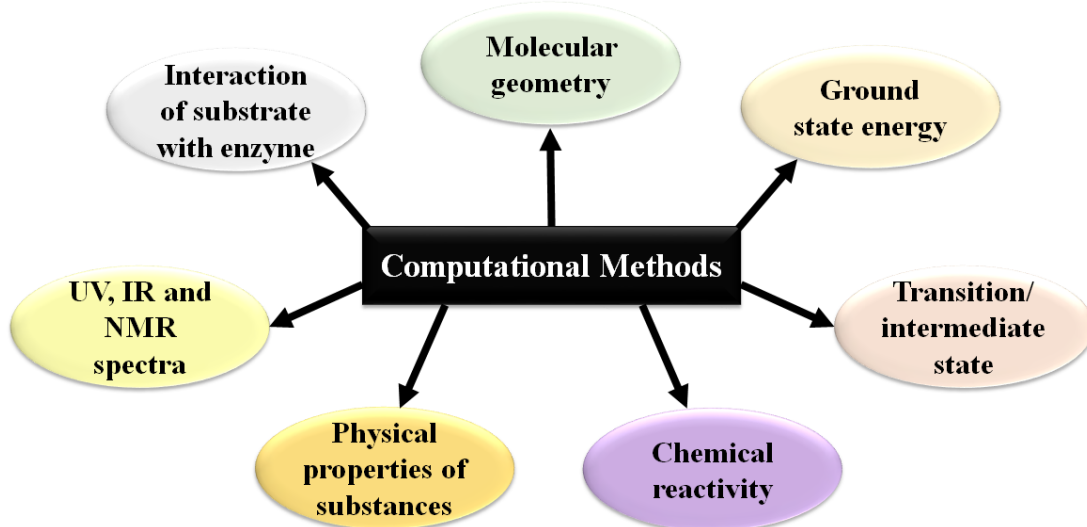


**Figure 3.1.** Questions that can be solved by computational chemistry.

The characteristics mentioned in Figure 2.1 are addressed using various tools of computational chemistry. There are five major techniques that are used in computational chemistry, *viz.*, molecular mechanics (MM), ab-initio calculations, semiempirical (SE)

method, density functional theory (DFT) calculations, and molecular dynamics.[1] In MM, the atoms and the bond linking them are considered as balls and spring, respectively. The change in energy is calculated in respect of different sets of position and momentum of the model, till a lowest energy state is obtained. As this stage, the molecule is said to be optimized, or simply geometry optimization. The method is fairly fast to perform, and within seconds we get the result. *Ab-initio* is a Latin word which means “from first principle.” Going well with the literal meaning of this term, the method utilizes the principle method of finding out the energy of a particular system, i.e., through the Schrödinger wave equation (SWE). In this technique, SWE is solved to obtain the molecular energy value along with the wave function. Since, SWE is very complicated to solve for many-body systems, thus approximations are implicated. The lesser approximations that are applied in this method, higher is the level of *ab-initio* calculations are considered. This method performs very slow calculations. The results for macromolecules takes weeks to obtain. The next is semiempirical (SE) method, which also solves SWE but with relatively more approximations. The complicated integrals of SWE made in *ab-initio* method are completely surpassed in the SE method. Furthermore, this technique mixes the theory and the experimental values. This means the integrals are solved by putting the experimental values to obtain results. This method is called *parametrization* based. The computational time is more than MM but less than *ab-initio*. The density functional calculations, popularly known as density functional theory (DFT) method, is also based on SWE, but unlike the other two methods (*ab-initio* and SE) it does not calculate the wave function. This theory rather is based on the electronic charge/density distribution across the system under consideration. The research in the field of DFT gained pace in the 1980s, while the *ab-initio* and SE have

been broadly explored in 1960s. The results obtained through this method takes lesser time than *ab-initio* calculations but more computational time than SE.[2] The molecular dynamics follows the laws of motions. It helps us to examine the changes that occur in the enzyme in terms of shape and position upon binding within a substrate.

In the present thesis, we have widely used the DFT method for different studies that have been discussed in the subsequent sections. Thus, in this chapter we shall now briefly discuss about DFT and its applications in computational chemistry.

### **3.2. Density Functional Theory**

#### **3.2.1. Basics of DFT**

The density functional theory (DFT) is based on the electron probability density function or simply electron density function, that is designated as  $\rho(x,y,z)$ . The symbol  $\rho$  represents the probability of finding an electron in a unit volume  $dxdydz$ . The unit of  $\rho$  is  $\text{volume}^{-1}$  and the electron probability value is represented as  $\rho(x,y,z)$   $dxdydz$ . Therefore, the electronic probability has no unit and is simply a numerical value. The DFT method is different from the ab-initio and SE as it focusses on the electronic charge distribution over a given space, rather than finding out the wavefunction value. In other words,  $\rho$  is a function of three spatial coordinates  $x, y, z$  only, irrespective of how many electrons are there in a molecular system. In a scatterplot of electron density, the variation in  $\rho$  with position can be pointed out by the density at a given point. In contrast to this, for an  $n$ -electron molecule, the wave function dependent on  $4n$  variables, viz. three spatial coordinates and one spin coordinate, for each electron. For this reason, as mentioned in the previous section the *ab-initio* and SE calculations are highly complicated and computationally expensive.

It takes nearly same time to perform DFT calculations as Hartree Fock (HF) and one obtains the result as close to that of MP2 calculations.[2–4]

The electronic density is not just the prime focus of DFT. There are other experimental characterization techniques that also deals with finding out the electronic density in a molecular system and then predicting the inferring the observations. The X-ray diffraction methods and electronic diffraction method are the examples of such techniques. In the year 1998, Noble prize was awarded to John Pople for his vital role in developing the practical wave function based methods, and also to Walter Kohn for the development of density functional theory.[1]

### ***3.2.2. Principle of DFT***

It was the vision of Enrico Fermi and P. A. M. Dirac, who independently performed calculations, that led to the establishment of atomic and molecular properties from electron density, the 1920s. This was popularly named as Fermi-Dirac statistics. The Thomas-Fermi-Dirac model was proved to be extremely good for atoms but it failed completely for molecules. It stated that the molecules are extremely unstable when dissociated into atoms. This indeed is a popularly known Thomas-Dirac theorem. The exchange correlation ( $X_\alpha$ , where X= exchange and  $\alpha$  is a parameter) was introduced to this theory to improvise the results for molecular systems. This modification was done by Slater in 1951. The  $X_\alpha$  method was found suitable for atoms and solids, it has also been implemented for molecules, but had limitations. The method was later replaced by more accurate Kohn-Sham type DFT method.[1–4]

### ***3.2.3. Theorems of DFT***

The modern DFT is based on Kohn-Sham approach. This approach revolves around two theorems given by Hohenberg and Kohn in the year 1964. The two theorems

were named as variational theorem and existence theorem. As per Hohenberg and Kohn, all the properties of a molecule at ground state can be calculated through ground state electron density function  $\rho_o(x,y,z)$ . for instance, the ground state energy has a relation with electronic density as stated in Eq. 3.1

$$\rho_o(x,y,z) \xrightarrow{\text{functional}} E_o \quad (\text{Eq. 3.1})$$

Here,  $E_o$  is a functional of  $\rho_o(x,y,z)$ . A function is rule that can change a number into another. See equation 3.2 as an example. In equation 3.2,  $x^2$  is the function applied on number 4, that yielded number 16. On the other hand, a functional is a rule that transforms a function into a number. See equation 3.3 for better understanding of functional.

$$4 \xrightarrow{x^2} 16 \quad (\text{Eq. 3.2})$$

$$f(x) = x^2 \xrightarrow{\int_0^2 f(x)dx} \left[ \frac{x^3}{3} \right]_0^2 = \frac{8}{3} \quad (\text{Eq. 3.3})$$

In other words, the functional is a function of a “definite” function. The understanding of functions and functional would now create a good base to perceive the two theorems of DFT. The first Hohenberg-Kohn theorem states that the ground state property of any molecule is a functional of its electron density function. The *existence theorem* indeed states the functional  $F$  exists (Eq. 3.4), but does not tell us how to find this functional. This is more like the existence of ghosts in the universe, and thus is a main disadvantage of DFT. The significance of this theorem is that it gives us the affirmation that molecular properties can be calculated through electron density function. Also, the approximate functional gives the result which are close to the real values (derived experimentally).

$$E_o = F[\rho_o] = E[\rho_o] \quad (\text{Eq. 3.4})$$

The second theorem *viz.* *variation theorem* states that any trial electronic density function will yield an energy which is larger than or equal to the true ground state energy of that system. At the ground state, the molecule is at rest and only potential energy is associated with it. Thus, at this point, as per the vibration theorem,

$$E_v[\rho_t] \geq E_o[\rho_o] \quad (\text{Eq. 3.5})$$

In equation 3.5,  $E_v$  is the potential energy of trial electron density function  $\rho_t$  is always greater than equal to the ground state energy  $E_o$  of ground state electron density function  $\rho_o$ .[1–4]

### 3.2.4. Applications of density functional theory

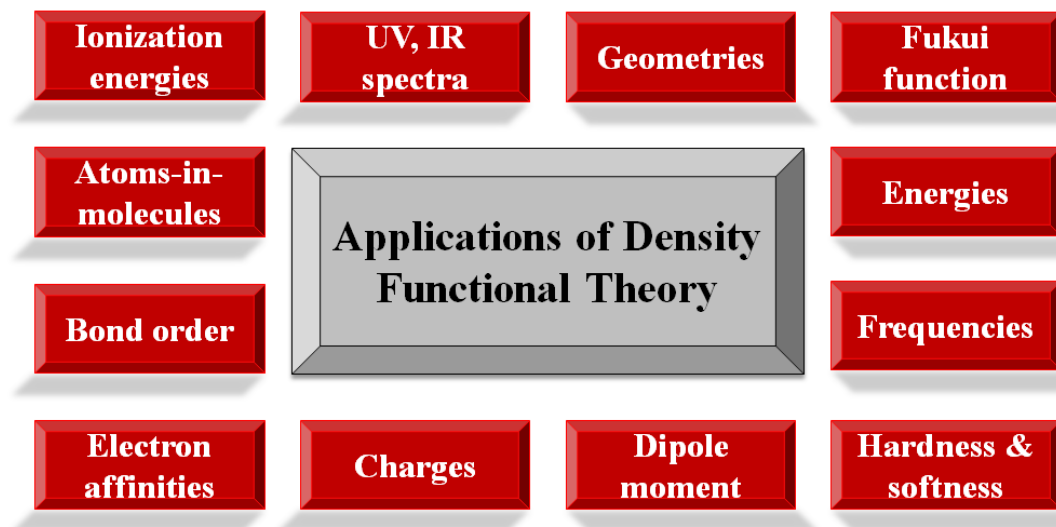


**Figure 3.2.** All the possible molecular properties that can be determined by DFT.

The optimized structure, which is the ground state structure gives information about the bond lengths and angles within the molecule. The *geometry* of the ground state is understood in this way. The output file of the DFT also yields the kinetic, potential and total *energy* of the molecule. The *frequency* calculation gives the global minima

of the optimized geometry, stating that no other force is associated with the molecule at this stage. Adding to this, one can also calculate the charges, net dipole moment, ionization energies, electronic affinities, bond orders, hardness and softness can be determined. The UV and NMR spectra can also be visualized through density functional theory results. The Fukui function was introduced by Yang and Parr in the year 1984. It is defined as the sensitivity of electronic density in species at different regions with respect to the change in the number of electron in that system. In other words, in a chemical reaction, the addition or removal of electrons from the frontier molecular orbital (LUMO and HOMO, respectively) leads to the change in number of electrons. The fukui function measures the change in electron density that occurs during a chemical reaction. The function is primarily employed in order to predict the variation of reactivity from site to site. Figure 3.2 summarizes all the possible properties that can be predicted through DFT.[1–4]

### 3.2.5. Basis functions and basis sets

The basis functions are defined as mathematical functions that are used to describe the one electron spatial orbitals. The popularly used atomic basis functions in the modern day quantum chemistry involves Slater-type orbitals (STO) and Gaussian-type orbitals (GTO).[5]

$$\phi_{l,m,n}^{STO}(r) = \frac{(2\xi)^{n+l/2}}{[(2n)!]^{1/2}} r^{(n-1)} e^{-\xi r} \quad (\text{Eq. 3.6})$$

$$\phi_{l,m,n}^{GTO}(r) = \left(\frac{2\xi}{\pi}\right)^{3/4} \left[\frac{(8\xi)^{i+j+k} i!j!k!}{(2i)!(2j)!(2k)!}\right]^{1/2} x^l y^m z^n e^{-\xi r^2} \quad (\text{Eq. 3.7})$$

Equation 3.6 and 3.7 represents the radial form of STOs and GTOs, respectively. The symbols l, m and n illustrates the azimuthal, magnetic and principle quantum

numbers, respectively.  $\xi$  represents an unknown positive number that is called as orbital exponent. Key points about the STOs and GTOs are listed in **Figure 3.3**.

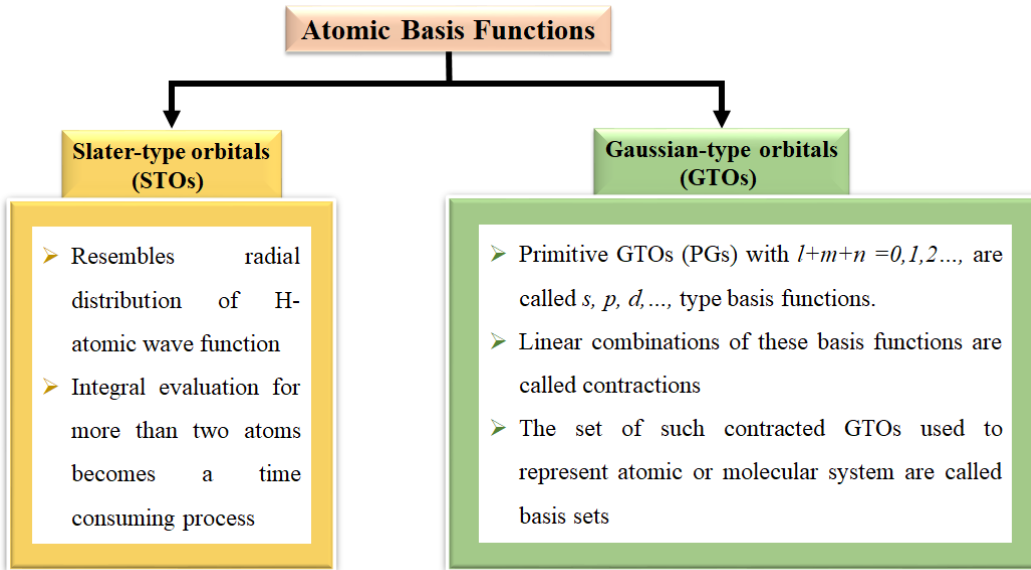


**Figure 3.3.** Key features of STOs and GTOs.[6]

Some of the popularly used Gaussian basis sets are discussed below:

- **Minimal basis set:** Those basis sets where one basis function is employed per occupied atomic orbital. In other words, when one contraction per atomic orbital is taken into account. For instance, STO-3G is a minimal basis set, wherein 3PGs combine to form one basis set for STO basis function.[1,6]
- **Double zeta (DZ) basis set:** Those basis sets where two basis functions are employed per atomic orbital are called double zeta (DZ) basis sets. Zeta here is used for exponent. In a similar fashion triple zeta (TZ), quadruple zeta (QZ) basis sets are also available in literature.[7]
- **Split-valence (SV) basis sets:** This basis set is minimal for inner shell electrons, where one contraction per atomic orbital is applied, along with double zeta for the valence shell electrons, i.e, two contractions per atomic orbital. For example,

6-31G, where 6 PGs are employed for inner core electrons and for the valence shell electrons combination of two basis function has been employed.[7–9]

- **Polarization function:** During the formation and breaking of bonds, electron polarization takes place in an atom, thus a basis function with higher flexibility is required. This is achieved by adding an extra function with one quantum number of higher angular momentum than the valence orbitals. These next shell orbitals are called as polarization functions, and are indicated by \* (or d) and \*\* (or d,p). Here, “d” function is added on the first and second row atoms, other than hydrogen while “p” function is added to hydrogen atom only.[10,11]
- **Diffuse function:** The systems having cations or lone pair of electrons, or free electrons, the electron density in such systems accumulates away from the nucleus. In order to count in their contribution in the overall charge distribution in a molecular system, diffuse function is added. These functions are indicated as “+” or “++”. The first “+” indicates the heavy atoms, other than H-atom, have been augmented with an additional one *s* and one set of *p* function bearing small exponent. The second “+” suggests the addition of diffuse *s* function on H-atoms.[12,13]
- **Effective core potential (ECP) basis sets:** With the increasing atomic number and large size of atoms, calculations becomes time consuming and computationally expensive. Thus, the chemistry of such heavy atoms deals with valence electron. Hellman suggested to replace the core-shell electron with analytical function which effectively represents nuclear electron core to valence shell electrons.[14] These analytical functions are called as effective core potential. The popularly used ECP includes Los Almos National laboratory pseudopotential (LANL) given by Hay and Wadt,[15,16] and Stuttgart-Dresden-Bonn (SDD) pseudopotential.[17,18]

## References

- [1] I.N. Levine, Quantum Chemistry Fifth Edition, 5th ed., Pearson, 2000.
- [2] Errol Lewars, Computational Chemistry- Introduction to theory and Applications of molecular and quantum mechanics, Kluwer Academic Publishers, 2003.
- [3] A.G. DeRocco, Modern Quantum Chemistry, Am. J. Phys. 35 (1967) 1097–1097. <https://doi.org/10.1119/1.1973756>.
- [4] X. Yang, S. Wang, X. Ma, Application of microwave technique in the preparation of catalyst, Chem. Bull. / Huaxue Tongbao. 67 (2004) 641–647.
- [5] S.F. Boys, P.R.S.L. A, The integral formulae for the variational solution of the molecular many-electron wave equation in terms of Gaussian functions with direct electronic correlation, Proc. R. Soc. London. Ser. A. Math. Phys. Sci. 258 (1960) 402–411. <https://doi.org/10.1098/rspa.1960.0195>.
- [6] S. Wilson, Quantum Chemistry: The Development of ab initio Methods in Molecular Electronic Structure Theory, Phys. Bull. 36 (1985) 392–392. <https://doi.org/10.1088/0031-9112/36/9/034>.
- [7] F. Weigend, R. Ahlrichs, Balanced basis sets of split valence, triple zeta valence and quadruple zeta valence quality for H to Rn: Design and assessment of accuracy, Phys. Chem. Chem. Phys. 7 (2005) 3297. <https://doi.org/10.1039/b508541a>.
- [8] J.S. Binkley, J.A. Pople, W.J. Hehre, Self-consistent molecular orbital methods. 21. Small split-valence basis sets for first-row elements, J. Am. Chem. Soc. 102 (1980) 939–947. <https://doi.org/10.1021/ja00523a008>.
- [9] M.S. Gordon, J.S. Binkley, J.A. Pople, W.J. Pietro, W.J. Hehre, Self-consistent molecular-orbital methods. 22. Small split-valence basis sets for second-row elements, J. Am. Chem. Soc. 104 (1982) 2797–2803. <https://doi.org/10.1021/ja00374a017>.

- [10] J.M.. Martin, O. Uzan, Basis set convergence in second-row compounds. The importance of core polarization functions, *Chem. Phys. Lett.* 282 (1998) 16–24. [https://doi.org/10.1016/S0009-2614\(97\)01128-7](https://doi.org/10.1016/S0009-2614(97)01128-7).
- [11] H. Guo, M. Karplus, Basis set and polarization function effects on optimized geometries and harmonic frequencies at the second- order Mo/lle–Plesset perturbation level, *J. Chem. Phys.* 91 (1989) 1719–1733. <https://doi.org/10.1063/1.457079>.
- [12] R.C. Raffenetti, General contraction of Gaussian atomic orbitals: Core, valence, polarization, and diffuse basis sets; Molecular integral evaluation, *J. Chem. Phys.* 58 (1973) 4452–4458. <https://doi.org/10.1063/1.1679007>.
- [13] B.J. Lynch, Y. Zhao, D.G. Truhlar, Effectiveness of Diffuse Basis Functions for Calculating Relative Energies by Density Functional Theory, *J. Phys. Chem. A.* 107 (2003) 1384–1388. <https://doi.org/10.1021/jp021590l>.
- [14] H. Hellmann, A new approximation method in the problem of many electrons, *J. Chem. Phys.* 3 (1935) 61. <https://doi.org/10.1063/1.1749559>.
- [15] P.J. Hay, W.R. Wadt, Ab initio effective core potentials for molecular calculations. Potentials for the transition metal atoms Sc to Hg, *J. Chem. Phys.* 82 (1985) 270–283. <https://doi.org/10.1063/1.448799>.
- [16] P.J. Hay, W.R. Wadt, Ab initio effective core potentials for molecular calculations. Potentials for K to Au including the outermost core orbitale, *J. Chem. Phys.* 82 (1985) 299–310. <https://doi.org/10.1063/1.448975>.
- [17] P. Taylor, A. Bergner, M. Dolg, W. Küchle, H. Stoll, H. Preuß, Molecular Physics : An International Journal at the Interface Between Chemistry and Physics Ab initio energy-adjusted pseudopotentials for elements of groups 13 – 17, (n.d.) 37–41.

- [18] M. Kaupp, P.V.R. Schleyer, H. Stoll, H. Preuss, Pseudopotential approaches to Ca, Sr, and Ba hydrides. Why are some alkaline earth MX<sub>2</sub> compounds bent?, J. Chem. Phys. 94 (1991) 1360–1366. <https://doi.org/10.1063/1.459993>.

## CHAPTER 4

### EFFECT OF SUBSTITUTIONS AT *meso*-POSITIONS

---

#### 4.1. Introduction

The core of *meta*-benzoporphodimethene consists of bifurcated hydrogen bonds between the H<sub>27</sub>—N<sub>25</sub> (HB1) and H<sub>27</sub>—N<sub>23</sub> (HB2) (**Figure 4.1**) atoms, which plays a crucial role in stabilizing the core of this unique metal sensor.[1-11] The concept of hydrogen bond was first highlighted by Pauling in the year 1931.[12-14] Classically, hydrogen-bonded neutral molecular system involve interactions such as O—H···O, N—H···N, S—H···O, etc. having variable strengths;  $\approx$ 1-4 kcal mol<sup>-1</sup> for weak,  $\approx$ 4-15 kcal mol<sup>-1</sup> for moderate and  $\approx$ 15-40 kcal mol<sup>-1</sup> for a very strong hydrogen bond.[15] Typically, H···Y distances for such strong, moderate and weak hydrogen bonds are  $\approx$ 1.2-3.0 Å and X—H···Y angles lie in the range 100-180° for such X—H···Y interactions.[16,17] Recently, the stability of *meta*-benzoporphodimethene molecules and its N-confused isomers containing  $\gamma$ -lactam ring have been reported from our laboratory.[11] The effect on geometries, relative stabilities, and N-confused oxygenated *meta*-benzoporphodimethene was investigated by changes in the position of N-confused ring and oxygenation at one of the pyrrole ring. Also, isomeric stability was examined.[11] Through this chapter, we intend to study the effect of H-bonding on the geometries of *meta*-benzoporphodimethene ligand employing density functional theory (DFT). We wish to demonstrate the effect of substituents on *sp*<sup>3</sup> and *sp*<sup>2</sup> *meso* carbon atoms on the core N—H···N hydrogen bond strength which plays a significant role in stabilization in solid-state structure.

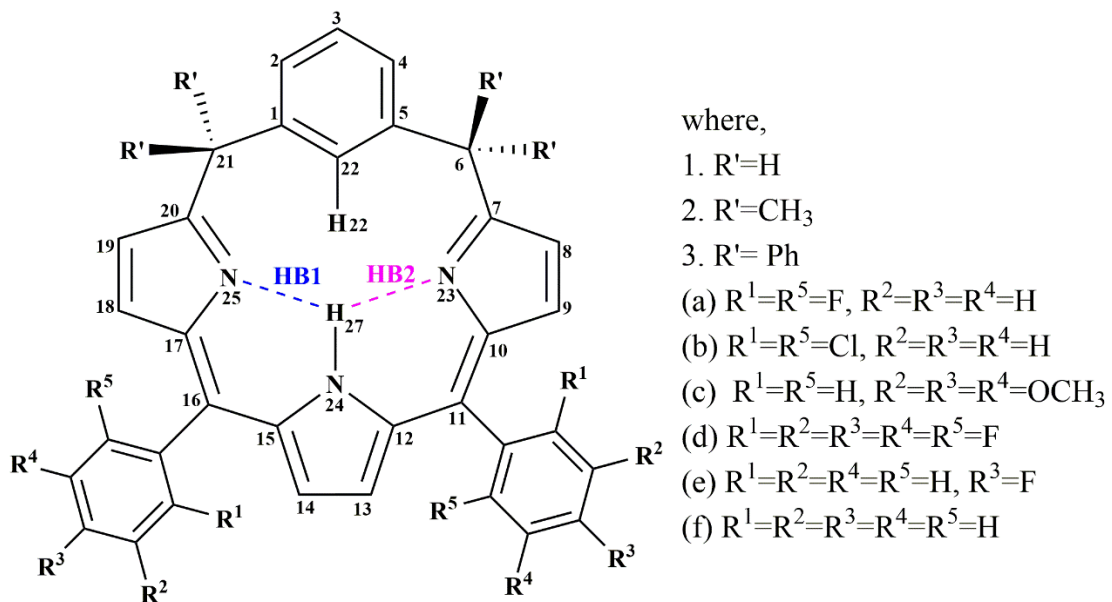


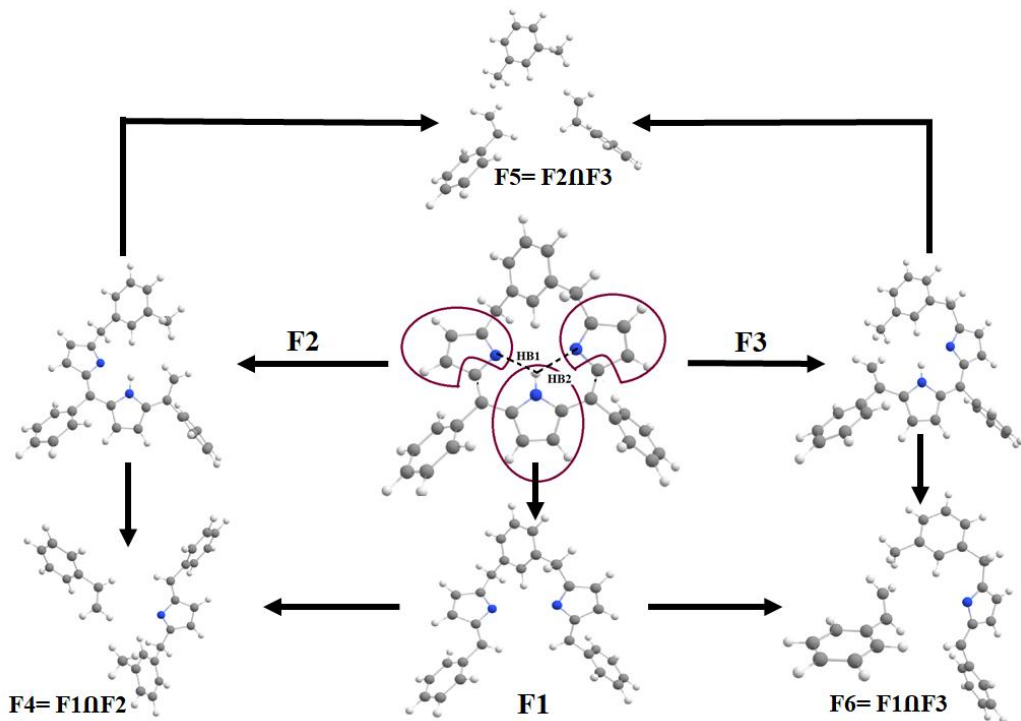
**Figure 4.1.** *meta*-benziporphodimethene analogues under consideration.

## 4.2. Models and Methods

### 4.2.1 Computational Details

Geometries of all species studied in this work were optimized under  $C_1$  symmetry by the DFT method with B3LYP functional. Two kinds of basis set systems, BS-I and BS-II, were used in this work. In BS-I, 6-31G(d,p) basis sets were employed for all atoms.[18,19] This BS-I was employed for geometry optimization. The choice of B3LYP/BS-I is excellent in the modeling of the geometry and relative stability of these types of molecules.[20] Vibrational frequencies were calculated with B3PW91/BS-I to confirm the optimized species to be in an equilibrium state. In a better basis set system BS-II, 6-311+G(d,p) basis sets were used for all the atoms. The intramolecular hydrogen bond energies were evaluated at B3LYP/BS-II level. All calculations were performed with Gaussian 09 program package.[21] All the molecular images were generated using chemcraft program package.[22]

#### 4.2.2 Fragmentation Method for Estimation of Hydrogen Bond Energy



**Scheme 4.1.** Fragmentation scheme for estimation of intramolecular  $\text{N}-\text{H}\cdots\text{N}$  hydrogen bond in **1f** (parent molecule).[11]

The energies of hydrogen bonds in these molecules were estimated employing molecular tailoring based approach (MTA). [11-15, 23, 24] A general fragmentation approach for the estimation of  $\text{N}-\text{H}\cdots\text{N}$  hydrogen bond strength in parent molecule (**1f**) is shown in **Scheme 4.1**. As seen in **Scheme 4.1**, the parent molecule (**1f**) is cut into three primary fragments F1, F2, and F3. These cuts have been shown by dotted regions on the parent molecule. To satisfy the valences of the cut regions, dummy hydrogen atoms were added at an appropriate C–H distance and direction. Fragments F4, F5, F6, and F7 are obtained by intersections of the primary fragments as  $(\text{F1} \cap \text{F2})$ ,  $(\text{F2} \cap \text{F3})$ ,  $(\text{F1} \cap \text{F3})$  and  $(\text{F1} \cap \text{F2} \cap \text{F3})$ , respectively (**Scheme 4.1**). Single point energy of all the fragments at B3LYP/BS-II level of theory was calculated. The fragments

were not optimized to avoid the conformational changes in them. The intramolecular hydrogen bond energy  $E_{HB2}$  in the parent molecule (**1f**) is calculated as  $((E_{F1} + E_{F3} - E_{F6}) - E_{1f}) = ((-1267.364461 + (-1306.722741) - (-1098.856506)) - (-1475.246703) = 0.016007 \text{ a.u.} = 10.04 \text{ kcal mol}^{-1}$  (**Scheme 4.1**). Likewise,  $E_{HB1}$  was calculated as  $((E_{F1} + E_{F2} - E_{F4}) - E_{1f})$  for (**1f**) molecule. In a similar fashion, hydrogen bond energies for all the eighteen molecules were evaluated.

### 4.3. Results and Discussion

#### 4.3.1. Geometries of *meta*-benzoporphodimethenes

It has been well documented by Kumar and coworkers that the quantum yield of *meta*-benzoporphodimethenes is highly dependent on the substituents present at  $sp^2$  *meso* carbon atoms.[8] But the substitution at the  $sp^3$  *meso* carbons at 6 and 21 positions may also affect the stability and respective quantum yield of these molecules.[5-8] Thus, to explore the substitution effect at  $sp^3$  *meso* carbons, in the present work, the starting geometries were taken from the X-ray crystal structures of 6,6,21,21-tetramethyl-11,16-bis(2,6-difluorobenzene)-*meta*-benzoporphodimethene and all other substituent modifications were made on this geometry and were further optimized. (**Scheme 4.1**).

The B3LYP/BS-I optimized structures are shown in Charts 1, 2 and 3 displaying N<sub>25</sub>-H<sub>27</sub> (HB1) and N<sub>23</sub>-H<sub>27</sub> (HB2) bond lengths on varying substituents at  $sp^2$  and  $sp^3$  *meso*-carbon atoms. The labels 1, 2 and 3 are employed to represent the H atom, CH<sub>3</sub> group and Phenyl group at the  $sp^3$  *meso*-carbon atoms at 6 and 21 positions. See **Appendix-I** for Cartesian coordinate and energies of these substituted molecules. The inner geometry of the molecules is explained by the change in angles with respect to the presence of sterically hindered groups (-Ph, -Me, -H) at  $sp^3$  *meso* carbon atoms.

The core cavity of *meta*-benzoporphodimethene was measured by passing planes through various atoms as shown in **Table 4.1**. The non-bonded angles (in degrees) for these structures were measured through different planes. See **Table 4.2** for pictorial representation of these non-bonded angles. For instance, the  $17/C_6$  angles depicted the angle between the 17 tripyrin atoms mean plane (plane consisting 3 pyrrole rings and 2  $sp^2$  *meso* carbon atoms, a plane of 17 atoms; N23, C7, C8, C9, C10, C11, C12, C13, C14, C15, N24, C16, C17, C18, C19, C20, N25) and benzene ring plane viz. C1, C2, C3, C4, C5, C22). Similarly,  $17/sp^3$  represents the angle between 17 tripyrrin mean plane and a vector along the  $sp^3$  *meso* carbon atoms, i.e., C6 and C21.

The above two angles gave an idea about the orientation of benzene ring and the planarity of the *meta*-benzoporphodimethene core which in turn may affect the intramolecular hydrogen bond strength (**Table 4.1**).[11]

Certain observations can be made on analyzing the angle between the pyrrole ring plane and 17 tripyrin atoms mean plane, i.e.,  $Py_i/17$  angle where  $i=0, 1$  and  $2$ , corresponds to pyrrole ring with N24, N25 and N23 atoms, respectively (**Figure 4.1**). For instance, in molecule **3(d)**,  $Py_i/17$  ( $i= 0,1,2$ ) is nearly the similar (24.630 to 25.444 degrees), which suggests that all the pyrrole rings lies in the same plane. Because of this planarity of these pyrrole rings, it is expected that the two N-H $\cdots$ N hydrogen bond (HB1 and HB2) distances are nearly same (See **Table 4.3**).

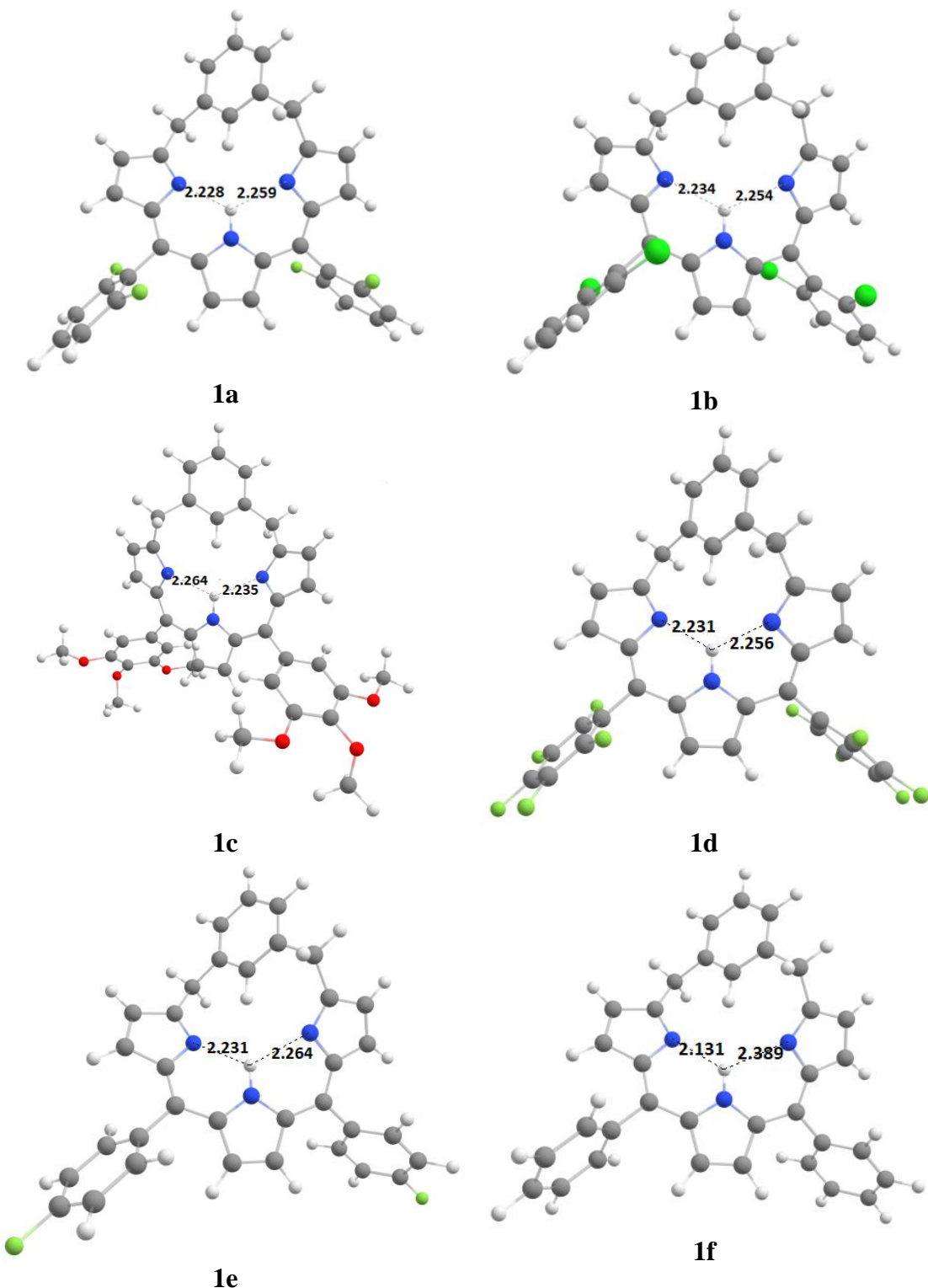


**Chart 4.1.** Geometries of H-bonded molecules along with H-bonded distances (in Angstrom) when R'=H.

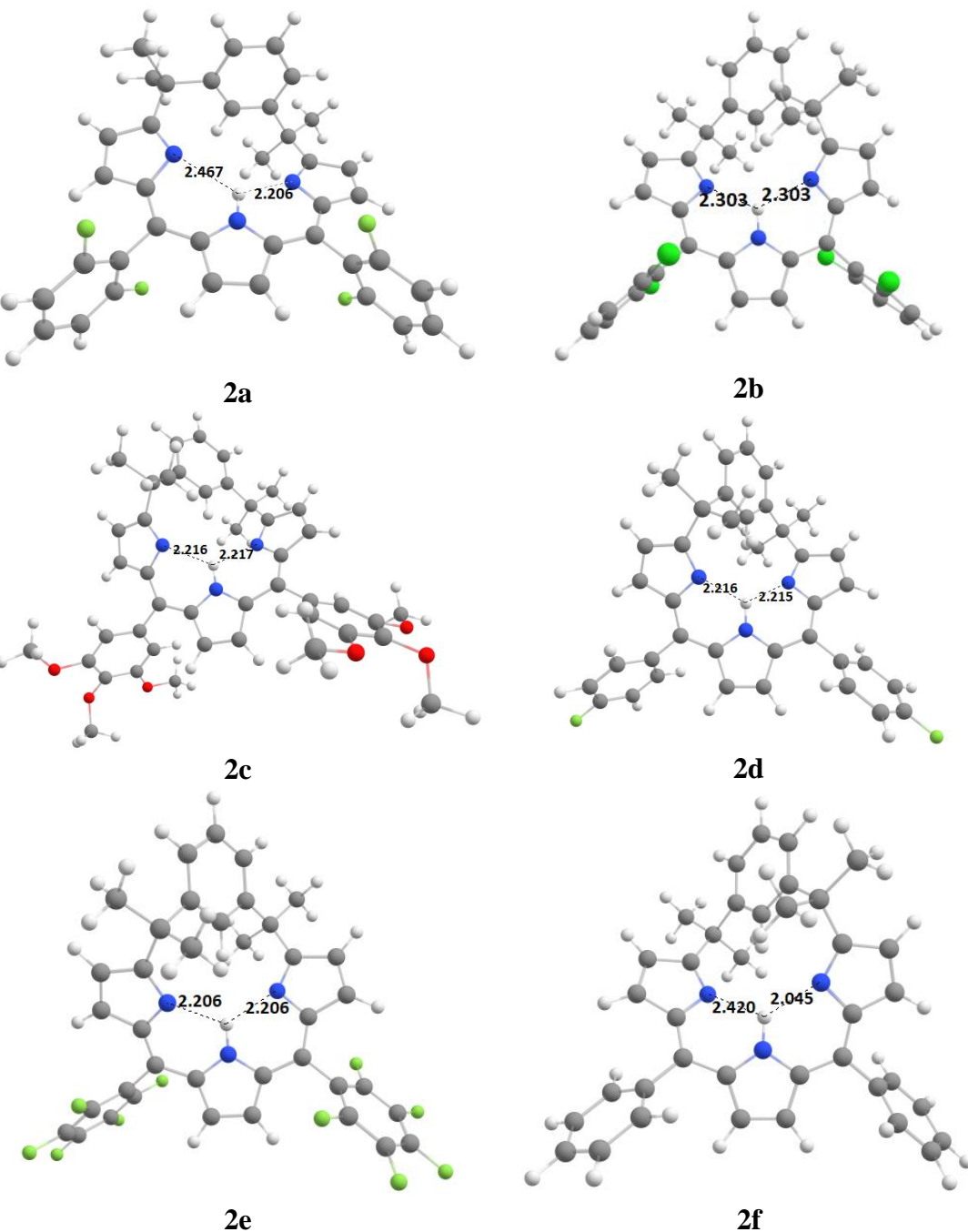


**Chart 4.2.** Geometries of H-bonded molecules along with H-bonded distances (in Angstrom) when  $R'=\text{CH}_3$ .

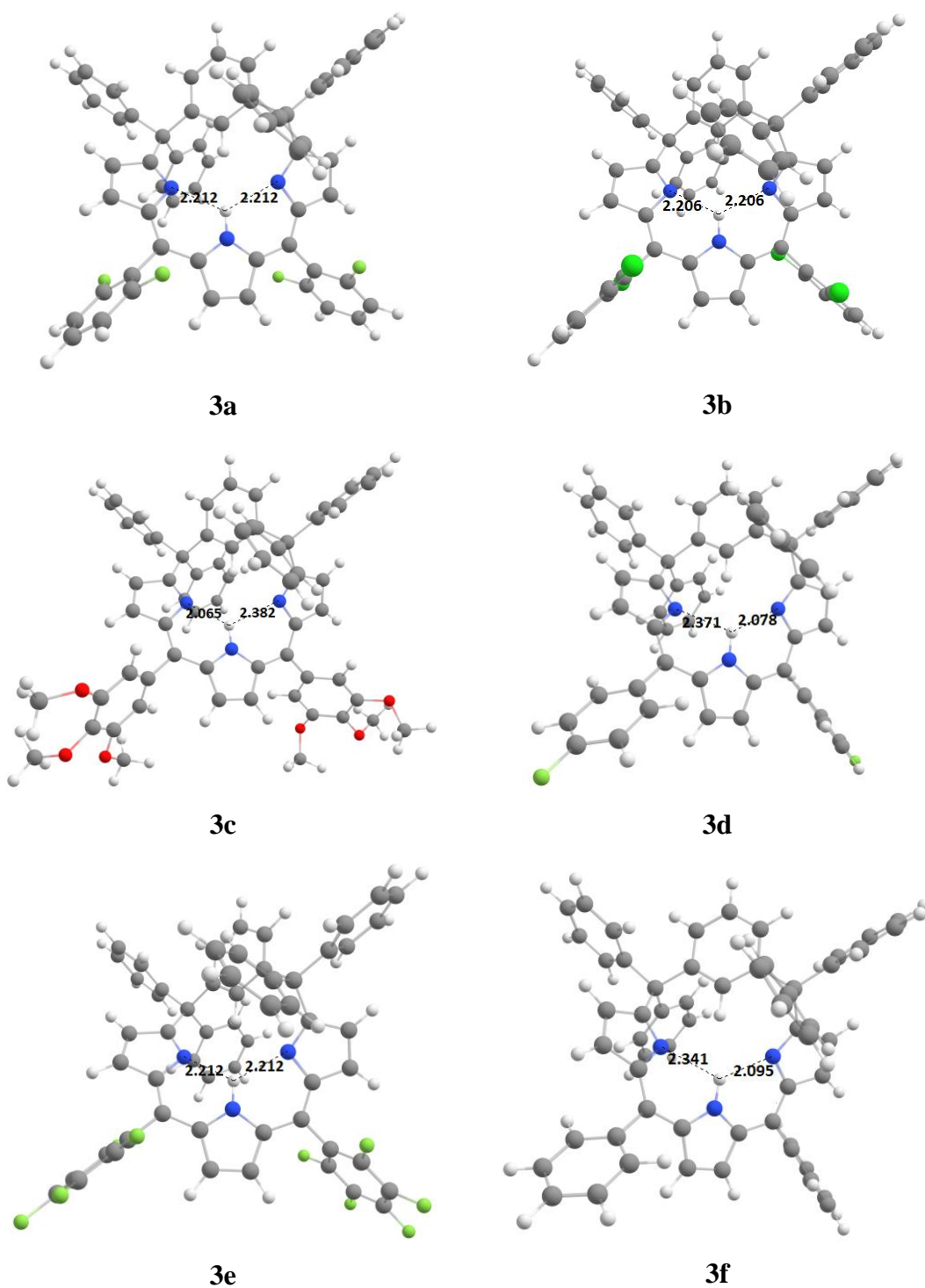


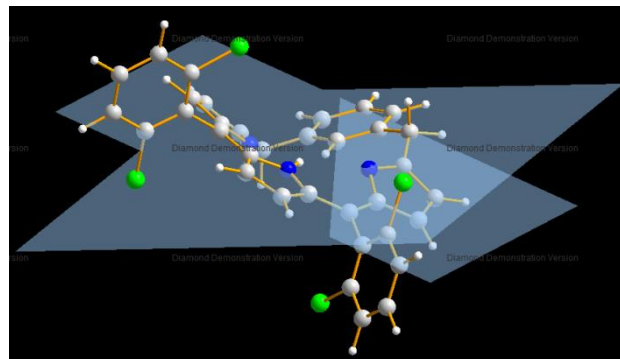
**Chart 4.3.** Geometries of H-bonded molecules along with H-bonded distances (in Angstrom) when R'=-Ph.

**Table 4.1:** Non-bonded angles (in degrees) for structures in **Charts 4.1, 4.2 and 4.3.**

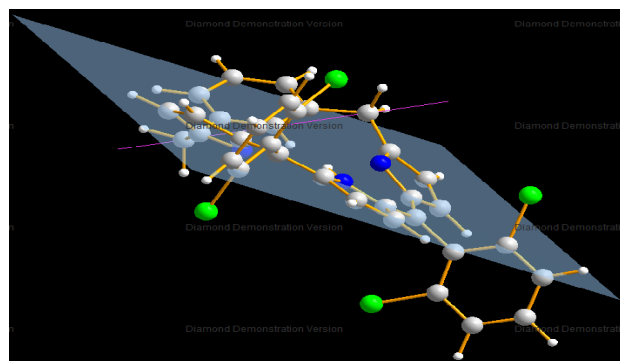
	<b>17/C<sub>6</sub></b> <sup>a</sup>	<b>17/sp<sup>3</sup></b> <sup>b</sup>	<b>P<sub>o</sub></b> <sup>c</sup>	<b>P<sub>core</sub></b> <sup>d</sup>	<b>C<sub>6</sub>/N<sub>3</sub></b> <sup>e</sup>	<b>Py<sub>o</sub>/17</b> <sup>f</sup>	<b>Py<sub>1</sub>/17</b> <sup>g</sup>	<b>Py<sub>2</sub>/17</b> <sup>h</sup>
<b>1(a)</b>	30.383	58.715	39.437	0.180	17.908	9.945	25.176	25.651
<b>1(b)</b>	30.018	59.767	37.376	0.272	19.129	9.734	23.982	24.114
<b>1(c)</b>	32.579	56.037	40.355	0.032	16.767	10.465	29.368	29.167
<b>1(d)</b>	30.550	58.657	37.825	0.109	18.101	9.901	25.414	25.576
<b>1(e)</b>	32.340	56.361	40.084	0.030	16.955	10.363	28.655	28.975
<b>1(f)</b>	30.612	57.937	38.702	2.012	18.931	11.705	21.437	31.591
<b>2(a)</b>	77.829	69.325	26.654	2.845	76.035	7.0270	22.294	12.742
<b>2(b)</b>	33.655	53.628	44.539	0.003	18.356	10.714	28.473	28.484
<b>2(c)</b>	36.467	51.117	45.009	0.001	18.008	11.300	32.794	32.816
<b>2(d)</b>	34.812	52.584	44.161	0.001	18.262	10.803	30.227	30.232
<b>2(e)</b>	36.514	51.157	44.870	0.001	18.130	10.991	32.798	32.789
<b>2(f)</b>	35.724	52.137	45.013	2.612	18.962	13.411	24.734	37.092
<b>3(a)</b>	32.505	56.446	42.949	0.003	21.629	11.633	24.829	24.817
<b>3(b)</b>	32.865	56.008	41.853	0.001	22.053	12.377	25.286	25.269
<b>3(c)</b>	35.505	54.415	45.307	2.875	22.411	13.963	34.304	20.931
<b>3(d)</b>	32.736	56.237	40.711	0.184	21.706	24.630	24.630	25.444
<b>3(e)</b>	34.970	54.830	45.258	2.513	22.389	14.501	32.701	21.443
<b>3(f)</b>	34.815	54.927	44.935	1.978	22.114	13.692	32.324	21.563

<sup>a</sup> angle between 17 tripyrin atoms mean plane and phenylene ring plane.<sup>b</sup> angle between the 17 tripyrin atoms mean plane and vector along *sp<sup>3</sup>* *meso* carbon.<sup>c</sup> dihedral angle between the four *meso* carbons C(6)-C(11)-C(16)-C(21).<sup>d</sup> dihedral angle between the inner core atoms C(22)-N(23)-N(24)-N(25).<sup>e</sup> angle between the phenylene ring plane and inner tri atom core.<sup>f,g,h</sup> angle between Pyrole Py<sub>i</sub>(i=0,1,2) rings and 17 tripyrin atoms mean plane.

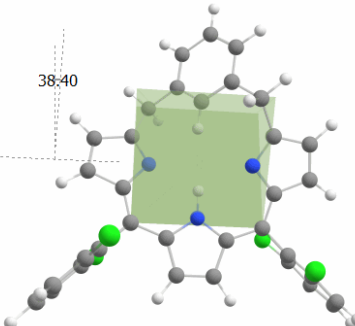
**Table 4.2.** Depiction of planes and dihedral angles reported in Table 4.1.



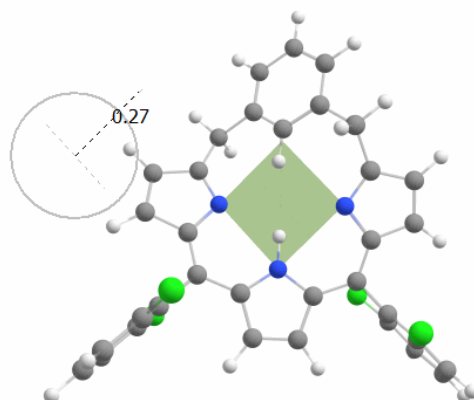
17/C6: angle between 17 tripyrin atoms mean plane and phenylene ring plane



17/sp<sup>3</sup>: angle between the 17 tripyrin atoms mean plane and vector along *sp*<sup>3</sup> *meso* carbon.

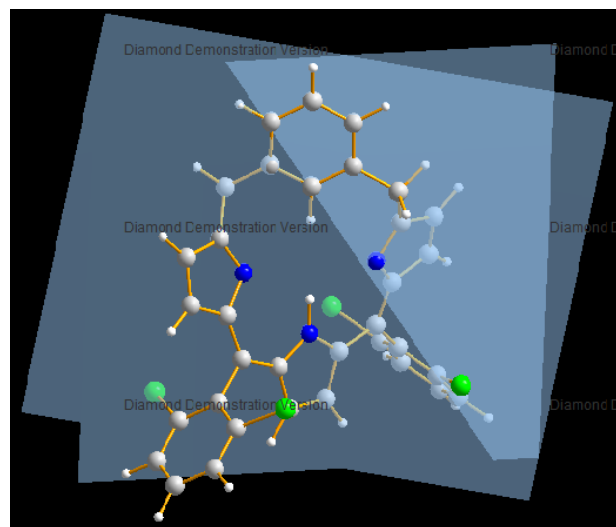


P<sub>o</sub>: dihedral angle between the four *meso* carbons C(6)-C(11)-C(16)-C(21).

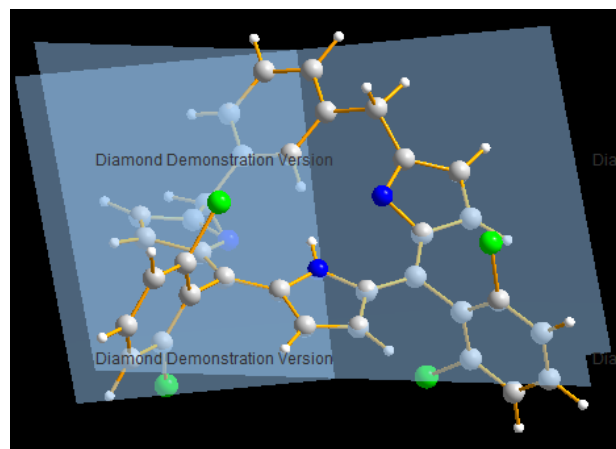


P<sub>core</sub>: dihedral angle between the inner core atoms C(22)-N(23)-N(24)-N(25).

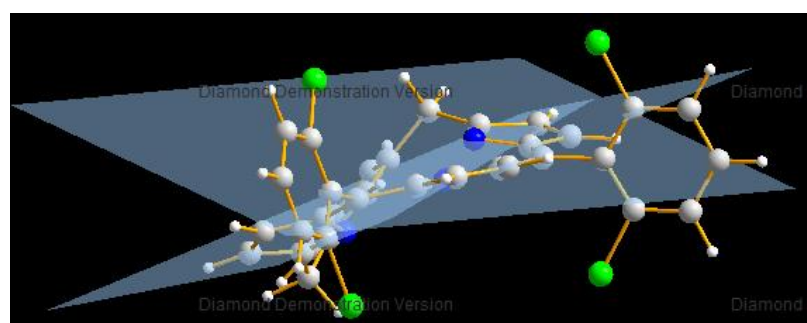
---



C6/N3: angle between the phenylene ring plane and inner tri N atom core.



Py<sub>0</sub>/17: angle between Pyrole Py<sub>0</sub> rings and 17 tripyrin atoms mean plane.



Py/17: angle between Pyrole Py<sub>i</sub> ( $i=1,2$ ) rings and 17 tripyrin atoms mean plane.

---

**Table 4.3:** Intramolecular hydrogen bond (H-Bond) energy (in kcal mol<sup>-1</sup>) and distance (in Å). See charts 4.1-4.3 for the corresponding geometries of these molecules.

Molecule	H-bond Distance (Å)		H-Bond Energy (kcal mol <sup>-1</sup> )	
	HB1 <sup>a</sup>	HB2 <sup>b</sup>	HB1 <sup>a</sup>	HB2 <sup>b</sup>
<b>1(a)</b>	2.234	2.254	8.64	7.96
<b>1(b)</b>	2.228	2.259	8.83	8.21
<b>1(c)</b>	2.264	2.235	7.13	7.69
<b>1(d)</b>	2.231	2.256	8.66	8.04
<b>1(e)</b>	2.231	2.264	7.83	7.22
<b>1(f)</b>	2.131	2.389	10.05	5.76
<b>2(a)</b>	2.467	2.206	8.05	10.15
<b>2(b)</b>	2.303	2.303	7.83	7.83
<b>2(c)</b>	2.216	2.217	6.67	6.65
<b>2(d)</b>	2.206	2.206	7.51	7.51
<b>2(e)</b>	2.216	2.215	6.75	6.76
<b>2(f)</b>	2.420	2.045	4.36	10.14
<b>3(a)</b>	2.212	2.212	7.64	7.63
<b>3(b)</b>	2.206	2.206	8.64	8.64
<b>3(c)</b>	2.065	2.382	10.33	5.69
<b>3(d)</b>	2.212	2.212	6.79	6.82
<b>3(e)</b>	2.371	2.078	5.10	0.78
<b>3(f)</b>	2.341	2.095	6.22	10.07

<sup>a</sup> HB1 corresponds to N25-H27 bond.<sup>b</sup> HB2 corresponds to N23-H27 bond.

But the same is not observed in the case of **1(d)** and **2(d)**. Thus, this planarity in **3(d)** may be attributed to the presence of -Ph groups at *sp*<sup>3</sup> *meso* positions. Planarity or flatness permits the overlapping of p-orbitals in both directions resulting in stabilization due to the delocalization of p-orbitals in the case of aromatic systems.[25,26] But, in the case of molecules like *meta*-benzoporphodimethenes,

where the ring current is attenuated due to the presence of two tetrahedral *meso* carbon atoms, planarity is still an important criterion as the stability of the inner core is greatly dependent on it.[27,28] Likewise, while studying the inner-geometry through Py<sub>i</sub>/17 (i= 0,1,2), it is observed that molecules **1(a)**, **1(b)**, **1(c)**, **1(d)**, **1(e)**, **2(b)**, **2(c)**, **2(d)**, **2(e)**, **3(a)** and **3(b)** have nearly alike Py<sub>1</sub>/17 and Py<sub>2</sub>/17 angles for their respective geometries (**Table 4.1** and **Chart 4.4**). This implies that the pyrrole rings Py<sub>1</sub> and Py<sub>2</sub> consisting of N23 and N25 atoms, respectively are coplanar in these molecules (**Figure 4.1**). Because of this co-planarity of Py<sub>1</sub> and Py<sub>2</sub> rings, one may expect that hydrogen bond distances HB1 and HB2 to be the same. However, this is not true, as the hydrogen bond length also depends on the orientation of Py<sub>0</sub> pyrrole ring consisting H27 atom, undergoing bifurcated hydrogen bonding. Also as seen in **Table 4.1**, the Py<sub>1</sub>/17 and Py<sub>2</sub>/17 angles may be approximately same for **1(d)** and **3(b)** molecules but HB1 and HB2 distances still vary for their respective geometries (**Table 4.3** and **Chart 4.4**). In other words, we can say that hydrogen bond strength in free base *meta*-benzoporphodimethene analogs is a functional of inner geometry of the molecule which is a function of the substituents at *sp*<sup>2</sup> and *sp*<sup>3</sup> *meso* positions. The substitution at *sp*<sup>3</sup> *meso*-carbon atoms also remarkably affect this planarity. For instance, in the case of **2(a)** molecule, where the ratio between P<sub>o</sub> (the dihedral angle between C6-C11-C16-C21 *meso* carbon atoms) and P<sub>core</sub> (the dihedral angle between the inner core atoms C22-N23-N24-N25), is smallest as compared to those in other molecules and hence exceptionally strong H-bond are expected. Indeed, the sum of HB1 (8.05 kcal mol<sup>-1</sup>) and HB2(10.15 kcal mol<sup>-1</sup>) is largest in **2(a)** (**Table 4.1** and

**Table 4.3**). Also the inner core consisting of a bifurcated hydrogen atom H27 (**Figure 4.1**) undergoes better interaction (with both the N atoms) when the structure of the molecule is less puckered. For example, in molecule **3(d)**, Py<sub>o</sub>/17, Py<sub>1</sub>/17 and Py<sub>2</sub>/17 angles are approximately the same (as seen in **Table 4.1**), and also the hydrogen atom H27 distance from N<sub>23</sub> and N<sub>25</sub> is same i.e. 2.212 Å and therefore, nearly same hydrogen bond energies (6.79 and 6.82 kcal mol<sup>-1</sup>) were obtained. This may further enhance the rate of metal binding in the free base compound.

In order to understand the stability of these molecules in terms of the strengthened inner core, we employed the MTA-based method (*cf. Scheme 4.1*) to estimate the energies of H-bonds in these molecules.[29] The results of estimated N-H $\cdots$ N H-bond energy are summarized in **Table 4.3** along with the respective N-H $\cdots$ N H-bond distances. As seen in **Table 4.3**, in general, the estimated H-bond energies are in agreement with the respective bond distances. For instance, the shorter H-bond length (eg. HB1 of **1(f)** and **3(c)**) results in higher hydrogen bond energy and vice versa. The estimated hydrogen bond energy also depends on the N-H $\cdots$ N angles (**Table 4.1**) and the planarity of pyrrole rings. In **Chart 4.4**, we compared estimated hydrogen bond energies in these substituted conformers with the planarity of Py<sub>o</sub>/17, Py<sub>1</sub>/17, and Py<sub>2</sub>/17 (See **Table 4.1** and **Chart 4.4**) corresponding to the pyrrole ring consisting of N<sub>24</sub>, N<sub>25</sub>, and N<sub>23</sub> nitrogen atoms, respectively (**Figure 4.1**).

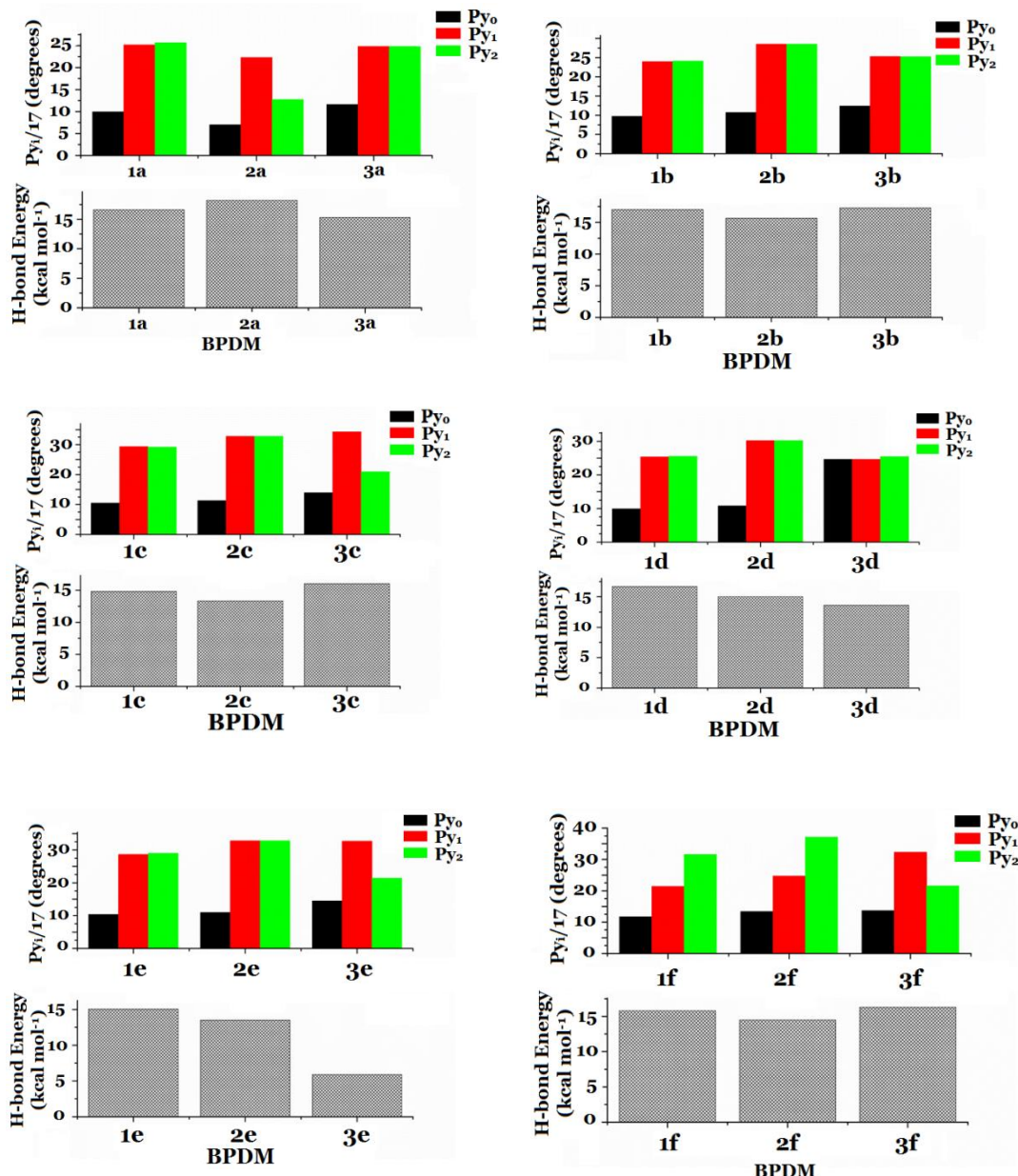


**Chart 4.4.** Comparison of inner geometry interms of Py<sub>0</sub>/17, Py<sub>1</sub>/17, and Py<sub>2</sub>/17 angles and the sum of intramolecular H-bond energy in different substituted *meta*-benzoporphodimethenes (BPDM)

#### 4.3.2. Effect of substituents at *sp*<sup>3</sup> meso-carbons

The substituents play an important role in stabilizing the porphodimethenes or phlorins. The reduced form of porphyrins, porphodimethenes or phlorins, is protected by two aryl or alkyl groups at *sp*<sup>3</sup> meso bridges. In the case of *meta*-benzoporphodimethenes, the substituents R' (**Scheme 4.3**) considerably changes the

inner core geometry and thus have a great impact on hydrogen bonding (HB1 and HB2) present in the inner core (**Figure 4.1**). For instance, molecules **1(b)**, **2(b)** and **3(b)** differes in the substitution at  $sp^3$  *meso* positions, (-H, -Me and -Ph, respectively). Upon comparing their inner geometries, it has been found that Py<sub>1</sub>/17 (28.473 degrees) and Py<sub>2</sub>/17 (28.484 degrees) angles for **2(b)** are close to each other (**Table 4.1, Chart 4.4**). This implies that the two pyrrole rings (consisting of N23 and N25) fall right opposite to each other in one plane. This was further reflected in their hydrogen bond distances (HB1 and HB2) which was found to be the same (2.303 Å). A similar feature can be seen in molecule **3(b)**. The Py<sub>1</sub>/17 and Py<sub>2</sub>/17 angles for **3(b)** were found to be similar (25.286, 25.269 degrees) but smaller than those in **2(b)**, which means the Py<sub>1</sub> and Py<sub>2</sub> rings are also in same plane but are closer to the tripyrin plane in **3(b)** than in **2(b)**. This suggests that the two hydrogen bond (HB1 and HB2) energies are similar (i.e., 8.64 kcal mol<sup>-1</sup>) but moderately larger in **3(b)** than in **2(b)** (i.e., 7.83 kcal mol<sup>-1</sup>) (**Chart 4.4**). The H-bonds HB1 and HB2 in **1(b)** are even stronger (i.e., 8.83 and 8.21 kcal mol<sup>-1</sup>, resepctively) than those in **2(b)** and **3(b)**. This may be attributed to smaller Py<sub>1</sub>/17 and Py<sub>2</sub>/17 angles (23.982 24.114 degrees); see **Chart 4.4**. It should be noted from **Chart 4.4** and **Table 4.1** that the Py<sub>1</sub>/17 angles are substantially different from Py<sub>2</sub>/17 ones in **1(f)**, **2(f)**, **3(c)**, **3(e)** and **(3f)** molecules suggesting that one of the pyrrole ring substantially deviates from the planarity. This deviation of one of the pyrrole ring could be the reason for the fact that one of the two bifurcated N-H••N hydrogen bond is substantially weak and other is strong, see **Table 4.3**. The substituents at  $sp^3$  *meso* carbons also affect the angle between the phenylene ring plane (C1, C2, C3, C4, C5, C22) and three pyrrolic nitrogen atom's plane (N23, N24 and N25), viz. C<sub>6</sub>/N<sub>3</sub> angle in **Table 4.1**. In general, with increasing

bulky substituent at  $sp^3$  *meso* carbon, C<sub>6</sub>/N<sub>3</sub> angle is seen to increase, **1(b)** is an exception. This suggest that the bulky substituents helps in strengthening the core of these molecules. Among all the molecules, **2(a)** has exceptionally different core angles (see **Table 4.1**). This is consistent with experimentally reported higher quantum yield of this molecule **2(a)**.

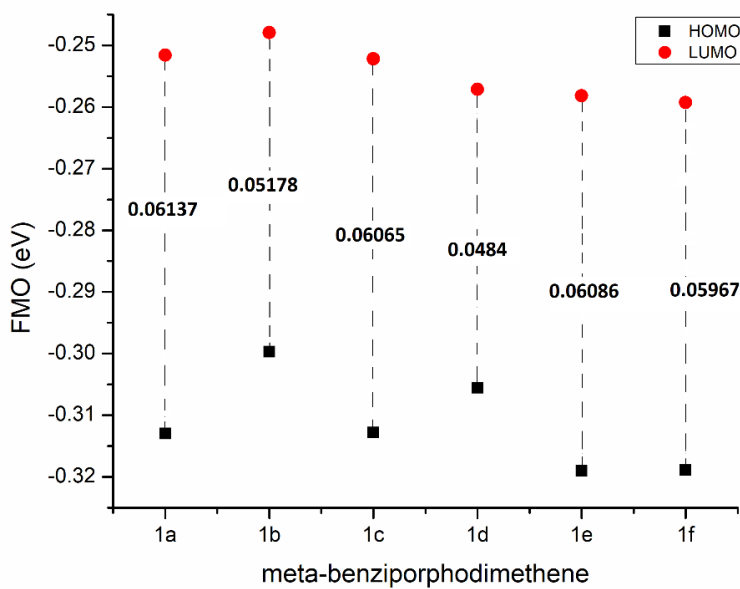
#### 4.3.3. Effect of substituents at $sp^2$ *meso*-carbons

Synthesis of benziporphodimethene is a difficult process as the compound is readily oxidizable and obtained in smaller yield ( $\approx$ 15-17%). Researchers have introduced many electron donating and withdrawing substituents as aldehyde precursors into these moieties to examine their photophysical properties.[8] It was recently reported by Kumar and coworkers that *meso* substituents may not affect the fluorescent spectra. Further, it was suggested that the aldehydic precursors play a vital role in increasing the quantum yield and stabilizing the molecule.[1,8] In this work, we have used six different substituents at 11, 16 positions (**Scheme 4.1**) and their effect were explored on the core geometry, frontier molecular orbital (FMO) energy levels, energy gaps and intramolecular hydrogen bond strength (**Chart 4.4**). **(a)** corresponding to 2,6-difluorobenzene at  $sp^2$  *meso* carbon atoms, fluoride groups here may show strong negative inductive effect and no negative mesomeric effect due to unavailability of vacant d-orbitals. Placement of chloro-substituents at ortho positions as seen in **(b)**, facilitates the 2p-Cl orbitals with the  $\pi$ -orbital of the *meso* carbon.[8] Thus, chloro substituents at 2, 6 position can exhibit strong negative mesomeric effects well as weak negative inductive effect (weak 3p-2p interactions). Ortho-chlorination facilitates smooth interactions between the halo-substituents and  $\pi$ -system of the macrocycle by locking the position of *meta*-benziporphodimethene and

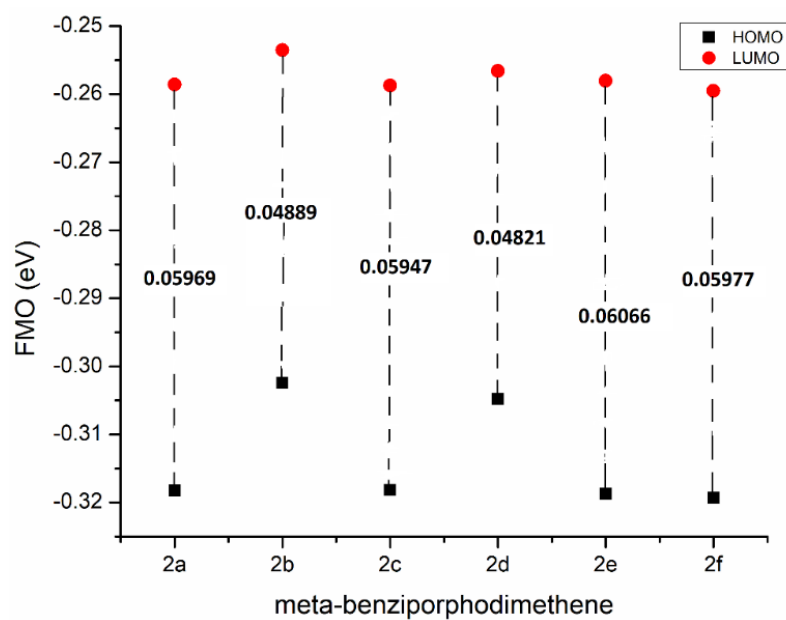
*meso* phenyl group in a perpendicular arrangement and inhibit the indirect conjugation between the induced electron withdrawing halogens and the macrocycle. The strong electronic communication between the  $\pi$ -systems of the macrocyclic ring and the ortho-chlorine overcomes the steric effect of the halogen.[8] Experimentally, it has been found that quantum yield is relatively on a higher side when *meso* phenyl (11, 16- positions) comprises electron withdrawing groups than electron donating groups.[8] Theoretical calculations of hydrogen bond energies for (**c**) systems are well in agreement with the experimental results. The hydrogen bond strengths are comparatively lower in (**c**) structure which may be accredited to three OMe groups at 3, 4, 5- positions. Methoxy group is an electron releasing group and can thus exhibit positive resonance effect, but the presence of three bulky substituents may introduce steric inhibition of resonance (SIR) effect in (**c**) systems.[30] (**d**) systems corresponding to penta-fluorobenzene at 11, 16 positions may possess strong negative inductive effect from ortho and para positions. Similarly, para-halogenation may withdraw electron density from the macrocycle which subsequently might weaken the electrostatic interactions between the macrocycle and central hydrogen atom (H27). The electron withdrawing groups stabilize the inner core, which has been documented experimentally.[8] When no substituent is present at  $sp^2$  *meso* phenyl, the system suffers a great distortion that can be seen by the asymmetric plane (**Chart 4.4**). Metalation of such non-planar moiety would be a very difficult process as the pyrrolic nitrogen atoms are not in a position to form effective coordinate bonds with such systems. Also, the total electronic energies suggested the lower stability of (**f**) systems (**Appendix-I**).

Frontier molecular orbitals (FMO) are very useful to get information about excitation properties of organic molecule.[31-33] The FMOs of all the molecules under study along with their corresponding energies in eV have been added as **Chart 4.5** to **4.7**, for visualization. The HOMO-LUMO energy levels along with their energy gaps for 1, 2 and 3 systems i.e. when R'= -H, -Me and -Ph, respectively, are as shown in **Figure 4.2**, **4.3** and **4.4** respectively. Among all the molecules studied, the band gaps for **1(b)**, **2(b)**, **3(b)**, **1(d)**, **2(d)** and **3(d)** systems viz. 0.05178 eV, 0.04889 eV, 0.04560 eV, 0.04840 eV, 0.04821 eV and 0.04644 eV, respectively, are found to be smallest, while the band gaps for (a), (c), (e), and (f) systems are nearly the same for their respective classes **1** ( ranging from 0.05967eV to 0.06137eV), **2** ( ranging from 0.05947eV to 0.06066eV) and **3** (ranging from 0.05839eV to 0.05960 eV), (R'=-H, -Me and -Ph) (**Figure 4.2**, **4.3** and **4.4**). This reveals that ortho-chlorinated (**b**) and penta-fluorinated (**d**) systems have lower band gaps, thus better bonding may be expected from these systems. The above statement can be further correlated with the Py<sub>i</sub>/17 (i=1, 2) angles which are nearly the same for their independent geometries, i.e., 23.982, 24.114 degrees for **1(b)**, 28.473, 28.484 degrees for **2(b)**, 25.286, 25.269 degrees for **3(b)**, 25.414, 25.576 degrees for **1(d)**, 30.227, 30.232 degrees for **2(d)** and 24.630, 25.444 degrees for **3(d)** as discussed above (**Table 4.1**, **Chart 4.4**). Also, the intramolecular hydrogen bond strengths were found to be comparatively higher among their respective classes **1**, **2** and **3**, i.e., when R'= -H, -Me and -Ph, respectively. For instance, HB1 and HB2 is 8.83 kcal mol<sup>-1</sup> and 8.21 kcal mol<sup>-1</sup> for **1(b)** system which is highest for R'=H (**Figure 4.1**, **Table 4.3**). HB1 for **1(f)** may appear highest which 10.05 kcal mol<sup>-1</sup> is but HB2 is 5.76 kcal mol<sup>-1</sup> which is lowest (**Table 4.3**). This variation reflects that the molecule is non-planar when R<sup>1</sup>=R<sup>2</sup>=R<sup>3</sup>=R<sup>4</sup>=R<sup>5</sup>=H at *sp*<sup>2</sup> *meso* phenyl (**Scheme 4.3**). The above statement was

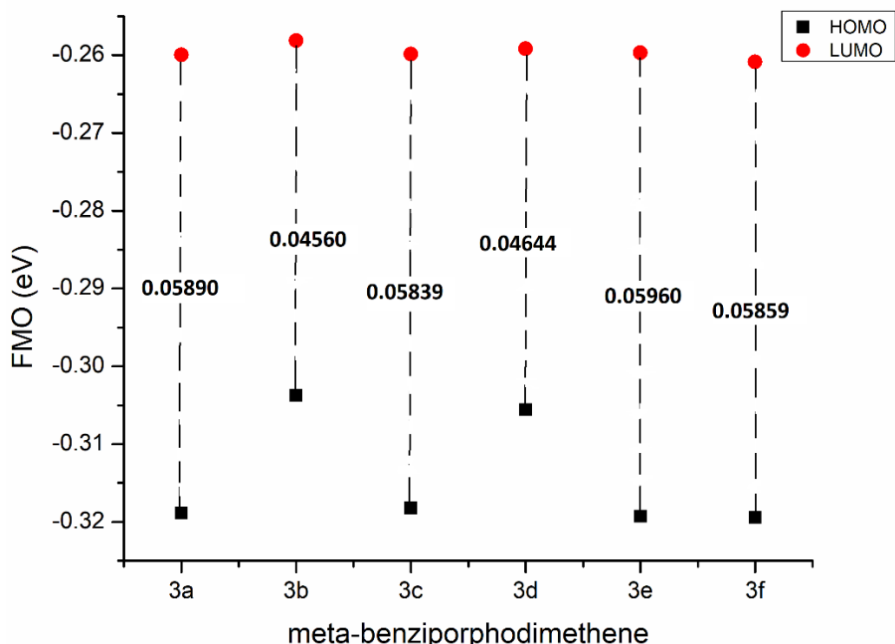
additionally supported by  $\text{Py}_i/17$  ( $i=0,1$  and 2) angles for **1(f)** molecule, i.e.,  $11.705^\circ$ ,  $21.437^\circ$  and  $31.591^\circ$ , respectively (**Table 4.1**). The difference in angles suggest that the molecule might be highly distorted. The similar variation in  $\text{Py}_i/17$  ( $i=0, 1, 2$ ) angles was seen in systems **2(f)** and **3(f)**. Thus, it may be assumed that placement of electron donating or withdrawing substituents at 11, 16  $sp^2$  *meso* phenyl, provides some planarity to the geometries of *meta*-benziporphodimethene molecules compared to **(f)** systems where  $R^1=R^2=R^3=R^4=R^5=H$  (Figure 3.1, Scheme 3). The hydrogen bond strength HB1 for systems (a), (c) and (e), are in the order **1(a)>1(e)>1(c)**, viz.  $8.64 > 7.83 > 7.13 \text{ kcal mol}^{-1}$ . The order for HB2 is **1(a)>1(c)>1(e)**. Hence, it may be assumed that presence of electron withdrawing substituents at  $sp^2$  *meso* phenyl strengthens the inner core and stronger intramolecular hydrogen bonding occurs. A similar trend of  $\text{Py}_i/17$  and hydrogen bond strengths was observed when  $R' = -\text{Me}$  and  $-\text{Ph}$ . As mentioned earlier in **section 4.3.2**, molecule 2(a) is an exception to this study.



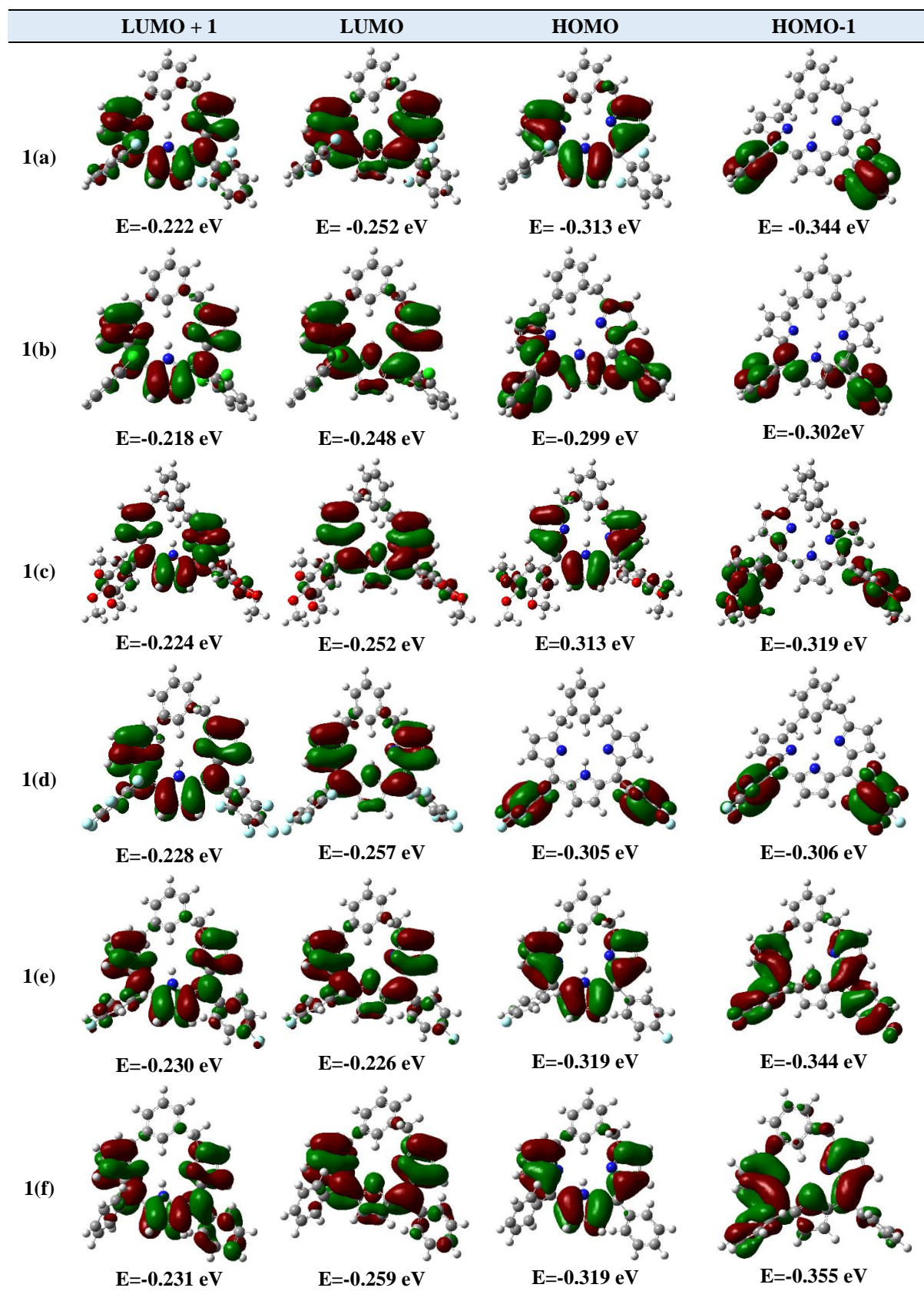
**Figure 4.2.** Frontier Molecular Orbital (FMO) energy level diagram with energy gap when  $R' = -\text{H}$  (1)

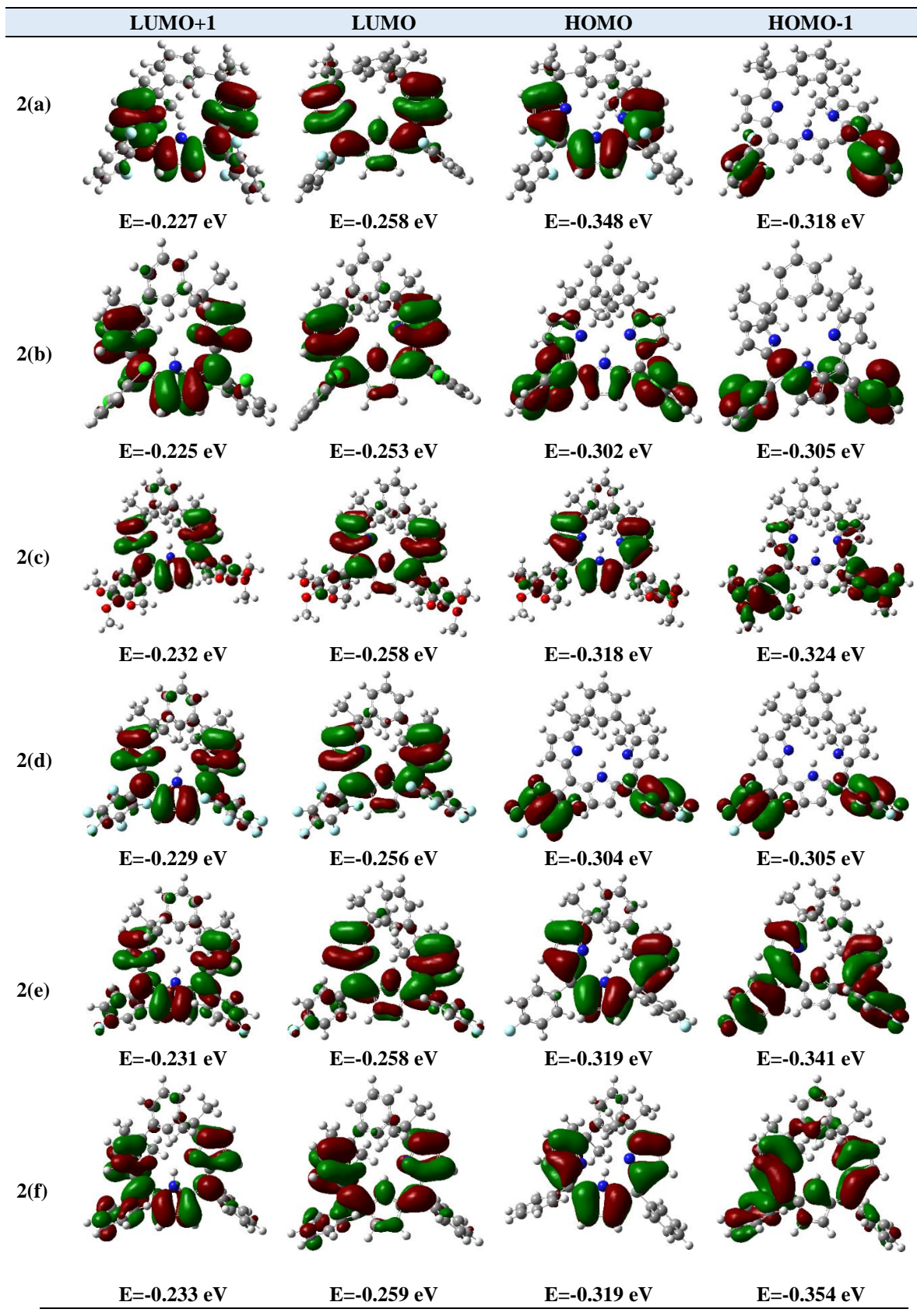


**Figure 4.3.** Frontier Molecular Orbital (FMO) energy level diagram with energy gap when  $R' = -Me$  (2).



**Figure 4.4.** Frontier Molecular Orbital (FMO) energy level diagram with energy gap when  $R' = -Ph$  (3).

Chart 4.5. Frontier molecular orbital diagrams and their respective energies for R' = -H (**1**).

Chart 4.6. Frontier molecular orbital diagrams and their respective energies for R' = -CH<sub>3</sub> (2).

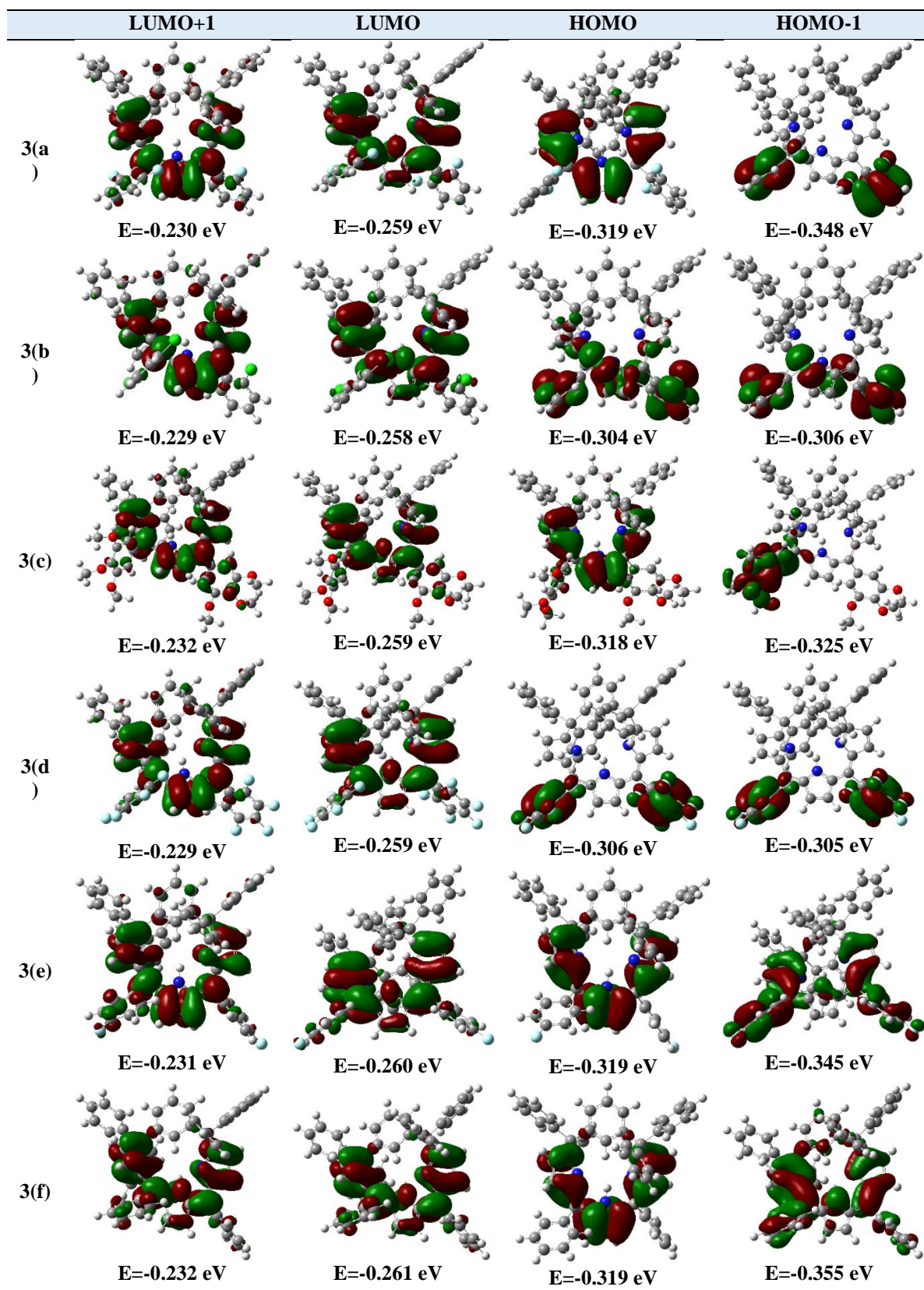


**Chart 4.7.** Frontier molecular orbital diagrams and their respective energies for R' = -Ph (3).

#### 4.4. Concluding Remarks

In this chapter, the effect of substitution on the geometry and the intramolecular hydrogen bond strength in substituted *meta*-benzoporphodimethene systems was explored with density functional theory. It is found that the substitution at both  $sp^3$  and  $sp^2$  *meso* carbon positions affect the inner core angles and hence geometry of the molecule. This further affects the bifurcated intramolecular N-H $\cdots$ N hydrogen bond strength in them. The calculated H-bond energies suggests that H-bonds in these molecules are moderately stronger (6.5 to 10.5 kcal mol $^{-1}$ ). It is found that the bulky substituents at  $sp^3$  *meso* carbon increased the intramolecular H-bond strength and hence strengthen the core of these molecules. On the other hand, ortho-chlorination and penta-fluorination of aromatic ring at  $sp^2$  *meso* position leads to increase in the H-bond strength. It is concluded that the presence of electron withdrawing substituents at  $sp^2$  *meso* phenyl strengthens the inner core and stronger intramolecular hydrogen bonding occurs.

The metal coordination is greatly dependent on the stability of the free base systems. It is worth noting that the shape of the core cavity is not symmetrical. The metal coordination can play a major role in providing the cavity a square shape. The present results of free-base *meta*-benzoporphodimethenes show that the core frame is flexible yet strong enough to accommodate sterically hindered groups.

## References

- [1] C. H. Hung, G. F. Chang, A. Kumar, G. F. Lin, L. Y. Luo, W. M. Ching, E. Wei-Guang Diau, m-Benzoporphodimethene: A New Porphyrin Analogue Fluorescence Zinc(II) Sensor. *Chem. Commun.* 8 (2008) 978–980.
- [2] M. Stepień, L. Łatos-Grażynski, Benziporphyrins: Exploring Arene Chemistry in a Macroyclic Environment. *Acc. Chem. Res.* 38 (2005) 88–98.
- [3] L. Szterenberg, L. Łatos-Grażynski, Structure and Stability of 2-Aza-21-Carbaporphyrin Tautomers Prearranged for Coordination. *Inorg. Chem.* 36 (1997) 6287-6291.
- [4] K. Berlin, E. Breitmaier, Benziporphyrin, a Benzene-Containing, Nonaromatic Porphyrin Analogue. *Angew. Chemie Int. Ed.* 33 (1994) 1246–1247.
- [5] M. Stepień, L. Łatos-Grażynski, L. Szterenberg, J. Panek, Z. Latajka, Cadmium (II) and Nickel (II) Complexes of Benziporphyrins. A Study of Weak Intramolecular Metal-Arene Interactions. *J. Am. Chem. Soc.* 126 (2004) 4566-4580.
- [6] G. F. Chang, A. Kumar, W. M. Ching, H. W. Chu, C. H. Hung, Tetramethyl-m-Benziporphodimethene and Isomeric  $\alpha,\beta$ -Unsaturated lactam Embedded N-Confused Tetramethyl-m-Benziporphodimethenes. *Chem. - An Asian J.* 4 (2009) 164–173.
- [7] G. F. Chang, C. H. Wang, H. C. Lu, L. S. Kan, I. Chao, W. H. Chen, A. Kumar, L. Lo, M. A. C. Dela Rosa, C. H. Hung, Factors That Regulate the Conformation of M-Benziporphodimethene Complexes: Agostic Metal-Arene Interaction, Hydrogen Bonding, and  $\hat{\lambda}\bullet 2,p$  Coordination. *Chem. – A Eur. J.* 17 (2011) 11332–11343.

- [8] R. K. Sharma, L. K. Gajanan, M. S. Mehata, F. Hussain, A. Kumar, Synthesis, Characterization and Fluorescence Turn-on Behavior of New Porphyrin Analogue: Meta-Benzoporphodimethenes. *Spectrochim. Acta - Part A Mol. Biomol. Spectrosc.* 169 (2016) 58–65.
- [9] M. Stepien, L. Latos-Grazynski, Tetraphenyl-p-Benzoporphyrin: A Carbaporphyrinoid with Two Linked Carbon Atoms in the Coordination Core. *J. Am. Chem. Soc.* 124 (2002) 3838–3839.
- [10] R. K. Sharma, A. Maurya, P. Rajamani, M. S. Mehata, A. Kumar, meta-Benzoporphodimethenes: New Cell-Imaging Porphyrin Analogue Molecules. *Chem. Select* 1 (2016) 3502–3509.
- [11] A. Kumar, C. H. Hung, S. Rana, M. M. Deshmukh, Study on the Structure, Stability and Tautomerisms of Meta-Benzoporphodimethene and N-Confused Isomers Containing  $\gamma$ -Lactam Ring. *J. Mol. Struct.* 1187 (2019) 138–150.
- [12] L. Pauling, The Nature of the Chemical Bond. Application of Results Obtained from the Quantum Mechanics and from a Theory of Paramagnetic Susceptibility to the Structure of Molecules. *J. Am. Chem. Soc.* 53 (1931) 1367–1400.
- [13] L. S. Kassel, The Limiting High Temperature Rotational Partition Function of Nonrigid Molecules: I. General Theory. II. CH<sub>4</sub>, C<sub>2</sub>H<sub>6</sub>, C<sub>3</sub>H<sub>8</sub>, CH(CH<sub>3</sub>)<sub>3</sub>, C(CH<sub>3</sub>)<sub>4</sub> and CH<sub>3</sub>(CH<sub>2</sub>)<sub>2</sub>CH<sub>3</sub>. III. Benzene and Its Eleven Methyl Derivatives. *J. Chem. Phys.* 4 (1936) 276–282.
- [14] P. A. Kollman, L. C. Allen, The Theory of the Hydrogen Bond. *Chem. Rev.* 72 (1972) 283–303.
- [15] M. M. Deshmukh, S. R. Gadre, L. J. Bartolotti, Estimation of Intramolecular Hydrogen Bond Energy via Molecular Tailoring Approach. *J. Phys. Chem. A* 110 (2006) 12519–12523.

- [16] M. M. Deshmukh, C. H. Suresh, S. R. Gadre, Intramolecular Hydrogen Bond Energy in Polyhydroxy Systems: A Critical Comparison of Molecular Tailoring and Isodesmic Approaches. *J. Phys. Chem. A* 111 (2007) 6472–6480.
- [17] M. M. Deshmukh, L. J. Bartolotti, S. R. Gadre, Intramolecular Hydrogen Bonding and Cooperative Interactions in Carbohydrates via the Molecular Tailoring Approach. *J. Phys. Chem. A* 112 (2008) 312–321.
- [18] P. C. Hariharan, J. A. Pople, The Influence of Polarization Functions on Molecular Orbital Hydrogenation Energies. *Theor. Chim. Acta* 28 (1973) 213–222.
- [19] W. J. Hehre, K. Ditchfield, J. A. Pople, Self-Consistent Molecular Orbital Methods. XII. Further Extensions of Gaussian-Type Basis Sets for Use in Molecular Orbital Studies of Organic Molecules. *J. Chem. Phys.* 56 (1972) 2257–2261.
- [20] A. D. Becke, Density-Functional Thermochemistry. III. The Role of Exact Exchange. *J. Chem. Phys.* 98 (1993) 5648–5652.
- [21] M. J. Frisch, G. W. Trucks, H. B. Schlegel, G. E. Scuseria, M. A. Robb, J. R. Cheeseman, G. Scalmani, V. Barone, B. Mennucci, G. A. Petersson, H. Nakatsuji, M. Caricato, X. Li, H. P. Hratchian, A. F. Izmaylov, J. Bloino, G. Zheng, J. L. Sonnenberg, M. Hada, M. Ehara, K. Toyota, R. Fukuda, J. Hasegawa, M. Ishida, T. Nakajima, Y. Honda, O. Kitao, H. Nakai, T. Vreven, J. A. Jr. Montgomery, J. E. Peralta, F. Ogliaro, M. Bearpark, J. J. Heyd, E. Brothers, K. N. Kudin, V. N. Staroverov, T. Keith, R. Kobayashi, J. Normand, K. Raghavachari, A. Rendell, J. C. Burant, S. S. Iyengar, J. Tomasi, M. Cossi, N. Rega, J. M. Millam, M. Klene, J. E. Knox, J. B. Cross, V. Bakken, C. Adamo, J. Jaramillo, R. Gomperts, R. E. Stratmann, O. Yazyev, A. J. Austin, R. Cammi, C. Pomelli, J. W. Ochterski, R. L. Martin, K. Morokuma, V. G.

- Zakrzewski, G. A. Voth, P. Salvador, J. J. Dannenberg, S. Dapprich, A. D. Daniels, O. Farkas, J. B. Foresman, J. V. Ortiz, J. Cioslowski, D. J. Fox, Gaussian, Inc. Wallingford CT, 2010.*Gaussian 09*, revision B.01.
- [22] Chemcraft - graphical software for visualization of quantum chemistry computations. <https://www.chemcraftprog.com>
- [23] N. Siddiqui, V. Singh, M. M. Deshmukh, R. Gurunath, Structures, Stability and Hydrogen Bonding in Inositol Conformers. *Phys. Chem. Chem. Phys.* 17 (2015) 18514–18523.
- [24] V. Ganesh, R. K. Dongare, P. Balanarayan, S. R. Gadre, Molecular Tailoring Approach for Geometry Optimization of Large Molecules: Energy Evaluation and Parallelization Strategies. *J. Chem. Phys.* 125 (2006) 104109.
- [25] J. Baker, P. M. Kozlowski, A. A. Jarzecki, P. Pulay, The Inner-Hydrogen Migration in Free Base Porphyrin. *Theor. Chem. Acc.* 97 (1997) 59–66.
- [26] H. R. Bigmore, J. Meyer, I. Krummenacher, H. Rüegger, E. Clot, P. Mountford, F. Breher, Syntheses, Reactivity and DFT Studies of Group 2 and Group 12 Metal Complexes of Tris(Pyrazolyl)Methanides Featuring “Free” Pyramidal Carbanions. *Chem. - A Eur. J.* 14 (2008) 5918–5934.
- [27] P. Belanzoni, M. Rosi, A. Sgamellotti, L. Bonomo, C. Floriani, A Theoretical Analysis of the Fundamental Stepwise Six-Electron Oxidation of Porphyrinogen to Porphyrins: The Energetics of Porphodimethene and Artificial Porphyrin Intermediates. *J. Chem. Soc. Dalt. Trans.* 9 (2001) 1492–1497.
- [28] D. Bhattacharya, S. Dey, S. Maji, K. Pal, S. Sarkar, Direct Incorporation of a Ferric Ion in the Porphyrinogen Core: Tetrakis(Cyclohexyl)Iron Porphyrinogen Anion with Different Conformers and Its Reaction with Iodine. *Inorg. Chem.* 44 (2005) 7699–7701.

- [29] S. R. Gadre, K. V. Jovan Jose, A. P. Rahalkar, Molecular Tailoring Approach for Exploring Structures, Energetics and Properties of Clusters. *J. Chem. Sci.* 122 (2010) 47–56.
- [30] M. B. Smith, March's Advanced Organic Chemistry; 2013; Vol. 53.
- [31] T. Sutradhar, A. Misra, Role of Electron-Donating and Electron-Withdrawing Groups in Tuning the Optoelectronic Properties of Difluoroboron-Naphthyridine Analogues. *J. Phys. Chem. A* 122 (2018) 4111–4120.
- [32] A. B. J. Parusel, T. Wondimagegn, A. Ghosh, Do Nonplanar Porphyrins Have Red-Shifted Electronic Spectra? A DFT/SCI Study and Reinvestigation of a Recent Proposal. *J. Am. Chem. Soc.* 122 (2000) 6371–6374.
- [33] Y. Mao, M. Head-Gordon, Y. Shao, Unraveling Substituent Effects on Frontier Orbitals of Conjugated Molecules Using an Absolutely Localized Molecular Orbital Based Analysis. *Chem. Sci.* 9 (2018) 8598–8607.

## CHAPTER 5

### EFFECT OF SUBSTITUTIONS AT C3-POSITION

---

#### **5.1. Introduction**

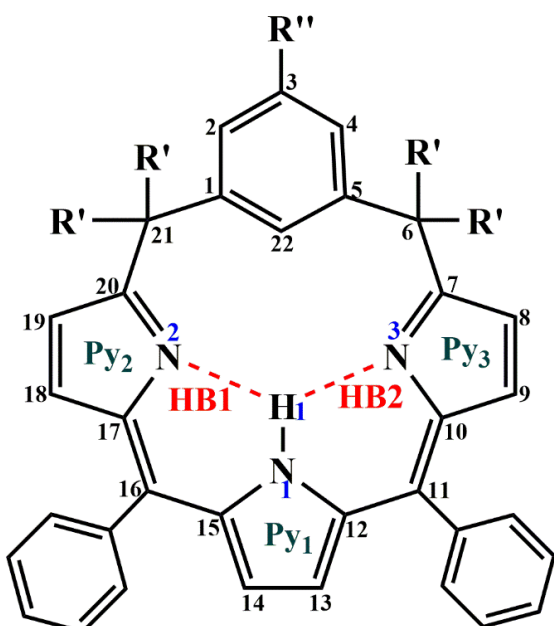
In this chapter, we intend to explore all the remaining factors that may or may not hamper the stability of free base *m*-BPDM,[1-11] thus herein we have placed different groups at C3-position alongside increasing the bulkiness at C6 and C21- positions. The basic characteristics of the substituents at C3-position invoked our interest to study its impact on the conventional (HB1 and HB2). For this purpose, the non-covalent interactions (NCI) analysis was done using Multiwfn.[12] The iso-surfaces and reduced density gradient (RDG) plots helped to visualize the presence of weak interactions at the inner core of these molecules. Further, the energies of these H-bonds was determined by molecular tailoring approach (MTA)-based approach. The optimized structures were also subjected to map molecular electrostatic potential surfaces, to understand the distribution of electron density throughout the system. The results of this work would give a clearer picture of the factors that could enhance the stability of *m*-BPDM molecules, in order to further explore its applications.

#### **5.2. Methodology**

##### ***5.2.1. Computational details***

Geometries of all the molecules studied in this work were optimized under C1 symmetry by the density functional theory (DFT) method employing B3LYP functional.[13-15] Two kinds of basis sets BS-I and BS-II i.e., 6-311G(d, p) and 6-311++G (d, p), respectively, are employed in the present work. Geometry and relative stability of these molecules were established using the B3LYP/BS-I level of theory.

The NCI analysis have been performed on these optimized systems using Multiwfn 3.8 software.[12] The iso-surfaces were generated using VMD 1.9.4a51 program. [16] In order to plot the colored 2D RDG graphs, gnuplot 5.4 software have been used. The intramolecular hydrogen bond (IHB) energy were evaluated at B3LYP-D3/BS-II level using molecular tailoring approach (MTA) based method developed by Deshmukh and Gadre.[18-24] All the calculations were performed with the Gaussian 09 program package.[25] All the molecular structures were generated using the Chemcraft program package.[26]



where,

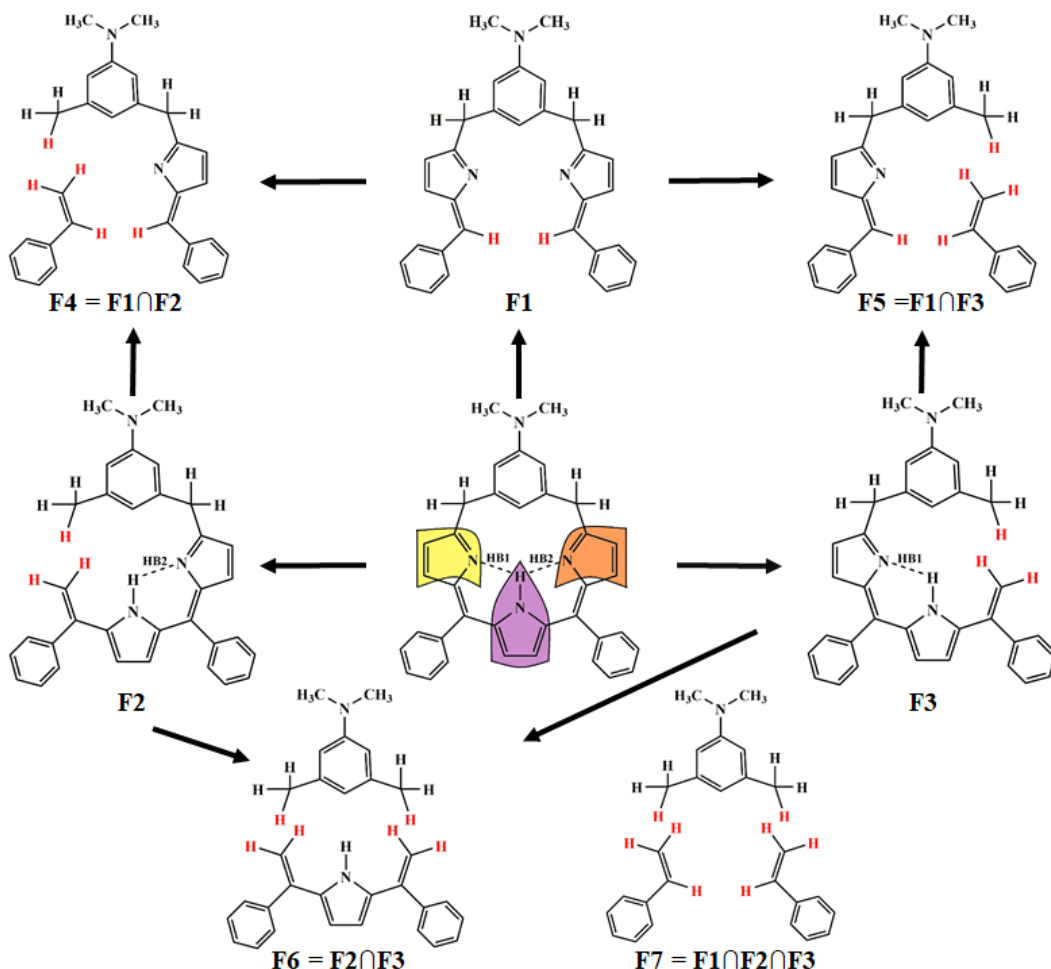
1.  $R' = H$
  2.  $R' = CH_3$
  3.  $R' = Ph$
- (a)  $R'' = N(CH_3)_2$
  - (b)  $R'' = OCH_3$
  - (c)  $R'' = CF_3$
  - (d)  $R'' = Cl$
  - (e)  $R'' = H$

**Figure 5.1.** *meta*-benziporphodimethene structures under study.

### 5.2.2. Fragmentation method for estimation of $N-H \cdots N$ hydrogen bond energy

The IHB energy in *m*-BPDM molecules were calculated using molecular tailoring approach (MTA). The general fragmentation procedure is depicted in **Scheme 5.1** for the estimation of **HB1** and **HB2** in parent molecule **1a**. As seen in **Figure 5.1**, **HB1** corresponds to the  $N1-H1 \cdots N2$  H-bond between the Py<sub>1</sub> and Py<sub>2</sub> pyrrole rings and

**HB2** corresponds to the N1-H1 $\cdots$ N3 H-bond between Py<sub>1</sub> and Py<sub>3</sub> pyrrole rings; See **Figure 5.1** for atomic numbering. In **Scheme 5.1**, the parent molecule **1a** is fragmented in three primary fragments, F1, F2 and F3. The fragment F1 was obtained by removing the Py<sub>1</sub> pyrrole ring. The fragments, F2 and F3 were similarly generated by cutting the portions of Py<sub>2</sub> and Py<sub>3</sub> rings, respectively. Here, the complete Py<sub>2</sub> and Py<sub>3</sub> rings were not cut in order to keep the hybridization of carbon atoms intact in these fragments as in the parent molecule **1a**.



**Scheme 5.1:** Fragmentation scheme for the estimation of N-H $\cdots$ N hydrogen bonds **HB1** and **HB2** in parent molecule **1a**; see Figure 5.1 and text for details.

The cut regions for all the three primary fragments are shown by appropriate colored portions. The valencies of cut regions (carbon atoms) were satisfied by adding the H-atoms at 1.0 Å along the cut C-C bonds. The added H-atoms in these fragments are shown in the red color. The secondary fragments were obtained by taking the appropriate intersections of these primary fragments. Here, intersection means a common structural part apart from added dummy H-atoms. For example, F4 is the intersection of two primary fragments F1 and F2 i.e.  $F4=F1\cap F2$ . Similarly,  $F5=F1\cap F3$  and  $F6 =F2\cap F3$  were obtained. The fragment F7 is the ternary overlap of three primary fragments i.e.  $F7=F1\cap F2\cap F3$ . The fragmented geometries were not optimized in order to prevent the conformational changes in them. The single point energy calculation at B3LYP-D3/BS-II level of theory was carried out on all the seven fragments. Using these fragment energies,  $E_{HB1}$  in the parent molecule **1a** is calculated as  $E_{HB1} = (E_{F1} + E_{F2} - E_{F4}) - E_{parent} = (-1401.444889 + (-1440.812301) - (-1232.924996)) - (-1609.344132) = 0.01193793$  a.u. = 7.49 kcal/mol. In a similar fashion, the IHB energies  $E_{HB1}$  and  $E_{HB2}$  were estimated in the substituted and unsubstituted *m*-BPDM molecules studied in the present work.

We wish to emphasize here that this  $E_{HB1}$  is estimated in the presence of hydrogen bond HB2. For instance, for the estimation of  $E_{HB1}$ , the energies of fragments F1, F2 and F4 were utilized along with energy of parent **1a**. It should be noted here that in the fragment F2, the hydrogen bond HB2 is intact. Thus, calculated  $E_{HB1}$  includes the cooperativity networking effect of other hydrogen bond (HB2). Similarly, fragment F3 utilized for the estimation of  $E_{HB2}$ , ensures the cooperativity contribution of HB1 towards HB2. If the  $E_{HB1}$  is estimated in the absence of cooperative networking of HB2, this  $E_{HB1}$  would be different than that discussed above. The difference in the

energy of HB1 in the presence of HB2 and with its absence is the cooperativity contribution of HB2 towards HB1. For details of the evaluation of cooperativity contributions in a multiple H-bonded system. [27-31]

### 5.3. Results and Discussion

As discussed above, in this work, 15 different analogues of free-base *m*-BPDM with varying the substituents at C3-position ( $R''$ ) and  $sp^3$  *meso* positions ( $R'$ ) are considered. The functional groups at C3-position considered here are:  $N(CH_3)_2$  (**a**),  $OCH_3$  (**b**),  $CF_3$  (**c**),  $Cl$  (**d**) and  $H$  (**e**). The prefix **1**, **2** and **3** in **Figure 5.1** signifies the molecules with  $R' = -H$ ,  $-CH_3$  and  $-Ph$  groups, respectively at C6 and C21 positions. Herein, we have only studied the effect of substitutions at C3-positions and not C2- and C4-positions (**Figure 5.1**) on *m*-BPDM because the synthesis of the precursor diol (for C2 and C4-positions) is not possible owing to the steric factor caused by the groups present at 1, 3-position of the diol.

#### 5.3.1. Geometries of meta-benziporphodimethene structures

The structures optimized under B3LYP/BS-I levels displaying N2-H1 (HB1), N3-H1 (HB2) (**Figure 5.1**), hydrogen bond distance is shown in **Chart 5.1**, **5.2** and **5.3**, for H atom, methyl and phenyl group, respectively placed at C6- and C21- positions. Refer to **Appendix-II** for Cartesian coordinates and energies of these structures. In order to study the inner geometry and core cavity of these structures, we have incorporated the study of non-bonded angles by passing the planes through various atoms in the molecules and calculating angles between them (refer to **Table 5.2** for visual depiction of these non-bonded angles). For instance, Py<sub>1</sub>/17 depicts the angle between the plane through middle pyrrole ring i.e., the plane involving C12, C13, C14, C15,

N1 atoms to the plane passing through tripyrrin atoms (involving all three pyrrole rings and two  $sp^2$  *meso* carbon atoms) i.e., plane involving 17 atoms- C7, C8, C9, C10, N3, C11, C12, C13, C14, C15, N1, C16, C17, C18, C19, C20, N2.[9,10] Likewise, Py<sub>i</sub>/17 ( $i = 2, 3$ ) represents the angle between the pyrrole ring consisting N2 and N3 atoms, respectively, with the tripyrrin plane or say, the mean plane of *meta*-benzoporphodimethene structures. Other non-bonded angles like 17/C6 represents the angle between the mean plane and the benzene ring of the molecule i.e., plane passing through C1, C2, C3, C4, C5, C22 atoms; 17/ $sp^3$  depicts the angle between tripyrrin plane and a vector passing through the two  $sp^3$  *meso* carbon atoms C6 and C21, etc. have also been calculated and reported in **Table 5.1**.

As seen in **Table 5.1** and **Table 5.2**, the calculated Py<sub>2</sub>/17 and Py<sub>3</sub>/17 angles are nearly similar in molecules **1d**, **2a**, **2d**, **3a** and **3d**. These nearly similar Py<sub>2</sub>/17 and Py<sub>3</sub>/17 angles suggests that the two pyrrole rings Py<sub>2</sub> and Py<sub>3</sub> are coplanar to each other with respect to the mean trypyrrin plane. The difference in the Py<sub>2</sub>/17 and Py<sub>3</sub>/17 angles for structures **1b**, **2b**, **3b** and **3c** were observed to be only moderately larger compared to the former discussed molecules, ranging from  $\pm 0.61^\circ$  to  $2.36^\circ$ . These two angles are distinctly different ( $\pm 10.15^\circ$  to  $12.36^\circ$ ) in the geometries of **1e**, **2e** and **3e**. Note that **1e**, **2e** and **3e** are the molecules without any substituents at C3-position; see **Figure 5.1**. These results suggests that the substitution at the C3-position enforces the planarity (or symmetry) to the core of C3-substituted *m*-BPDMs. Indeed, as seen in **Table 5.1**, the P<sub>core</sub> angles are very small (in between  $0.00$  to  $0.48^\circ$ ) in all the C3-substituted *m*-BPDMs (see **Table 5.2** for visualizing P<sub>o</sub> angle). On the other hand, when no substituent is present at the C3-position (R''), the Py<sub>2</sub> and Py<sub>3</sub> rings are majorly deviated from the mean plane. Also, the P<sub>core</sub> angles are distinctly larger (in between  $1.98^\circ$  to  $2.61^\circ$ ) when no substituent is present at C3-position.

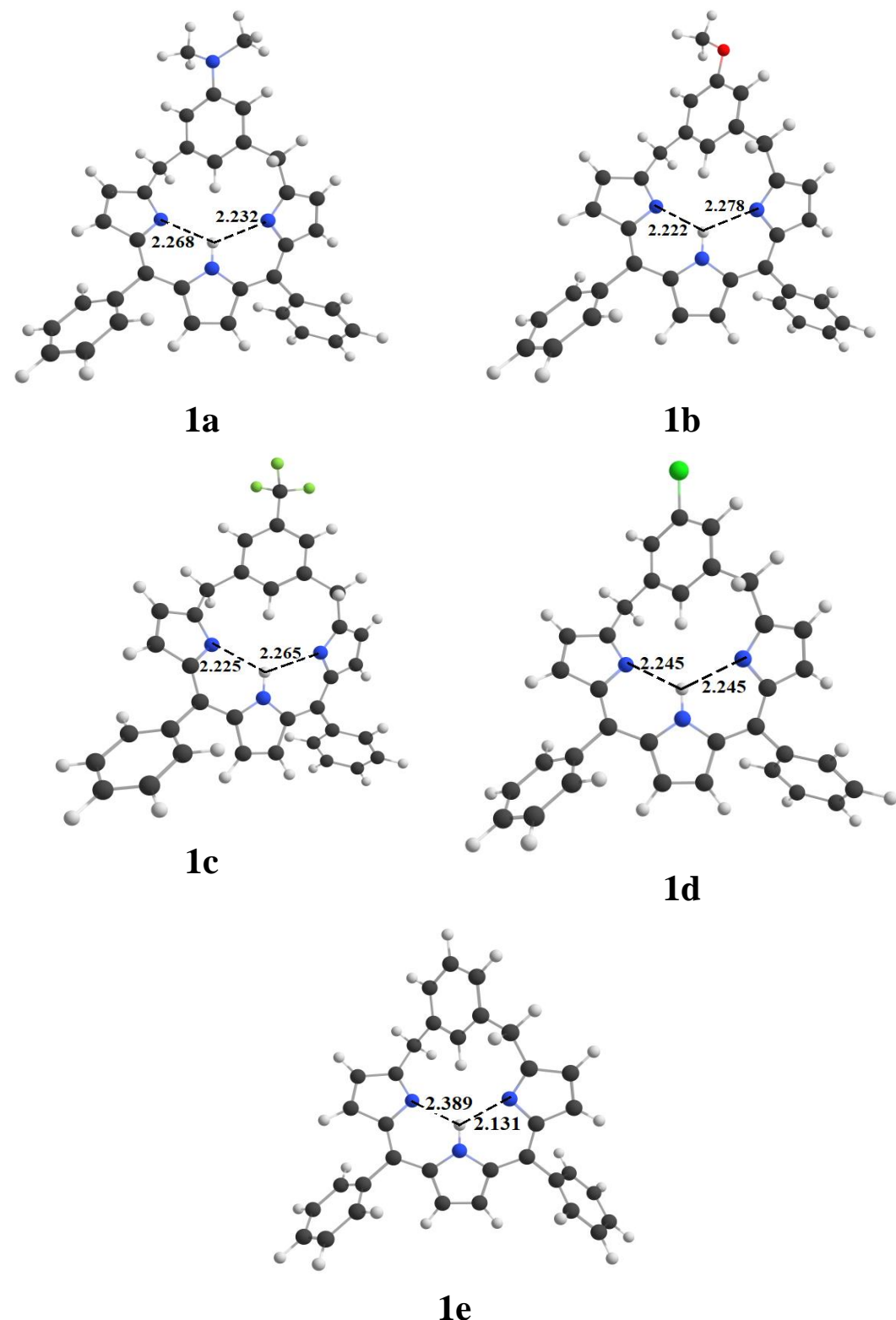


**Chart 5.1.** Geometries of molecules with H-bond distances (HB1, HB2; in Angstrom) when R' = -H (1)

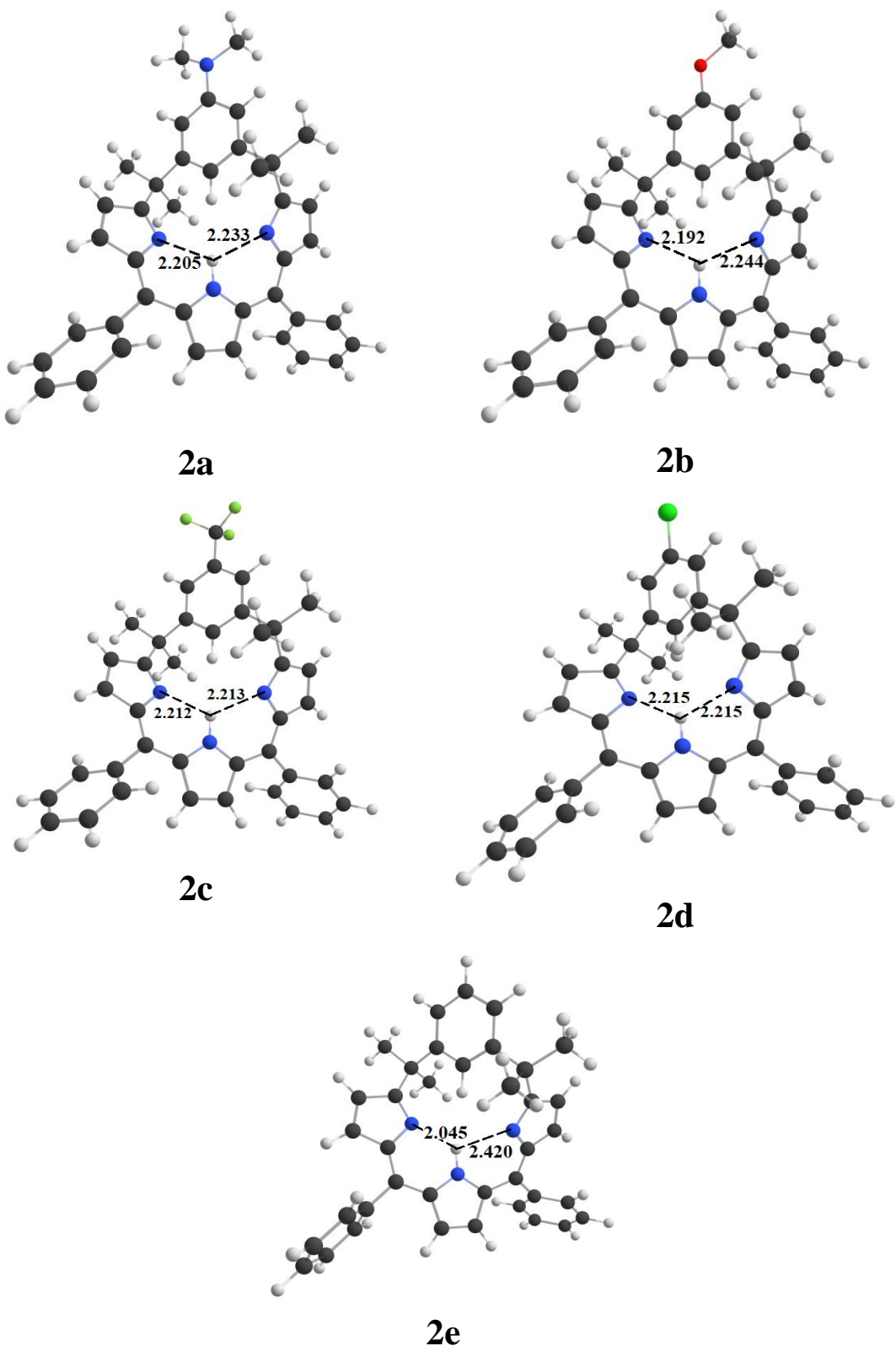


**Chart 5.2.** Geometries of molecules with H-bond distances (HB1, HB2; in Angstrom) when R' = -CH<sub>3</sub> (2)

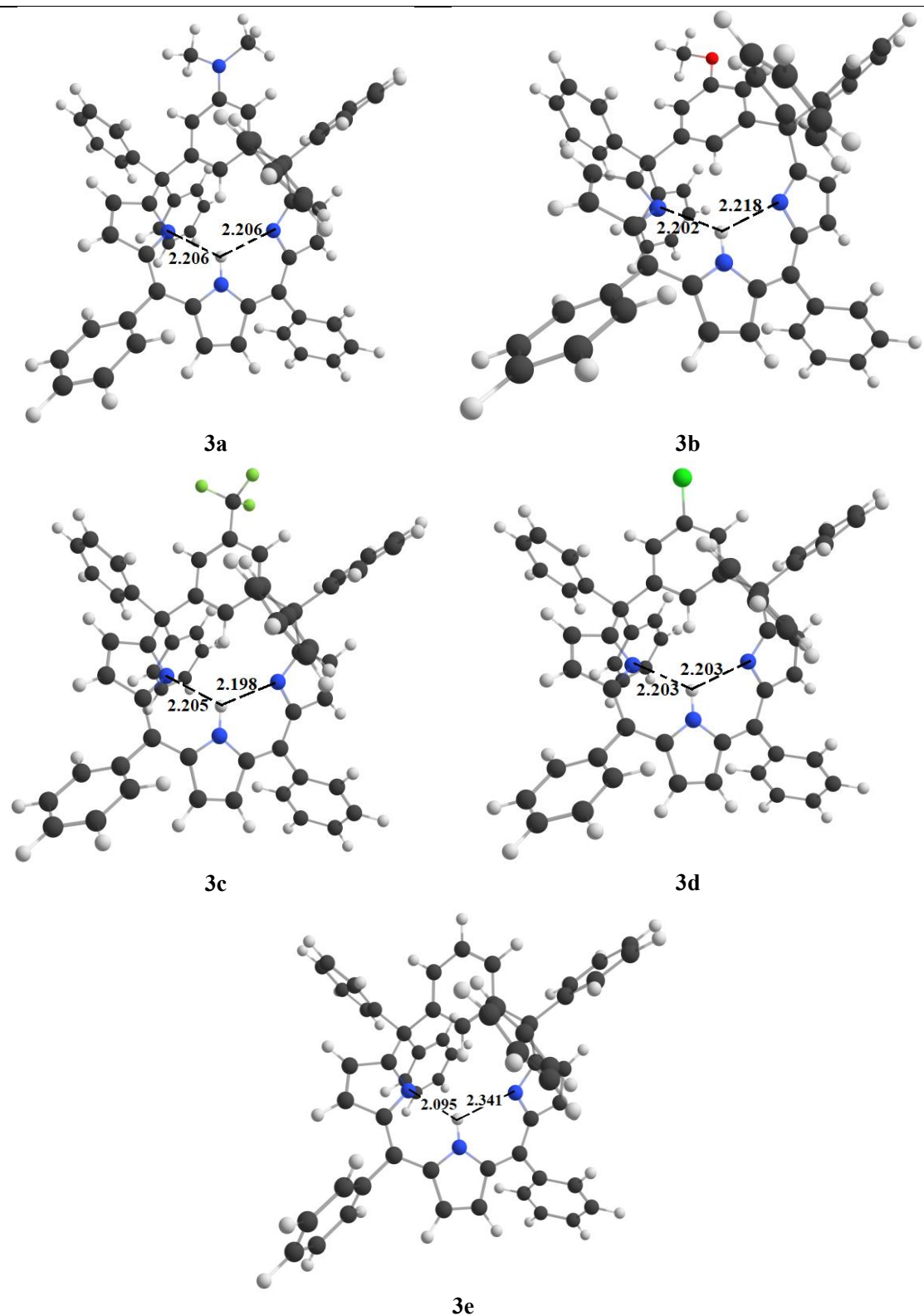


**Chart 5.3.** Geometries of molecules with H-bond distances (HB1, HB2; in Angstrom) when R' = -Ph (3).

These results suggest that the substitution affects the core structure which in turn may have affect on the strength on the N-H $\cdots$ N IHBs energies. The position of two pyrrole rings seems to be affecting the N-H $\cdots$ N IHB angles. As can be seen in **Table 5.3**, these two angles are distinctly different from each other when no substituent is present at C3-position. On the other hand, in case of C3-substituted *m*-BPDMs, these two H-bond angles have nearly similar values to each other. We shall discuss the energies of these H-bonds in the subsequent sections.

**Table 5.1.** Non-bonded angles in degrees for structures in Figure 5.1.\*

Structure	17/C <sub>6</sub> <sup>a</sup>	17/sp <sup>3b</sup>	P <sub>o</sub> <sup>c</sup>	P <sub>core</sub> <sup>d</sup>	C <sub>6</sub> /N <sub>3</sub> <sup>e</sup>	Py <sub>1</sub> /17 <sup>f</sup>	Py <sub>2</sub> /17 <sup>g</sup>	Py <sub>3</sub> /17 <sup>h</sup>
1a	32.10	56.52	40.70	0.13	16.66	10.40	28.83	28.56
1b	32.53	56.76	41.28	0.13	18.12	10.40	28.69	28.08
1c	32.09	56.81	39.70	0.09	17.43	10.50	27.88	28.20
1d	31.65	56.70	41.44	0.00	16.12	10.48	28.22	28.21
1e	30.61	57.94	38.70	2.01	18.93	11.71	21.44	31.59
2a	36.19	51.47	45.07	0.21	17.93	10.96	32.92	31.91
2b	36.23	51.51	45.12	0.17	18.11	11.06	33.39	31.03
2c	35.88	51.80	46.16	0.09	18.31	11.18	31.74	31.62
2d	35.90	51.77	46.16	0.00	18.19	11.12	31.83	31.83
2e	35.72	52.13	45.01	2.61	18.96	13.41	24.73	37.09
3a	35.21	53.82	43.18	0.00	21.21	12.39	28.17	28.17
3b	35.14	54.47	42.59	0.48	22.01	12.37	26.92	28.17
3c	35.37	53.98	45.54	0.16	22.01	12.70	27.43	28.25
3d	35.25	53.96	45.52	0.00	21.76	12.65	27.89	27.89
3e	34.82	54.93	44.94	1.98	22.11	13.69	32.32	21.56

<sup>a</sup>Angle between the 17 tripyrrin atoms mean plane and phenylene ring plane.

<sup>b</sup>Angle between the 17 tripyrrin atoms mean plane and a vector through *sp*<sup>3</sup> *meso* carbon

<sup>c</sup>Dihedral angle between four *meso* carbon atoms C6-C11-C16-C21.

<sup>d</sup>Dihedral angle between the inner core atoms C22-N3-N1-N2.

<sup>e</sup>Angle between the phenylene ring plane and inner N atom core (N3-N1-N2).

<sup>f,g,h</sup>Angle between the Pyrrole Py<sub>i</sub> (i=0,1,2) ring plane and 17 tripyrrin atoms mean plane.

\*Visuals of the planes and vectors across structure 1d have been displayed in Table 5.2.

### 5.3.2. Non-covalent Interactions

It is important to know the type of interactions present at the inner core of *m*-BPDM systems under consideration. Thus, herein the study of long-range interactions has been incorporated, which requires only the information about the molecular geometry. The prime feature of density functional theory (DFT) method is the determination of quantum-mechanical electron density ( $\rho$ ), which is further utilized to study all the possible chemical properties of a system.[32-34] Reduced gradient of density (RDG) on the other hand, is the density and its first derivative which is a dimensionless quantity that represents the divergence from homogeneous electronic distribution. The NCI index is a 2D plot based on the reduced density gradient,  $s$  and the electron density  $\rho$ , having a relation as shown in equation (1):

$$s = \frac{1}{(2(3\pi^2)^{1/3})} \frac{|\nabla\rho|}{\rho^{4/3}} \quad (1)$$

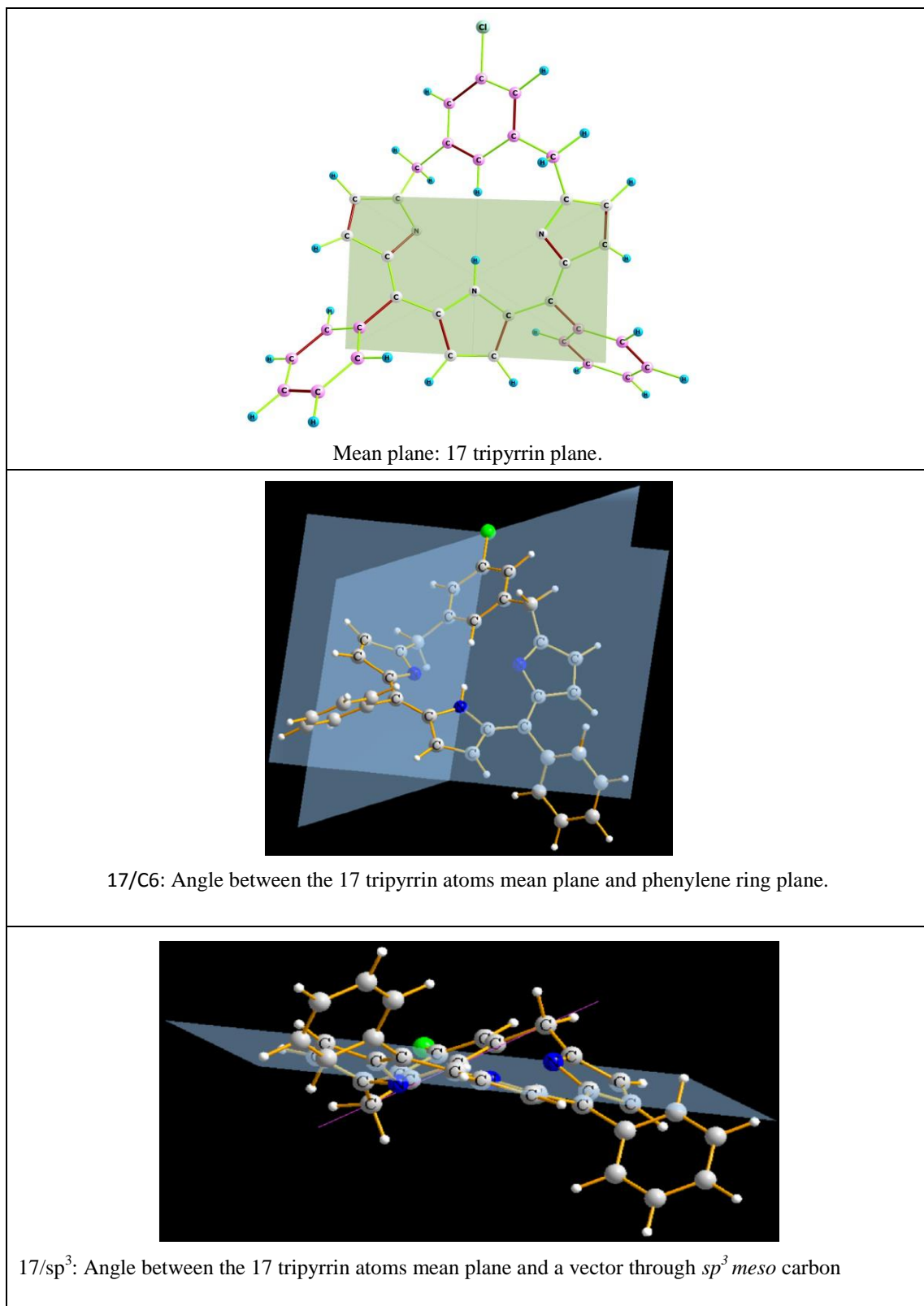
The plot not only determines the presence of long-range interactions but also enables us to find out the type of the weak interaction present in a certain system. The kind of interaction is further determined by the Laplacian of density,  $\nabla^2\rho$ . The Laplacian is the sum of three eigenvalue components  $\lambda_i$  of the electron density Hessian (second derivative) matrix, that is represented as  $\nabla^2\rho = \lambda_1 + \lambda_2 + \lambda_3$ . In a molecule,  $\lambda_3$  varies along the internuclear direction, whereas the  $\lambda_1$  and  $\lambda_2$  describes the variation of density in the plane normal to that of  $\lambda_3$  eigenvector. The value of the second eigenvector ( $\lambda_2$ ) differs in accordance to the type of interactions. For bonding interactions, such as H-bond, the value of  $\lambda_2 < 0$ , while for non-bonding interactions  $\lambda_2$  is greater than zero. The value of  $\lambda_2$  is nearly zero for weak van der Waals interactions. [35-37]

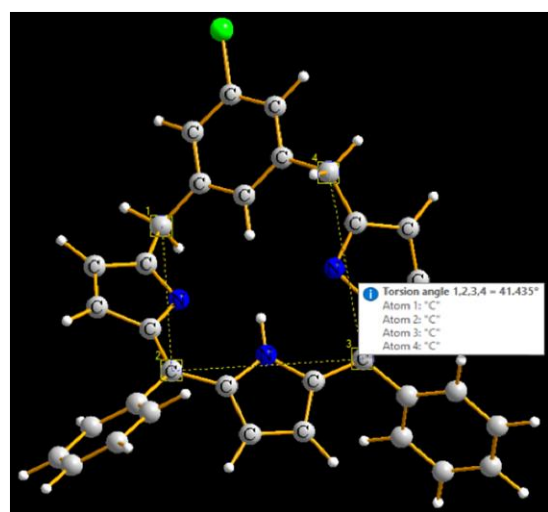
In our study, the iso-surfaces and RDG plots for all the 15 molecules were visualized. This analysis has been performed for a specific region between N2 and N3 atoms in Multiwfn software.[12] To visualize this phenomenon, colored 2D plots and iso-surfaces were drawn with the help of softwares like gnuplots [17] and VMD [16], respectively. The results have been compiled in **Chart 5.4**, **5.5** and **5.6**. All the RDG plots revealed the presence of hydrogen bond in all the systems. The presence of steric effect was also visualized by these plots. There is no van der Waals interactions present in these systems as per our results. Though the presence of H-bond has been visualized using RDG maps, it now becomes important to study the energy of these H-bonds present in these systems. Hence, we now apply molecular tailoring based approach to estimate HB1 and HB2 energies.

### **5.3.3. Effect of bulkiness at $sp^3$ meso-positions**

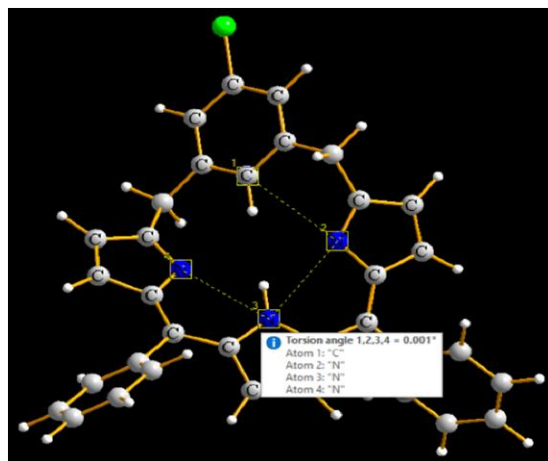
The N-H $\cdots$ N bond energy (HB1 and HB2) is greatly dependent upon the placement of N2 and N3 pyrrole rings i.e., Py<sub>2</sub> and Py<sub>3</sub> rings, respectively (**Figure 5.1**). **Table 5.3** summarizes the HB1 and HB2 bond energies, bond distances, N1-H1 bond length and N-H $\cdots$ N bond angles.

The estimated **HB1** and **HB2** for **1e**, **2e** and **3e** are merely for recognizing the difference when there is no substituents present at C3- position and  $sp^3$  meso carbon atoms. The bond distance HB1 and HB2 differ more as compared to values for other molecules. This may suggest that the pyrrole rings are not at equal distance from H1 atom (**Table 5.1** and **5.2**). It was further indicated by the deviation in N-H $\cdots$ N angle for this class (e) of molecules (**Table 5.3**). Henceforth, the deviation in the HB1 and HB2 bond energies is observed for (e) class of *m*-BPDM under study. Subsequently, shifting the focus to HB1 and HB2 bond lengths and energies of classes (a), (b), (c) and (d) of **1**, **2** and **3** type of *m*-BPDM, some interesting results were observed.

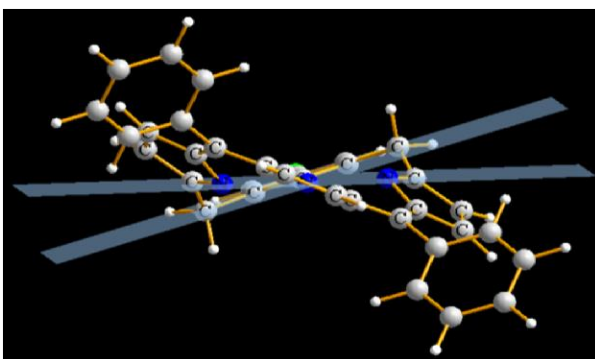
**Table 5.2.** Depiction of planes and dihedral angles discussed in section 5.3.1.



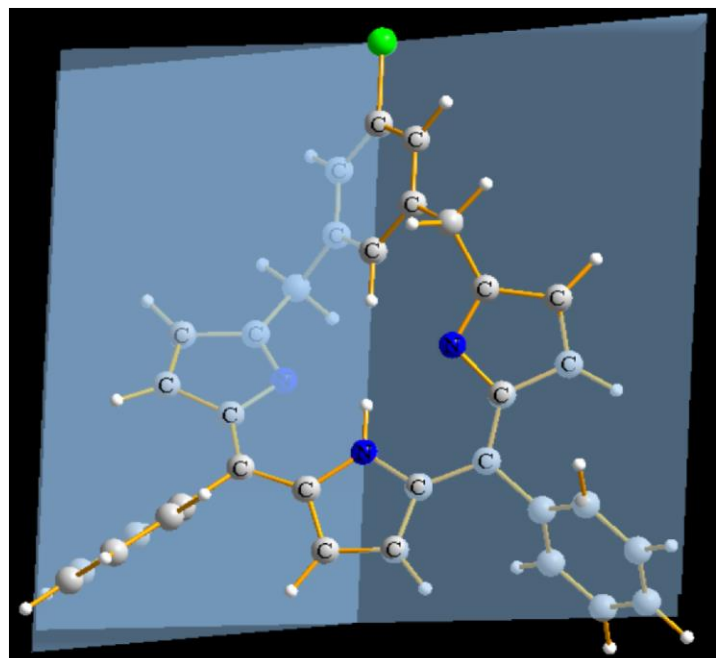
$P_o$ : Dihedral angle between four *meso* carbon atoms C6-C11-C16-C21.



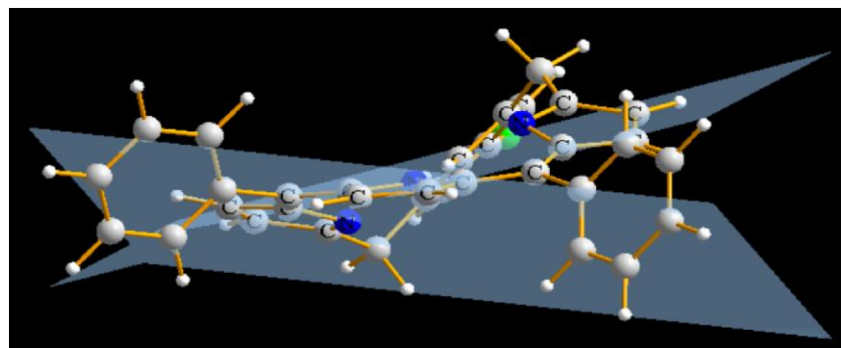
$P_{core}$ : Dihedral angle between the inner core atoms C22-N3-N1-N2.



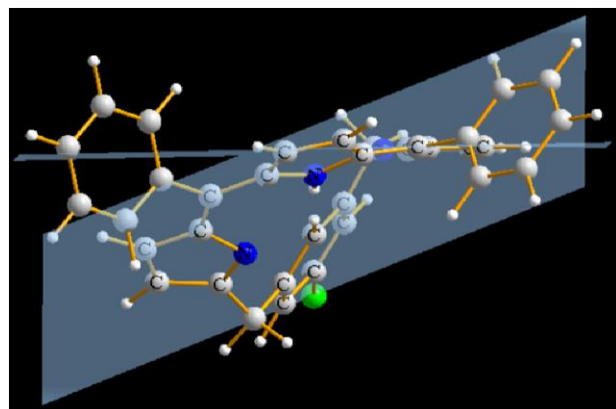
C6/N3: Angle between the phenylene ring plane and inner N atom core (N3-N1-N2).



Py<sub>1</sub>/17: Angle between the Pyrrole Py<sub>1</sub> ring plane and 17 tripyrrin atoms mean plane.



Py<sub>2</sub>/17: Angle between the Pyrrole Py<sub>2</sub> ring plane and 17 tripyrrin atoms mean plane.



Py<sub>3</sub>/17: Angle between the Pyrrole Py<sub>3</sub> ring plane and 17 tripyrrin atoms mean plane.

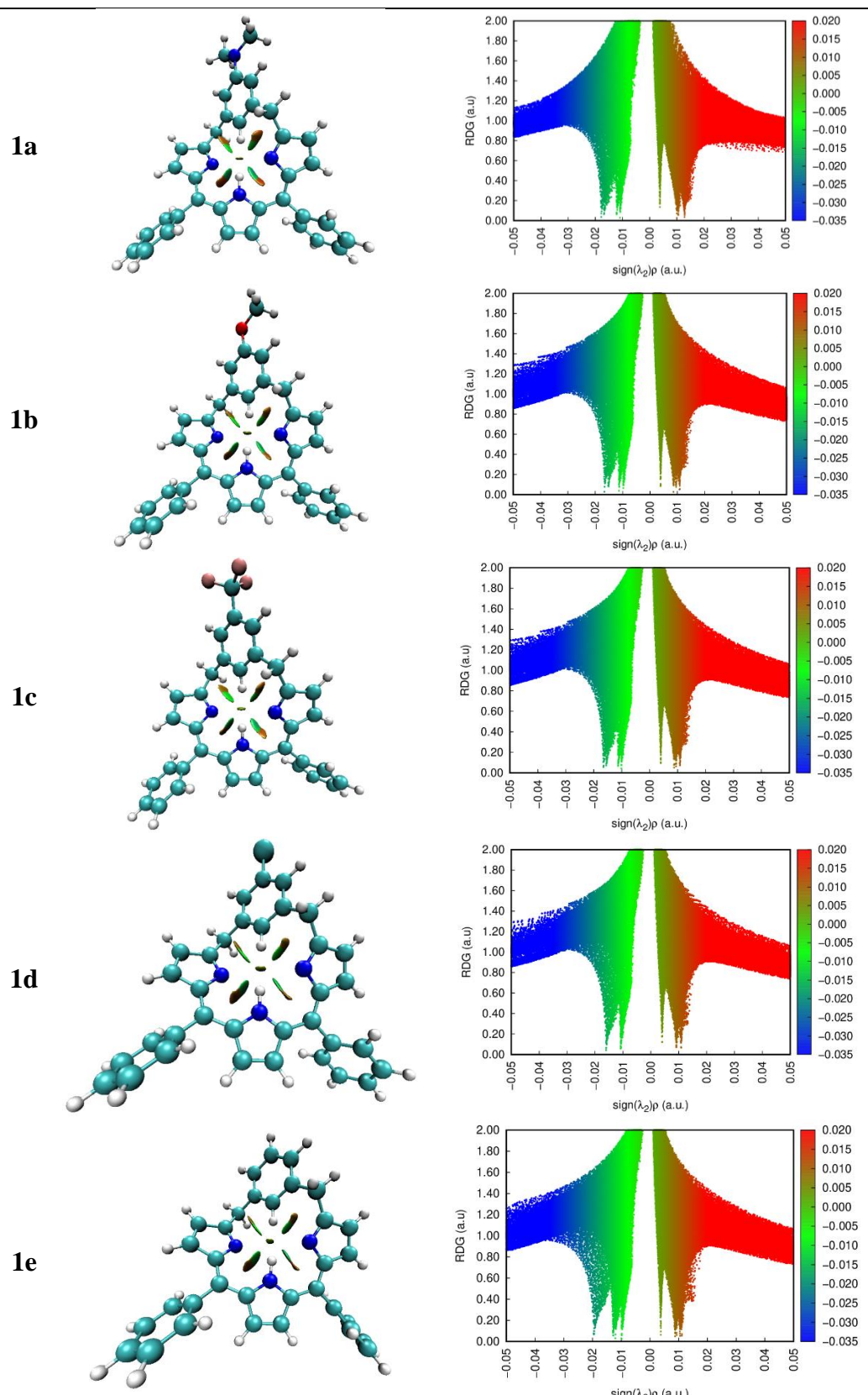


**Chart 5.4.** Non covalent interactions and RDG plots for R' = -H. (Isovalue= 0.5)

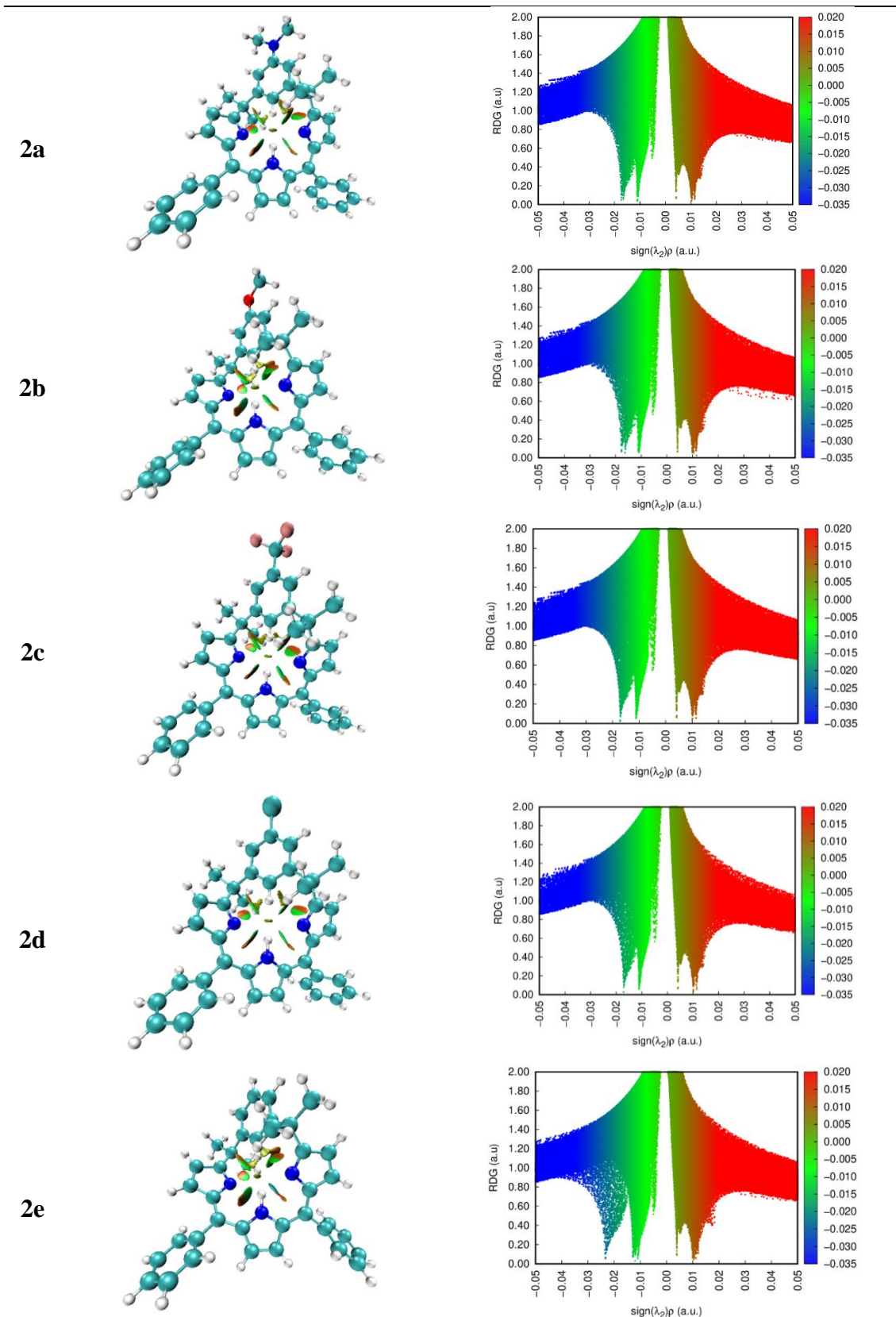


**Chart 5.5.** Non covalent interactions and RDG plots for  $R' = -CH_3$ . (Isovalue= 0.5)

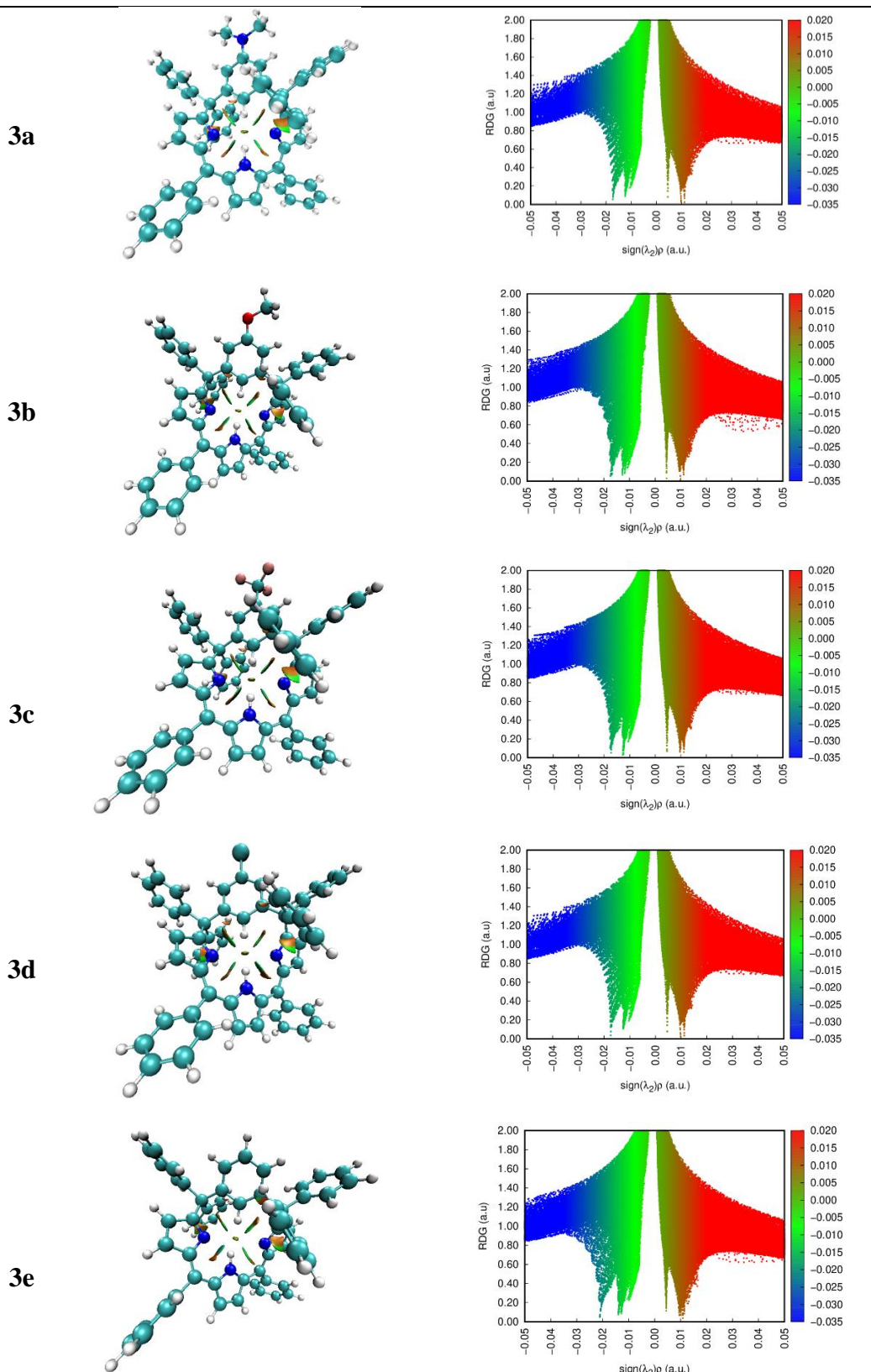


**Chart 5.6.** Non covalent interactions and RDG plots for  $R' = -\text{Ph}$ . (Isovalue= 0.5)

**Table 5.3.** Intramolecular Hydrogen Bond energy (in kcal mol<sup>-1</sup>) and distances (in Å). See Chart 5.1 to 5.3 for corresponding geometries of these molecules

	Bond Energy		Bond distance		N-H <sup>c</sup> (Å)	$\phi^d$	$\psi^e$
	(kcal/mol)		(NH•••N; Å)				
	HB1 <sup>a</sup>	HB2 <sup>b</sup>	HB1 <sup>a</sup>	HB2 <sup>b</sup>			
1a	7.49	7.63	2.27	2.23	1.014	115.25	113.13
1b	8.01	7.35	2.22	2.28	1.014	115.90	112.63
1c	7.78	7.67	2.23	2.27	1.014	115.51	113.36
1d	7.71	7.71	2.25	2.25	1.013	114.49	114.49
1e	5.92	10.05	2.39	2.13	1.016	107.45	121.27
2a	7.47	7.35	2.21	2.23	1.013	113.28	114.75
2b	7.21	6.70	2.19	2.24	1.013	115.46	112.65
2c	7.06	7.05	2.21	2.21	1.012	114.39	114.32
2d	7.05	7.05	2.22	2.22	1.012	114.28	114.28
2e	4.62	10.11	2.42	2.05	1.016	123.94	103.77
3a	8.12	8.12	2.21	2.21	1.015	115.32	115.32
3b	7.94	8.34	2.20	2.22	1.015	115.82	114.99
3c	16.03	15.97	2.21	2.20	1.014	115.38	115.76
3d	8.08	8.08	2.20	2.20	1.015	115.51	115.51
3e	6.33	10.05	2.34	2.10	1.017	122.22	108.79

<sup>a</sup>HB1 corresponds to N2-H1 bond.

<sup>b</sup>HB2 corresponds to N3-H1 bond.

<sup>c</sup>Bond distance of N1-H1.

<sup>d</sup>Angle between N1-H1-N2 in degrees.

<sup>e</sup>Angle between N1-H1-N3 in degrees.

It is well reported in literature that the delocalization of electrons in *m*-BPDM is obstructed due to the presence of two *sp*<sup>3</sup> *meso* carbon atoms at C6- and C21-position.[7,11] Hence, the increment in bulkiness at C6- and C21- positions may be held responsible for the positioning of Py<sub>2</sub> and Py<sub>3</sub> rings and thereby causing deviations in this N-H•••N IHB for their respective classes (**Figure 5.1**). The general observation

made amongst **(b)**, **(c)** and **(d)** sub-classes is such that upon increasing the bulkiness at C6- and C21- position, the IHB energy increased. For instance, **HB1** and **HB2** for R"= -OCH<sub>3</sub>, -CF<sub>3</sub> and Cl have the same order *viz.* -Ph > -H > -CH<sub>3</sub> (**Figure 5.1, Table 5.3**). Although, the estimated IHB energy value of HB1 and HB2 for **2b** is less than **1b**, but the Py<sub>i</sub>/17 (i= 2, 3) angles for R'= -CH<sub>3</sub> are less deviated compared to R'= H.

The order for energy of **HB1** when R'=H (**1**) is such that, **1b > 1c > 1a > 1d**, while for **HB2** of this class, it is **1c = 1a > 1d > 1b**, though the variation amongst **HB1** and **HB2** is not as much. The dissimilarity in the pattern of **HB1** and **HB2** may have aroused due to the difference in  $\phi^d$  and  $\phi^e$  angles. It is noteworthy that  $\phi^d$  and  $\phi^e$  for **1d** is same, and hence the bond energies **HB1** and **HB2** are equal for **1d**. Likewise, for 2d and 3d, **HB1** and **HB2** are equal owing to equal  $\phi^d$  and  $\phi^e$  angles. As observed in **Table 5.1, 5.2**, Py<sub>i</sub>/17 (i=2, 3) values for **1d**, **2d** and **3d** are also equal (**Figure 5.2, 5.3 and 5.4**). It is thus worthy highlighting here, that the presence of -Cl group at C3-position of *m*-BPDM may be responsible for this planarity in these structures, irrespective of the bulky groups present at C6- and C21- positions.

The order of energy for **HB1** and **HB2** when R'= CH<sub>3</sub> (**2**) is **2a > 2b > 2c ≥ 2d** and **2a > 2c = 2d > 2b**, respectively. It has been observed that the estimated energy of **HB1**, **HB2** for **2c** and **2d** are nearly the same i.e., (7.06 kcal/mol) and (7.05 kcal/mol), respectively and so is their  $\phi^d$  and  $\phi^e$  angles. **2a** and **2b** showed deviation in  $\phi^d$  and  $\phi^e$  angles, and thus the IHBs for their respective geometries varied. Although, the range of the IHB energies for R'= -CH<sub>3</sub> (**2**) lies between (7.05 to 7.47 kcal/mol) for **HB1** and (6.70 to 7.35 kcal/mol) for **HB2**, which implied for subclasses **a**, **b**, **c** and **d**, the **HB1** and **HB2** did not show much divergence. The IHB energies were quite contrasting in case of R'= -Ph (**3**). The

order of energy for **HB1** and **HB2** for this class is **3c > 3a > 3d > 3b** for **HB1** and **3c > 3b > 3a > 3d** for **HB2**. Exceptionally high IHB energies is observed for **3c** molecule. It must not be ruled out that the IHB energies of **3a**, **3b**, **3c** and **3d** are on the higher side compared to all the other geometries under study. This may be attributed to the presence of bulky phenyl groups at C6- and C21- positions. The molecular electrostatic potential surface of **3c** (**Chart 5.9**), discussed in later section of this chapter, also showed electron deficiency at H1 atom (displayed via blue region). The  $\phi^d$  and  $\phi^e$  angles for **3a**, **3b**, **3c** and **3d** were also found to be in a close proximity each other in their respective systems, suggesting the two pyrrole rings i.e., Py<sub>2</sub> and Py<sub>3</sub> lied nearly in the same plane to each other and are equidistance from H1 atom. The trend of these systems invoked our interest to study the effect of substituents at C3-position upon the geometry and inner-core strength of *m*-BPDM molecules.

#### **5.3.4. Effect of substitutions at C3-positions**

As expected by the substituent placed at C3- position of the phenyl ring of *m*-BPDM, change in the electron density may occur due to their presence. In order to understand this distribution of electron density, molecular electrostatic potential (MESP) surfaces were studied (**Chart 5.7**, **5.8** and **5.9**). The MESP surfaces depicts the dimension and overall charge distribution of a molecule with respect to the negative, positive and neutral electrostatic charge, in the form of electron density represented by different colors. It thus gives the insights to chemically reactive sites of the molecule. The nucleophilic sites or electron rich regions are denoted by red while blue color displayed electron deficient centers and neutral sites were shown by other colors on the scale (**Chart 5.7**, **5.8**, and **5.9**). [38-41] The region around N1-H1 indicated blue

color, thus a good H-bond donor capacity is contemplated from this site and thus it may foreshow typically strong IHB energy.

The substituent  $R'' = N(CH_3)_2$ , is expected to behave as an electron-withdrawing group, due to the electronegativity of N atom. The lone pair on N atom may not participate in the delocalization of electrons with the phenylene ring of *m*-BPDM, owing to the steric inhibition of resonance (SIR) effect, which may lead to shifting of the lone pair out of the resonating plane. Thus, this group can only exhibit negative inductive effect (-I). But, the -I effect is operative up to 3 adjacent carbons only (**Figure 5.2 (i)**). For  $R'' = OCH_3$ , the methoxy group is expected to show positive mesomeric effect, making the *ortho* and *para*- groups electronically rich centers as shown in **Figure 5.2(ii)**.

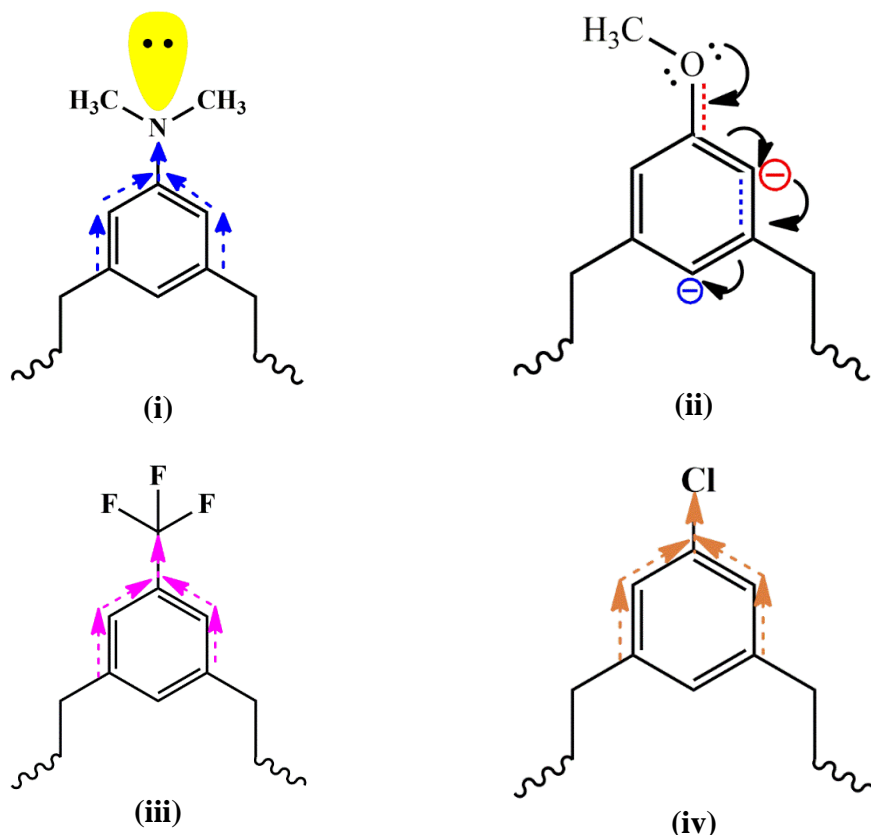


**Figure 5.2.** Effect of substituents at C3-position on the phenylene ring.

When R"= CF<sub>3</sub>, exceptionally high **HB1** and **HB2** energy values were observed for **3c** molecule. It may be attributed to the presence of the strong electron-withdrawing nature, (-I) effect of CF<sub>3</sub> group. The 2p-2p orbital interaction occurring in this molecule, summed up with the bulkiness of -Ph group placed at C6- and C21-position may have played a major role in this (**Figure 5.2 (iii)**). The N1-H1 bond in **Chart 5.9 (3c)** is in blue region, hence it also gives significant idea about the electron deficiency at this H atom and the electron richness at N2 and N3 is also visual (red region). Another unusual characteristic observed in this particular structure (3c) is that, the C3-subsituted phenyl ring showcased blue color while for all the other structures under consideration, nucleophilicity has been visualized on this ring. This suggested that the electron density is majorly pulled by the -CF<sub>3</sub> group. Additionally, the two bulky -Ph (R') groups further cancel out the distortion that could have been there, had the molecule been unsubstituted (like **3e**), thus nearly same  $\phi^d$  and  $\phi^e$  were observed (**Table 5.3**). Therefore, we may interpret this occurrence of high **HB1**, **HB2** value for this particular molecule. Another interesting fact noticed in conventional IHB is that for R"= -Cl (**d**), the values of **HB1**, **HB2** as well as  $\phi^d$ ,  $\phi^e$  angles viz, (7.71 kcal/mol; 114.49 degrees), (7.05 kcal/mol; 114.28 degrees) and (8.08 kcal/mol; 115.51 degrees) for classes **1**, **2** and **3**, respectively, are the same (**Table 5.3**). Thus, we may infer that -Cl group is providing some kind of planarity to *m*-BPDM molecules through its negative inductive effect (**Figure 5.2 (iv)**). Also, chloro-group can facilitate the smooth interaction of 2p-Cl orbital with the  $\pi$ -cloud system of the macrocycle (weak 2p- 3p interactions). This may be responsible for imparting this planarity to **1d**, **2d** and **3d** molecules.

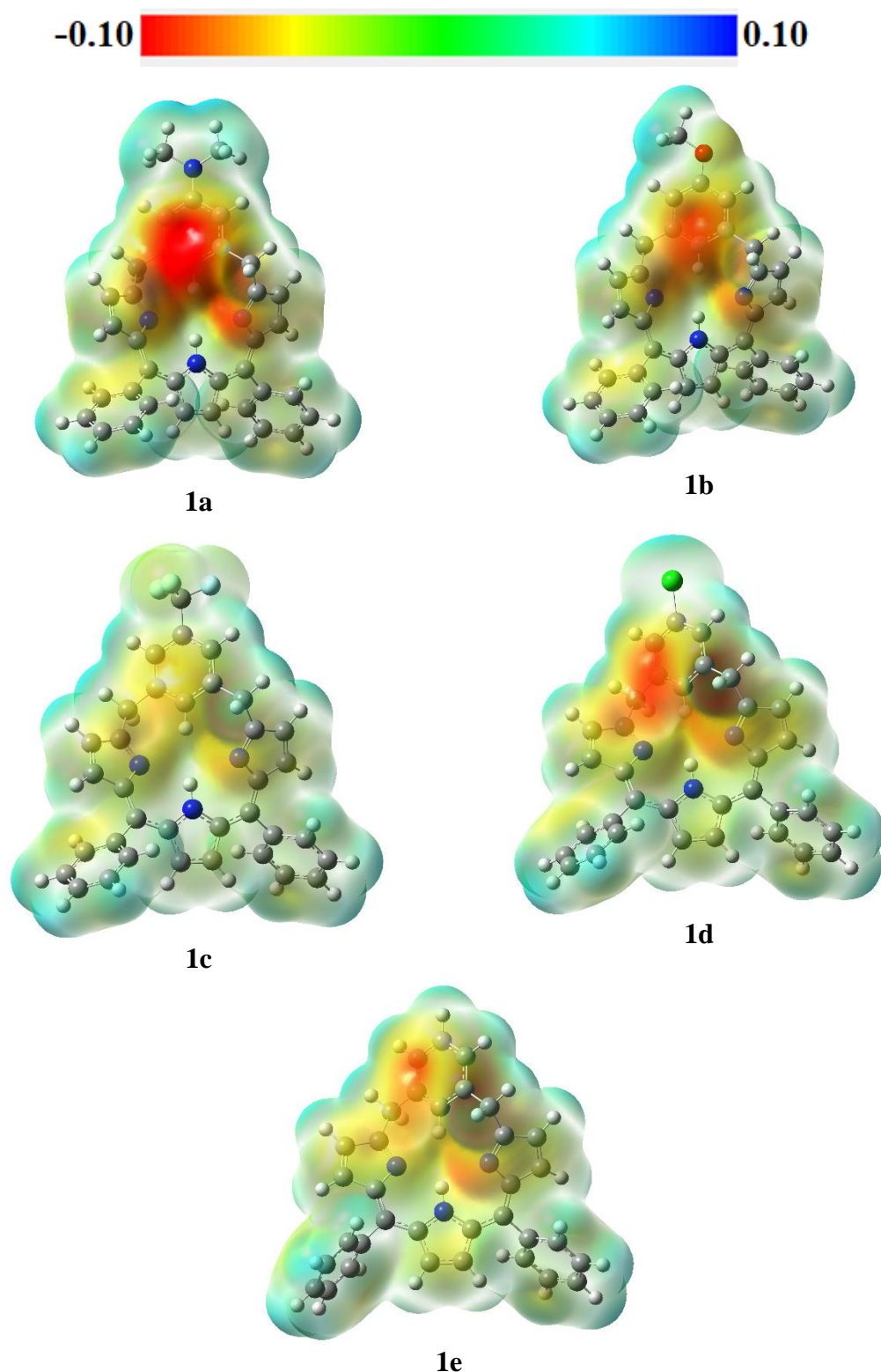


**Chart 5.7.** MESP surfaces of *m*-BPDM molecules when R' = -H. The electron density isosurface of value 0.001 a.u. was chosen.

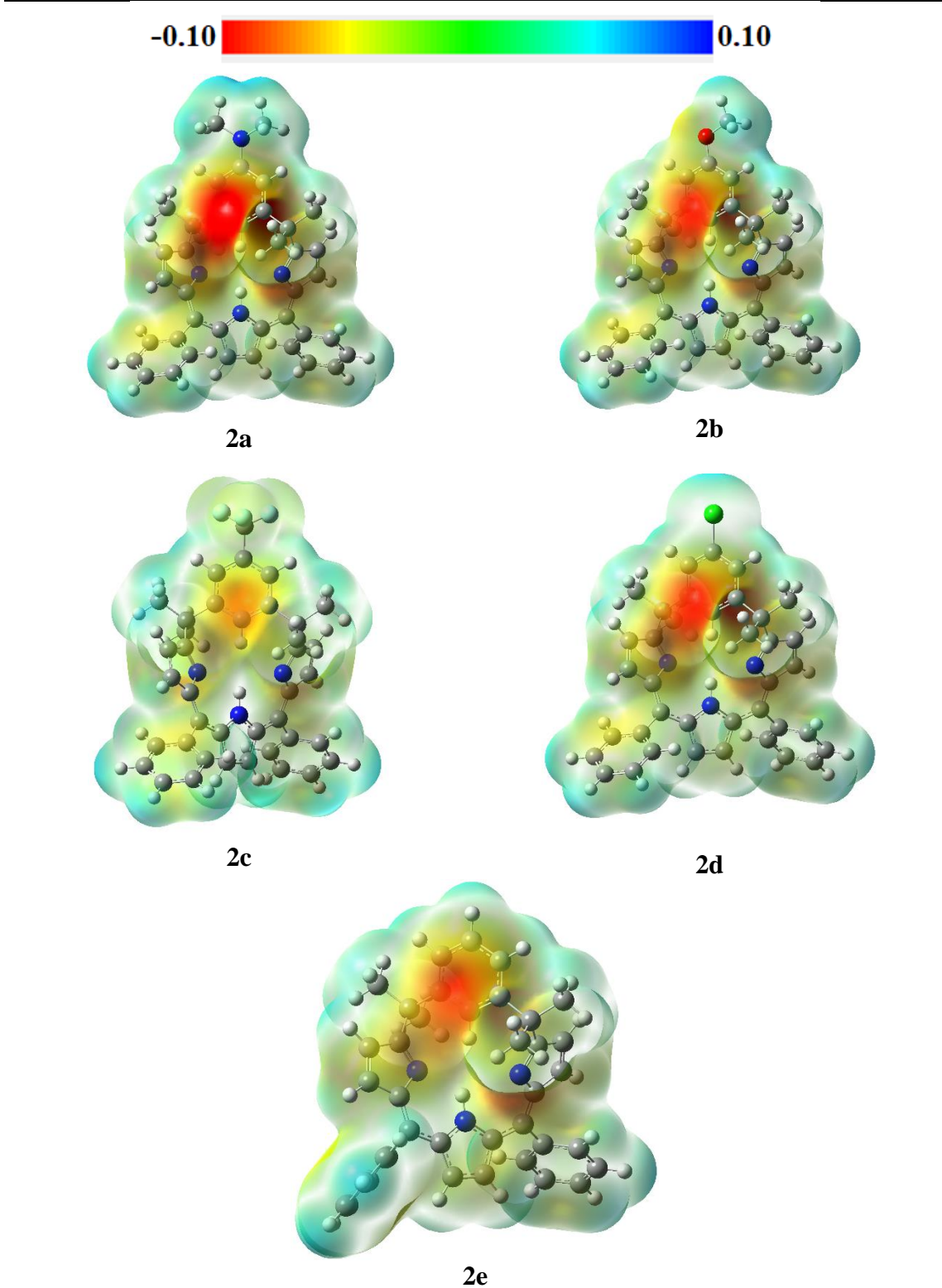


**Chart 5.8.** MESP surfaces of *m*-BPDM molecules when  $R' = -CH_3$ . The electron density isosurface of value 0.001 a.u. was chosen.

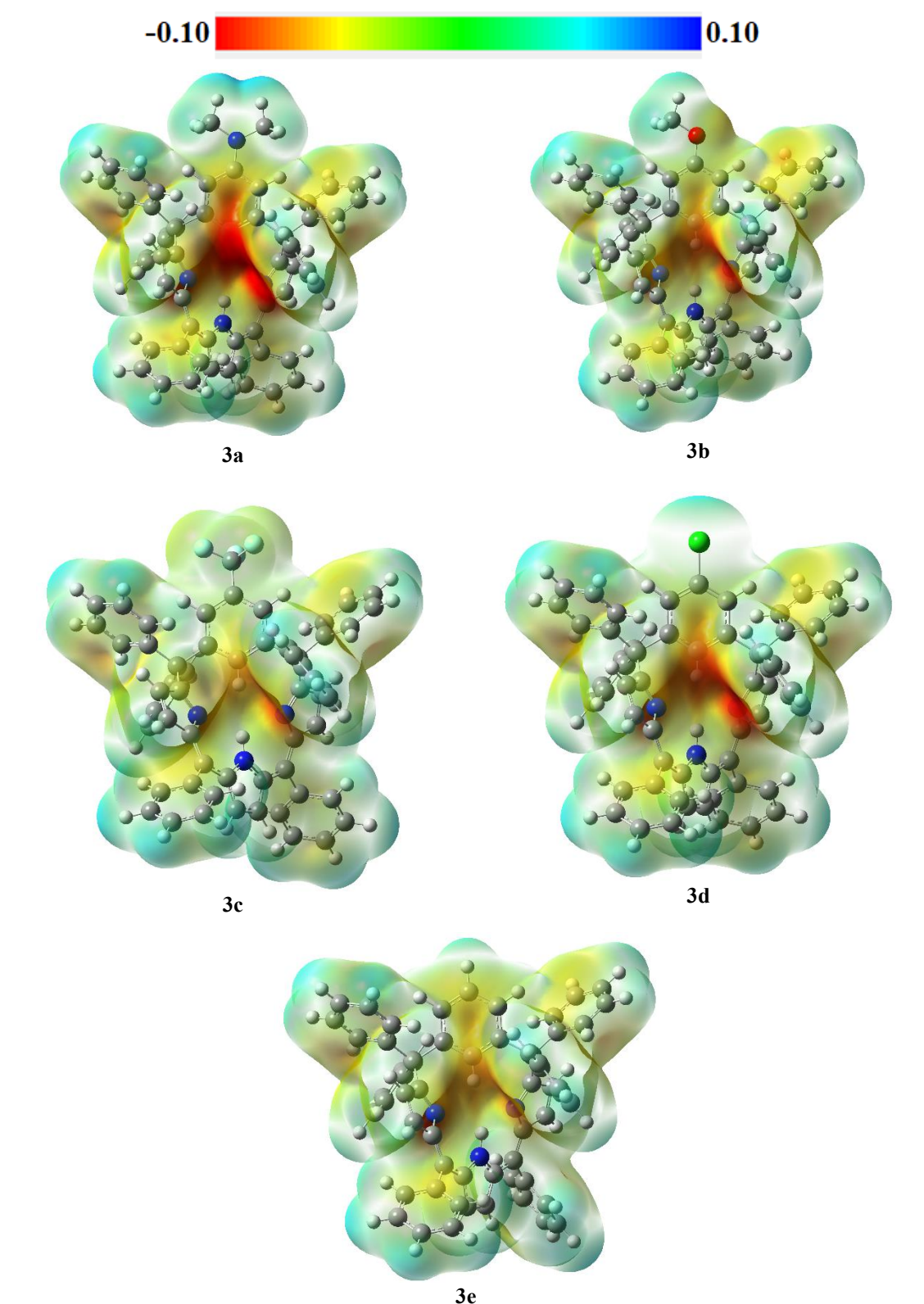


**Chart 5.9.** MESP surfaces of *m*-BPDM molecules when R' = -Ph. The electron density isosurface of value 0.001 a.u. was chosen.

## 5.4. Concluding Remarks

In this chapter, we investigated the intramolecular non-covalent interaction viz. N-H $\cdots$ N hydrogen bonding in substituted *m*-BPDM analogues. Initially, non-covalent interactions (NCI) plots revealed the presence of H-bond, steric factor and no vdW forces. The 2D RDG plots and iso-surfaces are visualized that go well with our expectations about the presence of H-bond in the inner core region. Furthermore, molecular tailoring approach is used to investigate the numerical value of these IHB energies (**HB1** and **HB2**). The investigation of N-H $\cdots$ N intramolecular IHBs energies leads us to a new way of exploring the synthetic routes of *m*-BPDM molecules. The N-H $\cdots$ N IHB falls under the range 4.6 to 16.0 kcal/mol, which is actually the moderate to strong type of intramolecular hydrogen bond. Interesting results were observed while calculating IHB, as the molecule **3c** exhibiting comparatively higher HB1 and HB2 values. The estimated values were then checked and went well in agreement with the MESP surfaces. This discovery of a distinguished substitution at C3-position of phenylene ring of *m*-BPDM also inferred that the substitution of -Cl group irrespective of bulkiness at C6- and C21- position provides a planarity in the molecule as observed in **1d**, **2d** and **3d**. The metalation of these molecule shall be easier compared to those having distorted geometry and we may expect a higher yield in these cases.

## References

- [1] C.H. Hung, G.F. Chang, A. Kumar, G.F. Lin, L.Y. Luo, W.M. Ching, E. Wei-Guang Diau, m-Benziporphodimethene: A new porphyrin analogue fluorescence zinc(II) sensor, *Chem. Commun.* (2008) 978–980. <https://doi.org/10.1039/b714412a>.
- [2] R.K. Sharma, L.K. Gajanan, M.S. Mehata, F. Hussain, A. Kumar, Synthesis, characterization and fluorescence turn-on behavior of new porphyrin analogue: meta-benziporphodimethenes, *Spectrochim. Acta - Part A Mol. Biomol. Spectrosc.* 169 (2016) 58–65. <https://doi.org/10.1016/j.saa.2016.06.020>.
- [3] R.K. Sharma, A. Maurya, P. Rajamani, M.S. Mehata, A. Kumar, meta - Benziporphodimethenes: New Cell-Imaging Porphyrin Analogue Molecules, *ChemistrySelect.* 1 (2016) 3502–3509. <https://doi.org/10.1002/slct.201600812>.
- [4] D. Chauhan, A. Kumar, S.G. Warkar, An efficient adsorbent for the removal of  $Zn^{2+}$   $Cd^{2+}$  and  $Hg^{2+}$  from the real industrial effluents. *Int. J. Environ. Sci. Technol.* (2021). <https://doi.org/10.1007/s13762-021-03615-5>
- [5] D. Chauhan, A. Kumar, S. G. Warkar, Modified polymeric hydrogels for the detection of  $Zn^{2+}$  in *E.coli* bacterial cells and  $Zn^{2+}$ ,  $Cd^{2+}$  and  $Hg^{2+}$  in industrial effluents (2021) *Environmental Technology*, DOI: 10.1080/0959330.2021.1928294
- [6] D. Chauhan, A. Kumar, S.G. Warkar, Synthesis, characterization and metal ions sensing applications of meta-benziporphodimethene-embedded polyacrylamide/carboxymethyl guar gum polymeric hydrogels in water, *Environ. Tech.* (2020), DOI: 10.1080/0959330.2020.1812730
- [7] M. Stępień, L. Latos-Grażyński, L. Szterenberg, J. Panek, Z. Latajka, Cadmium(II) and Nickel(II) Complexes of Benziporphyrins. A Study of Weak Intramolecular Metal-Arene Interactions, *J. Am. Chem. Soc.* 126 (2004) 4566–4580. <https://doi.org/10.1021/ja039384u>.

- [8] G.F. Chang, C.H. Wang, H.C. Lu, L.S. Kan, I. Chao, W.H. Chen, A. Kumar, L. Lo, M.A.C. Dela Rosa, C.H. Hung, Factors that regulate the conformation of m-benziporphodimethene complexes: Agostic metal-arene interaction, hydrogen bonding, and  $\tilde{\Gamma} \cdot 2,\pi$  coordination, *Chem. - A Eur. J.* 17 (2011) 11332–11343. <https://doi.org/10.1002/chem.201100780>.
- [9] A. Kumar, C.H. Hung, S. Rana, M.M. Deshmukh, Study on the structure, stability and tautomerisms of meta-benziporphodimethene and N-Confused isomers containing  $\gamma$ -lactam ring, *J. Mol. Struct.* 1187 (2019) 138–150. <https://doi.org/10.1016/j.molstruc.2019.03.064>.
- [10] D. Ahluwalia, A. Kumar, S.G. Warkar, M.M. Deshmukh, Effect of substitutions on the geometry and intramolecular hydrogen bond strength in meta-benziporphodimethenes: A new porphyrin analogue, *J. Mol. Struct.* 1220 (2020) 128773–128783. <https://doi.org/10.1016/j.molstruc.2020.128773>.
- [11] D. Ahluwalia, A. Kumar, S.G. Warkar, Recent developments in meta-benziporphodimethene: A new porphyrin analogue, *J. Mol. Struct.* 1228 (2021) 129672. <https://doi.org/10.1016/j.molstruc.2020.129672>.
- [12] T. Lu, F. Chen, Multiwfn: A multifunctional wavefunction analyzer. *J. Comput. Chem.*, 33 (2012) 580-592. <https://doi.org/10.1002/jcc.22885>
- [13] A.D. Becke, Density-functional exchange-energy approximation with correct asymptotic behavior, *Phys. Rev. A* 38 (1988) 3098-3100. doi: 10.1103/PhysRevA.38.3098.
- [14] A.D. Becke, Density-functional thermochemistry. III. The role of exact exchange, *J. Chem. Phys.* 98 (1993) 5648-5652. doi: 10.1063/1.464913.
- [15] C. Lee, W. Yang, R.G. Parr, Development of the colic-salvetti correlation energy formula into a functional of the electron density, *Phys. Rev. B* 37 (1988) 785-789. doi: 10.1103/PhysRevB.37.785.

- [16] W. Humphrey, A. Dalke, K. Schulten, VMD: Visual molecular dynamics, *J. Mol. Graph.* 14 (1996), 33-38. [https://doi.org/10.1016/0263-7855\(96\)00018-5](https://doi.org/10.1016/0263-7855(96)00018-5).
- [17] T. Williams, C. Kelly, gnuplot 5.4 An Interactive Plotting Program. <http://sourceforge.net/projects/gnuplot>
- [18] M.M. Deshmukh, S.R. Gadre, Molecular Tailoring Approach for the Estimation of Intramolecular Hydrogen Bond Energy, *Molecules* 26 (2021) 2928. <https://doi.org/10.3390/molecules26102928>
- [19] V. Singh, I. Ibnusaud, S. R. Gadre, M. M. Deshmukh, Fragmentation Method Reveals a Wide Spectrum of Intramolecular Hydrogen Bond Energies in Antioxidant Natural Products, *New J. Chem.* 44 (2020) 5841-5849. doi: 10.1039/D0NJ00304B.
- [20] M. B. Ahirwar, S. R. Gadre, M. M. Deshmukh, Direct and Reliable Method for Estimating the Hydrogen Bond Energies and Cooperativity in Water Clusters  $W_n$ ,  $n = 3$  to 8, *J. Phys. Chem. A* 124 (2020) 6699-6706. doi: 10.1021/acs.jpca.0c05631.
- [21] D. Patkar, M.B. Ahirwar, M. M. Deshmukh, Assessment of hydrogen bond strengths and cooperativity in self- and cross-associating cyclic  $(HF)_m(H_2O)_n$  ( $m + n = 2$  to 8) clusters, *New J. Chem.* (2022). <http://dx.doi.org/10.1039/D1NJ05431G>.
- [22] D. Patkar, M.B. Ahirwar, S.R. Gadre, M. M. Deshmukh, Unusually Large Hydrogen-Bond Cooperativity in Hydrogen Fluoride Clusters,  $(HF)_n$ ,  $n = 3$  to 8, Revealed by the Molecular Tailoring Approach, *J. Phys. Chem. A*, 125 (2021), 8836-45. <https://doi.org/10.1021/acs.jpca.1c06478>
- [23] M.B. Ahirwar, N.D. Gurav, S.R. Gadre, M.M. Deshmukh, Molecular Tailoring Approach for Estimating Individual Intermolecular Interaction Energies in Benzene Clusters, *J. Phys. Chem. A*, 125 (2021), 6131-6140. DOI: 10.1021/acs.jpca.1c03907

- [24] M.B. Ahirwar, D. Patkar, I. Yadav, M.M. Deshmukh, Appraisal of individual hydrogen bond strengths and cooperativity in ammonia clusters via a molecular tailoring approach, *Phys. Chem. Chem. Phys.*, 23 (2021), 17224-17231. <http://dx.doi.org/10.1039/D1CP02839A>
- [25] M.J. Frisch, G.W. Trucks, H.B. Schlegel, G.E. Scuseria, G.A.P. J.R. Cheeseman, G. Scalmani, V. Barone, B. Mennucci, J.B. H. Nakatsuji, M. Caricato, X. Li, H.P. Hratchian, A.F. Izmaylov, R.F. G. Zheng, J.L. Sonnenberg, M. Hada, M. Ehara, K. Toyota, T.V. J. Hasegawa, M. Ishida, T. Nakajima, Y. Honda, O. Kitao, H. Nakai, E.B. J.A. Montgomery Jr., J.E. Peralta, F. Ogliaro, M. Bearpark, J.J. Heyd, J.N. K.N. Kudin, V.N. Staroverov, T. Keith, R. Kobayashi, M.C. K. Raghavachari, A. Rendell, J.C. Burant, S.S. Iyengar, J. Tomasi, C.A. N. Rega, J.M. Millam, M. Klene, J.E. Knox, J.B. Cross, V. Bakken, R.C. J. Jaramillo, R. Gomperts, R.E. Stratmann, O. Yazyev, A.J. Austin, V.G.Z. C. Pomelli, J.W. Ochterski, R.L. Martin, K. Morokuma, O.F. G.A. Voth, P. Salvador, J.J. Dannenberg, S. Dapprich, A.D. Daniels, D.J.F. J.B. Foresman, J.V. Ortiz, J. Cioslowski, Gaussian 09 Suites, (2016). <https://gaussian.com/g09citation>.
- [26] Chemcraft graphical software for visualization of quantum chemistry computations. <https://www.chemcraftprog.com>.
- [27] M. M. Deshmukh, S. R. Gadre, L. J. Bartolotti, Estimation of Intramolecular Hydrogen Bond Energy via Molecular Tailoring Approach, *J. Phys. Chem. A.* 110 (2006) 12519-12523. doi: 10.1021/jp065836o.
- [28] M. M. Deshmukh, C. H. Suresh, S. R. Gadre, Intramolecular Hydrogen Bond Energy in Polyhydroxy Systems: A Critical Comparison of Molecular Tailoring and Isodesmic Approaches, *J. Phys. Chem. A.* 111 (2007) 6472-6480. doi: 10.1021/jp071337r.

- [29] M. M. Deshmukh, L. J. Bartolotti, S. R. Gadre, Intramolecular Hydrogen Bonding and Cooperative Interactions in Carbohydrates via the Molecular Tailoring Approach, *J. Phys. Chem. A.* 112 (2008) 312-321. doi: 10.1021/jp076316b.
- [30] M. M. Deshmukh, S. R. Gadre, Estimation of N-H···O=C Intramolecular Hydrogen Bond Energy in Polypeptides. *J. Phys. Chem. A.* 113 (2009) 7927-7932. doi: 10.1021/jp9031207.
- [31] M. M. Deshmukh, L. J. Bartolotti, S. R. Gadre, Intramolecular Hydrogen Bond Energy and Cooperative Interactions in  $\alpha$ -,  $\beta$ -, and  $\gamma$ -cyclodextrin Conformers, *J. Comput. Chem.* 32 (2011) 2996-3004. doi: 10.1002/jcc.21881.
- [32] Friesecke, G. The Multiconfiguration Equations for Atoms and Molecules: Charge Quantization and Existence of Solutions. *Arch. Rational Mech. Anal.* 169, 35–71 (2003). <https://doi.org/10.1007/s00205-003-0252-y>
- [33] A.D. Becke, D.R. Yarkony, “Modern electronic structure theory.” (1995), Ed.; World Scientific: River Edge, NJ, 1995; pp 1022-1046.
- [34] A. J. Cohen, P. Mori-Sánchez, W. Yang, Insights into Current Limitations of Density Functional Theory, *Science*, 321 (2008), 792–794. Doi: 10.1126/science.1158722
- [35] C. Lefebvre, G. Rubez, H. Khartabil, J.-C. Boisson, J. C.-García, E. Hénon, Accurately extracting the signature of intermolecular interactions present in the NCI plot of the reduced density gradient versus electron density, *Phys. Chem. Chem. Phys.* 19 (2017), 17928-17936. <https://doi.org/10.1039/C7CP02110K>
- [36] E. R. Johnson, S. Keinan, P. Mori-Sánchez, J. Contreras- García, A. J. Cohen and W. Yang, *J. Am. Chem. Soc.* 132 (2010), 6498–6506. <https://doi.org/10.1107/S2056989019001129>

- [37] E. R. Johnson, S. Keinan, P. Mori-Sánchez, J. Contreras-García, A. J. Cohen, W. Yang, Revealing noncovalent interactions, *J. Am. Chem. Soc.* 132 (2010), 6498–6506. <https://doi.org/10.1021/ja100936w>
- [38] C. H. Suresh, S. R. Gadre, A Novel Electrostatic Approach to Substituent Constants: Doubly Substituted Benzenes *J. Am. Chem. Soc.* 120 (1998), 7049–7055. <https://doi.org/10.1021/ja973105j>
- [39] A. Kumar, S. R. Gadre, N. Mohan, C. H. Suresh, Lone Pairs: An Electrostatic Viewpoint. *J. Phys. Chem. A* 118 (2014) 526–532. <https://doi.org/10.1021/jp4117003>
- [40] M. M. Deshmukh, S. R. Gadre, R. Tonner, G. Frenking, Molecular electrostatic potentials of divalent carbon(0) compounds, *Phys. Chem. Chem. Phys.* 10, (2008), 2298–2301. <https://doi.org/10.1039/B803068E>
- [41] S. R. Gadre, M. M. Deshmukh, T. Chakraborty, Electrostatics-guided ab initio studies on weakly bonded complexes of substituted naphthalenes *Chem. Phys. Lett.* 384 (2004), 350–356. <https://doi.org/10.1016/j.cplett.2003.11.099>

# CHAPTER 6

## SYNTHESIS AND CHARACTERIZATIONS OF A NEW STERICALLY HINDERED FREE BASE *meta*-BENZIPORPHODIMETHENE AND ITS METAL COMPLEXES

---

### **6.1. Introduction**

Although, Stepien and co-workers reported the very first 11,16-bis(p-nitrophenyl)-6,6,21,21-tetraphenyl-*meta*-benzi-6,21-porphodimethene, having a yield as low as 14%,[2] the derivatives of sterically hindered compound were not synthesized. All the studies henceforth, focused on the development of series of tetramethylene *m*-BPDM (TMBPDM) analogues and its derivatives. [3-7] Thus, in this chapter, we present a novel sterically hindered free base 11,16-bis(phenyl)-6,6,21,21-tetraphenyl-*meta*-benzi-6,21-porphodimethene (TPBPDM) along with its zinc and cadmium metal complexes. Furthermore, the time-dependent DFT optimizations were performed on all the three compounds and the electronic structures have been studied rigorously.

### **6.2. Experimental section**

#### **6.2.1. Reagents**

Pyrrole and benzaldehyde (liquid) were distilled prior to use. DDQ and boron trifluoride ethyl ether complex were used without further purifications. Anhydrous zinc chloride ( $ZnCl_2$ ) and anhydrous cadmium chloride ( $CdCl_2$ ) were received from Sigma-Aldrich. All other solvents and reagents were ordered from E. Merck Ltd. and were brought to use as received.

#### **6.2.2. General information**

$^1H$ , NMR spectra were recorded on Bruker Avance III 400 spectrometer (400 MHz for  $^1H$ ). Chemical shifts are reported in ppm relative to the residual hydrogen atoms

in the deuterated solvent  $\text{CDCl}_3$  ( $\delta = 7.26$ ),  $\text{CD}_3\text{COCD}_3$  ( $\delta = 2.05$ ). High-resolution mass spectra for the compounds were performed on a Bruker MaXis Impact mass spectrometer. MesteRenova v6.0.2-5475 software used for the analysis of NMR spectra. Absorption spectra were recorded using an Agilent Cary 8454 UV-Visible spectrophotometer.

### 6.2.3. Synthetic procedure

**1,3-Bis(diphenylhydroxymethyl)benzene (1)** was synthesized as described previously by Stepien and co-workers, [2] 10 mmol of dimethyl isophthalate was dispersed in 150 mL of degassed dry tetrahydrofuran (THF). 44 mmol of 1M solution in  $\text{Et}_2\text{O}$  of phenylmagnesiumbromide ( $\text{PhMgBr}$ ) was dissolved into the reaction mixture. The solution was then stirred for 1 hour and then hydrolyzed using aqueous solution of ammonium chloride (aq.  $\text{NH}_4\text{Cl}$ ). Dichloromethane ( $\text{CH}_2\text{Cl}_2$ , DCM) was used for the extraction of the product. The extracted product was washed several times with water and the solvent was evaporated under reduced pressure. The yellowish viscous liquid so obtained was compound **1** that slowly crystallized upon standing. The yield obtained was nearly 80 % (**Scheme 6.1**).  $^1\text{H}$  NMR ( $\text{CDCl}_3$ , 298 K, numbering corresponds to that of **2**, **Scheme 6.2**): 7.49 (t, 1H, 22-H), 7.15–7.35 (m, 23H, 6,6,21,21-Ph, 2,4-H, 3-H), 3.25 (b, 2H, OH). Refer to **Figure 6.2** for NMR spectra of this diol (compound 1) precursor.

**11,16-Bis(phenyl)-6,6,21,21-tetraphenyl-*meta*-benzi-6,21-porphoodimethene (2):** 1 mmol of Precursor (**1**), 3 mmol pyrrole and 2 mmol benzaldehyde were added to 900 mL of DCM. Inert atmosphere was provided by bubbling  $\text{N}_2$  gas into the solution for 15 minutes. The round bottomed flask was covered with septum caps and 100  $\mu\text{L}$

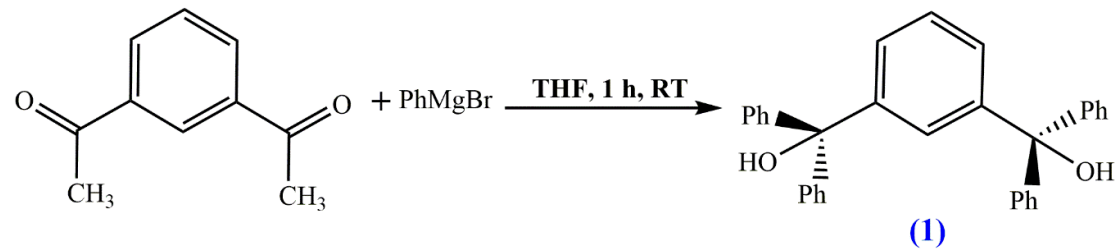
$\text{Et}_2\text{O} \cdot \text{BF}_3$  was added. The solution was kept in dark and stirred for 2 hours. After this, 2 mmol of DDQ was added slowly, with continuous stirring. The reaction mixture was evaporated in reduced pressure. With the help of column chromatography, the compound was eluted from the mixture. The yield obtained is 20% (**Scheme 6.2**) [1-9].  $^1\text{H}$  NMR ( $\text{CD}_3\text{COCD}_3$ , 298 K, numbering corresponds to that of **2**, **Scheme 6.2**): 12.33 (b, 1H, 24-H), 6.08 (s, 2H, 13,14-H), 6.52 (d, 2H, 8,19-H) 6.65 (d, 2H, 9,18-H), 6.90 (t, 4H, p 6,6,21,21-H), 7.13 (m, 8H, o 6,6,21,21-H), 7.27 (m, 8H, m 6,6,21,21-H), 7.08 (d, 2H, 2,4-H), 7.10 (t, 1H, 3-H), 7.43 (m, 4H, o 11,16-H), 7.49 (m, 4H, m 11,16-H), 7.56 (t, 2H, p 11,16-H), 7.88 (s, 1H, 22-H). UV-vis ( $\text{CH}_2\text{Cl}_2$ ,  $\lambda_{\max}$  [nm] ( $\log \epsilon$ )): 365 (3.78), 618 (3.32), 667 (3.62). HRMS (APCI, positive mode) for  $\text{C}_{58}\text{H}_{41}\text{N}_3$  ( $\text{M}^+$ ):  $m/z = 779.3300$  (calculated), 779.3274 (observed). Refer to **Figure 6.3** and **6.6** for NMR spectra and mass spectrum, respectively, of compound **2**.

**Chlorozinc(II) 11,16-Bis(phenyl)-6,6,21,21-tetraphenyl-*meta*-benzi-6,21-porphoiodimethene (3):** 10 mg of compound **2** was dissolved in 25 mL of DCM/ $\text{CH}_3\text{CN}$  in the ratio 1:2. Anhydrous solution of  $\text{ZnCl}_2$  which was pre-dissolved in  $\text{CH}_3\text{CN}$  was added to the reaction mixture, followed by 1 drop of 2, 6-lutadiene. The solution was stirred for 2 minutes, then the solvent was removed under reduced pressure. The residue was dissolved in DCM and excess of Zn(II) was removed using distilled water. The organic layer was collected and residue was removed using vacuum. The product was recrystallized using n-hexane.[1-9]  $^1\text{H}$  NMR ( $\text{CD}_3\text{COCD}_3$ , 298 K, numbering corresponds to that of **2**, **Scheme 6.2**): 6.16 (s, 2H, 13,14-H), 6.20 (d, 2H, 8,19-H) 6.60 (d, 2H, 9,18-H), 6.72 (t, 4H, p 6,6,21,21-H), 7.07 (m, 8H, o 6,6,21,21-H), 7.13 (m, 8H, m 6,6,21,21-H), 7.21 (d, 2H, 2,4-H), 7.19 (t, 1H, 3-H), 7.37 (m, 4H, o 11,16-H), 7.39 (m, 4H, m 11,16-H), 7.32 (t, 2H, p 11,16-H), 7.30 (s, 1H, 22-H). UV-vis ( $\text{CH}_2\text{Cl}_2$ ,  $\lambda_{\max}$  [nm] ( $\log \epsilon$ )): 365 (3.78), 618 (3.32), 667 (3.62). HRMS (APCI, positive mode) for  $\text{C}_{58}\text{H}_{40}\text{N}_3\text{ZnCl}$  ( $\text{M-Cl}^+$ ):  $m/z = 842.2513$

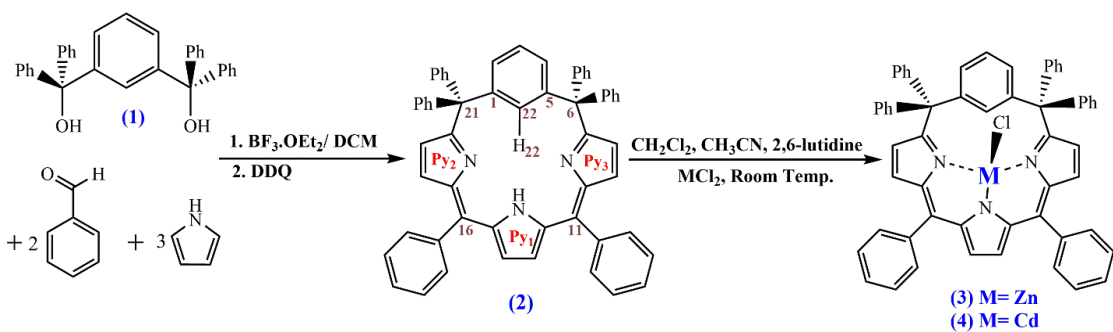
(calculated), 842.2524 (observed). **Figure 6.4** and **6.7** for NMR spectra and mass spectrum, respectively, of compound **3**.

**Chlorocadmium(II)11,16-Bis(phenyl)-6,6,21,21-tetraphenyl-*meta*-benz-6,21-porphoodimethene (**4**):**

10 mg of compound **2** was dissolved in 25 mL of DCM/CH<sub>3</sub>CN in the ratio 1:2. Anhydrous solution of CdCl<sub>2</sub> which was pre-dissolved in CH<sub>3</sub>CN was added to the reaction mixture, followed by 1 drop of 2, 6-lutadiene. The solution was stirred for 2 minutes, then the solvent was removed under reduced pressure. The residue was dissolved in DCM and excess of Zn(II) was removed using distilled water. The organic layer was collected and residue was removed using vacuum. The product was recrystallized using n-hexane (**Scheme 6.2**) [1-9]. <sup>1</sup>H NMR (CD<sub>3</sub>COCD<sub>3</sub>, 298 K, numbering corresponds to that of **2**, **Scheme 6.2**): 6.29 (s, 2H, 13,14-H), 6.08 (d, 2H, 8,19-H) 6.17 (d, 2H, 9,18-H), 6.52 (d, 2H, p 6,21-H), 6.66 (t, 4H, o 6,21-H), 6.78 (dd, 4H, m 6,21-H), 7.09 (d, 2H, p 6',21'-H), 7.18 (m, 4H, o 6',21'-H), 7.27 (m, 4H, m 6',21'-H), 7.35 (d, 2H, 2,4-H), 7.40 (t, 1H, 3-H), 7.44 (m, 4H, o 11,16-H), 7.49 (m, 4H, m 11,16-H), 7.56 (t, 2H, p 11,16-H), 7.13 (s, 1H, 22-H). UV-vis (CH<sub>2</sub>Cl<sub>2</sub>,  $\lambda_{\text{max}}$  [nm] (log ε)): 360 (3.36), 413 (2.96), 615 (2.85), 668 (3.21). HRMS (APCI, positive mode) for C<sub>58</sub>H<sub>40</sub>N<sub>3</sub>CdCl (M-Cl)+: m/z = 892.2255 (calculated), 892.2298 (observed). **Figure 6.5** and **6.8** for the NMR spectra and mass spectrum of compound **4**, respectively.



**Scheme 6.1.** Synthesis of 1,3-Bis(diphenylhydroxymethyl)benzene (**1**) precursor.[2]



**Scheme 6.2.** Synthesis of free base hexaaryl-*m*-benziporphodimethene and its metal complexes.[2-5]

### 6.3. Computational details

Density functional theory has been employed for studying the electronic structures of 2, 3, and 4. Geometries of all the species were optimized under C1 symmetry employing B3LYP functional.[10,11] LANL2DZ basis set has been utilized for these geometries, keeping in mind the presence of transition metal in 3 and 4.[11,12] The optimized geometries were then subjected to time-dependent DFT calculations for further analysis of electronic distribution. All the calculations were performed on Gaussian 16 suites of program.[13] Further, the frontier molecular orbitals were visualized using Multiwfn 3.8 software.[14] The topological analysis was done to understand the nature of bonding in these systems. The formatted checkpoint file (.fch) obtained from Gaussian 16 was used as an input file in Multiwfn package. The total density of states (TDOS)/partial density of states (PDOS)/overlapping partial density of states (OPDOS) plots, have been generated through this program. The molecular electrostatic surfaces and frontier molecular orbitals were visualized in GaussView5.0 software.[15]

## 6.4. Results and discussion

### 6.4.1. Synthesis and spectroscopy

The compound **1** which is a precursor for further synthesis of sterically hindered free base *meta*-benzoporphodimethenes and its metalated analogues was successfully synthesized. The synthesis was confirmed after recording the  $^1\text{H}$ -NMR spectra attached as **Figure 6.2**. This diol (compound **1**) precursor was utilized for the synthesis of free base 11,16-bis(phenyl)-6,6,21,21-tetraphenyl-*meta*-benzi-6,21-porphodimethene (**2**). The acid catalyzed condensation reaction led to the formation of desired red-colored product with a yield of 20%.[2] Product **2** so obtained was fully characterized by UV-visible, NMR and mass spectra. This sterically hindered free base *m*-BPDM was then subjected to metalation at room temperature using metal (Zn(II) and Cd(II)) chloride metal salt in presence of 2,6-lutidine. The insertion of metal ion was validated by the change in color of the product *viz.*, green for chlorozinc(II) 11,16-Bis(phenyl)-6,6,21,21-tetraphenyl-*meta*-benzi-6,21-porphodimethene (**3**) and bluish-green for chlorocadmium(II) 11,16-Bis(phenyl)-6,6,21,21-tetraphenyl-*meta*-benzi-6,21-porphodimethene (**4**) complexes.[1-5]

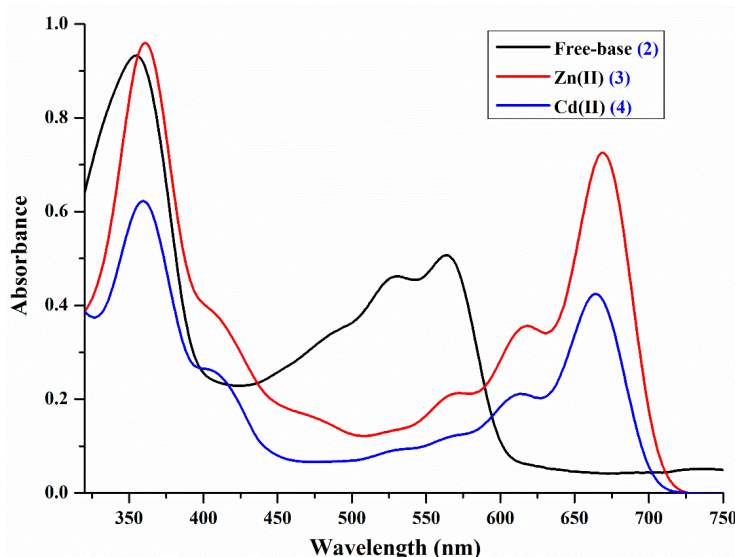


**Figure 6.1.** UV-Vis plots for compound **2**, **3** and **4**.

While the chemosensing applications of *meta*-benzoporphodimethenes serves as a blessing for the research community, the rapid oxidation tendency and low yield are the disguise.[1] The low yield and instability of tetramethylene analogue of *m*-BPDM has been a well talked about topic in the literature.[1-9] The tetraphenylene derivative is much cohesive to that of tetramethylene *m*-BPDM analogue, not only in terms of low yield, but also UV-vis characteristic plots. The plot in **Figure 6.1** represents the overlapping UV-Visible curve for **2**, **3** and **4**. The bathochromic shift in Q-bands of the Zn(II) (**3**) and Cd(II) (**4**) *m*-BPDM complexes when compared to that of free base (**2**), has been observed. The widened nature of the peaks is attributed to the presence of  $sp^3$ - $sp^2$  *meso* carbon atoms, in a non-conjugated system.[1,5] For compound **2**, the Soret like high energy band is observed at nearly 350-360 nm. On the other hand, the Soret like high energy band for compound **3** and **4** are observed at 360-370 nm. The disparity arises on moving towards the higher wavelength, where a significant red shift is observed at the Q-bands of free base and metalated complexes. The Q-band for free base *m*-BPDM lies in the range of 500-575 nm while that of Zn(II) and Cd(II) complexes lies at 600-700 nm and 600-675 nm, respectively. This bathochromic shift is anticipated due to the interactions of d-orbital of the transition metals (Zn and Cd) to the macrocyclic ring.[5] These interactions may further be responsible for introducing a symmetry to the highly puckered free base *m*-BPDM molecules, upon metalation. The H22 in compound **2** has a chemical shift value of 7.8 ppm, singlet, while in the case of metal complexes, a deshielding of this H22 atom is observed. This downfield shift indicates the agostic interactions present between the metal center with that of the H22 atom. The recorded NMR spectra have been attached as **Figure 6.3**, **6.4** and **6.5** for compound **2**, **3** and **4**, respectively. The APCI-Mass

spectrum recorded a peak at m/z at  $[M-1]^+$  for free base **2** and  $[M-\text{Cl}]^+$  for **3** and **4**, attached as **Figure 6.6**, **6.7** and **6.8**, respectively.

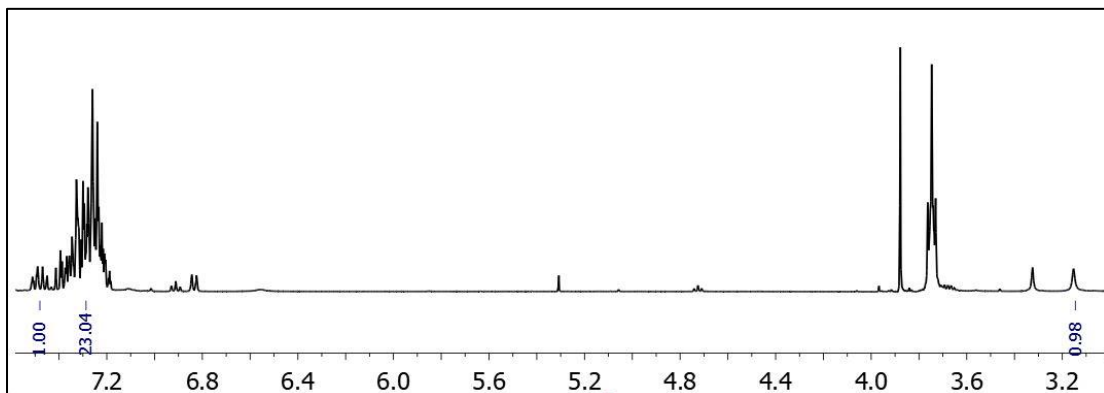


**Figure 6.2.**  $^1\text{H}$ -NMR of 1,3-Bis(diphenylhydroxymethyl)benzene (**1**) precursor.

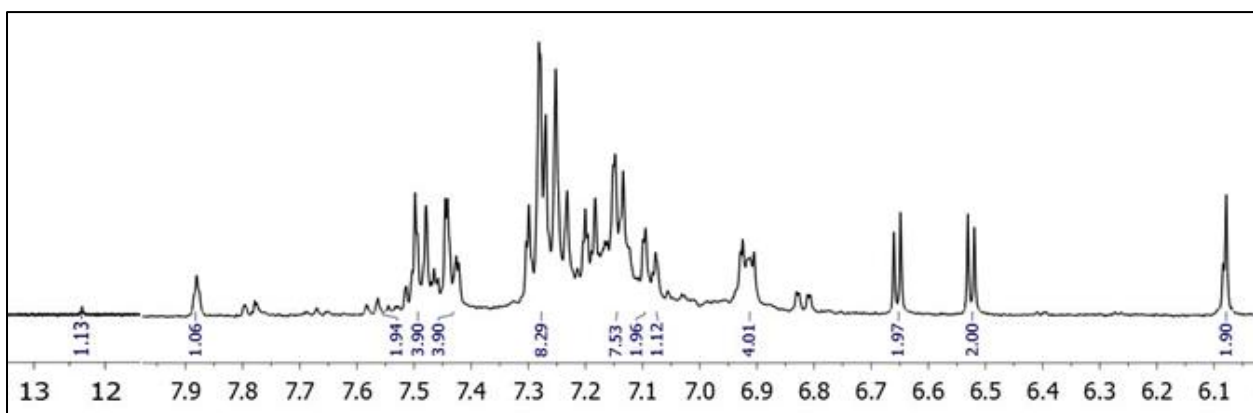


**Figure 6.3.**  $^1\text{H}$ -NMR of 11,16-Bis(phenyl)-6,6,21,21-tetraphenyl-meta-benzi-6,21-porphrodimethene (**2**) in  $\text{CD}_3\text{OCD}_3$ .

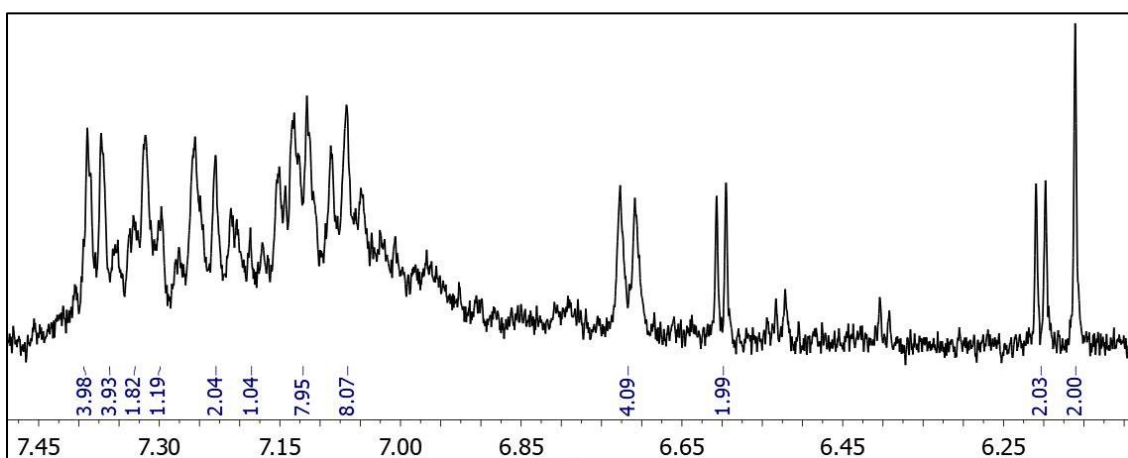


**Figure 6.4.**  $^1\text{H}$ -NMR of chlorozinc(II) 11,16-Bis(phenyl)-6,6,21,21-tetraphenyl-meta-benzi-6,21-porphrodimethene (**3**) in  $\text{CD}_3\text{OCD}_3$ .

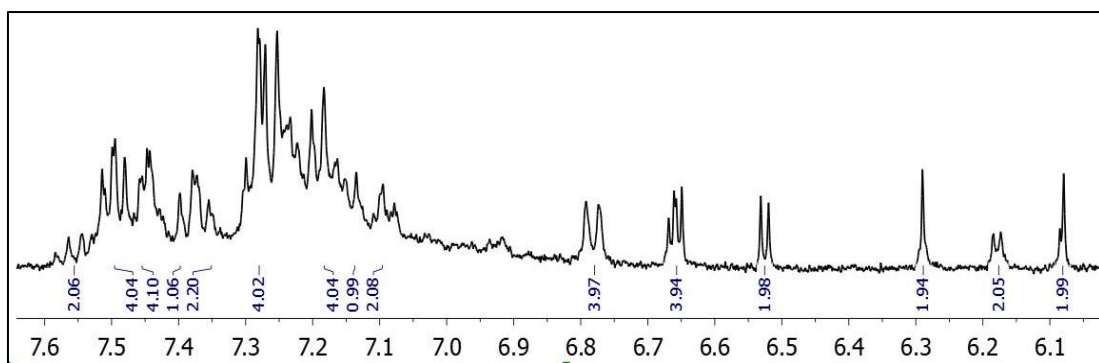


**Figure 6.5.**  $^1\text{H}$ -NMR of chlorocadmium(II) 11,16-Bis(phenyl)-6,6,21,21-tetraphenyl-*meta*-benzi-6,21-porphooidimethene (**4**) in  $\text{CD}_3\text{OCD}_3$ .

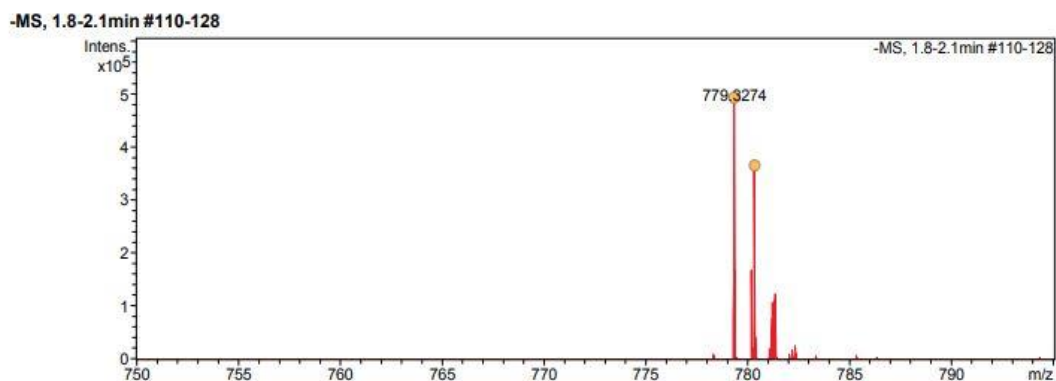


**Figure 6.6.** HRMS of 11,16-Bis(phenyl)-6,6,21,21-tetraphenyl-*meta*-benzi-6,21-porphorodimethene (**2**) in APCI positive mode.

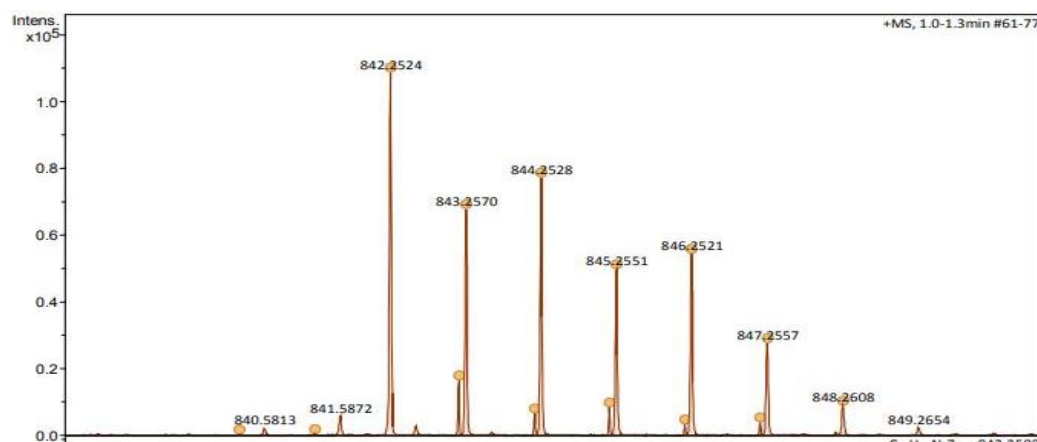


**Figure 6.7.** HRMS of chlorozinc(II) 11,16-Bis(phenyl)-6,6,21,21-tetraphenyl-*meta*-benzo-6,21-porphroodimethene (**3**) in APCI positive mode.

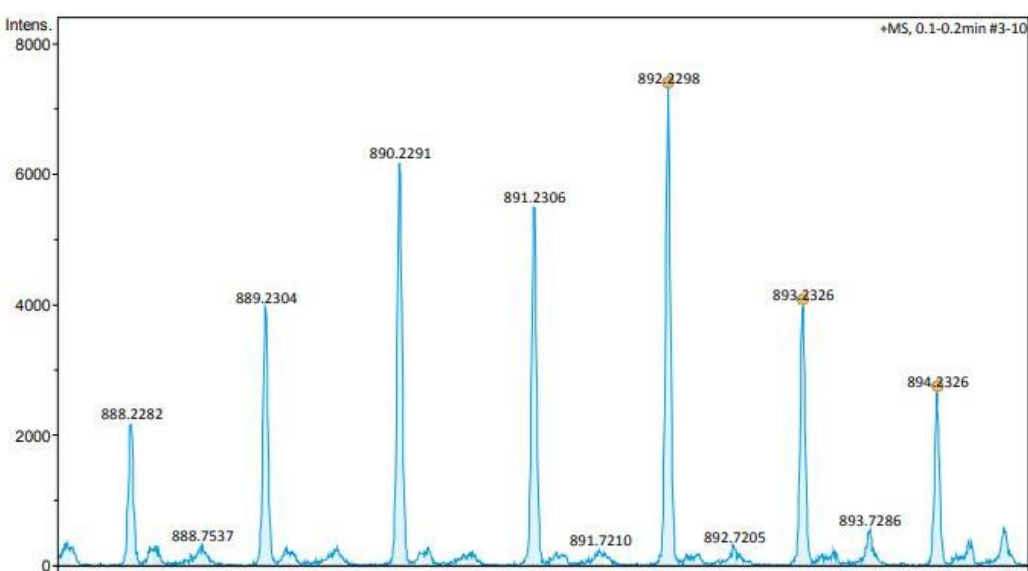


**Figure 6.8.** HRMS of chlorocadmium(II) 11,16-Bis(phenyl)-6,6,21,21-tetraphenyl-*meta*-benzo-6,21-porphorodimethene (**4**) in APCI positive mode.

#### 6.4.2. Frontier molecular orbitals

The prime reason for this analysis is to get an insight of electron density distribution within a molecule at its lowest energy state. Herein, using TDDFT results, the highest occupied molecular orbital (HOMO) and lowest unoccupied molecular orbital (LUMO) have been visualized for **2**, **3** and **4** (Scheme 6.2). The HOMO and LUMO enables one to understand the chemical reactivity and kinetic stability of the molecule.

Figure 6.9 shows the electronic charge distribution within the *m*-BPDM systems under consideration. The red colored region depicts the positive phase while the negative phase is denoted by the green region. It is well documented that the electronic delocalization is hampered due to the presence of C6- and C21- *sp*<sup>3</sup> *meso* carbon atoms. Consequently, an even distribution of electron density is observed below these *sp*<sup>3</sup> carbon atoms, in all the three systems. The HOMO of free base *m*-BPDM (**2**) lies at -8.34 eV while the LUMO is at -6.91 eV. Likewise, the HOMO-1, HOMO, LUMO and LUMO+1 orbital energies for the molecules **2**, **3** and **4** have been

summarized in **Table 6.1**. These HOMO-LUMO energy gap ( $\Delta E$ ) is very low, which is much in agreement with the fluorescent nature of these compounds. Having said that, the  $\Delta E$  values lies in the order **2 > 3 > 4**. It is noteworthy that the applications of these systems as conductors or semiconductors have not been studied yet.

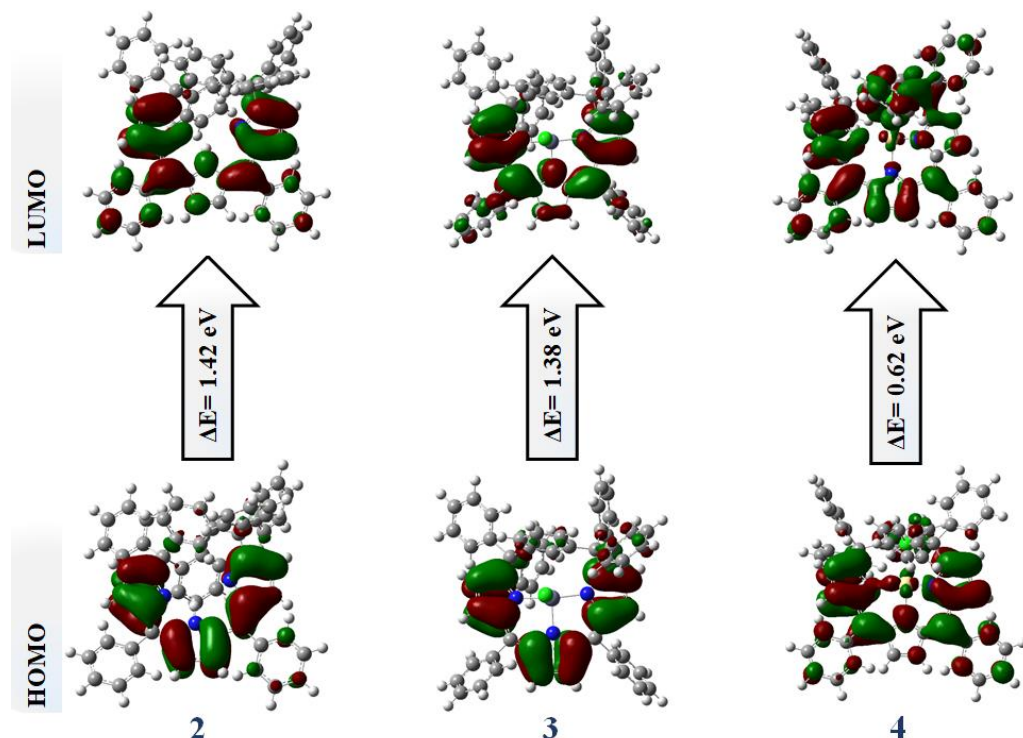


**Figure 6.9.** Depiction of frontier molecular orbitals and their energy gap in **2**, **3** and **4** *meta*-benzoporphphdimethene systems (Isovalue = 0.02).

**Table 6.1.** Energy of frontier molecular orbitals and HOMO-LUMO energy gap.

<b>m-BPDM</b>	Frontier Molecular Orbital Energy			
	HOMO-1 (eV)	HOMO (eV)	LUMO (eV)	LUMO+1 (eV)
<b>2</b>	-9.04	-8.34	-6.91	-6.26
<b>3</b>	-9.22	-8.48	-7.10	-6.04
<b>4</b>	-6.89	-6.56	-5.94	-5.86

### 6.4.3. Density-of-states

The conductivity of a molecule does not depend on just the HOMO-LUMO gap, the population of states (or MOs) is of great importance too.[16] Hence, to understand the molecular orbital compositions and their contributions to chemical bonding, graphical representation of MOs in form of curves has been done. The total density of states (TDOS), partial density of states (PDOS) and overlapping partial density of states (OPDOS) have been plotted. In the total density of states (TDOS) plot each discrete line represents a molecular orbital energy level.[17,18] **Figure 6.10** describes the TDOS plot in correlation with the FMOs. The elongated dashed vertical line represents HOMO, the small vertical lines adjacent to it are present in two colors: black and grey. The black lines signifies the occupied orbitals, while, the grey lines denotes the unoccupied molecular orbitals. The right Y-axis plots the density of these states and the right Y-axis reveals the degenerate energy levels.[14]

Though, the band gap value of the free base and Zn(II) complex of tetraphenyl-*m*-BPDM lies in the range wherein mostly semiconductor band gaps have been reported (**Figure 6.10**), yet no literature is present on the conductivity of these materials. For a compound to be conducting or semiconducting in nature, the prime requirement is the number of energy states near the highest occupied molecular orbital (HOMO).[19] **Figure 6.10** depicts the absence of the discrete lines around the HOMO level, which should be available for electron transfer for conduction, in all the three systems. In PDOS, each molecular structure (**2**, **3**, and **4**) have been fragmented to understand the contribution of these parts in the chemical bonding of the structures.[20,21] In contrast to this, the OPDOS represents the presence of bonding, anti-bonding and non-bonding interactions. The positive OPDOS curve denotes the bonding

interactions, the negative curve signifies anti-bonding and when the non-bonding interactions are shown when the curve reaches at zero.[20-22] **Figure 6.11** represents TDOS/PDOS/OPDOS curve for **2**, **3** and **4**.

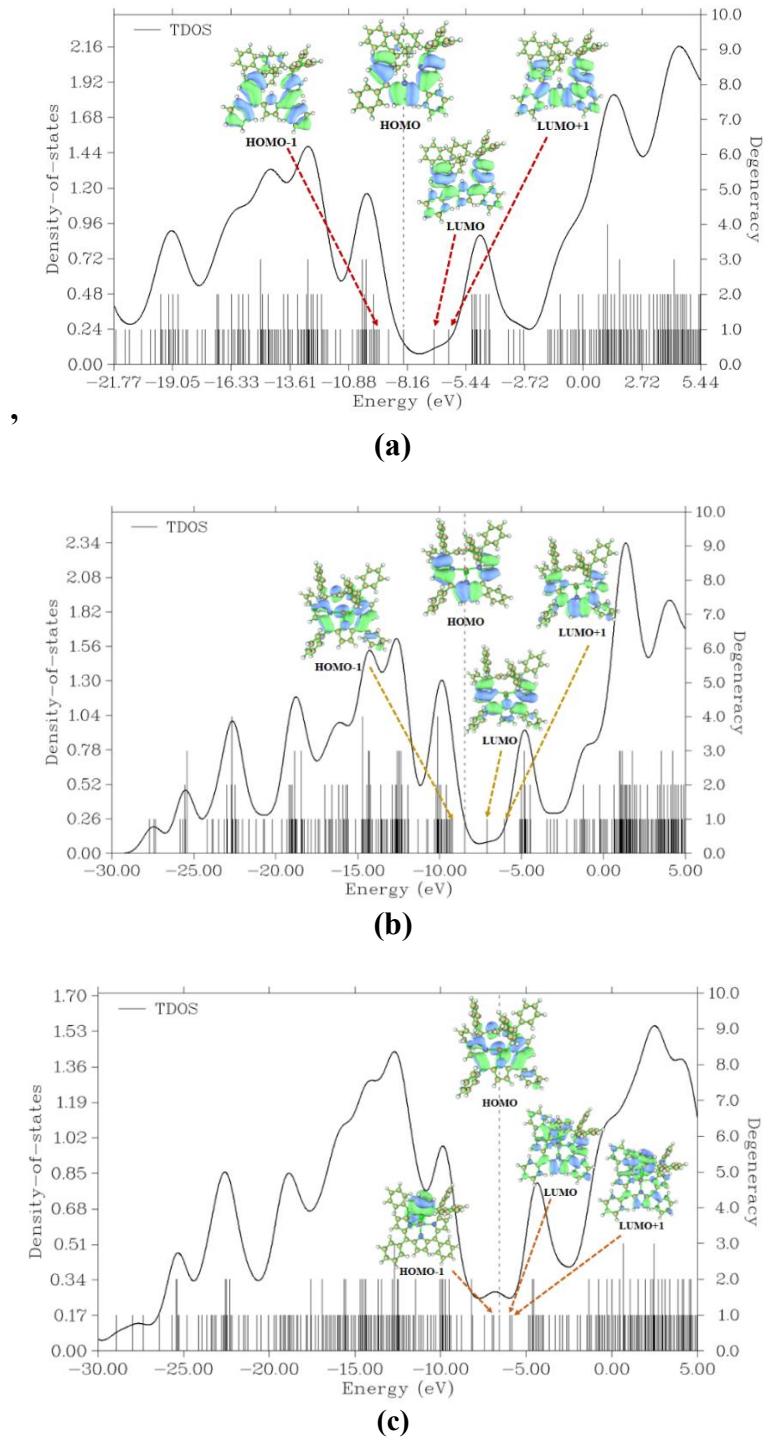


**Figure 6.10.** TDOS plot for (a) free base *m*-BPDM (**2**) (b) Zn(II) *m*-BPDM complex (**3**) and (c) Cd(II) *m*-BPDM complex (**4**).

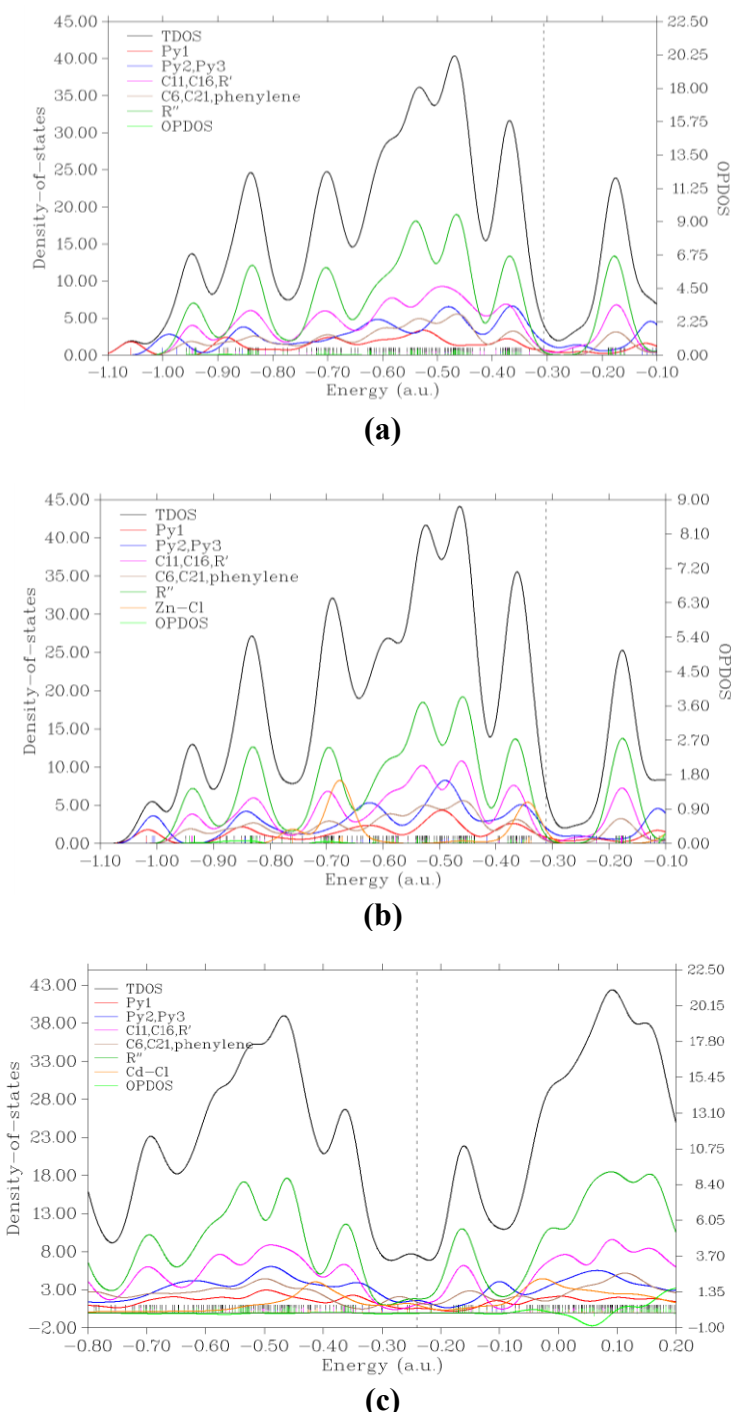


**Figure 6.11.** TDOS/PDOS/OPDOS plot for (a) 2, (b) 3 and (c) 4.

Each molecular system has been fragmented into five to six parts as labelled in the graphs in **Figure 6.11**. Refer to **Scheme 6.2** for labelling and numbering within the system. It was observed that in the region around HOMO, the PDOS reaches a

minimal value, though are in positive direction. This suggests that the electron density is evenly localized close to the FMOs, thus suggesting a uniform distribution of electron density. In contrary to this, when the energy values are lower than -0.3 a.u. or higher than 0.2 a.u., most of the electron density is seemed to be localized at hexa-aryl groups ( $R''$ -green lines; C11, C16,  $R'$ - pink lines). See **Figure 6.11** and **Scheme 6.2** for all the labels and lines. The OPDOS for both free base and Zn(II) complex of *m*-BPDM (**Figure 6.11 (a and b)**) appears to be at the bonding side or nearly zero throughout the energy axis, while for Cd(II) complex, the anti-bonding interactions are also observed in 0.0 to 0.1 a.u. range.

### 6.5. Concluding remarks

The synthesis of 1,3-Bis(diphenylhydroxymethyl)benzene (**1**) precursor was successfully achieved which was confirmed through NMR spectra. This precursor was further utilized for the synthesis of sterically hindered *meta*-benziporphodimethene compound. Much in agreement with the previously reported data, the UV-Vis plots showed the bathochromic shift upon metalation in 11, 16-Bis(phenyl)-6,6,21,21-tetraphenyl-*meta*-benzi-6,21-porphodimethenes. At the same time, the NMR spectra revealed the presence of agostic interactions between the metal center and the H22 atom of the benziporphodimethene macrocycle. The synthesized compounds were subjected to electronic structural analysis employing density functional theory method. Using TDDFT, at B3LYP function and LANL2DZ basis set, the frontier molecular orbitals and density of state plots were visualized. The plots inferred that despite the low band gap (HOMO-LUMO gap), the *m*-BPDM materials have not been utilized as conductor, owing to the absence of unoccupied energy states like LUMO+1, LUMO+2, LUMO+3, and so on, in the near proximity of HOMO.

## References

- [1] D. Ahluwalia, A. Kumar, S.G. Warkar, Recent developments in meta-benziporphodimethene: A new porphyrin analogue, *J. Mol. Struct.* 1228 (2021) 129672. <https://doi.org/10.1016/j.molstruc.2020.129672>.
- [2] M. Stępień, L. Latos-Grażyński, L. Szterenberg, J. Panek, Z. Latajka, Cadmium(II) and Nickel(II) Complexes of Benziporphyrins. A Study of Weak Intramolecular Metal-Arene Interactions, *J. Am. Chem. Soc.* 126 (2004) 4566–4580. <https://doi.org/10.1021/ja039384u>.
- [3] C.H. Hung, G.F. Chang, A. Kumar, G.F. Lin, L.Y. Luo, W.M. Ching, E. Wei-Guang Diau, m-Benziporphodimethene: A new porphyrin analogue fluorescence zinc(II) sensor, *Chem. Commun.* (2008) 978–980. <https://doi.org/10.1039/b714412a>.
- [4] R.K. Sharma, A. Maurya, P. Rajamani, M.S. Mehata, A. Kumar, meta-Benziporphodimethenes: New Cell-Imaging Porphyrin Analogue Molecules, *ChemistrySelect*. 1 (2016) 3502–3509. <https://doi.org/10.1002/slct.201600812>.
- [5] R.K. Sharma, L.K. Gajanan, M.S. Mehata, F. Hussain, A. Kumar, Synthesis, characterization and fluorescence turn-on behavior of new porphyrin analogue: meta-benziporphodimethenes, *Spectrochim. Acta - Part A Mol. Biomol. Spectrosc.* 169 (2016) 58–65. <https://doi.org/10.1016/j.saa.2016.06.020>.
- [6] G.F. Chang, C.H. Wang, H.C. Lu, L.S. Kan, I. Chao, W.H. Chen, A. Kumar, L. Lo, M.A.C. Dela Rosa, C.H. Hung, Factors that regulate the conformation of m-benziporphodimethene complexes: Agostic metal-arene interaction, hydrogen bonding, and  $\hat{\imath}\cdot 2,\pi$  coordination, *Chem. - A Eur. J.* 17 (2011) 11332–11343. <https://doi.org/10.1002/chem.201100780>.
- [7] D. Ahluwalia, A. Kumar, S.G. Warkar, M.M. Deshmukh, A. Bag, Uncovering the geometrical aspects of intramolecular hydrogen bond in meta-

- benziporphodimethenes through molecular tailoring approach, *Comput. Theor. Chem.* 1209 (2022) 113631. <https://doi.org/10.1016/j.comptc.2022.113631>.
- [8] D. Ahluwalia, A. Kumar, S.G. Warkar, M.M. Deshmukh, Effect of substitutions on the geometry and intramolecular hydrogen bond strength in meta-benziporphodimethenes: A new porphyrin analogue, *J. Mol. Struct.* 1220 (2020) 128773–128783. <https://doi.org/10.1016/j.molstruc.2020.128773>.
- [9] A. Kumar, C.H. Hung, S. Rana, M.M. Deshmukh, Study on the structure, stability and tautomerisms of meta-benziporphodimethene and N-Confused isomers containing  $\gamma$ -lactam ring, *J. Mol. Struct.* 1187 (2019) 138–150. <https://doi.org/10.1016/j.molstruc.2019.03.064>.
- [10] A.D. Becke, Density-functional thermochemistry. III. The role of exact exchange, *J. Chem. Phys.* 98 (1993) 5648–5652. <https://doi.org/10.1063/1.464913>.
- [11] L.S. Kassel, The limiting high temperature rotational partition function of nonrigid molecules: I. General theory. II. CH<sub>4</sub>, C<sub>2</sub>H<sub>6</sub>, C<sub>3</sub>H<sub>8</sub>, CH(CH<sub>3</sub>)<sub>3</sub>, C(CH<sub>3</sub>)<sub>4</sub> and CH<sub>3</sub>(CH<sub>2</sub>)<sub>2</sub>CH<sub>3</sub>. III. Benzene and its eleven methyl derivatives, *J. Chem. Phys.* 4 (1936) 276–282. <https://doi.org/10.1063/1.1749835>.
- [12] C. Lee, W. Yang, R.G. Parr, Development of the Colle-Salvetti correlation-energy formula into a functional of the electron density, *Phys. Rev. B* 37 (1988) 785–789. <https://doi.org/10.1103/PhysRevB.37.785>.
- [13] M.J. Frisch, G.W. Trucks, H.B. Schlegel, G.E. Scuseria, M. a. Robb, J.R. Cheeseman, G. Scalmani, V. Barone, G. a. Petersson, H. Nakatsuji, X. Li, M. Caricato, a. V. Marenich, J. Bloino, B.G. Janesko, R. Gomperts, B. Mennucci, H.P. Hratchian, J. V. Ortiz, a. F. Izmaylov, J.L. Sonnenberg, Williams, F. Ding, F. Lipparini, F. Egidi, J. Goings, B. Peng, A. Petrone, T. Henderson, D. Ranasinghe, V.G. Zakrzewski, J. Gao, N. Rega, G. Zheng, W. Liang, M. Hada,

M. Ehara, K. Toyota, R. Fukuda, J. Hasegawa, M. Ishida, T. Nakajima, Y. Honda, O. Kitao, H. Nakai, T. Vreven, K. Throssell, J. a. Montgomery Jr., J.E. Peralta, F. Ogliaro, M.J. Bearpark, J.J. Heyd, E.N. Brothers, K.N. Kudin, V.N. Staroverov, T. a. Keith, R. Kobayashi, J. Normand, K. Raghavachari, a. P. Rendell, J.C. Burant, S.S. Iyengar, J. Tomasi, M. Cossi, J.M. Millam, M. Klene, C. Adamo, R. Cammi, J.W. Ochterski, R.L. Martin, K. Morokuma, O. Farkas, J.B. Foresman, D.J. Fox, G16\_C01, (2016) Gaussian 16, Revision C.01, Gaussian, Inc., Wallin.

- [14] F.C. T. Lu, Multiwfn: A multifunctional wavefunction analyzer, *J. Comput. Chem.* 33 (2012) 580–592. <https://doi.org/https://doi.org/10.1002/jcc.22885>.
- [15] J.M.M. Roy Dennington, Todd A. Keith, GaussView5.0, (2016). <https://gaussian.com/citation/>.
- [16] M. Karabacak, E. Kose, A. Atac, E.B. Sas, A.M. Asiri, M. Kurt, Experimental (FT-IR, FT-Raman, UV-Vis,  $^1\text{H}$  and  $^{13}\text{C}$  NMR) and computational (density functional theory) studies on 3-bromophenylboronic acid, *J. Mol. Struct.* 1076 (2014) 358–372. <https://doi.org/10.1016/j.molstruc.2014.07.058>.
- [17] P.E. Contreras, L. Seijas, D. Osorio, TDOS quantum mechanical visual analysis for single molecules, ArXiv. (2021).
- [18] M. Prasath, S. Muthu, R.A. Balaji, Vibrational spectroscopy investigation using ab initio and DFT vibrational analysis of 7-chloro-2-methylamino-5-phenyl-3H-1, 4-benzodiazepine-4-oxide, *Spectrochim. Acta - Part A Mol. Biomol. Spectrosc.* 113 (2013) 224–235. <https://doi.org/10.1016/j.saa.2013.04.104>.
- [18] A.R. Zanatta, Revisiting the optical bandgap of semiconductors and the proposal of a unified methodology to its determination, *Sci. Rep.* 9 (2019) 11225. <https://doi.org/10.1038/s41598-019-47670-y>.

- [19] C. Karaca, A. Atac, M. Karabacak, Quantum chemical calculation (electronic and topologic) and experimental (FT-IR, FT-Raman and UV) analysis of isonicotinic acid N-oxide, *Spectrochim. Acta - Part A Mol. Biomol. Spectrosc.* 140 (2015) 85–95. <https://doi.org/10.1016/j.saa.2014.12.084>.
- [20] E. Kose, A. Atac, M. Karabacak, C. Karaca, M. Eskici, A. Karanfil, Synthesis, spectroscopic characterization and quantum chemical computational studies of (S)-N-benzyl-1-phenyl-5-(pyridin-2-yl)-pent-4-yn-2- amine, *Spectrochim. Acta - Part A Mol. Biomol. Spectrosc.* 97 (2012) 435–448. <https://doi.org/10.1016/j.saa.2012.06.041>.
- [21] S. Christopher Jeyaseelan, A. Milton Franklin Benial, K. Kaviyarasu, Vibrational, spectroscopic, chemical reactivity, molecular docking and in vitro anticancer activity studies against A549 lung cancer cell lines of 5-Bromo-indole-3-carboxaldehyde, *J. Mol. Recognit.* 34 (2021). <https://doi.org/10.1002/jmr.2873>.
- [22] C. Charanya, S. Sampathkrishnan, N. Balamurugan, Molecular Docking and Quantum Chemical Computations of 4-Chloro-2-[(furan-2-ylmethyl)amino]-5-sulfamoylbenzoic Acid Based on Density Functional Theory, *Polycycl. Aromat. Compd.* 0 (2021) 1–24. <https://doi.org/10.1080/10406638.2021.2020309>.

# CHAPTER 7

## CONFORMATIONAL ANALYSIS OF METALATED *meta*-BENZIPORPHODIMETHENES

### 7.1. Introduction

Benziporphodimethene like benzoporphyrin macrocycles are generally more flexible than regular porphyrins, as can be judged from the puckered structures observed in the solid state for the free bases and their metal complexes.[1,2] This may be due the loss of aromaticity and introduction of phenylene ring in the macrocyclic structure which creates steric constraints.

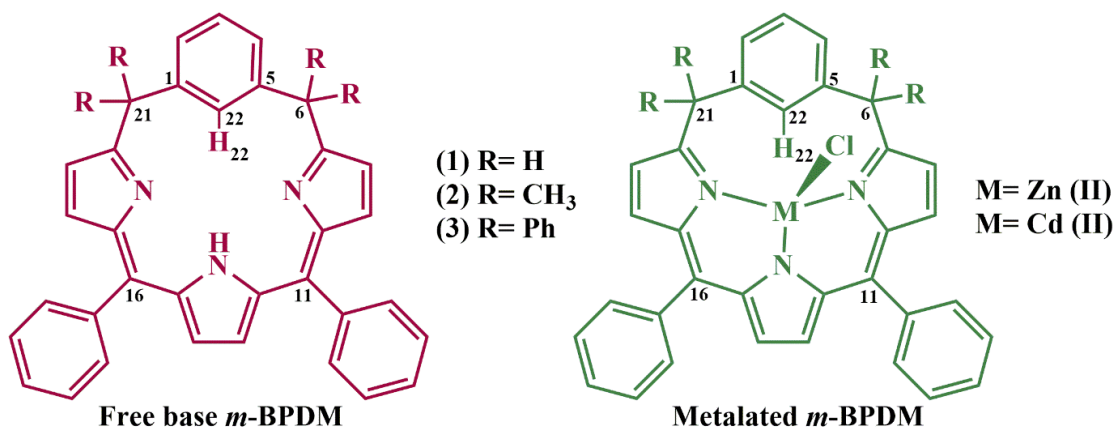


**Figure 7.1.** Geometries of *meta*-benziporphodimethene structures under study.

The labeling of metalated complexes as *syn* and *anti* was first done by Grazynski and co-workers,[1,3–5] while performing a similar study for *meta*- and *para*-benzoporphyrin systems. Basically, the *anti*- conformers refers to the geometry of *m*-BPDM wherein the chloride group attached to the metal ion is oriented opposite to the H22 atom. Refer to **Figure 7.1** and **7.2** for numbering and visualization, respectively. On the other hand, the *syn* conformers have chloride and H22 atom oriented in the same direction, as can be observed in **Figure 7.2**. Back in 2004, Grazynski and co-workers reported the first ever compound of *m*-BPDM, i.e., Zn(II) and Cd(II) chloride of 11,16-bis(4-nitrobenzene)-6,6,21,21-tetraphenyl-*meta*-beziporphodimethene.[5]

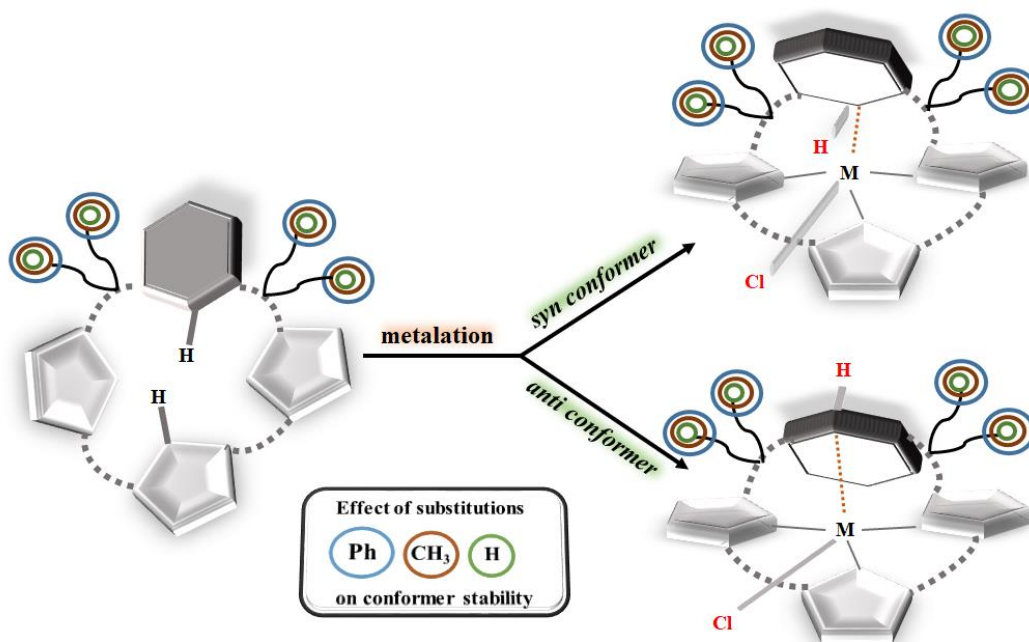


**Figure 7.2.** 3D-representation of *anti*- and *syn*- conformers of *m*-BPDM metal complex.

The compound was not further pursued by other research groups owing to the extremely low yield.[6] The X-ray crystal structure reported by them had *anti*-conformation.[5] Several years later, in 2009 when Hung and co-workers synthesized the tetramethyl (at C6- and C21-positions) derivative of *m*-BPDM using the same aldehyde group (*p*-nitrobenzaldehyde), found that the X-ray crystal structure of their compound was a *syn*-conformer.[2,7] Furthermore, Kumar *et. al.* also reported different analogues of tetramethyl (at C6- and C21-positions) substituted *m*-BPDM systems, which were again found as *syn*-conformers.[8,9] This invoked our interest to understand, whether the solid state structures are actually the lowest energy structures. If the variation in the groups placed at C6- and C21- position affecting the ground state conformation of these compounds. To answer all these queries, this study has been attempted.

In this chapter, we have incorporated detailed computational studies on the *syn*- and *anti*-conformers of *m*-BPDMs complexes in light of their stabilization in solid state

structures. The computational chemistry has been used to demonstrate the effect of substituents at  $sp^3$  *meso* carbons. Prior to this, many theoretical studies have been performed focusing on stabilization of the free base *m*-BPDM. The present study stands as the very first DFT analysis of these metalated *m*-BPDM structures stating the effect of bulkiness at  $sp^3$  positions. The results were found to be more impressive than previously reported results from DFT optimized geometries for different free base *m*-BPDM.

## 7.2. Computational details

In order to study the conformations of metalated *m*-BPDM systems, the input X-ray crystallographic information files have been taken from ref number [2]. The subsequent modifications for *syn* and *anti*-conformations along with the substituents placed at C6 and C21 positions have been incorporated using Gauss view 5.0 package [10]. Becke's three parameters exchange functional with the gradient corrected correlation formula of Lee, Yang and Parr [DFT-B3LYP] [11] was used with the effective core potential basis set LANL2DZ to optimize the geometry obtained after semiempirical calculation at restricted Hartree-Fock level [12]. Harmonic vibrational frequencies were calculated using analytical second derivatives for all systems. Calculated vibrational frequencies show that the obtained geometries represent true minima since no imaginary frequencies were found. In all calculations, convergence was reached when the relative change in the density matrix between subsequent iterations was less than  $1 \times 10^{-8}$ .[13,14]

### 7.3. Result and discussion

#### 7.3.1. Lowest energy conformers

In 2004, Grazynski *et. al.* have shown that the preferred conformation for both metal complexes of zinc and cadmium with *meta*-benzoporphyrin as well as for *m*-BPDM macrocycle having phenyl rings at  $sp^3$  *meso* carbons has the phenylene ring tilted away from the metal center with the inner C-H bonds and the axial M-X bond in an *anti*- orientation [1]. They found that the lowest energy conformation for the metal complexes Zn(II) and Cd(II) with 11, 16-bis(4-nitrophenyl)-6,6,21,21-tetraphenyl-*meta*-benzi-6,21-porphodimethene are *anti*- conformers by DFT studies.

But as observed from the metal complexes of zinc (II) and cadmium (II) with the ligand 11,16-bis(phenyl)-6,6,21,21-tetramethyl-*meta*-benzi-6,21-porphodimethene, the *syn* geometry corresponds to the solid state geometry (single crystal X-ray structure) [2]. So, two questions arose in our minds; firstly whether the obtained geometries from the single crystal X-ray structures are the lowest energy conformers for all metal complexes? Secondly, do substituents at  $sp^3$  *meso* carbons play an important role to drive the conformer orientations? In order to address these issues, we have carried out density functional theory calculations on *syn* and *anti*- conformers of zinc, and cadmium metal complexes on varying the substituents at  $sp^3$  *meso* carbons including their free base *m*-BPDMs (**Figure 7.1**) on B3LYP/LANL2DZ level of theory. Vibrational frequencies were calculated to ensure that all optimized geometries correspond to true minima on the potential energy surface.

Starting geometries for the metal complexes having *syn* conformation were taken from the crystal structure of chloro-(11,16-diphenyl-6,6,21,21-tetramethyl-*meta*-

benzoporphodimethene) zinc (II), and chloro-(11,16-diphenyl-6,6,21,21-tetramethyl-*meta*-benzoporphodimethene) cadmium (II), reported by Chang *et. al.* [2] and subsequent modifications were made employing GaussView 5.0 software [34]. The geometries obtained from the crystal structure (*syn*) and by modification in the phenylene ring angle (*anti*) were first subjected to PM3 calculation. Subsequently, semiempirical calculations were performed at restricted Hartree-Fock level by using PM3 optimized geometries. The geometries obtained after semiempirical calculations were then subjected to DFT optimization at the B3LYP/LANL2DZ level of theory for all systems discussed in this chapter. In each case, a genuine energy minima was obtained since no imaginary frequencies were found during vibrational frequencies calculation.

DFT optimized structures of *syn*- and *anti*-conformers of Zn-Cl and Cd-Cl, are shown in **Chart 7.1, 7.2** and **7.3** for R= H, CH<sub>3</sub> and Ph, respectively at *sp*<sup>3</sup> *meso* carbons (C6- and C21- positions). The xyz coordinates of the output geometries have been attached in **Appendix-III**. **Chart 7.4** depicts the DFT optimized geometries of free base *m*-BPDMs for different substituents placed at *sp*<sup>3</sup> *meso* carbons. Selected geometrical parameters for *syn* and *anti*-conformer for zinc and cadmium metal complexes including X-ray structure geometries optimized on B3LYP/LANL2DZ level of theory are given in **Table 7.2**. A comparison of various bond lengths and angles for free base geometries and their metal complexes are given **Table 7.2**. For each metalated system, there are three *syn* and three *anti* (R"= H, -CH<sub>3</sub> and -Ph) conformers that differ only for substituents at *sp*<sup>3</sup> *meso* carbons. Each conformer can be uniquely characterized by the signs of the torsion angles φ<sub>1</sub>- φ<sub>4</sub>, as defined in the footnote of **Table 7.2**. The distinction between *anti* and *syn* conformers is made on the basis of

the signs of  $\phi_1$  and  $\phi_2$  ( $^+\phi_1 \ ^-\phi_2$  for *syn* and  $^-\phi_1 \ ^+\phi_2$  for *anti*), whereas the remaining two angles  $\phi_3$  and  $\phi_4$  define the orientation of 6-21-methyls and 6-21-phenyls.[1]

*Syn* conformers for the metal complexes of zinc and cadmium correspond to the solid state geometry, as could be expected, have the lowest energies. The comparison of total electronic energies including zero-point vibrational energies and their relative energies are given in **Table 7.1** for all systems discussed herein. Refer to **Figure 7.1** for numbering and labelings. It is clear from Table 7.1 that *syn* conformers have the lowest energies ( $\Delta E_{Znsyn} < \Delta E_{Znanti}$ ;  $\Delta E_{Cdsyn} < \Delta E_{Cdanti}$ ) in all systems, when R= -H and -CH<sub>3</sub>. But, when R= -Ph at *sp*<sup>3</sup> *meso* carbons, the trend is different i.e., *anti*-conformer have the lowest energy for zinc and cadmium complexes. The energy order of the *syn* conformers were found as  $\Delta E_{Znsyn} < \Delta E_{Cdsyn}$  and the same trend in energies was also observed for the *anti*-conformers i.e.,  $\Delta E_{Znanti} < \Delta E_{Cdanti}$  for R= -H and -CH<sub>3</sub>. The single point (SP) calculations were performed on the solid state structures obtained from the X-ray data. The SP calculation of the *syn* conformers (obtained from X-ray crystallographic data) also follow the same trend  $\Delta E_{Znsyn} < \Delta E_{Cdsyn}$ . The energy difference between the SP energy and the optimized structure energy are 284.1773162, and 345.8948072 kcal/mol for zinc, and cadmium complexes, respectively for R= -CH<sub>3</sub>. It means that the optimized structure are the lowest energy structure. Also, in case of free base *m*-BPDMs, DFT optimized structures have the lowest energy and having a difference of 397.9718621 kcal/mol from the single point calculation of energy for *m*-BPDM (R = -CH<sub>3</sub>) discussed here. Free base *m*-BPDM (R= -H, -CH<sub>3</sub>) is higher in energy than its metal complexes (**Table 7.1**). This may be attributed to the fact that the structure of the free base is highly puckered than its metal complex which in fact is more symmetrical than free base. As per the

observations, in case of *anti*-conformers, structure is more twisted than their corresponding *syn* conformers for Zn(II) and Cd(II) complexes when R= -H, -CH<sub>3</sub>. Consequently, *syn*- conformers are energetically more favorable than *anti*- conformers in the case of substituents like -H and -CH<sub>3</sub> at C6- and C21- positions. In contrast to this, the *syn* conformer is more symmetrical than its *anti*- conformer in the case of substituents like -Ph, but the steric factor play an important role in stabilizing the *anti*-conformer than their corresponding *syn* conformers.

**Table 7.1.** LANL2DZ total electronic energies ( $E_{\text{total}}$ ) and relative energies ( $E_{\text{rel}}$ ) for the DFT optimized structures. For all systems the values including the zero-point vibrational energies (ZPV) are also given; where a= Energy relative to the most stable conformer separately for R= -H(1), -CH<sub>3</sub>(2) and -Ph(3)). ZPV= Zero-point vibrational energy.

Structure	$E_{\text{total}}$ , Hartree	$E_{\text{total}} (+\text{ZPV})$ , Hartree
Zn- <i>syn</i> (1)	-1998.04	-1997.55
Zn- <i>syn</i> (2)	-2155.28	-2154.74
Zn- <i>syn</i> (3)	-2922.17	-2921.36
Cd- <i>syn</i> (1)	-1980.48	-1979.99
Cd- <i>syn</i> (2)	-2137.72	-2137.19
Cd- <i>syn</i> (3)	-2904.61	-2903.79
Zn- <i>anti</i> (1)	-1998.04	-1997.55
Zn- <i>anti</i> (2)	-2155.27	-2154.74
Zn- <i>anti</i> (3)	-2922.18	-2921.36
Cd- <i>anti</i> (1)	-1980.48	-1979.99
Cd- <i>anti</i> (2)	-2137.72	-2137.18
Cd- <i>anti</i> (3)	-2904.62	-2903.81
Free base (1)	-1474.94	-1474.45
Free base (2)	-1632.19	-1631.59
Free base (3)	-2399.13	-2398.31

**Chart 7.1.** B3LYP/LANL2DZ optimized geometries for (a) Zinc *syn* conformer ; (b) Zinc *anti* conformer; (c) Cd *syn* conformer; (d) Cd *anti*-conformer; when R= H (1). at  $sp^3$  *meso* carbons.

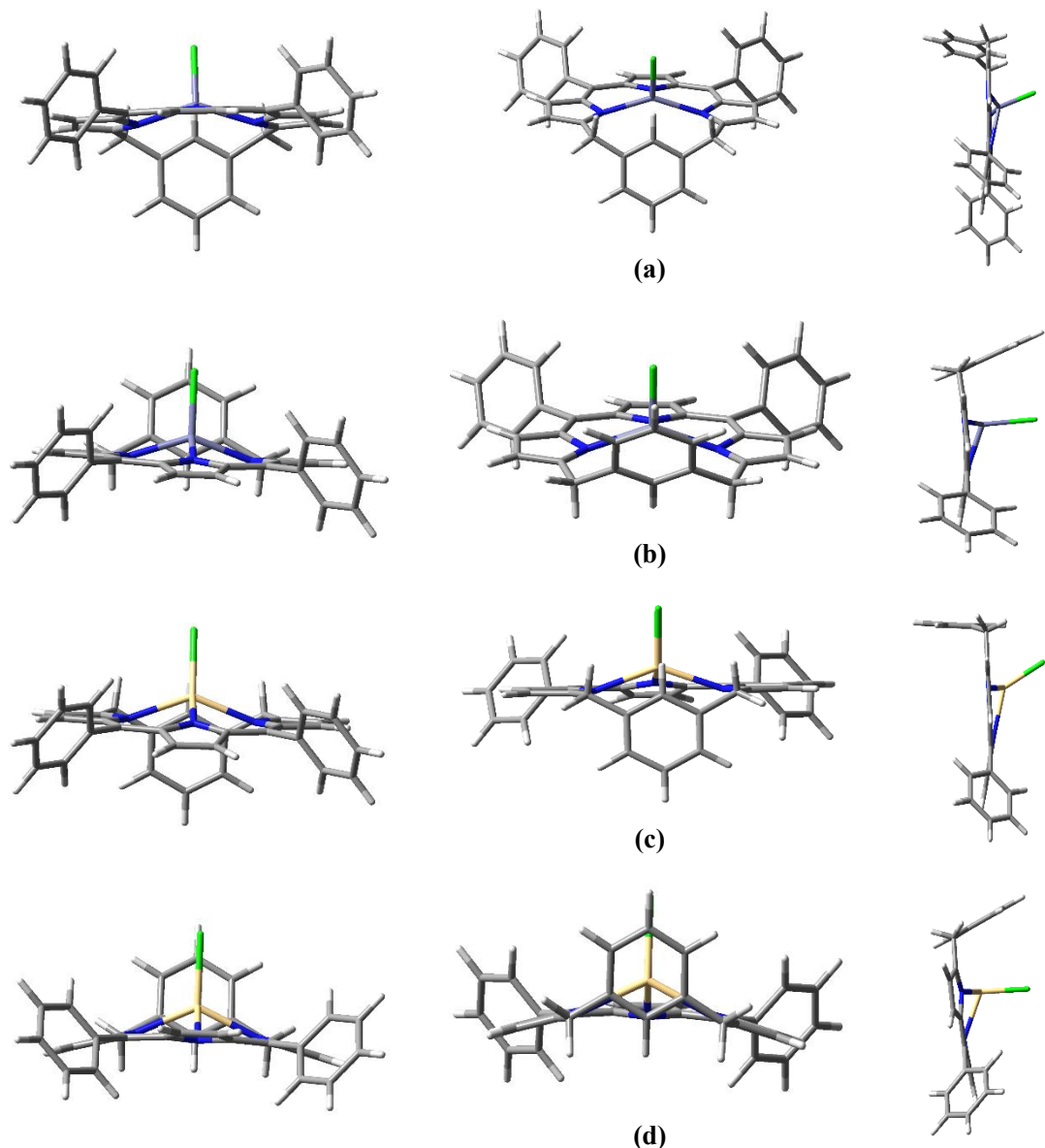


**Chart 7.2.** B3LYP/LANL2DZ optimized geometries for (a) Zinc *syn* conformer; (b) Zinc *anti* conformer; (c) Cd *syn* conformer (d) Cd *anti* conformer; when R= -CH<sub>3</sub> (2), at *sp*<sup>3</sup> *meso* carbons.

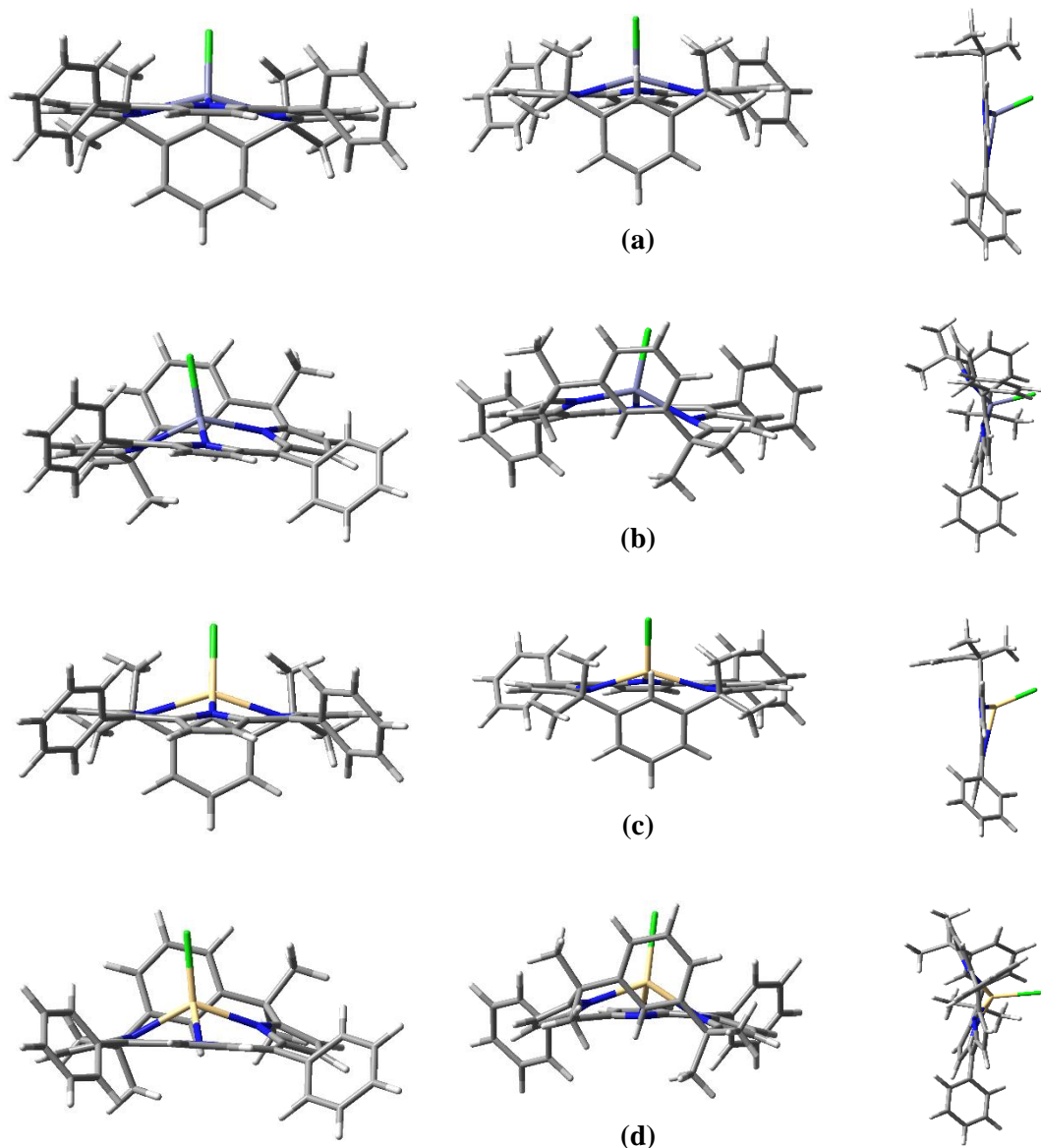


**Chart 7.3.** B3LYP/LANL2DZ optimized geometries for (a) Zinc syn conformer ; (b) Zinc anti conformer; (c) Cd syn conformer; (d) Cd anti conformer; when R= Ph(3) at  $sp^3$  meso carbons.

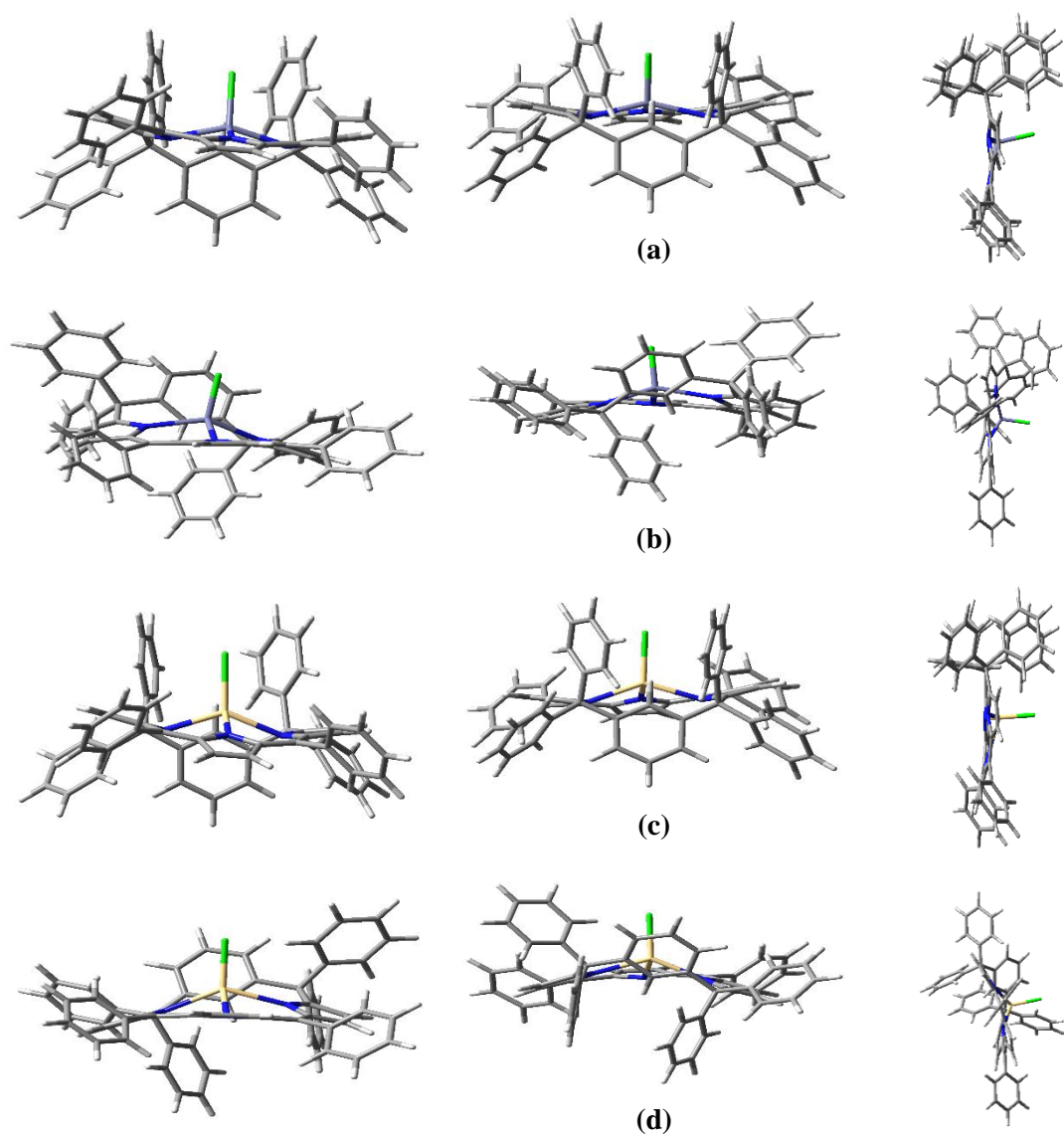


**Chart 7.4.** B3LYP/LANL2DZ optimized geometries for free base *m*-BPDM when (a) R= H (1); (b) R= methyl (2); (c) R = Phenyl (3) at *sp*<sup>3</sup> *meso* carbons.

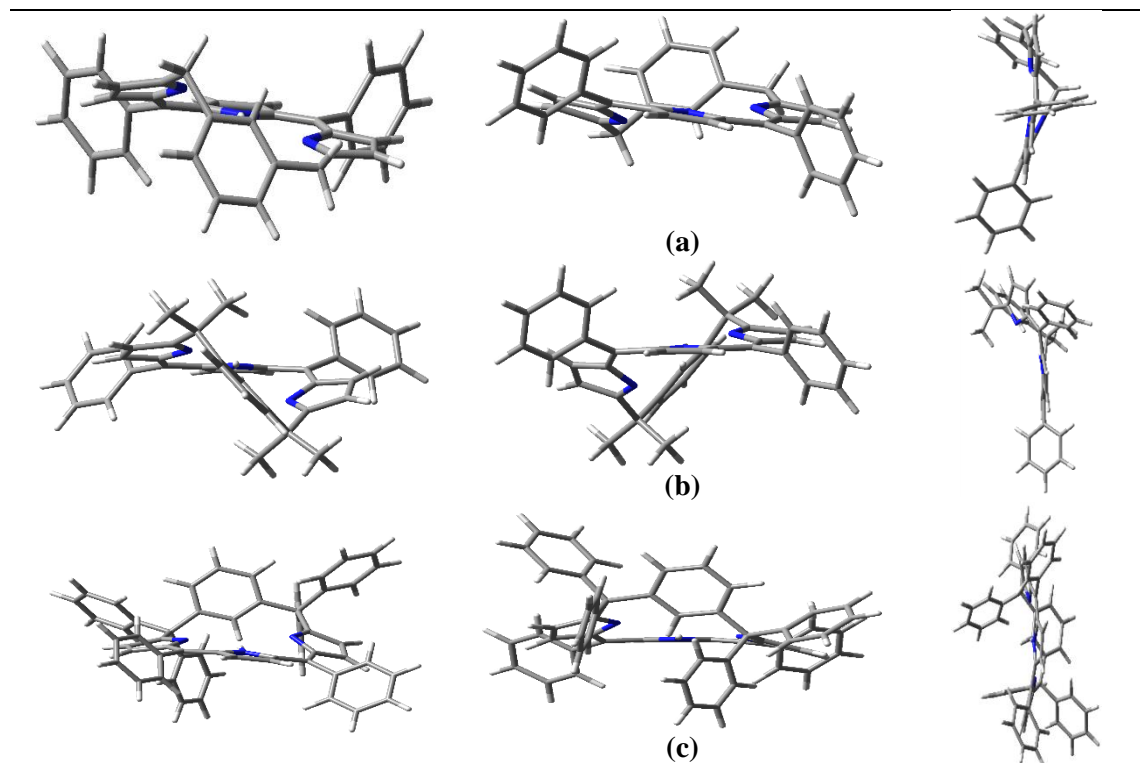
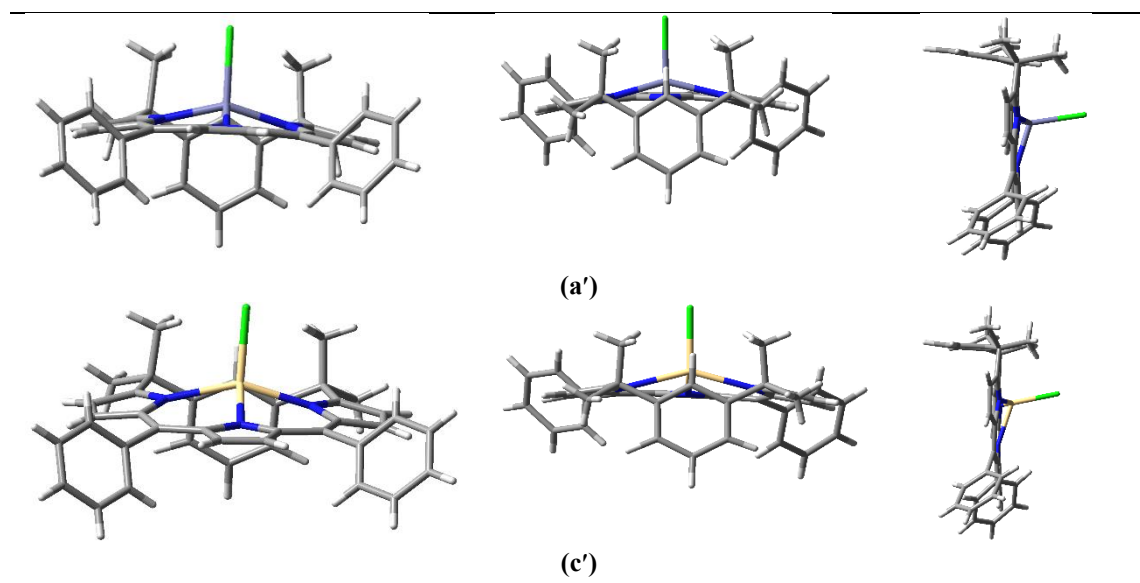


**Chart 7.5.** X-Ray geometries for (a') Zinc *syn* conformer; (c') Cd *syn*-conformer ; when R= -CH<sub>3</sub>, at *sp*<sup>3</sup> *meso* carbons.



The introduction of bulkier ions like cadmium causes an additional increase in the energy of both *syn* and *anti*-conformers when compared to that of zinc. The relative energy (energy relative to the zinc complex) differences between the *syn* and *anti*-conformers from Cd(II) complexes are more and have been summarized in **Table 7.2**.

### 7.3.2. Comparison of DFT optimized and X-ray geometries

Important geometrical parameters of the DFT-optimized structures and X-ray geometries are given in **Table 7.2** for metal complexes. The DFT optimized free base *m*-BPDMs and X-ray structure (of R= -CH<sub>3</sub>) important parameters are given in **Table 7.2**. The deviations of 0.0382 Å, and 0.0922 Å, have been observed for zinc, and cadmium, respectively, from their X-ray geometry in M-C22 bond distance for R= -CH<sub>3</sub>. Refer to **Figure 7.1** for numbering and labeling of atoms discussed herein. A decrease in the M-C22 bond distance as the size of substituents at *sp*<sup>3</sup> *meso* carbons for *syn*- and *anti*-conformers was observed. The M-H22 bond distances becomes longer as the size of metal ion increase except for cadmium when R= -CH<sub>3</sub> and increase in M-H22 distances were measured as the size of the substituents increase from -H to -CH<sub>3</sub> but the same trend were not found if the substituents is phenyl (*vide infra*) for *syn* and *anti*-conformers. The M-C22 and M-H22 bond distances are longer in DFT optimized structures than their corresponding X-ray structures (R= -CH<sub>3</sub>). The deviation of 0.2102 Å, and 0.0085 Å for M-H22 bond distance have been observed for zinc, and cadmium, respectively from their X-ray geometry. But in case of DFT-optimized *anti*- conformers, the M-C22 bond distances are shorter than their corresponding *syn* conformers. On the other hand, M-H22 bond distances are longer than their corresponding *syn* conformers. The maximum deviation for M-H22 was found to be 0.2075 Å with DFT optimized structure and X-ray geometry for zinc complexes.

### 7.3.3. Geometrical studies

The metal ion lies above the three pyrrolic nitrogen's plane ( $N_3$ ) both in X-ray geometries (for methyl substituted) as well as for DFT optimized geometries in both conformers in all the systems discussed herein. The *anti*-conformers metal ion lies at a higher distance above the  $N_3$  plane in comparison to both X-ray geometry as well as DFT-optimized *syn* conformers. Refer to **Chart 7.6** for pictorial representations of all the non-bonded angles.

The angle between the phenylene plane and the plane of the three pyrrolic nitrogen's ( $C_6-N_3$ ) is markedly dependent on the orientation of the substituents at  $sp^3$  *meso* carbons, which in turn affects the M-C22 and M-H22 distances in the conformation core (**Table 7.2**). The  $C_6-N_3$  angle obtained for the DFT optimized *syn* conformers ( $R = -H$ ,  $-CH_3$  and  $-Ph$ ) and X-ray geometries for  $R = -CH_3$  are in such a way that the phenylene rings remain perpendicular to the  $N_3$  plane. This reflects the inherent flexibility of the *m*-BPDM. In case of *anti*-conformers, the angle between the phenylene ring and plane of the three pyrrolic nitrogen are lesser than their corresponding *syn* conformers for both zinc, and cadmium complexes, which in fact emphasizes on the flexibility of *m*-BPDM metal complexes. Large deviations were calculated between *syn* and *anti*-conformers  $C_6-N_3$  plane angle (**Table 7.2**). The angle between the Cl-M-C22 are small as compared to their *anti*-conformers and the values are more closer to the  $120^\circ$  while in *syn* conformers it is very close to  $90^\circ$  (see **Chart 7.1 to 7.3** for structures) The angle between the phenylene plane and three pyrrolic nitrogen's plane in free base DFT-optimized structure and X-ray geometry ( $R = -CH_3$ ) are  $19.829$  and  $52.406^\circ$ , respectively. In X-ray geometry the phenylene ring is more tilted towards the pyrrolic nitrogen's plane (**Chart 7.5**) and structure is more

puckered as compared to the DFT-optimized geometry. This is further supported by the energy difference between the DFT-optimized and X-ray geometry ( $R = -CH_3$ ). DFT-optimized structure is energetically more favorable than the X-ray geometry with the difference of 397.972 kcal/mol (**Table 7.2**).

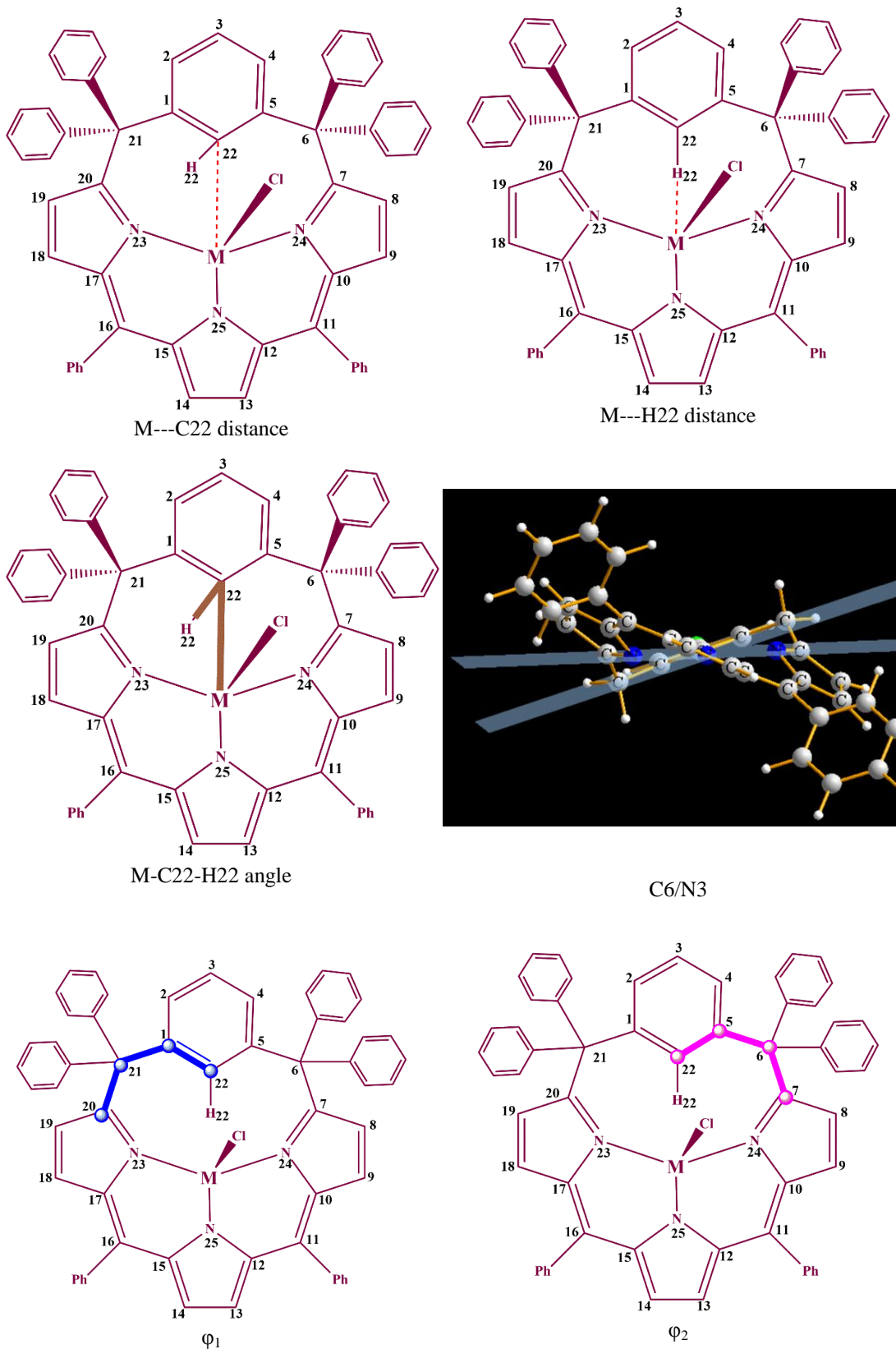
The M-C22 and M-H22 bond distances are very small as compared to the van der Waal contact and evidence the formation of weak yet influential agostic bonds. In addition to this, careful analysis of available *syn* conformer crystal structure (**Chart 7.5**) and DFT-optimized structure for *syn* (**Chart 7.2**) confirms that the C22-H22 bond is not coplanar with the phenylene ring, which is also indicative of agostic interactions. The distance between the H22 atom and the phenylene plane is 0.2344 Å ( $R = -CH_3$ ) in the cadmium complex. The dihedral angle between the phenylene plane and hydrogen atom on the phenylene ring is 2.388° for cadmium complexes in X-ray geometry. The dihedral angle and distance between the H22 atom and the phenylene ring plane is 0.929° and 0.0644 Å, respectively. The C22-H22 bond distance in X-ray geometry and DFT-optimized geometry are 1.1186 Å and 1.0819 Å, respectively for this complex. In the case of zinc(II) complex, X-ray and DFT optimized geometry, the distance and dihedral angle between the H22 atom and the phenylene plane are very less in comparison to the Cd(II) complex, i.e., 0.0157 Å and 1.168°, 0.0380 Å and 0.556°, respectively. The C22-H22 bond distance are 0.9501 Å and 1.0794 Å in X-ray geometry and DFT-optimized geometry, respectively for zinc (II) complex. The agostic interaction is negligible in the case of zinc complex but a considerable amount of agostic interaction exist in cadmium complex (**Chart 7.2** and **7.5**) both in the X-ray geometry and DFT-optimized geometry. Due to this interaction, the M-N<sub>3</sub> distance in cadmium shows large deviation (**Table 7.2**) in DFT-optimized geometry with their X-

ray geometry. This interaction should affect the H22 chemical shift in the NMR but this effect was less noticeable in the *m*-BPDM in comparison to that of benziporphyrin [9,43] (at most 0.64 ppm for zinc, and 0.44 ppm for cadmium with their free base). It is noteworthy that the variations of chemical shifts (especially  $^1\text{H}$ ) can be influenced by conformational and electronic effects not related to the metal-arene interaction. Also, it should be noted that, as the electrophilicity of cationic center increases, the metal-arene interaction becomes stronger. Cd(II) ions in the benziporphodimethene environment are poor electrophiles, and hence the observed interactions are very weak.[1,2]

The substituents play an important role in stabilizing the porphodimethenes or phlorins. The reduced form of porphyrins, benziporphyrin and porphodimethene, is protected by two aryl or alkyl groups at  $sp^3$  *meso* bridges.[2] In the case of *m*-BPDMs, the substituents drive the stabilities and twisting of geometries to form *syn*- and *anti*-conformers. The isolated form of zinc, and cadmium metal complexes of 11,16-bis(phenyl)-6,6,21,21-tetramethyl-*meta*-benzi-6,21-porphodimethene have the *syn* conformer which, obviously, are the lowest energy conformer. So, in order to have the better idea on effect of substituents at  $sp^3$  *meso* carbons, we have carried out the DFT calculation on varying the substituents at  $sp^3$  *meso* carbons on free base *m*-BPDMs and their metal complexes with zinc, and cadmium (**Figure 7.2**). On the basis of theoretical calculation, it has been observed the increase in the bulkiness of the substituents decreases the energy of the molecule and thus stabilizing the bulkier group substituted free base *m*-BPDMs and their metal complexes ( $\Delta E_{\text{Ph}} < \Delta E_{\text{CH}_3} < \Delta E_{\text{H}}$ ; **Table 7.2**). Also, DFT calculation demonstrate that the isolated form of zinc, and

cadmium metal complexes i.e., *syn*, with the ligand when R= -CH<sub>3</sub> as the substituents, is the lowest energy conformer. The *syn* conformer are the most stable when substituents are lesser bulky (R= -H, -CH<sub>3</sub>). The *anti*-conformers have the lowest energy in the case of bulkier substituent (R=Ph). The substituents also affect the angle between the phenylene ring and three pyrrolic nitrogen's plane (C<sub>6</sub>-N<sub>3</sub>) and increase as the size of the substituents increase (**Table 7.2**). On the basis of NMR and DFT calculations, we can propose that substituents affect the dynamic broadening in NMR and relative stabilities of the conformers.

It was also observed, when R= H at *sp*<sup>3</sup> *meso* carbons, the optimized *syn* and *anti*-geometries are very symmetrical. We did not observe any twisting in the geometries (**Chart 7.3**) which in turn affects the torsion angles,  $\varphi_1$  and  $\varphi_2$ , measured for these geometries are almost numerically same (see **Table 7.2**). The same phenomena were also observed when R= -CH<sub>3</sub>. The DFT optimized *syn* geometries are symmetrical (see **Chart 7.2**). The torsion angles,  $\varphi_1$  and  $\varphi_2$ , measured for *syn* geometries are almost numerically same. In addition, for all systems discussed herein, the ionic radius of the coordinated metal ion has an evident effect on the relative stabilities of the conformers and probably also on the activation barrier.[1] All the relative energy and important parameters are given in **Table 7.2**.

**Chart 7.6.** Depiction of angles and bond distances measured in Table 7.2.

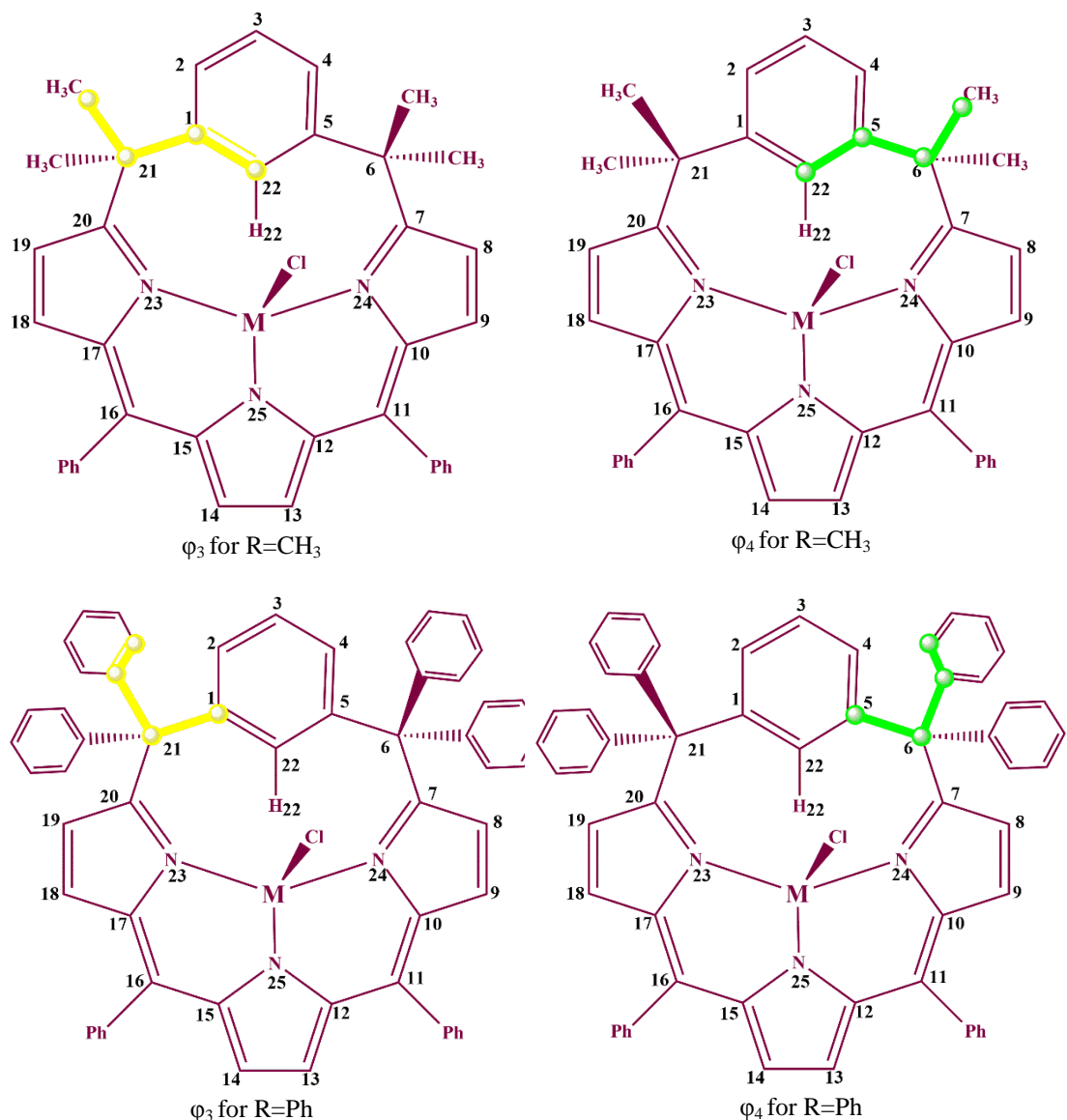


**Table 7.2.** Relative Energies and Selected Geometrical Parameters of the X-ray and DFT Optimized Structures of the Zn, and Cd *m*-BPDMs (where R= H (1); CH<sub>3</sub> (2); Ph (3)).

Structure	$\Delta E^a$ , kcal/mol	Distance (Å)		Angles (°)		Torsional angles <sup>b, c</sup> (°)			
		M---C22	M—H22	M-H22-C22	C6/N3 <sup>d</sup>	$\varphi_1$	$\varphi_2$	$\varphi_3$	$\varphi_4$
Zn-syn (1)	0.00 (0.00)	2.8862	2.6214	92.75	74.52	-87.71	87.61	--	--
Zn-anti (1)	3.19 (2.83)	2.8636	2.9520	74.66	66.03	79.31	-79.35	--	--
Cd-syn (1)	0.00 (0.00)	2.8410	2.6415	89.08	81.08	-94.57	94.57	--	--
Cd-anti (1)	1.06 (0.69)	2.8382	3.0857	66.75	6.03	78.06	-78.06	--	--
Zn-syn (2)	0.00 (0.00)	2.8714	2.8641	79.54	88.78	-97.95	97.95	20.61 (140.92)	-20.61 (-140.92)
Zn-syn (2) X-ray*	--	2.8332	2.6539	90.93	81.54	-93.46	90.38	25.57 (140.92)	-28.52 (149.92)
Zn-anti (2)	3.44 (2.96)	2.7738	2.9029	72.35	68.91	96.28	-49.82	-142.92 (-21.89)	-169.75 (71.59)
Cd-syn (2)	0.00 (0.00)	2.8056	2.8378	77.28	86.88	-	102.35	17.09 (137.85)	-17.12 (-137.07)
Cd-syn (2) X-ray*	--	2.7134	2.8293	72.59	89.43	-99.24	95.59	19.22 (137.85)	-23.63 (-144.19)
Cd-anti (2)	3.07 (2.78)	2.7983	3.0634	65.74	68.11	96.12	-58.59	-141.68 (22.14)	-178.75 (62.85)
Zn-syn (3)	5.80 (3.37)	2.7880	2.5400	91.42	75.86	-75.12	79.96	52.66 (62.42)	-47.07 (-73.17)
Zn-anti (3)	0.00 (0.00)	2.6763	2.6982	77.22	60.88	45.38	-81.62	-47.57 (-71.98)	74.03 (42.41)
Cd-syn (3)	7.11 (6.91)	2.7902	2.6113	87.81	82.45	-82.19	90.25	52.78 (72.54)	-45.07 (-78.17)
Cd-anti (3)	0.00 (0.00)	2.7056	2.8305	72.29	58.57	81.62	-48.22	-75.35 (-44.34)	48.45 (70.64)

<sup>a</sup>Energies relative to the most stable conformer. Values in parentheses were calculated with the ZPV contribution included.

<sup>b</sup>Torsion angles in are defined as follows.  $\varphi_1$ , C(20)-C(21)-C(1)-C(22);  $\varphi_2$ , C(22)-C(5)-C(6)-C(7);  $\varphi_3$ , C(1)-C(21)-C(ipso)-C(ortho);  $\varphi_4$ , C(5)-C(6)-C(ipso)-C(ortho) when R=Ph but when R=CH<sub>3</sub>, torsion angles were defined as follows.  $\varphi_1$ , C(20)-C(21)-C(1)-C(22);  $\varphi_2$ , C(22)-C(5)-C(6)-C(7);  $\varphi_3$ , C(22)-C(1)-C(21)-C(-CH<sub>3</sub>);  $\varphi_4$ , C(22)-C(5)-C(6)-C(-CH<sub>3</sub>). The angles with smaller absolute values are chosen for  $\varphi_3$  and  $\varphi_4$ . Numberings follows scheme 2; the axial ligand pointing toward the viewer.

<sup>c</sup>For all M-Cl complexes when R and R", the top values of  $\varphi_3$  and  $\varphi_4$  correspond to the phenyl substituents *syn* to the Cl ligand. When R' methyl substituents *syn* to the Cl ligand.

<sup>d</sup>Angle between the phenylene mean plane and plane of N(23)-N(24)-N(25) atoms. There is no  $\varphi_3$  and  $\varphi_4$  for the substituents R at *sp*<sup>3</sup> *meso* carbons.

\*X-ray data taken from reference number 2.

#### 7.4. Concluding remarks

This chapter focused on the conformational analysis (*syn* and *anti*-conformers) of metalated *m*-BPDM complexes, upon increasing the bulkiness at *sp*<sup>3</sup> *meso* carbon atoms. The X-ray crystallographic data for R"= -CH<sub>3</sub> confirmed that *syn* conformers were more stable for both zinc and cadmium metal complexes. Upon comparing this data with the DFT optimized structures of these molecules, it was confirmed that the *syn* conformers were bearing lower energies in comparison to that of *anti*-conformers, and hence the solid state structures were obtained as *syn* conformers. It is also important to note that the DFT optimized structures for free base *m*-BPDM were having higher energy than its metalated complexes for R= -H and -CH<sub>3</sub>. Also, the extremely puckered structure of free base *m*-BPDM obtained some symmetry upon metalation. The calculations also concluded that the *anti*-conformer was a more stable form for R=-Ph, which means that the presence of bulkier group renders stability to this *anti* conformer of both zinc and cadmium *m*-BPDM complexes.

## References

- [1] M. Stępień, L. Latos-Grazyński, L. Szterenberg, Conformational Flexibility of Nickel (II) Benziporphyrins, *Inorg. Chem.* 43 (2004) 6654–6662. <https://doi.org/https://doi.org/10.1021/ic049172d>.
- [2] G.F. Chang, C.H. Wang, H.C. Lu, L.S. Kan, I. Chao, W.H. Chen, A. Kumar, L. Lo, M.A.C. Dela Rosa, C.H. Hung, Factors that regulate the conformation of m-benziporphodimethene complexes: Agostic metal-arene interaction, hydrogen bonding, and  $\hat{1}\cdot 2,\pi$  coordination, *Chem. - A Eur. J.* 17 (2011) 11332–11343. <https://doi.org/10.1002/chem.201100780>.
- [3] M. Stępień, L. Latos-Grazyński, Tetraphenylbenziporphyrin - A ligand for organometallic chemistry, *Chem. - A Eur. J.* 7 (2001) 5113–5117. [https://doi.org/10.1002/1521-3765\(20011203\)7:23<5113::AID-CHEM5113>3.0.CO;2-V](https://doi.org/10.1002/1521-3765(20011203)7:23<5113::AID-CHEM5113>3.0.CO;2-V).
- [4] M. Stępień, L. Latos-Grazyński, Tetraphenyl-p-benziporphyrin: A carbaporphyrinoid with two linked carbon atoms in the coordination core, *J. Am. Chem. Soc.* 124 (2002) 3838–3839. <https://doi.org/10.1021/ja017852z>.
- [5] M. Stępień, L. Latos-Grazyński, L. Szterenberg, J. Panek, Z. Latajka, Cadmium(II) and Nickel(II) Complexes of Benziporphyrins. A Study of Weak Intramolecular Metal-Arene Interactions, *J. Am. Chem. Soc.* 126 (2004) 4566–4580. <https://doi.org/10.1021/ja039384u>.
- [6] D. Ahluwalia, A. Kumar, S.G. Warkar, Recent developments in meta-benziporphodimethene: A new porphyrin analogue, *J. Mol. Struct.* 1228 (2021) 129672. <https://doi.org/10.1016/j.molstruc.2020.129672>.
- [7] C.H. Hung, G.F. Chang, A. Kumar, G.F. Lin, L.Y. Luo, W.M. Ching, E. Wei-Guang Diau, m-Benziporphodimethene: A new porphyrin analogue fluorescence zinc(II) sensor, *Chem. Commun.* (2008) 978–980. <https://doi.org/10.1039/b714412a>.

- [8] R.K. Sharma, L.K. Gajanan, M.S. Mehata, F. Hussain, A. Kumar, Synthesis, characterization and fluorescence turn-on behavior of new porphyrin analogue: meta-benziporphodimethenes, *Spectrochim. Acta - Part A Mol. Biomol. Spectrosc.* 169 (2016) 58–65. <https://doi.org/10.1016/j.saa.2016.06.020>.
- [9] R.K. Sharma, A. Maurya, P. Rajamani, M.S. Mehata, A. Kumar, meta-Benziporphodimethenes: New Cell-Imaging Porphyrin Analogue Molecules, *ChemistrySelect*. 1 (2016) 3502–3509. <https://doi.org/10.1002/slct.201600812>.
- [10] T.A.K. J.M.M. Roy Dennington, GaussView 5.0, (n.d.).  
<https://doi.org/https://gaussian.com/citation/>.
- [11] A.D. Becke, Density functional thermochemistry. III. The role of exact exchange, *J. Chem. Phys.* 98 (1993) 5648–5652. <https://doi.org/10.1063/1.464913>.
- [12] F. Sim, A. St-Amant, I. Papai, D.R. Salahub, Gaussian Density Functional Calculations on Hydrogen-Bonded systems, *J. Am. Chem. Soc.* 114 (1992) 4391–4400. <https://doi.org/10.1021/ja00037a055>.
- [13] D. Ahluwalia, A. Kumar, S.G. Warkar, M.M. Deshmukh, A. Bag, Uncovering the geometrical aspects of intramolecular hydrogen bond in meta-benziporphodimethenes through molecular tailoring approach, *Comput. Theor. Chem.* 1209 (2022) 113631. <https://doi.org/10.1016/j.comptc.2022.113631>.
- [14] D. Ahluwalia, A. Kumar, S.G. Warkar, M.M. Deshmukh, Effect of substitutions on the geometry and intramolecular hydrogen bond strength in meta-benziporphodimethenes: A new porphyrin analogue, *J. Mol. Struct.* 1220 (2020) 128773–128783. <https://doi.org/10.1016/j.molstruc.2020.128773>.

## CHAPTER 8

### CONCLUSION AND FUTURE PROSPECTS

---

#### 8.1. Conclusion

- The present study aims to draw the attention of the chemists towards *meta*-benzoporphodimethene analogues, providing various factors that may enhance the product yield, as concluded from their computational studies.
- The study of *meso*-substituted free base *meta*-benzoporphodimethenes suggests that orthochlorinated and pentafluorinated phenyl rings at  $sp^2$  *meso*-positions tend to be more symmetrical and show stronger intramolecular hydrogen bond strength. Furthermore, the highly puckered methyl substituted free base *m*-BPDM molecules obtain symmetry upon the placement of bulkier groups at  $sp^3$  *meso* carbon atoms, i.e., C6- and C21- positions.
- The study of non-covalent interactions pointed out the presence of H-bond interaction within the *m*-BPDM systems. The C3-substitutions on the free base *m*-BPDM molecule suggests that -CF<sub>3</sub> placement along with -Ph group and  $sp^3$  *meso*- carbon atoms yields stronger intramolecular H-bond interaction, thus, helping the core of this system to stay intact. In addition to this, -Cl group at C3-position imparted symmetry to the puckered ring, that could lead to easy metalation.
- The synthesis of 11,16-bis(phenyl)-6,6,21,21-tetraphenyl-*meta*-benz-6,21-porphodimethene and its zinc and cadmium complexes was achieved successfully. The synthesis was confirmed by UV-Vis, NMR and mass

spectrometry. The frontier molecular orbitals were also visualized along with the density-of-states plot (TDOS/PDOS/OPDOS).

- The conformational analysis of the metalated complexes of tetramethyl and tetraphenyl substituted *m*-BPDM metal complexes of Zn(II) and Cd(II) chlorides have been done. It was clear from this study, that computationally optimized structures of tetramethyl substituted *m*-BPDM complexes of Zn(II) and Cd(II) chlorides bears *syn* conformation, that is well in agreement with its solid state geometry (X-ray crystallographic data). In contrast to this, the tetraphenyl substituted *m*-BPDM metalated complexes bears *anti*-conformation as suggested from their computational studies. Thus, the bulkiness at *sp*<sup>3</sup> *meso* carbon atom is responsible for this change in conformations from *syn* to *anti*.

## 8.2. Future prospects

- We are convinced that the most stable structures obtained from the studies documented in **Chapter 4** and **5** of this thesis, will be energetically more stable.
- We believe that merging the best results of **Chapter 4** and **5** will lead to the development of a new *meta*-benzoporphodimethene molecule, which may help overcoming the low yield and rapid oxidation setbacks of this compound.
- The synthesis of *para*-benzoporphodimethenes and its electronic structural studies have not been attempted by far.
- Development of a water soluble *meta*-benzoporphodimethene systems could serve as a challenge to the research groups working in this area.

## LIST OF PUBLICATIONS/CONFERENCES

---

---

1. **Deepali Ahluwalia**, Anil Kumar, Sudhir G. Warkar, Recent developments in *meta*-benzoporphodimethene: a new porphyrin analogue, *Journal of Molecular Structure*, 1228 (2021), 129672. <https://doi.org/10.1016/j.molstruc.2020.129672>
2. **Deepali Ahluwalia**, Anil Kumar\*, Sudhir G. Warkar, Milind M. Deshmukh, Effect of Substitutions on the Geometry and Intramolecular Hydrogen Bond Strength in *meta*-benzoporphodimethes: A New Porphyrin Analogue, *Journal of Molecular Structure*, 1220 (2020), 128773-128783. <https://doi.org/10.1016/j.molstruc.2020.128773>
3. **Deepali Ahluwalia**, Anil Kumar\*, Sudhir G. Warkar, Milind M. Deshmukh, Uncovering the geometrical aspects of intramolecular hydrogen bond in *meta*-benzoporphodimethenes through molecular tailoring approach, *Computational and Theoretical Chemistry*, 1209 (2022), 113631. <https://doi.org/10.1016/j.comptc.2022.113631>
4. **Deepali Ahluwalia**, Atul Varshney, Sachin Kumar, Anil Kumar\*, Sudhir G. Warkar, Narender Singh, Prashant Dubey, One-pot Synthesis of Magnetic Iron Phosphide Nanoparticles. *Inorganic and Nano-Metal Chemistry Journal*, Taylor and Francis. 50 (2020), 908-913 <https://doi.org/10.1080/24701556.2020.1728551>
5. **Deepali Ahluwalia**, Sachin Kumar, Anil Kumar\*, Sudhir G. Warkar, Synthesis, characterization and electronic structural studies of newly synthesized sterically hindered analogue of *meta*-benzoporphodimethene systems and its metal complexes. (*under revision*)
6. Atul Varshney, **Deepali Ahluwalia**, Ritika Kubba, Jyoti, Anil Kumar\*, Corrole as a sensor. (*under revision*)

## **CONFERENCES AND AWARDS**

1. Oral Presentation: *Uncovering the geometrical aspects, non-covalent interactions and intramolecular H-bond strength in meta-benziporphodimethenes- a new porphyrin analogue*, Recent Advancements in Chemical Sciences: Health, Environment and Society, International e-conference, Deshbandhu College, University of Delhi, April 8-10, 2022. (**Best Presentation Award**)
2. Oral Presentation: *Effect of substitution on Geometry and Intramolecular Hydrogen-Bond Strength on meta-benziporphodimethenes: a new porphyrin analogue*, Recent Advances in Bis and Tetra-Pyrrolic Molecular Materials, Central University of Kerala, August 24-26, 2020. (**Second Best Presentation Award**)
3. Poster Presentation: *Uncovering the conventional and non-conventional intramolecular hydrogen bond strengths in substituted meta-benziporphodimethenes*, Online International Conference on Chemistry for Substantial Development, Department of Chemistry, Central University of Jharkhand, July 2-4, 2021.
4. Poster Presentation: *Exploring m-benziporphodimethene and its derivative using density functional theory*, 1<sup>st</sup> Indian Analytical Congress (IAC-2019), Amity University, Noida, December 12-14, 2019.
5. Poster Presentation: *Estimation of Intramolecular H-bond Energies in substituted meta-Benziporphodimethenes using Molecular Tailoring Approach*, 2<sup>nd</sup> Indian Analytical Congress (An International Analytical Conference and Exhibition), Graphic Era University, Dehradun, May 26-28, 2022.

6. Poster Presentation: *Estimation of Intramolecular Hydrogen Bond strength in meso-substituted free base meta-benziporphodimethene analogues*, International Conference on Advances in Chemical Sciences and Nanocomposites, Zakir Husain Delhi College, University of Delhi, April 1-2, 2022.
7. Poster Presentation: *Study of Non-Covalent Interactions and Intramolecular Hydrogen Bond Strength in substituted meta-Benziporphodimethenes: A new porphyrin analogue*, National Conference on Molecular Modelling and Simulations (NCMMS) 2022, VIT Bhopal, February 28- March 2, 2022.

## ABOUT THE AUTHOR

---

**Name: Deepali Ahluwalia**

Father's Name: Rakesh Ahluwalia

Nationality: Indian



The author completed her schooling from Delhi Police Public School, Delhi. She then pursued her bachelor's and master's degree in Chemistry from University of Delhi. She qualified CSIR-UGC-NET JRF exam in Chemical Sciences during her M.Sc and joined DTU as a UGC-NET JRF in the year 2017. She started her Ph.D. journey in July 2018 under the supervision of Prof. Anil Kumar and Prof. S. G. Warkar at the Department of Applied Chemistry, DTU. Her research work revolves around the computational studies of *meta*-benzoporphodimethene systems. During her Ph.D. she has received Commendable research excellence award, consecutively in 2021 and 2022, by Delhi Technological University. She has also received best oral presentation awards in both National and International conferences, during her Ph.D. tenure. She wishes to work as an academician along with exploring the wider perspective of computational chemistry in her future.

## APPENDIX -I

---

<b>1(a) :</b> B3LYP/BS-II energy = -1872.29532378 a.u.	<b>1(b):</b> B3LYP/BS-II energy = -3313.71568938 a.u.
N 0.036766000 -0.620545000 0.000163000	N 0.029325000 -0.444191000 0.002092000
H 0.000360000 0.393369000 0.007814000	H -0.004203000 0.570469000 -0.001123000
N 1.827730000 1.437478000 0.740257000	N 1.838488000 1.627388000 0.690309000
N -1.908043000 1.258565000 -0.837277000	N -1.908596000 1.451492000 -0.824748000
C 1.190022000 -1.353132000 -0.005710000	C 1.178824000 -1.183059000 0.012745000
C 0.814575000 -2.713838000 -0.013826000	C 0.798035000 -2.542384000 0.013137000
H 1.497192000 -3.548116000 -0.019531000	H 1.477398000 -3.379327000 0.018551000
C -0.573661000 -2.768360000 0.016282000	C -0.590350000 -2.590825000 0.033294000
H -1.189712000 -3.652967000 0.019586000	H -1.210263000 -3.472686000 0.041526000
C -1.054375000 -1.441321000 0.005417000	C -1.064729000 -1.261735000 0.004713000
C 2.797551000 0.521927000 0.310955000	C 2.801357000 0.686161000 0.301896000
C 4.101803000 1.169191000 0.288707000	C 4.119977000 1.303596000 0.311320000
H 5.032389000 0.712492000 -0.011447000	H 5.049062000 0.819505000 0.051786000
C 3.893791000 2.444675000 0.702390000	C 3.927775000 2.587628000 0.704518000
H 4.625276000 3.231692000 0.818827000	H 4.672811000 3.359136000 0.837663000
C 2.464631000 2.558606000 0.985906000	C 2.492525000 2.736657000 0.942907000
C -2.804467000 0.288037000 -0.370174000	C -2.809336000 0.471788000 -0.385295000
C -4.154276000 0.836601000 -0.360582000	C -4.165766000 1.002058000 -0.425098000
H -5.046616000 0.321679000 -0.039176000	H -5.062047000 0.472737000 -0.139712000
C -4.043975000 2.109844000 -0.815665000	C -4.055525000 2.274249000 -0.882430000
H -4.832530000 2.836286000 -0.951531000	H -4.847896000 2.989166000 -1.052756000
C -2.627743000 2.319286000 -1.112962000	C -2.631586000 2.501016000 -1.130313000
C 2.511503000 -0.790536000 0.014529000	C 2.501391000 -0.627329000 0.034792000
C 3.631016000 -1.729786000 -0.288252000	C 3.620532000 -1.583225000 -0.240058000
C 3.822218000 -2.260198000 -1.567133000	C 4.013520000 -1.892525000 -1.551031000
C 4.849798000 -3.135749000 -1.881063000	C 5.049121000 -2.779153000 -1.826345000
H 4.942619000 -3.498927000 -2.896203000	H 5.320661000 -2.981537000 -2.853731000
C 4.545136000 -2.145239000 0.683199000	C 4.321591000 -2.224185000 0.792265000
C 5.586071000 -3.023043000 0.418433000	C 5.358721000 -3.117468000 0.541424000
H 6.254742000 -3.305219000 1.221134000	H 5.870362000 -3.588258000 1.370165000
C 5.733527000 -3.515645000 -0.874600000	C 5.718973000 -3.390347000 -0.772764000
H 6.542387000 -4.199928000 -1.099936000	H 6.526383000 -4.083314000 -0.977321000
C -2.417735000 -0.986223000 -0.028083000	C -2.423895000 -0.801247000 -0.045815000
C -3.457705000 -2.001200000 0.309705000	C -3.475628000 -1.816464000 0.277557000
C -4.346398000 -2.511529000 -0.640188000	C -4.133222000 -2.551069000 -0.720581000
C -5.311014000 -3.462724000 -0.341897000	C -5.108358000 -3.498436000 -0.423648000
H -5.963387000 -3.816574000 -1.129468000	H -5.588249000 -4.040811000 -1.227253000
C -5.404695000 -3.934170000 0.963988000	C -5.448311000 -3.732331000 0.903373000
H -6.153846000 -4.674981000 1.215443000	H -6.207605000 -4.466993000 1.143573000
C -4.543111000 -3.461049000 1.950036000	C -4.819312000 -3.029195000 1.924311000
H -4.595722000 -3.805902000 2.974405000	H -5.075639000 -3.200558000 2.961193000
C -3.592198000 -2.514517000 1.602895000	C -3.845444000 -2.089696000 1.603279000
C -2.040787000 3.566397000 -1.719757000	C -2.043370000 3.751343000 -1.730437000
C 1.799507000 3.769641000 1.581820000	C 1.847050000 3.967261000 1.520053000
C -1.148143000 4.383029000 -0.792735000	C -1.149167000 4.563905000 -0.802404000
C -0.117844000 3.757302000 -0.089348000	C -0.096177000 3.942191000 -0.128208000
H 0.009709000 2.690090000 -0.184553000	H 0.049062000 2.879701000 -0.247002000
C 0.740093000 4.474423000 0.740557000	C 0.759554000 4.658475000 0.704300000
C 0.567818000 5.858229000 0.850879000	C 0.562369000 6.036679000 0.845937000
H 1.229089000 6.437001000 1.488221000	H 1.222245000 6.614549000 1.485625000
C -0.454767000 6.495829000 0.154266000	C -0.481533000 6.669376000 0.178220000
H -0.583602000 7.568806000 0.247599000	H -0.628728000 7.737587000 0.295793000
C -1.315350000 5.762447000 -0.661358000	C -1.340404000 5.936463000 -0.639853000
H -2.112295000 6.266668000 -1.198582000	H -2.154985000 6.436175000 -1.154320000
F -4.256787000 -2.069767000 -1.908952000	Cl -3.720932000 -2.296212000 -2.407004000
F -2.763092000 -2.056067000 2.559517000	Cl -3.076327000 -1.215848000 2.914950000
F 2.971454000 -1.891482000 -2.543420000	Cl 3.887308000 -1.916561000 2.464185000
F 4.405118000 -1.681441000 1.939474000	Cl 3.193264000 -1.134976000 -2.903539000
H 2.570326000 4.492683000 1.860418000	H -2.853717000 4.385493000 -2.097869000
H 1.323549000 3.448310000 2.517330000	H -1.454075000 3.450064000 -2.604479000
H -2.850904000 4.198922000 -2.090745000	H 1.404290000 3.674212000 2.481490000
H -1.449324000 3.261703000 -2.590941000	H 2.629107000 4.694163000 1.754021000

1(c) B3LYP/BS-II energy = -2162.54590213 a.u.			
C	-3.913653000	-2.913738000	-3.769151000
H	-4.242550000	-3.539786000	-4.596788000
H	-2.906689000	-3.217245000	-3.462585000
H	-3.895708000	-1.867292000	-4.091324000
C	-6.571743000	-4.835433000	-0.764418000
H	-7.520264000	-5.315418000	-1.004056000
H	-6.282990000	-5.095804000	0.259344000
H	-5.804947000	-5.173341000	-1.467081000
C	-6.645526000	-1.598122000	2.759952000
H	-7.530963000	-1.960275000	3.279566000
H	-6.717994000	-0.512523000	2.634165000
H	-5.755305000	-1.836190000	3.352810000
C	-4.708118000	-2.431157000	-1.565797000
C	-5.718021000	-2.636958000	-0.610251000
C	-5.638954000	-1.978868000	0.627701000
C	-4.586855000	-1.095988000	0.888738000
H	-4.513512000	-0.587887000	1.838841000
C	-3.589858000	-0.888644000	-0.070957000
C	-3.645196000	-1.567965000	-1.294000000
H	-2.873007000	-1.393648000	-2.028995000
C	-2.471055000	0.052171000	0.208047000
C	-1.134192000	-0.473528000	0.077424000
C	-0.716625000	-1.821965000	0.032484000
H	-1.372952000	-2.675241000	0.078596000
C	0.671679000	-1.833621000	-0.050378000
H	1.313349000	-2.697417000	-0.106704000
C	1.112332000	-0.492344000	-0.084075000
C	2.458474000	0.009597000	-0.221474000
C	2.749821000	1.300532000	-0.617907000
C	4.052347000	1.952456000	-0.631946000
H	4.982505000	1.514221000	-0.306386000
C	3.837337000	3.214880000	-1.088472000
H	4.565046000	4.002163000	-1.226347000
C	2.409272000	3.315323000	-1.358969000
C	1.706557000	4.522792000	-1.920658000
C	0.898096000	5.317954000	-0.900979000
C	0.993007000	6.708624000	-0.820268000
H	1.676679000	7.244851000	-1.470821000
C	0.205176000	7.410889000	0.090739000
H	0.277573000	8.491868000	0.144841000
C	-0.672639000	6.733089000	0.933383000
H	-1.277148000	7.288560000	1.643581000
C	-0.769433000	5.339624000	0.873964000
C	0.014001000	4.654103000	-0.051167000
H	-0.058879000	3.578794000	-0.108071000
C	-1.657018000	4.575945000	1.852294000
C	-2.371317000	3.376159000	1.291458000
C	-3.800191000	3.292337000	1.022504000
H	-4.515953000	4.092542000	1.147939000
C	-4.034576000	2.025737000	0.586617000
H	-4.971482000	1.596203000	0.268965000
C	-2.742798000	1.354029000	0.583706000

1(d) : B3LYP/BS-II energy = -2467.80895160 a.u.				1(e) : B3LYP/BS-II energy = -1673.77699835 a.u.			
N	0.011180000	-0.041339000	-0.004705000	N	-0.025150000	-0.608569000	-0.005601000
H	-0.004971000	0.973284000	0.003010000	H	-0.002432000	0.404753000	-0.018791000
N	1.801742000	1.974204000	0.846729000	N	-1.767355000	1.382420000	-0.971435000
N	-1.840391000	1.881006000	-0.944685000	N	1.811539000	1.273347000	1.021229000
C	1.146504000	-0.798818000	0.054145000	C	-1.168961000	-1.354954000	-0.060510000
C	0.743730000	-2.150964000	0.020806000	C	-0.773683000	-2.710245000	-0.024169000
H	1.405020000	-3.001639000	0.053677000	H	-1.441878000	-3.554887000	-0.059210000
C	-0.644936000	-2.175766000	-0.029563000	C	0.615543000	-2.745120000	0.032207000
H	-1.275964000	-3.049016000	-0.065720000	H	1.240821000	-3.621579000	0.077835000
C	-1.095265000	-0.838908000	-0.064899000	C	1.078530000	-1.411346000	0.057607000
C	2.775052000	1.041306000	0.466286000	C	-2.759972000	0.500028000	-0.525023000
C	4.092605000	1.662965000	0.515740000	C	-4.045059000	1.186201000	-0.513206000
H	5.029935000	1.191579000	0.262899000	H	-4.985345000	0.768925000	-0.188751000
C	3.887574000	2.939894000	0.922457000	C	-3.801096000	2.450058000	-0.949195000
H	4.626778000	3.712093000	1.080485000	H	-4.509360000	3.257815000	-1.067700000
C	2.446073000	3.081337000	1.130970000	C	-2.373079000	2.518806000	-1.233062000
C	-2.784136000	0.930075000	-0.534652000	C	2.759353000	0.352978000	0.553948000
C	-4.121296000	1.508686000	-0.602630000	C	4.076945000	0.976301000	0.552568000
H	-5.043583000	1.015747000	-0.335859000	H	4.995269000	0.521022000	0.216413000
C	-3.955914000	2.778772000	-1.046121000	C	3.895383000	2.241245000	1.014113000
H	-4.718499000	3.522919000	-1.226067000	H	4.642167000	3.011334000	1.146177000
C	-2.518642000	2.957579000	-1.259452000	C	2.472280000	2.372563000	1.303215000
C	2.475485000	-0.262161000	0.149216000	C	-2.498598000	-0.806659000	-0.163038000
C	3.590911000	-1.223137000	-0.097969000	C	-3.625469000	-1.733151000	0.130062000
C	3.827101000	-1.740461000	-1.372997000	C	-3.687829000	-2.422896000	1.350488000
C	4.858825000	-2.636368000	-1.621889000	C	-4.746089000	-3.277323000	1.638495000
C	4.431164000	-1.650338000	0.931125000	H	-4.811970000	-3.801543000	2.583639000
C	5.467309000	-2.548934000	0.704755000	C	-4.648827000	-1.937938000	-0.806725000
C	5.681236000	-3.041299000	-0.576728000	C	-5.707661000	-2.799502000	-0.536442000
C	-2.443133000	-0.351321000	-0.175157000	H	-6.496406000	-2.973699000	-1.257556000
C	-3.524002000	-1.342937000	0.100669000	C	-5.739472000	-3.452242000	0.685964000
C	-4.355875000	-1.822722000	-0.912142000	C	2.434802000	-0.931849000	0.167412000
C	-5.357495000	-2.752549000	-0.657946000	C	3.513109000	-1.909600000	-0.139442000
C	-5.544544000	-3.223715000	0.635637000	C	4.530493000	-2.172024000	0.789642000
C	-4.729894000	-2.766351000	1.665163000	C	5.544159000	-3.082422000	0.506713000
C	-3.732724000	-1.840122000	1.388631000	H	6.327322000	-3.300751000	1.221854000
C	-1.871214000	4.192825000	-1.826298000	C	5.536716000	-3.726703000	-0.720594000
C	1.774521000	4.303504000	1.694105000	C	4.547214000	-3.496530000	-1.665392000
C	-1.017892000	4.986463000	-0.843545000	H	4.581419000	-4.016772000	-2.614419000
C	-0.040702000	4.337071000	-0.087975000	C	3.533956000	-2.593273000	-1.364875000
H	0.074160000	3.268787000	-0.185772000	C	1.805483000	3.592688000	1.880730000
C	0.778954000	5.032610000	0.796894000	C	-1.654103000	3.710213000	-1.805147000
C	0.624314000	6.418191000	0.909515000	C	0.986033000	4.401961000	0.881076000
H	1.256623000	6.980209000	1.589606000	C	0.066060000	3.754744000	0.056774000
C	-0.344752000	7.079081000	0.160281000	H	-0.027588000	2.681396000	0.118531000
H	-0.460385000	8.153243000	0.255421000	C	-0.726383000	4.454815000	-0.849509000
C	-1.169108000	6.367347000	-0.710107000	C	-0.602072000	5.845844000	-0.915040000
H	-1.924916000	6.889579000	-1.287845000	H	-1.212865000	6.412483000	-1.610830000
F	-4.197295000	-1.401113000	-2.171644000	C	0.311196000	6.506813000	-0.097261000
F	-2.968694000	-1.414169000	2.400603000	H	0.404653000	7.585878000	-0.155982000
F	3.056144000	-1.364490000	-2.399476000	C	1.107900000	5.790068000	0.794560000
F	4.248103000	-1.206116000	2.179449000	H	1.819546000	6.313143000	1.425452000
F	-6.136520000	-3.198315000	-1.647531000	H	2.758835000	-2.399684000	-2.096245000
F	-6.504310000	-4.113162000	0.889975000	H	4.514774000	-1.670903000	1.749419000
F	-4.914894000	-3.215776000	2.909386000	H	-4.603059000	-1.430676000	-1.762344000
F	5.069344000	-3.106136000	-2.854484000	H	-2.908973000	-2.272438000	2.088007000
F	6.674524000	-3.900745000	-0.804269000	F	-6.765363000	-4.286907000	0.956547000
F	6.254444000	-2.944142000	1.709264000	F	6.518627000	-4.608691000	-1.003720000
H	-2.644979000	4.843558000	-2.240134000	H	-1.054318000	3.357531000	-2.652781000
H	-1.237015000	3.877788000	-2.662961000	H	-2.389489000	4.410994000	-2.208796000
H	1.240132000	3.988304000	2.599582000	H	1.142228000	3.260617000	2.687223000
H	2.543357000	5.008934000	2.018905000	H	2.563223000	4.237735000	2.332383000

<b>1(f) :</b> B3LYP/BS-II energy = -1475.24670300 a.u.	C 2.349337000 -1.369201000 0.074642000 C 3.328864000 -2.440619000 -0.249537000 C 4.398794000 -2.721382000 0.613052000 C 5.314086000 -3.724589000 0.306133000 H 6.128936000 -3.935189000 0.989619000 C 5.180024000 -4.459527000 -0.869541000 H 5.894640000 -5.238705000 -1.109540000 C 4.118756000 -4.192690000 -1.733424000 H 4.009916000 -4.758731000 -2.651693000 C 3.195780000 -3.199624000 -1.422416000 C 2.159658000 3.203564000 1.748383000 C -1.543869000 3.568570000 -1.686365000 C 1.332194000 4.064191000 0.800467000 C 0.300123000 3.481377000 0.063529000 H 0.119319000 2.421895000 0.163693000 C -0.491910000 4.230576000 -0.802729000 C -0.253829000 5.604946000 -0.911245000 H -0.862922000 6.208887000 -1.576659000 C 0.767971000 6.200794000 -0.177390000 H 0.946988000 7.266722000 -0.269152000 C 1.565225000 5.434143000 0.671519000 H 2.364454000 5.904678000 1.235369000 H 2.989395000 3.795213000 2.143337000 H 1.532096000 2.917620000 2.599641000 H -1.040038000 3.213379000 -2.595039000 H -2.262241000 4.325669000 -2.010851000 H -4.053793000 -0.933244000 2.224092000 H -3.728158000 -2.803935000 -1.619293000 H 4.494527000 -2.161779000 1.535466000 H 2.373903000 -2.993218000 -2.097602000
--	--

<b>2(a)</b> B3LYP/BS-II energy = -2029.57913889 a.u.	H	-5.405500000	-4.576649000	1.464095000			
F	3.409065000	-1.590886000	2.697189000	C	-4.957407000	-4.792727000	-0.647950000
C	4.107939000	-2.187855000	1.709474000	C	5.879168000	-3.643595000	1.039783000
F	-2.685765000	-2.728144000	-2.556324000	H	6.699577000	-4.305391000	1.289553000
C	-3.389594000	-3.210869000	-1.510654000	H	5.154278000	0.445987000	-0.222766000
F	4.196275000	-2.349805000	-1.885171000	C	-0.798950000	4.317965000	1.953692000
C	4.506475000	-2.560262000	-0.588521000	H	5.383066000	-3.187696000	3.102976000
N	0.116343000	-0.874793000	0.002258000	H	6.105983000	-3.880719000	-1.105130000
H	0.063727000	0.131803000	-0.143677000	C	-1.394926000	4.480268000	2.841586000
C	1.296222000	-1.562994000	0.142432000	H	0.552335000	4.664107000	1.981079000
C	-0.941938000	-1.743351000	0.059613000	H	2.409433000	4.704290000	0.928911000
F	-3.896804000	-2.565940000	1.993515000	C	-4.225621000	-4.295835000	-1.723858000
C	-4.002323000	-3.121875000	0.768198000	C	0.975133000	3.182305000	-2.764802000
N	1.908864000	1.195730000	-0.719718000	C	2.692720000	4.717268000	-1.808659000
C	2.896097000	0.283502000	-0.344692000	H	-5.081295000	-0.573321000	-0.482871000
C	2.530883000	2.306580000	-1.035438000	C	-3.492044000	4.372732000	-0.363236000
N	-2.200559000	1.023149000	0.263470000	C	-3.602089000	3.636389000	2.032013000
C	-2.896705000	-0.159688000	-0.036514000	H	-4.293167000	-4.729077000	-2.713331000
C	-3.099688000	1.977626000	0.285519000	H	0.978733000	5.090256000	2.882903000
C	3.745434000	-1.916476000	0.388611000	H	-5.350612000	2.050166000	-0.096175000
C	2.612397000	-1.000272000	0.050470000	H	0.340172000	4.016609000	-3.076192000
C	0.970008000	-2.922412000	0.322876000	H	1.681584000	2.973172000	-3.572275000
C	-2.332113000	-1.409598000	-0.078236000	H	0.359699000	2.293835000	-2.629195000
C	-3.246111000	-2.581189000	-0.272922000	H	2.103766000	5.588863000	-2.103841000
C	-0.411571000	-3.036336000	0.254487000	H	3.319786000	5.010458000	-0.965526000
C	5.559851000	-3.413781000	-0.295776000	H	3.351868000	4.457595000	-2.641691000
C	-4.309838000	0.138066000	-0.230458000	H	-3.322143000	5.411922000	-0.071178000
C	4.206144000	0.909711000	-0.449616000	H	-3.054551000	4.224192000	-1.352110000
C	5.153307000	-3.029243000	2.057303000	H	-4.570428000	4.214661000	-0.440781000
H	1.681394000	-3.719947000	0.463573000	H	-3.542858000	4.681330000	2.347277000
C	3.980991000	2.178059000	-0.881049000	H	-4.658528000	3.385477000	1.919779000
C	1.751579000	3.540196000	-1.477469000	H	-3.190710000	3.006493000	2.823590000
C	0.822148000	3.891952000	-0.298016000				
C	-0.532523000	3.569134000	-0.309343000				
C	1.357260000	4.452747000	0.871070000				
H	-0.992500000	-3.939707000	0.343939000				
H	-0.961469000	3.115701000	-1.191125000				
C	-1.362032000	3.767075000	0.802482000				
H	4.717896000	2.941672000	-1.078096000				
C	-2.852647000	3.425913000	0.692339000				
C	-4.441479000	1.470747000	-0.037873000				
C	-4.850464000	-4.208199000	0.611134000				

2(b) B3LYP/BS-II energy = -3471.00000259 a.u.				H	-0.432387000	-3.631923000	3.424062000
N	0.000063000	0.863865000	-0.000011000	H	-1.535981000	-2.252757000	3.622471000
H	-0.000130000	-0.150031000	0.000361000	H	-0.174731000	-2.138171000	2.502074000
N	1.832522000	-1.099085000	-0.770423000	C	-2.919115000	-4.252873000	2.411433000
N	-1.832552000	-1.098668000	0.770638000	H	-2.473900000	-5.010057000	3.059841000
C	1.121508000	1.637186000	0.053021000	H	-3.533274000	-4.765452000	1.667189000
C	0.694429000	2.983225000	0.046213000	H	-3.575341000	-3.637324000	3.031063000
H	1.343257000	3.843611000	0.080868000	C	0.931273000	-2.811721000	-2.901854000
C	-0.693899000	2.983351000	-0.047010000	H	0.432410000	-3.632447000	-3.423724000
H	-1.342553000	3.843848000	-0.082065000	H	1.536304000	-2.253513000	-3.622088000
C	-1.121220000	1.637383000	-0.053356000	H	0.174859000	-2.138527000	-2.501950000
C	2.765514000	-0.202507000	-0.232977000	C	2.918825000	-4.253779000	-2.410412000
C	4.066559000	-0.848638000	-0.157502000	H	2.473677000	-5.010755000	-3.059106000
H	4.975231000	-0.405132000	0.220740000	H	3.532444000	-4.766633000	-1.665909000
C	3.892968000	-2.102939000	-0.644717000	H	3.575540000	-3.638408000	-3.029699000
H	4.644589000	-2.870624000	-0.744597000	C	-0.918251000	-4.191428000	0.813993000
C	2.483067000	-2.205474000	-1.039501000	C	-0.000098000	-3.522328000	0.000406000
C	-2.765463000	-0.202018000	0.233154000	H	0.000293000	-2.443521000	0.000657000
C	-4.066659000	-0.847900000	0.158103000	C	0.917494000	-4.191684000	-0.813574000
H	-4.975308000	-0.404282000	-0.220067000	C	0.911611000	-5.590295000	-0.796717000
C	-3.893232000	-2.102116000	0.645585000	H	1.604337000	-6.157596000	-1.404119000
H	-4.644990000	-2.869615000	0.745832000	C	-0.001197000	-6.276576000	-0.000365000
C	-2.483248000	-2.204884000	1.040034000	H	-0.001613000	-7.361498000	-0.000660000
C	2.451138000	1.095875000	0.088777000	C	-0.913487000	-5.590017000	0.796363000
C	3.542909000	2.037604000	0.487745000	H	-1.606657000	-6.157108000	1.403451000
C	3.827886000	2.301101000	1.836269000	Cl	-4.022879000	2.470782000	2.172718000
C	4.835572000	3.177012000	2.225369000	Cl	-2.905176000	1.493496000	-3.090539000
H	5.022861000	3.343029000	3.277787000	Cl	4.023958000	2.469104000	-2.173050000
C	4.323459000	2.714408000	-0.461585000	Cl	2.904772000	1.494330000	3.090387000
C	5.334429000	3.598174000	-0.096462000				
H	5.909906000	4.098031000	-0.864062000				
C	5.586776000	3.824485000	1.251282000				
H	6.373298000	4.509645000	1.544365000				
C	-2.450935000	1.096248000	-0.088880000				
C	-3.542614000	2.038041000	-0.488000000				
C	-4.322747000	2.715447000	0.461230000				
C	-5.333625000	3.599264000	0.095968000				
H	-5.908777000	4.099617000	0.863491000				
C	-5.586295000	3.824982000	-1.251813000				
H	-6.372753000	4.510167000	-1.545010000				
C	-4.835503000	3.176889000	-2.225806000				
H	-5.023065000	3.342449000	-3.278247000				
C	-3.827891000	2.300952000	-1.836570000				
C	-1.826149000	-3.377093000	1.767262000				
C	1.825869000	-3.377667000	-1.766653000				
C	-0.931205000	-2.811171000	2.902185000				

<b>2(c): B3LYP/BS-II energy = -2319.83124354 a.u.</b>	C	2.698901000	-0.895851000	0.600472000
C	C	-0.437306000	-3.455285000	-3.008459000
C 3.775100000	3.353277000	-3.836662000	H 0.134746000	-4.271543000
H 4.077629000	3.976309000	-4.676539000	H 0.248807000	-2.791633000
H 2.797782000	3.686586000	-3.470890000	H -0.917713000	-2.882091000
H 3.704056000	2.311229000	-4.165713000	C -2.479671000	-4.896424000
C 6.648764000	5.166648000	-0.979440000	H -1.937963000	-5.645405000
H 7.597586000	5.617510000	-1.269139000	H -3.031000000	-4.269277000
H 6.422066000	5.435902000	0.057573000	H -3.203911000	-5.417941000
H 5.856882000	5.527372000	-1.641626000	C 0.438353000	-3.455613000
C 6.811750000	1.902229000	2.527222000	H -0.133622000	-4.271984000
H 7.735784000	2.231789000	2.999128000	H -0.247833000	-2.791815000
H 6.842055000	0.815944000	2.390631000	H 0.918888000	-2.882601000
H 5.963901000	2.163541000	3.170311000	C 2.480838000	-4.896547000
C 4.672470000	2.826790000	-1.683597000	H 1.939306000	-5.645533000
C 5.737704000	2.994264000	-0.782021000	H 3.032403000	-4.269435000
C 5.703635000	2.330062000	0.454917000	H 3.204854000	-5.418050000
C 4.639318000	1.479749000	0.767345000	C -3.586569000	1.308790000
H 4.598838000	0.970732000	1.718826000	C -4.639288000	1.479413000
C 3.586341000	1.309256000	-0.139287000	H -4.598505000	0.970621000
C 3.598702000	1.995942000	-1.360132000	C -5.703779000	2.329551000
H 2.784526000	1.849598000	-2.054677000	C -5.738279000	2.993411000
C 2.456493000	0.403118000	0.191959000	C -4.673308000	2.825770000
C 1.123896000	0.945090000	0.072356000	C -3.599358000	1.995120000
C 0.695302000	2.290620000	0.035954000	H -2.785363000	1.848674000
H 1.344170000	3.149877000	0.081772000	C -3.776934000	3.351270000
C -0.695613000	2.290559000	-0.034498000	H -4.079925000	3.973821000
H -1.344588000	3.149767000	-0.079635000	H -2.799382000	3.684748000
C -1.124019000	0.944995000	-0.071846000	H -3.706147000	2.309020000
C -2.456513000	0.402864000	-0.191796000	C -6.649564000	5.165665000
C -2.698696000	-0.896083000	-0.600510000	H -7.598569000	5.616319000
C -3.957865000	-1.623220000	-0.572499000	H -6.422376000	5.435395000
H -4.898029000	-1.247755000	-0.200045000	H -5.858042000	5.526153000
C -3.690433000	-2.865707000	-1.056162000	C -6.811268000	1.902065000
H -4.386755000	-3.682676000	-1.168978000	H -7.735200000	2.231639000
C -2.269329000	-2.880916000	-1.395615000	H -6.841516000	0.815746000
C -1.502180000	-4.031741000	-2.041220000	H -5.963264000	2.163578000
C -0.764893000	-4.857075000	-0.959239000	N -0.000012000	0.175317000
C -0.761942000	-6.255608000	-0.942467000	N -1.696739000	-1.734127000
H -1.339716000	-6.822215000	-1.661086000	N 1.697172000	-1.734016000
C 0.000382000	-6.941599000	-0.0000118000	O 4.787019000	3.518276000
H 0.000391000	-8.026577000	-0.0000125000	O 6.824494000	3.752365000
C 0.762711000	-6.255620000	0.942244000	O 6.753880000	2.583011000
H 1.340539000	-6.822251000	1.660803000	O -4.788268000	3.516908000
C 0.765621000	-4.857088000	0.959081000	O -6.825256000	3.751307000
C 0.000321000	-4.189746000	-0.000040000	O -6.753807000	2.582590000
H 0.000302000	-3.110471000	-0.0000010000	H -0.000103000	-0.837008000
C 1.503066000	-4.031827000	2.041002000		-0.0000697000
C 2.269933000	-2.880828000	1.395369000		
C 3.690931000	-2.865473000	1.055463000		
H 4.387339000	-3.682430000	1.167884000		
C 3.958124000	-1.622891000	0.571915000		
H 4.898142000	-1.247314000	0.199203000		

<b>2(d) : B3LYP/BS-II energy = -2625.09306526 a.u.</b>				H	-3.263199000	-3.986779000	-3.367690000
C	4.697218000	3.120822000	-1.822538000	H	-3.343303000	-5.130971000	-2.016697000
C	5.668448000	3.427846000	-0.872247000	C	0.633686000	-3.164720000	2.979235000
C	5.601791000	2.856692000	0.395916000	H	0.091407000	-3.984562000	3.460234000
C	4.563225000	1.980938000	0.704243000	H	-0.086729000	-2.499935000	2.501604000
C	3.572046000	1.648919000	-0.228498000	H	1.161640000	-2.593725000	3.750152000
C	3.667250000	2.244237000	-1.493638000	C	2.663834000	-4.607300000	2.695440000
C	2.455154000	0.721963000	0.106922000	H	2.157733000	-5.357904000	3.308594000
C	1.123705000	1.267114000	0.038204000	H	3.263477000	-3.986674000	3.367666000
C	0.696235000	2.614208000	0.011576000	H	3.343657000	-5.130820000	2.016639000
H	1.345045000	3.477281000	0.035663000	C	-3.572151000	1.648745000	0.228515000
C	-0.696360000	2.614186000	-0.011167000	C	-4.563272000	1.980777000	-0.704281000
H	-1.345198000	3.477244000	-0.035033000	C	-5.601913000	2.856449000	-0.395971000
C	-1.123778000	1.267082000	-0.038101000	C	-5.668705000	3.427503000	0.872231000
C	-2.455187000	0.721865000	-0.106890000	C	-4.697535000	3.120460000	1.822576000
C	-2.732936000	-0.578552000	-0.475457000	N	-0.0000018000	0.493750000	-0.000032000
C	-4.021465000	-1.258492000	-0.463067000	N	-1.750434000	-1.447401000	-0.971017000
H	-4.958615000	-0.844698000	-0.117645000	N	1.750546000	-1.447342000	0.971060000
C	-3.791502000	-2.508689000	-0.943108000	H	-0.0000056000	-0.520644000	-0.000236000
H	-4.516229000	-3.299000000	-1.078884000	F	2.762328000	1.959994000	-2.437960000
C	-2.361786000	-2.573561000	-1.269479000	F	4.764183000	3.661512000	-3.043576000
C	-1.636607000	-3.736714000	-1.942552000	F	6.660557000	4.266237000	-1.177290000
C	-0.829847000	-4.557288000	-0.905659000	F	6.527839000	3.158014000	1.312405000
C	-0.826619000	-5.958029000	-0.888549000	F	4.527815000	1.470931000	1.941100000
H	-1.453399000	-6.525376000	-1.566870000	F	-2.762626000	1.959697000	2.438064000
C	0.000242000	-6.645346000	-0.000074000	F	-4.764628000	3.661053000	3.043650000
H	0.000289000	-7.731972000	-0.000106000	F	-6.660885000	4.265816000	1.177256000
C	0.827047000	-5.958008000	0.888438000	F	-6.527906000	3.157787000	-1.312510000
H	1.453883000	-6.525339000	1.566722000	F	-4.527735000	1.470859000	-1.941170000
C	0.830149000	-4.557269000	0.905631000				
C	0.000116000	-3.887339000	0.000011000				
H	0.000065000	-2.806478000	0.000051000				
C	1.636866000	-3.736676000	1.942542000				
C	2.361964000	-2.573475000	1.269464000				
C	3.791663000	-2.508544000	0.942999000				
H	4.516432000	-3.298827000	1.078714000				
C	4.021544000	-1.258329000	0.462972000				
H	4.958654000	-0.844490000	0.117496000				
C	2.732980000	-0.578444000	0.475452000				
C	-0.633447000	-3.164685000	-2.979226000				
H	-0.091130000	-3.984490000	-3.460244000				
H	0.086940000	-2.499885000	-2.501573000				
H	-1.161421000	-2.593691000	-3.750131000				
C	-2.663516000	-4.607385000	-2.695481000				
H	-2.157363000	-5.357935000	-3.308658000				

2(e): B3LYP/BS-II energy = -1831.06177697 a.u.			
C	4.578673000	3.797297000	-1.836399000
C	5.677730000	3.897219000	-0.989954000
C	5.758390000	3.181209000	0.198601000
C	4.706437000	2.335297000	0.542489000
C	3.578544000	2.201924000	-0.287433000
C	3.531226000	2.954273000	-1.475705000
C	2.464072000	1.293058000	0.083619000
C	1.126784000	1.837250000	0.025602000
C	0.696878000	3.184504000	0.007426000
H	1.346603000	4.046425000	0.030125000
C	-0.696996000	3.184479000	-0.006922000
H	-1.346750000	4.046384000	-0.029345000
C	-1.126847000	1.837213000	-0.025477000
C	-2.464098000	1.292960000	-0.083595000
C	-2.724963000	-0.010908000	-0.473631000
C	-3.984004000	-0.737587000	-0.386304000
H	-4.908584000	-0.363120000	0.029315000
C	-3.738353000	-1.981773000	-0.882587000
H	-4.439986000	-2.799969000	-0.967388000
C	-2.333746000	-1.996733000	-1.287754000
C	-1.598312000	-3.148195000	-1.969295000
C	-0.809569000	-3.975234000	-0.924333000
C	-0.805498000	-5.375996000	-0.908280000
H	-1.416065000	-5.942900000	-1.601914000
C	0.000203000	-6.063159000	-0.000022000
H	0.000260000	-7.149909000	-0.000044000
C	0.805836000	-5.375947000	0.908261000
H	1.416472000	-5.942811000	1.601865000
C	0.809753000	-3.975186000	0.924371000
C	0.000048000	-3.306453000	0.000039000
H	-0.000018000	-2.225296000	0.000074000
C	1.598445000	-3.148097000	1.969333000
C	2.333835000	-1.996633000	1.287751000
C	3.738409000	-1.981682000	0.882445000
H	4.440045000	-2.799884000	0.967162000
C	3.984012000	-0.737507000	0.386119000
H	4.908542000	-0.363058000	-0.029625000
C	2.724984000	-0.010810000	0.473611000
C	-0.580857000	-2.569658000	-2.986201000
H	-0.030995000	-3.385592000	-3.465601000
H	0.132057000	-1.907345000	-2.494207000
H	-1.098060000	-1.992908000	-3.760229000
C	-2.614947000	-4.013173000	-2.742663000
H	-2.101559000	-4.759824000	-3.355216000
H	-3.206218000	-3.386178000	-3.416508000
H	-3.304045000	-4.541274000	-2.077104000
C	0.580958000	-2.569573000	2.986210000
H	0.031101000	-3.385512000	3.465606000
H	-0.131955000	-1.907274000	2.494194000
H	1.098133000	-1.992805000	3.760243000
C	2.615105000	-4.013018000	2.742730000
H	2.101740000	-4.759665000	3.355308000
H	3.206354000	-3.385979000	3.416553000
H	3.304223000	-4.541123000	2.077194000
C	-3.578635000	2.201766000	0.287422000
C	-4.706433000	2.335187000	-0.542615000
C	-5.758445000	3.181045000	-0.198770000
C	-5.677938000	3.896945000	0.989862000
C	-4.578981000	3.796959000	1.836429000
C	-3.531473000	2.953991000	1.475776000
N	-0.000013000	1.065994000	-0.000038000
N	-1.744621000	-0.847356000	-1.026722000
N	1.744694000	-0.847251000	1.026800000
H	-0.000063000	0.052426000	-0.000298000
F	6.691635000	4.717510000	-1.329962000
F	-6.691901000	4.717181000	1.329830000
H	2.671371000	2.860331000	-2.130207000
H	4.557301000	4.369067000	-2.757590000
H	6.626080000	3.298982000	0.838278000
H	4.744901000	1.783947000	1.475549000
H	-4.744783000	1.783913000	-1.475726000
H	-6.626065000	3.298856000	-0.838535000
H	-4.557731000	4.368637000	2.757680000
H	-2.671696000	2.860001000	2.130374000

2(f): B3LYP/BS-II energy = -1632.53149058 a.u.			
N	0.145529000	-1.326304000	0.070732000
H	0.094693000	-0.332945000	0.278288000
N	1.704010000	0.802131000	0.828666000
N	-1.883871000	0.402289000	-0.904709000
C	1.340148000	-1.960086000	-0.128436000
C	1.043452000	-3.315688000	-0.392444000
H	1.769274000	-4.080230000	-0.616258000
C	-0.338305000	-3.467597000	-0.310942000
H	-0.903734000	-4.371710000	-0.468995000
C	-0.895234000	-2.198048000	-0.042904000
C	2.758147000	0.029217000	0.321566000
C	3.984355000	0.806535000	0.372764000
H	4.960971000	0.470050000	0.061076000
C	3.646237000	2.016698000	0.891235000
H	4.305574000	2.850044000	1.078035000
C	2.214418000	1.961152000	1.180153000
C	-2.711759000	-0.533323000	-0.270361000
C	-4.020484000	0.063482000	-0.040652000
H	-4.852775000	-0.403933000	0.462304000
C	-3.951731000	1.326963000	-0.535017000
H	-4.733645000	2.071332000	-0.527966000
C	-2.604170000	1.482723000	-1.087146000
C	2.606247000	-1.280981000	-0.084083000
C	3.805867000	-2.063698000	-0.511378000
C	4.436206000	-1.790283000	-1.730602000
C	5.554248000	-2.520514000	-2.127578000
H	6.030412000	-2.299164000	-3.076186000
C	4.315211000	-3.084440000	0.300310000
C	5.435327000	-3.810535000	-0.096591000
H	5.824251000	-4.591996000	0.546625000
C	6.057115000	-3.531448000	-1.311970000
C	-2.285117000	-1.808064000	0.045201000
C	-3.252505000	-2.852945000	0.463715000
C	-4.431684000	-3.078026000	-0.263525000
C	-5.336482000	-4.057569000	0.135323000
H	-6.237086000	-4.224457000	-0.444802000
C	-5.082456000	-4.826942000	1.268611000
C	-3.912338000	-4.617631000	1.997040000
H	-3.709414000	-5.210751000	2.881634000
C	-3.001368000	-3.647298000	1.594078000
C	-2.060150000	2.702137000	-1.826350000
C	1.388185000	3.039510000	1.879769000
C	-1.079715000	2.233451000	-2.930873000

<b>3(a): B3LYP/BS-II energy = -2796.63682525 a.u.</b>			
N	0.002108000	2.091570000	0.000242000
H	0.001197000	1.075829000	0.000270000
N	-1.980729000	0.094316000	-0.054323000
N	1.981105000	0.090582000	0.055170000
C	-1.021980000	2.869506000	-0.452823000
C	-0.626775000	4.215729000	-0.290349000
H	-1.221523000	5.075370000	-0.553547000
C	0.634930000	4.214588000	0.290645000
H	1.231287000	5.073156000	0.553707000
C	1.027633000	2.867650000	0.453265000
C	-2.689704000	1.055467000	-0.786883000
C	-3.966985000	0.503931000	-1.200699000
H	-4.720836000	1.009366000	-1.784320000
C	-4.021396000	-0.748770000	-0.686752000
H	-4.841467000	-1.442086000	-0.759172000
C	-2.758369000	-0.959334000	0.032250000
C	2.692060000	1.050575000	0.787319000
C	3.968564000	0.496871000	1.200639000
H	4.723508000	1.001050000	1.783932000
C	4.020719000	-0.755856000	0.686512000
H	4.839698000	-1.450508000	0.758485000
C	2.757000000	-0.964315000	-0.031871000
C	-2.267859000	2.355702000	-0.939810000
C	-3.172797000	3.343898000	-1.598635000
C	-2.898357000	3.860665000	-2.867156000
C	-3.713272000	4.784411000	-3.503047000
H	-3.443871000	5.134885000	-4.490788000
C	-4.330260000	3.826074000	-0.983656000
C	-5.174364000	4.752775000	-1.577345000
H	-6.054077000	5.084577000	-1.041559000
C	-4.857464000	5.228783000	-2.846186000
H	-5.506180000	5.951139000	-3.326434000
C	2.272617000	2.351604000	0.940127000
C	3.179591000	3.338344000	1.598374000
C	4.337445000	3.818556000	0.982594000
C	5.183412000	4.743983000	1.575619000
H	6.063331000	5.074296000	1.039251000
C	4.868056000	5.220683000	2.844580000
H	5.518230000	5.942061000	3.324325000
C	3.723543000	4.778273000	3.502214000
H	3.455319000	5.129364000	4.490056000
C	2.906742000	3.855746000	2.866969000
C	2.406722000	-2.173127000	-0.928912000
C	-2.410650000	-2.168719000	0.929504000
C	1.154073000	-2.947291000	-0.404810000
C	-0.001942000	-2.267359000	0.000454000
H	-0.001124000	-1.189768000	-0.000169000
C	-1.158935000	-2.945084000	0.406434000
C	-1.131650000	-4.344340000	0.429862000
H	-1.987208000	-4.905278000	0.777136000
C	-0.003987000	-5.033688000	0.002014000
H	-0.004783000	-6.118391000	0.002595000
C	1.124719000	-4.346477000	-0.426657000
H	1.979377000	-4.909101000	-0.773414000
F	4.644159000	3.368781000	-0.249775000
F	1.800212000	3.429304000	3.503835000
F	-1.792172000	3.432291000	-3.503330000
F	-4.638476000	3.376961000	0.248578000
C	-3.640518000	-3.119380000	0.952209000
C	-4.381989000	-3.371205000	2.107529000
C	-4.041835000	-3.760100000	-0.232047000
C	-5.487873000	-4.225111000	2.084262000
H	-4.101814000	-2.903561000	3.041226000
C	-5.141917000	-4.608586000	-0.259898000
H	-3.478007000	-3.596951000	-1.143375000
C	-5.874654000	-4.846122000	0.903737000
H	-6.042882000	-4.400178000	2.999378000
H	-5.425588000	-5.088226000	-1.190400000
H	-6.732404000	-5.509141000	0.885704000
C	-2.117354000	-1.640586000	2.362432000
C	-1.212620000	-2.291727000	3.206017000
C	-2.813651000	-0.537634000	2.874382000
C	-1.005822000	-1.854786000	4.514145000
H	-0.656512000	-3.145949000	2.843324000
C	-2.609239000	-0.099947000	4.179449000
H	-3.523149000	-0.009075000	2.250393000
C	-1.701012000	-0.755932000	5.007625000
H	-0.292160000	-2.375556000	5.143300000
H	-3.158292000	0.760503000	4.545920000
H	-1.535162000	-0.410961000	6.022131000
C	2.113083000	-1.644761000	-2.361675000
C	2.809754000	-0.542280000	-2.874108000
C	1.207642000	-2.295581000	-3.204775000
C	2.604975000	-0.104697000	-4.179164000
H	3.519809000	-0.013993000	-2.250538000
C	1.000504000	-1.858767000	-4.512880000
H	0.651292000	-3.149480000	-2.841675000
C	1.696046000	-0.760338000	-5.006831000
H	3.154322000	0.755399000	-4.546024000
H	0.286321000	-2.379280000	-5.141655000
H	1.529935000	-0.415451000	-6.021324000
C	3.634996000	-3.125810000	-0.952581000
C	4.374971000	-3.379038000	-2.108566000
C	4.036368000	-3.767056000	0.231373000
C	5.479388000	-4.234857000	-2.086242000
H	4.094745000	-2.911010000	-3.042053000
C	5.135004000	-4.617451000	0.258285000
H	3.473713000	-3.602831000	1.143233000
C	5.866216000	-4.856403000	-0.906012000
H	6.033229000	-4.410975000	-3.001863000
H	5.418725000	-5.097450000	1.188587000
H	6.722832000	-5.520906000	-0.888717000

<b>3(b): B3LYP/BS-II energy = -4238.08325559 a.u.</b>	H 0.000942000 6.320083000 0.001103000 C -1.113896000 4.547714000 -0.463126000 H -1.957351000 5.110016000 -0.836877000 Cl -4.380191000 -3.589933000 -0.828701000 Cl -1.866842000 -2.506681000 3.903586000 Cl 4.379038000 -3.590801000 0.828789000 Cl 1.865437000 -2.508298000 -3.903522000 C 2.027076000 1.830762000 2.424829000 C 2.711404000 0.731224000 2.959411000 C 1.080934000 2.467886000 3.232941000 C 2.455444000 0.282506000 4.251510000 H 3.453011000 0.215169000 2.362926000 C 0.822156000 2.020114000 4.528110000 H 0.532452000 3.319136000 2.852275000 C 1.505872000 0.924328000 5.044067000 H 2.997229000 -0.574520000 4.636359000 H 0.077441000 2.530191000 5.129352000 H 1.301125000 0.572097000 6.048953000 C 3.602555000 3.319348000 1.083570000 C 4.054063000 3.960610000 -0.082153000 C 4.291111000 3.574213000 2.270588000 C 5.152562000 4.811481000 -0.061920000 H 3.530928000 3.796229000 -1.017226000 C 5.394990000 4.430563000 2.295629000 H 3.970630000 3.107155000 3.191477000 C 5.832620000 5.051180000 1.132775000 H 5.475940000 5.291389000 -0.979224000 H 5.908299000 4.607884000 3.234345000 H 6.689027000 5.715881000 1.152230000 C -3.601520000 3.320479000 -1.083997000 C -4.289986000 3.574764000 -2.271200000 C -4.053156000 3.962329000 0.081358000 C -5.393828000 4.431141000 -2.296781000 H -3.969485000 3.107195000 -3.191821000 C -5.151613000 4.813244000 0.060586000 H -3.530138000 3.798419000 1.016576000 C -5.831543000 5.052378000 -1.134290000 H -5.907051000 4.607981000 -3.235635000 H -5.475056000 5.293620000 0.977622000 H -6.687937000 5.717083000 -1.154155000 C -2.025924000 1.831607000 -2.424620000 C -1.079750000 2.468910000 -3.232578000 C -2.709959000 0.731959000 -2.959304000 C -0.820694000 2.021223000 -4.527709000 H -0.531457000 3.320232000 -2.851793000 C -2.453710000 0.283313000 -4.251382000 H -3.451546000 0.215748000 -2.362937000 C -1.504149000 0.925324000 -5.043790000 H -0.075981000 2.531442000 -5.128833000 H -2.995288000 -0.573801000 -4.636326000 H -1.299186000 0.573145000 -6.048651000
---	---

<b>3(c): B3LYP/BS-II energy = -3086.90446595 a.u.</b>				H	2.885551000	6.837587000	1.920365000
N	-0.057700000	1.230644000	-0.068323000	H	3.509172000	7.124971000	3.566799000
H	-0.085841000	0.239430000	0.163477000	H	4.640312000	7.078810000	2.184073000
N	-1.825166000	-0.785241000	0.600028000	O	3.867779000	5.256283000	2.870594000
N	1.916705000	-0.720452000	-0.698102000	C	-7.421445000	2.622129000	-3.741594000
C	-1.186504000	1.940829000	-0.375118000	H	-7.700733000	1.955380000	-4.560490000
C	-0.773603000	3.257393000	-0.687873000	H	-8.036788000	2.384675000	-2.865371000
H	-1.427518000	4.057920000	-0.997527000	H	-7.591335000	3.660075000	-4.032190000
C	0.606892000	3.314028000	-0.523753000	C	-7.881792000	4.954469000	-1.245317000
H	1.250607000	4.164745000	-0.688699000	H	-8.551375000	5.616344000	-1.798318000
C	1.049571000	2.022777000	-0.153587000	H	-8.387287000	3.996609000	-1.066761000
C	-2.791949000	0.096484000	0.094353000	H	-7.619812000	5.412287000	-0.289104000
C	-4.111559000	-0.477058000	0.279676000	C	-4.585443000	5.810307000	1.289572000
H	-5.047502000	-0.015053000	0.001830000	H	-5.020619000	6.756542000	1.613782000
C	-3.923140000	-1.672275000	0.901966000	H	-4.647112000	5.083707000	2.109251000
H	-4.686291000	-2.359707000	1.229909000	H	-3.532047000	5.967306000	1.027443000
C	-2.479853000	-1.822734000	1.086194000	O	-5.346645000	5.398017000	0.163819000
C	2.778063000	0.240839000	-0.149629000	O	-6.727758000	4.779102000	-2.075124000
C	4.087287000	-0.351349000	0.071241000	O	-6.041286000	2.356397000	-3.494298000
H	4.943836000	0.137373000	0.511959000	C	1.273221000	-2.615256000	-2.835039000
C	4.003192000	-1.632669000	-0.376599000	C	0.152260000	-3.323365000	-3.285430000
C	2.631441000	-1.814404000	-0.859846000	C	1.725303000	-1.539626000	-3.615912000
C	-2.507970000	1.377088000	-0.349025000	C	-0.502972000	-2.964636000	-4.465673000
C	-3.628632000	2.261169000	-0.790524000	H	-0.222047000	-4.161693000	-2.709924000
C	-4.376583000	1.940331000	-1.919323000	C	1.075096000	-1.180846000	-4.795393000
C	-5.439436000	2.757541000	-2.338417000	H	2.592497000	-0.972549000	-3.297666000
C	-3.941791000	3.419414000	-0.057905000	C	-0.047255000	-1.890226000	-5.226318000
C	-4.991771000	4.239026000	-0.467996000	H	-1.374727000	-3.529233000	-4.784642000
C	-5.760054000	3.917589000	-1.613064000	H	1.445558000	-0.340356000	-5.375741000
C	2.404766000	1.560600000	0.033904000	H	-0.558830000	-1.606441000	-6.141574000
C	3.415701000	2.593842000	0.381929000	C	3.237579000	-3.988101000	-1.964544000
C	4.620922000	2.696893000	-0.331586000	C	3.608955000	-4.212653000	-3.294821000
C	5.566752000	3.662866000	0.007744000	C	3.990517000	-4.630722000	-0.963547000
C	5.331474000	4.544870000	1.076509000	C	4.693307000	-5.036265000	-3.615306000
C	4.115775000	4.461833000	1.778389000	H	3.051028000	-3.746040000	-4.096889000
C	3.166994000	3.503887000	1.422593000	C	5.071657000	-5.450073000	-1.278150000
C	2.051954000	-3.061630000	-1.566016000	H	3.717047000	-4.493706000	0.077797000
C	-1.771963000	-2.944142000	1.884127000	C	5.431304000	-5.657451000	-2.612167000
C	1.074780000	-3.821041000	-0.610672000	H	4.953843000	-5.189080000	-4.658890000
C	0.130839000	-3.115524000	0.149462000	H	5.630377000	-5.930667000	-0.479852000
H	0.110759000	-2.037827000	0.083232000	H	6.272265000	-6.297974000	-2.861663000
C	-0.789534000	-3.764962000	0.986349000	C	-0.972780000	-2.280956000	3.041949000
C	-0.730784000	-5.163375000	1.071501000	C	0.225200000	-2.829970000	3.515861000
H	-1.388700000	-5.702824000	1.739847000	C	-1.480235000	-1.148017000	3.697697000
C	0.170934000	-5.880898000	0.289725000	C	0.900947000	-2.259875000	4.597513000
H	0.184307000	-6.966000000	0.344168000	H	0.642119000	-3.707663000	3.036061000
C	1.057450000	-5.222009000	-0.556736000	C	-0.809249000	-0.578883000	4.778653000
H	1.737867000	-5.804492000	-1.164603000	H	-2.411045000	-0.704560000	3.360837000
H	2.248869000	3.453592000	1.996404000	C	0.389823000	-1.130225000	5.233223000
H	4.831168000	2.038262000	-1.165771000	H	1.832361000	-2.703589000	4.938001000
H	-3.363816000	3.659771000	0.824518000	H	-1.224477000	0.300143000	5.263943000
H	-4.152418000	1.058122000	-2.507333000	H	0.917626000	-0.683786000	6.071068000
C	6.957609000	4.847903000	-1.505027000	C	-2.862786000	-3.889379000	2.461430000
H	7.931972000	4.717165000	-1.979530000	C	-3.075556000	-4.058661000	3.833213000
H	6.183642000	4.907207000	-2.280254000	C	-3.680672000	-4.620571000	1.579460000
H	6.955205000	5.767136000	-0.912101000	C	-4.073664000	-4.915849000	4.309895000
O	6.758824000	3.693750000	-0.678966000	H	-2.461138000	-3.521743000	4.545186000
C	7.359423000	4.979032000	2.198632000	C	-4.676288000	-5.472581000	2.049612000
H	8.015223000	5.827559000	2.402590000	H	-3.527920000	-4.522853000	0.509031000
H	7.000160000	4.558992000	3.144605000	C	-4.879833000	-5.624226000	3.424008000
H	7.906909000	4.216189000	1.636250000	H	-4.213493000	-5.024694000	5.381742000
O	6.263931000	5.494691000	1.426498000	H	-5.291033000	-6.021771000	1.341917000
C	3.724197000	6.655798000	2.604741000	H	-5.654482000	-6.289397000	3.794415000
				H	4.795932000	-2.363484000	-0.396317000

<b>3(d): B3LYP/BS-II energy = -3086.90446595 a.u.</b>	C 4.015079000 3.835630000 2.850495000 C 4.062646000 4.237346000 0.488317000 C 5.118953000 4.677446000 3.010935000 H 3.581498000 3.369279000 3.724309000 C 5.161477000 5.073590000 0.643506000 H 3.650394000 4.086181000 -0.502916000 C 5.698835000 5.297481000 1.911802000 H 5.519570000 4.844031000 4.004761000 H 5.596443000 5.554674000 -0.225720000 H 6.555204000 5.950549000 2.036657000 C 1.720177000 2.120193000 2.717889000 C 0.661600000 2.739409000 3.387607000 C 2.343476000 1.031392000 3.343026000 C 0.235976000 2.285953000 4.636261000 H 0.154177000 3.580933000 2.935222000 C 1.921458000 0.577800000 4.588706000 H 3.168592000 0.526210000 2.856043000 C 0.861596000 1.202666000 5.243068000 H -0.592448000 2.783116000 5.128982000 H 2.420285000 -0.269996000 5.045291000 H 0.527384000 0.845720000 6.210751000 C -3.337572000 3.723201000 -1.605407000 C -3.819513000 3.992347000 -2.887481000 C -3.966757000 4.365000000 -0.525364000 C -4.895379000 4.861345000 -3.086964000 H -3.358354000 3.526263000 -3.747097000 C -5.038204000 5.228510000 -0.719244000 H -3.605721000 4.191922000 0.482011000 C -5.511088000 5.481254000 -2.007454000 H -5.246316000 5.048655000 -4.095759000 C -5.501895000 5.707983000 0.135906000 H -6.345946000 6.155358000 -2.162516000 C -1.585755000 2.218897000 -2.683322000 C -0.513981000 2.847758000 -3.323062000 C -2.190131000 1.133512000 -3.331548000 C -0.055681000 2.404845000 -4.563605000 H -0.023569000 3.689880000 -2.852974000 C -1.735152000 0.689962000 -4.569571000 H -3.025893000 0.622712000 -2.869816000 C -0.661625000 1.322654000 -5.192744000 H 0.781989000 2.909126000 -5.032897000 H -2.219557000 -0.156155000 -5.044429000 H -0.301845000 0.973454000 -6.154070000 F -4.296936000 -4.594225000 4.038709000 F -6.427760000 -4.513041000 -0.170199000 F -4.592945000 -2.755790000 -1.076080000 F -2.453613000 -2.833609000 3.145245000 F 6.258794000 -4.723829000 0.134078000 F 4.491929000 -2.903986000 1.050465000 F 2.300057000 -2.939441000 -3.144780000 F 4.075795000 -4.762785000 -4.048559000
---	---

<b>3(e): B3LYP/BS-II energy = -2598.12471105 a.u.</b>				H	-0.444558000	-6.049486000	0.163004000
N	0.226000000	2.113452000	-0.085123000	C	-1.380817000	-4.190902000	0.681097000
H	0.231931000	1.105467000	-0.220555000	H	-2.213487000	-4.679519000	1.166625000
N	1.967609000	-0.035646000	-0.173464000	H	-1.517135000	4.097876000	-2.881656000
N	-1.958580000	0.319143000	0.231288000	H	-4.615507000	3.381001000	-0.002654000
C	1.303565000	2.793516000	0.409056000	H	3.930095000	4.259616000	-0.357508000
C	0.926545000	4.151998000	0.503278000	H	3.500923000	1.992593000	3.258067000
H	1.545807000	4.947608000	0.882941000	F	6.471291000	5.371691000	3.182754000
C	-0.374304000	4.260075000	0.025085000	F	-5.294181000	6.521552000	-3.148542000
H	-0.973861000	5.153778000	-0.033119000	C	-3.723886000	-2.755052000	1.448851000
C	-0.813160000	2.962492000	-0.320034000	C	-4.353771000	-2.900053000	2.686560000
C	2.850566000	0.848190000	0.460842000	C	-4.294237000	-3.418559000	0.349176000
C	4.141386000	0.205001000	0.617861000	H	-5.515167000	-3.664718000	2.822233000
H	5.024444000	0.647721000	1.051226000	H	-3.940171000	-2.420071000	3.562409000
C	4.021051000	-1.028641000	0.064586000	C	-5.450345000	-4.178705000	0.479327000
H	4.795946000	-1.768651000	-0.037764000	H	-3.817021000	-3.349329000	-0.621322000
C	2.643430000	-1.136553000	-0.418338000	C	-6.071421000	-4.304482000	1.722213000
C	-2.624601000	1.281845000	-0.537746000	H	-5.978745000	-3.756909000	3.798314000
C	-3.917488000	0.759135000	-0.946504000	H	-5.863767000	-4.678335000	-0.390046000
H	-4.640921000	1.257956000	-1.571956000	H	-6.972240000	-4.898603000	1.827711000
C	-4.018986000	-0.475421000	-0.392374000	C	-1.931745000	-1.370789000	2.620146000
H	-4.860546000	-1.143211000	-0.459179000	C	-0.939581000	-2.032577000	3.347924000
C	-2.772123000	-0.704110000	0.344533000	C	-2.520215000	-0.237495000	3.198127000
C	2.554496000	2.169221000	0.730644000	C	-0.544751000	-1.578707000	4.606806000
C	3.592893000	3.027627000	1.375487000	H	-0.459339000	-2.908630000	2.932868000
C	3.973831000	2.793332000	2.702439000	C	-2.130327000	0.216669000	4.453661000
C	4.941652000	3.581423000	3.319171000	H	-3.292838000	0.299583000	2.662468000
H	5.240021000	3.413692000	4.346452000	C	-1.136318000	-0.451856000	5.166353000
C	4.205646000	4.073467000	0.673679000	H	0.231797000	-2.111140000	5.145259000
C	5.179681000	4.864674000	1.275606000	H	-2.601925000	1.098588000	4.873479000
H	5.669593000	5.668223000	0.740026000	C	-0.827700000	-0.095828000	6.143036000
C	5.529294000	4.604688000	2.592139000	C	3.180191000	-3.347947000	-1.479733000
C	-2.127745000	2.551600000	-0.746089000	C	3.667034000	-3.671627000	-2.747172000
C	-2.973019000	3.600755000	-1.375304000	C	3.740283000	-4.014953000	-0.377318000
C	-4.247189000	3.906260000	-0.874821000	H	4.681637000	-4.618415000	-2.911263000
C	-5.033023000	4.891087000	-1.465442000	H	3.257014000	-3.188413000	-3.623188000
H	-6.012822000	5.142929000	-1.079409000	C	4.750909000	-4.955397000	-0.535764000
C	-4.535757000	5.567398000	-2.568549000	H	3.372507000	-3.798697000	0.619108000
C	-3.278734000	5.298422000	-3.090477000	C	5.229903000	-5.262726000	-1.809878000
H	-2.929157000	5.847861000	-3.955554000	H	5.038046000	-4.847180000	-3.909623000
C	-2.499128000	4.321117000	-2.482741000	H	5.162389000	-5.452254000	0.336064000
C	-2.433758000	-1.909076000	1.252016000	H	6.017200000	-5.997251000	-1.937296000
C	2.055382000	-2.300658000	-1.249452000	C	1.574910000	-1.727136000	-2.611861000
C	-1.318672000	-2.794568000	0.607257000	C	0.482205000	-2.276670000	-3.288808000
C	-0.189156000	-2.211390000	0.021112000	C	2.277301000	-0.688126000	-3.236817000
H	-0.115870000	-1.136446000	-0.005223000	C	0.098754000	-1.801928000	-4.542817000
C	0.847950000	-2.979771000	-0.524426000	H	-0.081533000	-3.081917000	-2.836789000
C	0.721583000	-4.373105000	-0.492804000	C	1.897460000	-0.212970000	-4.488608000
H	1.473585000	-5.005041000	-0.942172000	H	3.133061000	-0.243556000	-2.744037000
C	-0.374018000	-4.967848000	0.122418000	C	0.802430000	-0.766673000	-5.148999000
				H	-0.756846000	-2.244324000	-5.041288000
				H	2.458942000	0.594106000	-4.946739000
				H	0.502344000	-0.393958000	-6.122050000

3(f) B3LYP/BS-II energy = -2399.61405162 a.u.			
N	0.274442000	2.342972000	-0.055290000
H	0.271403000	1.331234000	-0.155057000
N	2.003871000	0.179593000	0.089554000
N	-1.936851000	0.566636000	-0.017949000
C	1.298605000	3.023922000	0.540045000
C	0.941012000	4.390950000	0.539928000
H	1.530944000	5.189682000	0.958045000
C	-0.290706000	4.501738000	-0.094841000
H	-0.859194000	5.402114000	-0.260955000
C	-0.710658000	3.199203000	-0.446297000
C	2.806438000	1.067413000	0.818630000
C	4.058182000	0.416846000	1.154735000
H	4.878322000	0.860727000	1.696999000
C	3.999038000	-0.825153000	0.609728000
H	4.772886000	-1.573246000	0.622503000
C	2.695634000	-0.929694000	-0.048522000
C	-2.491678000	1.526346000	-0.874608000
C	-3.723386000	1.007204000	-1.443279000
H	-4.355017000	1.506029000	-2.161177000
C	-3.903989000	-0.222318000	-0.897616000
H	-4.733506000	-0.886835000	-1.068899000
C	-2.766121000	-0.450689000	-0.002402000
C	2.493438000	2.395614000	1.023609000
C	3.458723000	3.262913000	1.765842000
C	3.627538000	3.105734000	3.146265000
C	4.527342000	3.908309000	3.844100000
H	4.645056000	3.777633000	4.913949000
C	4.208291000	4.238893000	1.098064000
C	5.111898000	5.035682000	1.796560000
H	5.693804000	5.780366000	1.265053000
C	5.272285000	4.874019000	3.171381000
H	5.974755000	5.496258000	3.714211000
C	-1.963913000	2.791898000	-1.029266000
C	-2.715242000	3.836976000	-1.776434000
C	-4.038485000	4.15816000	-1.442032000
C	-4.729604000	5.141496000	-2.145916000
H	-5.748833000	5.384480000	-1.867355000
C	-4.113145000	5.814100000	-3.198418000
H	-4.652902000	6.576918000	-3.748123000
C	-2.796842000	5.505631000	-3.538158000
H	-2.311517000	6.022939000	-4.358128000
C	-2.100182000	4.533388000	-2.827910000
C	-2.565036000	-1.646996000	0.956545000
C	2.206836000	-2.102499000	-0.930466000
C	-1.377833000	-2.547641000	0.487055000
C	-0.178302000	-1.981753000	0.040826000
H	-0.096124000	-0.908096000	-0.004820000
C	0.917645000	-2.765653000	-0.344660000
C	5.006176000	-4.438550000	-2.246974000
H	3.682845000	-3.009550000	-3.134317000
C	4.787931000	-4.759296000	0.121563000
H	3.285807000	-3.590183000	1.095049000
C	0.782609000	-4.157252000	-0.292762000
H	1.583939000	-4.801568000	-0.623782000
C	-0.387612000	-4.734395000	0.187761000
H	-0.468023000	-5.814564000	0.246349000
C	-1.455919000	-3.941940000	0.586922000
H	-2.348816000	-4.416678000	0.968301000
C	3.346805000	-3.154751000	-1.015081000
C	3.982294000	-3.488296000	-2.212351000
C	3.769129000	-3.814718000	0.151289000
C	5.415629000	-5.076899000	-1.083498000
H	5.479491000	-4.674773000	-3.193703000
H	5.089988000	-5.250857000	1.039963000
H	6.209921000	-5.814472000	-1.110315000
C	1.888664000	-1.549040000	-2.347976000
C	0.897720000	-2.126410000	-3.147800000
C	2.644964000	-0.503891000	-2.894205000
C	0.664404000	-1.672141000	-4.445357000
H	0.296386000	-2.936959000	-2.757834000
C	2.414820000	-0.049030000	-4.189420000
H	3.424197000	-0.038003000	-2.304412000
C	1.419779000	-0.629943000	-4.972795000
H	-0.115296000	-2.135276000	-5.040216000
H	3.014132000	0.764005000	-4.584764000
H	1.235318000	-0.272657000	-5.979857000
C	-2.258078000	-1.096150000	2.376594000
C	-2.905309000	0.053973000	2.848690000
C	-1.392985000	-1.761448000	3.249130000
C	-2.693664000	0.521640000	4.141510000
H	-3.583633000	0.593139000	2.199754000
C	-1.176804000	-1.293958000	4.545803000
H	-0.873410000	-2.651223000	2.919502000
C	-1.824031000	-0.149964000	4.999024000
H	-3.206122000	1.416864000	4.476778000
H	-0.494284000	-1.828561000	5.197589000
H	-1.652751000	0.217019000	6.004970000
C	-3.877379000	-2.481464000	0.977898000
C	-4.685178000	-2.594327000	2.111240000
C	-4.286369000	-3.163509000	-0.180667000
C	-5.862742000	-3.345898000	2.088364000
H	-4.400805000	-2.099246000	3.029209000
C	-5.457544000	-3.911171000	-0.208145000
H	-3.670866000	-3.117154000	-1.071347000
C	-6.257096000	-4.005006000	0.931266000
H	-6.466917000	-3.413133000	2.986515000
H	-5.743688000	-4.425432000	-1.119202000
H	-7.170241000	-4.589437000	0.914210000
H	-4.514835000	3.648029000	-0.614179000
H	-1.078125000	4.294083000	-3.096666000
H	4.092202000	4.360504000	0.027190000
H	3.045295000	2.356312000	3.669710000

## APPENDIX -II

---



---

<b>(1a)</b> B3LYP/BS-I energy = -1609.24854319 a.u.			
N	1.617217000	0.040769000	-0.003664000
H	0.604518000	-0.003143000	-0.013825000
N	-0.258868000	-1.873202000	-0.874771000
N	-0.375087000	1.799978000	0.951493000
C	2.436701000	-1.053368000	-0.008421000
C	3.763465000	-0.569488000	0.001867000
H	4.648609000	-1.184065000	-0.003738000
C	3.707569000	0.820098000	-0.009879000
H	4.540686000	1.503584000	-0.002004000
C	2.346443000	1.196220000	0.002145000
C	0.689424000	-2.782617000	-0.388965000
C	0.089552000	-4.107842000	-0.307613000
H	0.572214000	-5.001357000	0.056095000
C	-1.191472000	-3.967737000	-0.739232000
H	-1.952109000	-4.732103000	-0.813592000
C	-1.356053000	-2.562782000	-1.092419000
C	0.480561000	2.782115000	0.435531000
C	-0.227457000	4.054817000	0.373655000
H	0.168904000	4.983771000	-0.005161000
C	-1.478439000	3.812163000	0.845063000
H	-2.296495000	4.511897000	0.942695000
C	-1.516477000	2.398513000	1.202479000
C	1.976748000	-2.419057000	-0.046831000
C	2.976019000	-3.469406000	0.293721000
C	3.658133000	-3.438781000	1.519093000
C	4.578966000	-4.430305000	1.842848000
H	5.085901000	-4.399969000	2.800800000
C	3.255666000	-4.508914000	-0.604452000
C	4.187034000	-5.493200000	-0.283755000
H	4.398051000	-6.284517000	-0.994282000
C	4.848013000	-5.459507000	0.941861000
H	5.570346000	-6.228001000	1.192999000
C	1.780921000	2.522395000	0.052337000
C	2.684127000	3.645957000	-0.319495000
C	2.898056000	4.715741000	0.561327000
C	3.739066000	5.768154000	0.209186000
H	3.900717000	6.582575000	0.906448000
C	4.374273000	5.772936000	-1.030430000
H	5.026266000	6.594280000	-1.305633000
C	4.170788000	4.714099000	-1.914124000

(1b) B3LYP/BS-I energy = -1589.80165686 a.u.			
N	-1.375162000	-0.025064000	-0.006059000
H	-0.361841000	0.008347000	-0.000512000
N	0.569728000	-1.810755000	1.005114000
N	0.552418000	1.867122000	-0.804063000
C	-2.118858000	-1.171013000	-0.013554000
C	-3.474842000	-0.778381000	-0.052849000
H	-4.316184000	-1.451685000	-0.059995000
C	-3.513973000	0.611518000	-0.043695000
H	-4.391395000	1.236603000	-0.066758000
C	-2.181377000	1.079234000	-0.027466000
C	-0.286483000	-2.781646000	0.468352000
C	0.401525000	-4.066363000	0.434332000
H	0.001337000	-4.990374000	0.047642000
C	1.640550000	-3.843005000	0.944975000
H	2.442749000	-4.555996000	1.072992000
C	1.690864000	-2.428410000	1.296314000
C	-0.403342000	2.788115000	-0.356117000
C	0.204285000	4.108382000	-0.264903000
H	-0.282366000	5.008414000	0.076626000
C	1.497285000	3.955261000	-0.655496000
H	2.265692000	4.713330000	-0.711981000
C	1.661229000	2.547202000	-0.992469000
C	-1.572827000	-2.504796000	0.052010000
C	-2.483583000	-3.616508000	-0.336586000
C	-3.113092000	-3.620231000	-1.590385000
C	-3.950751000	-4.667658000	-1.960168000
H	-4.416697000	-4.662461000	-2.939135000
C	-2.732568000	-4.680086000	0.542564000
C	-3.581205000	-5.721091000	0.175221000
H	-3.770136000	-6.530654000	0.871240000
C	-4.189128000	-5.720485000	-1.078026000
H	-4.847078000	-6.532966000	-1.365020000
C	-1.705321000	2.438791000	-0.055859000
C	-2.703718000	3.501810000	0.246366000
C	-2.947266000	4.534636000	-0.669801000
C	-3.878531000	5.530243000	-0.385994000
H	-4.061660000	6.316224000	-1.110038000
C	-4.574924000	5.514863000	0.820192000
H	-5.296981000	6.292386000	1.042639000

(1c) B3LYP/BS-I energy = -1812.38923479 a.u.							
N	1.816518000	-0.050298000	0.003450000	C	5.124789000	5.415846000	-0.871566000
H	0.804481000	0.003907000	0.010634000	H	5.860762000	6.176799000	-1.105176000
N	-0.055520000	1.881482000	0.837517000	C	1.957768000	-2.532826000	-0.052344000
N	-0.197705000	-1.790165000	-0.941393000	C	2.854326000	-3.665482000	0.307925000
C	2.646833000	1.035550000	0.010151000	C	3.066261000	-4.724747000	-0.585933000
C	3.969127000	0.538769000	0.006673000	C	3.902283000	-5.784515000	-0.244394000
H	4.860042000	1.144776000	0.015575000	H	4.063215000	-6.590623000	-0.951305000
C	3.899609000	-0.849719000	0.019332000	C	4.533149000	-5.807328000	0.997248000
H	4.725908000	-1.541347000	0.015418000	H	5.180824000	-6.634715000	1.264155000
C	2.534628000	-1.212478000	0.002388000	C	4.331056000	-4.759118000	1.893788000
C	0.912856000	2.782261000	0.373780000	H	4.814958000	-4.772279000	2.863862000
C	0.337764000	4.118134000	0.311198000	C	3.506696000	-3.692617000	1.549568000
H	0.838895000	5.008473000	-0.034483000	C	-2.499327000	-1.663855000	-1.838447000
C	-0.947277000	3.996417000	0.738234000	C	-2.389692000	1.995896000	1.653889000
H	-1.692392000	4.774389000	0.825609000	C	-3.249684000	-0.735234000	-0.892086000
C	-1.138583000	2.590560000	1.065253000	C	-2.543392000	0.185172000	-0.117254000
C	0.654638000	-2.781319000	-0.435107000	H	-1.466045000	0.203169000	-0.179781000
C	-0.053080000	-4.053978000	-0.400426000	C	-3.188204000	1.068759000	0.744218000
H	0.340518000	-4.988819000	-0.033758000	C	-4.582623000	1.040405000	0.814539000
C	-1.298772000	-3.806393000	-0.884671000	C	-5.300089000	0.127949000	0.043722000
H	-2.113346000	-4.506251000	-1.006295000	C	-4.640279000	-0.762735000	-0.804364000
C	-1.333538000	-2.388612000	-1.217497000	H	3.695324000	2.639578000	-2.207008000
C	2.200979000	2.405058000	0.047774000	H	2.989949000	4.483949000	1.600078000
C	3.217842000	3.445974000	-0.269061000	H	2.586346000	-4.702245000	-1.556864000
C	3.910692000	3.421518000	-1.488422000	H	3.348218000	-2.882336000	2.251342000
C	4.849016000	4.403710000	-1.789635000	H	-5.213843000	-1.473754000	-1.387037000
H	5.364320000	4.379366000	-2.743199000	H	-5.111702000	1.714661000	1.477450000
C	3.503728000	4.468442000	0.646467000	H	-3.039760000	2.802687000	2.001494000
C	4.453036000	5.442555000	0.348358000	H	-2.096849000	1.422766000	2.541957000
H	4.669281000	6.220524000	1.071821000	H	-2.115918000	-1.068263000	-2.674413000

(1d) B3LYP/BS-I energy = -1934.87143920 a.u.			
N	1.374985000	0.000160000	-0.000008000
H	0.361570000	-0.000007000	-0.000048000
N	-0.569126000	1.834898000	0.898755000
N	-0.568629000	-1.835162000	-0.898584000
C	2.149766000	1.125810000	0.005499000
C	3.495161000	0.695643000	-0.005175000
H	4.355038000	1.345044000	0.002044000
C	3.495375000	-0.694676000	0.005196000
H	4.355450000	-1.343814000	-0.002001000
C	2.150111000	-1.125254000	-0.005500000
C	0.339950000	2.783583000	0.411021000
C	-0.305889000	4.088147000	0.360049000
H	0.139553000	5.003113000	0.002446000
C	-1.572789000	3.899991000	0.815199000
H	-2.356053000	4.637733000	0.917181000
C	-1.682389000	2.486084000	1.148495000
C	0.340771000	-2.783572000	-0.410921000
C	-0.304664000	-4.088332000	-0.359914000
H	0.141084000	-5.003164000	-0.002349000
C	-1.571655000	-3.900560000	-0.814973000
H	-2.354699000	-4.638543000	-0.916906000
C	-1.681712000	-2.486687000	-1.148253000
C	1.636862000	2.472119000	0.053462000
C	2.592639000	3.561455000	-0.288685000
C	3.264862000	3.561799000	-1.519914000
C	4.144651000	4.588967000	-1.846516000
H	4.643807000	4.582583000	-2.808933000
C	2.840547000	4.606156000	0.612829000
C	3.731677000	5.625988000	0.289163000
H	3.919520000	6.421038000	1.001959000
C	4.382473000	5.623038000	-0.942358000
H	5.073039000	6.419476000	-1.195628000
C	1.637613000	-2.471716000	-0.053447000
C	2.593740000	-3.560770000	0.288624000
C	2.841927000	-4.605362000	-0.612940000
C	3.733386000	-5.624932000	-0.289353000
H	3.921440000	-6.419897000	-1.002187000
C	4.384236000	-5.621828000	0.942139000
H	5.075059000	-6.418062000	1.195348000
C	4.146136000	-4.587864000	1.846346000
H	4.645333000	-4.581363000	2.808741000
C	3.266016000	-3.560954000	1.519823000
C	-2.891288000	-1.823838000	-1.752550000
C	-2.891733000	1.822850000	1.752842000
C	-3.665721000	-0.899524000	-0.819237000
C	-2.986915000	-0.000530000	0.000186000
H	-1.908343000	-0.000486000	0.000297000
C	-3.665953000	0.898430000	0.819462000
C	-5.062954000	0.901751000	0.814642000
C	-5.736713000	-0.000629000	-0.000085000
C	-5.062727000	-0.902948000	-0.814686000
H	3.078518000	2.762785000	-2.227740000
H	2.343924000	4.603444000	1.575595000
H	2.345256000	-4.602768000	-1.575681000
H	3.079457000	-2.762025000	2.227688000
H	-5.621652000	-1.590015000	-1.438104000
H	-5.622053000	1.588784000	1.437942000
Cl	-7.502876000	-0.000702000	-0.000249000
H	-3.196369000	-2.393329000	-2.257639000
C	-6.802115000	0.137461000	0.080182000
F	-7.325762000	0.931841000	-0.886185000
F	-7.326447000	-1.094376000	-0.112901000
F	-7.285836000	0.595303000	1.256825000

(1e) B3LYP/BS-I energy = -1475.24670299 a.u.			
N	-0.091613000	-0.880787000	-0.053972000
H	-0.031041000	0.123183000	-0.196057000
N	-1.733652000	1.261663000	-0.785320000
N	1.941854000	0.889303000	0.911655000
C	-1.284948000	-1.544371000	0.048237000
C	-0.980573000	-2.906402000	0.262048000
H	-1.706293000	-3.690241000	0.403660000
C	0.403836000	-3.035547000	0.251530000
H	0.974047000	-3.938831000	0.394414000
C	0.955540000	-1.748196000	0.072708000
C	-2.771737000	0.401800000	-0.398800000
C	-4.043344000	1.100549000	-0.505670000
H	-5.013262000	0.684806000	-0.281377000
C	-3.748394000	2.353053000	-0.941845000
H	-4.434560000	3.162776000	-1.145845000
C	-2.300951000	2.400991000	-1.112559000
C	2.787348000	-0.100203000	0.392390000
C	4.141637000	0.428851000	0.282947000
H	4.996910000	-0.094921000	-0.114078000
C	4.082786000	1.707901000	0.736749000
H	4.888820000	2.425174000	0.801797000
C	2.696858000	1.939674000	1.130868000
C	-2.572913000	-0.914744000	-0.044387000
C	-3.758708000	-1.773197000	0.268106000
C	-4.414538000	-1.652544000	1.497936000
C	-5.517940000	-2.450898000	1.791551000
H	-6.016016000	-2.347153000	2.749009000
C	-4.226674000	-2.709020000	-0.661326000
C	-5.331730000	-3.504348000	-0.367175000
H	-5.688497000	-4.219893000	-1.099566000
C	-5.979184000	-3.378373000	0.860216000
H	-6.838687000	-3.998427000	1.088486000
C	2.349337000	-1.369201000	0.074642000
C	3.328864000	-2.440619000	-0.249537000
C	4.398794000	-2.721382000	0.613052000
C	5.314086000	-3.724589000	0.306133000
H	6.128936000	-3.935189000	0.989619000
C	5.180024000	-4.459527000	-0.869541000
H	5.894640000	-5.238705000	-1.109540000
C	4.118756000	-4.192690000	-1.733424000
H	4.009916000	-4.758731000	-2.651693000

(2a) B3LYP/BS-I energy = -1766.53331354 a.u.			
N	1.945998000	0.011847000	-0.001262000
H	0.933631000	-0.001012000	-0.014990000
N	0.045501000	-1.817177000	-0.894595000
N	0.015395000	1.817785000	0.899440000
C	2.726212000	-1.105707000	0.058670000
C	4.068000000	-0.663883000	0.059825000
H	4.934000000	-1.304547000	0.095423000
C	4.055937000	0.725930000	-0.026001000
H	4.910378000	1.382636000	-0.045416000
C	2.706572000	1.143258000	-0.048718000
C	0.899424000	-2.747471000	-0.288299000
C	0.189863000	-4.006839000	-0.120301000
H	0.579527000	-4.898831000	0.345023000
C	-1.058747000	-3.807885000	-0.618339000
H	-1.866485000	-4.523034000	-0.649432000
C	-1.095340000	-2.431168000	-1.110417000
C	0.850633000	2.755639000	0.279172000
C	0.116585000	3.998416000	0.092827000
H	0.488493000	4.890551000	-0.386568000
C	-1.127844000	3.782283000	0.594216000
H	-1.949588000	4.481694000	0.615068000
C	-1.136830000	2.412677000	1.107669000
C	2.195677000	-2.446799000	0.084441000
C	3.114416000	-3.527582000	0.530576000
C	3.797042000	-3.428998000	1.752686000
C	4.643971000	-4.448041000	2.176244000
H	5.151576000	-4.362668000	3.130489000
C	3.319787000	-4.666008000	-0.262499000
C	4.177092000	-5.679145000	0.157964000
H	4.331674000	-6.547685000	-0.472351000
C	4.838291000	-5.575471000	1.379659000
H	5.503486000	-6.366133000	1.708025000
C	2.153151000	2.475087000	-0.087340000
C	3.055230000	3.567355000	-0.538541000
C	3.229396000	4.720636000	0.240730000
C	4.072524000	5.743889000	-0.183729000
H	4.203352000	6.623723000	0.436213000
C	4.750580000	5.635777000	-1.395762000
H	5.405044000	6.434129000	-1.727085000
C	4.587292000	4.493908000	-2.178671000
H	5.108286000	4.404851000	-3.125330000
C	3.754590000	3.465006000	-1.750966000
C	-2.284845000	1.727762000	1.844723000
C	-2.259697000	-1.756420000	-1.830812000
C	-3.093341000	0.836455000	0.868574000
C	-2.404279000	-0.024390000	0.014777000
H	-1.326921000	-0.005221000	0.003754000
C	-3.080575000	-0.904043000	-0.830456000
C	-4.474685000	-0.928609000	-0.807662000
C	-5.204949000	-0.081777000	0.051961000
C	-4.487991000	0.811621000	0.874520000
H	3.643390000	-2.557284000	2.377464000
H	2.817173000	-4.740734000	-1.219129000
H	2.714496000	4.798912000	1.190485000
H	3.625279000	2.581846000	-2.365038000
N	-6.598058000	-0.136636000	0.098290000
C	-7.314906000	-0.874454000	-0.926930000
H	-8.382198000	-0.837235000	-0.709846000
H	-7.155326000	-0.473576000	-1.940132000
H	-7.020984000	-1.927827000	-0.931300000
C	-7.327093000	0.911550000	0.790760000
H	-7.161372000	1.911015000	0.359435000
H	-8.393540000	0.692382000	0.743806000
H	-7.049972000	0.951144000	1.848136000
H	-5.005419000	-1.599479000	-1.463942000
H	-5.028959000	1.477816000	1.527224000
C	-3.160740000	2.800738000	2.523063000
H	-3.694295000	3.420569000	1.798878000
H	-3.900150000	2.337383000	3.179888000
H	-2.539458000	3.454873000	3.139532000
C	-1.701678000	0.811511000	2.950670000
H	-1.143475000	1.403629000	3.681732000
H	-2.513587000	0.291243000	3.465438000
H	-1.024110000	0.072231000	2.527370000
C	-3.116070000	-2.833646000	-2.526804000
H	-3.629236000	-3.482495000	-1.813435000
H	-3.871346000	-2.372254000	-3.166829000
H	-2.484931000	-3.459043000	-3.162784000
C	-1.701305000	-0.806886000	-2.921067000
H	-1.132525000	-1.372324000	-3.664927000
H	-2.526706000	-0.295706000	-3.423371000
H	-1.039146000	-0.059922000	-2.487095000

(2b) B3LYP/BS-I energy = -1747.08695069 a.u.						
N	-1.740416000	0.086966000	-0.014042000	C	3.353342000	0.647264000
H	-0.731494000	0.018255000	0.036514000	C	4.750691000	0.530549000
N	0.301977000	1.789070000	-0.874964000	C	5.361369000	-0.393022000
N	0.043738000	-1.828459000	0.927508000	C	4.595444000	-1.201096000
C	-2.442261000	1.256579000	0.005047000	H	-3.361581000	2.735284000
C	-3.810014000	0.909628000	-0.059802000	H	-2.214034000	4.915793000
H	-4.629045000	1.610146000	-0.071165000	H	-2.895138000	-4.597073000
C	-3.891803000	-0.478117000	-0.139969000	H	-3.502703000	-2.417622000
H	-4.788317000	-1.073168000	-0.201064000	C	7.563166000	0.200624000
C	-2.575429000	-0.988817000	-0.094264000	H	8.579167000	-0.112097000
C	-0.497739000	2.770222000	-0.275190000	H	7.372864000	0.026823000
C	0.295777000	3.972588000	-0.070410000	H	7.455872000	1.270031000
H	-0.040374000	4.883280000	0.400347000	H	5.127849000	-1.893566000
C	1.539157000	3.691296000	-0.541931000	H	5.353984000	1.143232000
H	2.396852000	4.346475000	-0.542636000	O	6.714135000	-0.586401000
C	1.488203000	2.322967000	-1.054921000	C	1.785081000	-0.895170000
C	-0.845784000	-2.720168000	0.313813000	H	2.623063000	-0.424162000
C	-0.205920000	-4.021206000	0.189689000	H	1.173909000	-0.118029000
H	-0.633864000	-4.898646000	-0.269573000	H	1.168365000	-1.423286000
C	1.036538000	-3.885736000	0.723244000	C	3.106845000	-2.993777000
H	1.799119000	-4.646159000	0.794218000	H	3.595470000	-3.679058000
C	1.139371000	-2.503796000	1.189708000	H	3.877403000	-2.562424000
C	-1.822360000	2.558347000	0.057894000	H	2.434573000	-3.575143000
C	-2.677974000	3.695982000	0.485792000	C	2.014721000	0.688306000
C	-3.421961000	3.626719000	1.673842000	H	1.286337000	-0.010848000
C	-4.211001000	4.697726000	2.080285000	H	1.509921000	1.307033000
H	-4.767131000	4.632988000	3.008739000	H	2.810490000	0.122535000
C	-2.762922000	4.860953000	-0.291340000	C	3.566262000	2.598987000
C	-3.562458000	5.926871000	0.111655000	H	4.115128000	3.189021000
H	-3.624554000	6.815264000	-0.506759000	H	4.294234000	2.096398000
C	-4.285475000	5.850500000	1.299827000	H	2.997200000	3.286199000
H	-4.906094000	6.681886000	1.614571000			
C	-2.114539000	-2.355694000	-0.094979000			
C	-3.077766000	-3.391730000	-0.553890000			
C	-3.366282000	-4.507263000	0.245624000			
C	-4.265081000	-5.478132000	-0.187792000			
H	-4.483536000	-6.329116000	0.447532000			
C	-4.885590000	-5.354549000	-1.428847000			
H	-5.583022000	-6.112531000	-1.767176000			
C	-4.608644000	-4.249265000	-2.231952000			
H	-5.084066000	-4.148775000	-3.201178000			
C	-3.720002000	-3.271896000	-1.795814000			
C	2.319515000	-1.883920000	1.934016000			
C	2.616243000	1.576147000	-1.761684000			
C	3.209135000	-1.087057000	0.949919000			
C	2.608324000	-0.159876000	0.089980000			
H	1.533908000	-0.072577000	0.086628000			

(2c) B3LYP/BS-I energy = -1969.67497650 a.u.			
N	2.115183000	0.006748000	0.000564000
H	1.102802000	0.001809000	0.001829000
N	0.183519000	1.814948000	0.876944000
N	0.196876000	-1.818855000	-0.869099000
C	2.880495000	1.134498000	-0.056997000
C	4.228477000	0.711329000	-0.046527000
H	5.085629000	1.363969000	-0.076417000
C	4.235164000	-0.677895000	0.041782000
H	5.098524000	-1.322403000	0.069314000
C	2.891232000	-1.113724000	0.055850000
C	1.032461000	2.755640000	0.278530000
C	0.318606000	4.013904000	0.128964000
H	0.703386000	4.912708000	-0.327001000
C	-0.925586000	3.808143000	0.636745000
H	-1.732806000	4.522736000	0.685608000
C	-0.955242000	2.426628000	1.111101000
C	1.057392000	-2.751957000	-0.275312000
C	0.356965000	-4.017797000	-0.125962000
H	0.752452000	-4.913561000	0.326824000
C	-0.890829000	-3.823901000	-0.629491000
H	-1.690623000	-4.546869000	-0.677452000
C	-0.936225000	-2.441820000	-1.100947000
C	2.334291000	2.468734000	-0.086827000
C	3.245884000	3.559889000	-0.522037000
C	3.934645000	3.473059000	-1.741552000
C	4.775380000	4.501170000	-2.155295000
H	5.287715000	4.425604000	-3.107757000
C	3.438631000	4.694879000	0.279088000
C	4.290596000	5.716508000	-0.131331000
H	4.436349000	6.582158000	0.504906000
C	4.957637000	5.624984000	-1.350806000
H	5.618293000	6.422515000	-1.671440000
C	2.357658000	-2.453032000	0.085967000
C	3.281050000	-3.536146000	0.516470000
C	3.482526000	-4.667669000	-0.287366000
C	4.345331000	-5.681885000	0.118791000
H	4.497579000	-6.544912000	-0.519486000
C	5.014785000	-5.586284000	1.336630000
H	5.683880000	-6.378080000	1.653961000
C	4.824042000	-4.465744000	2.143709000
H	5.338294000	-4.387025000	3.094882000
C	3.972374000	-3.444947000	1.734203000
C	-2.097978000	-1.767135000	-1.827478000
C	-2.107451000	1.741429000	1.842754000
C	-2.917079000	-0.898196000	-0.844564000
C	-2.252018000	-0.009905000	0.004046000
H	-1.172787000	-0.000477000	-0.002546000

<b>(2d)</b> B3LYP/BS-I energy = -2092.15704463 a.u.			
N	1.734554000	0.000000000	0.000000000
H	0.722146000	0.000001000	0.000003000
N	-0.188390000	1.816885000	0.880323000
N	-0.188389000	-1.816886000	-0.880324000
C	2.505245000	1.124272000	-0.054461000
C	3.851182000	0.694707000	-0.043001000
H	4.711448000	1.343354000	-0.070649000
C	3.851182000	-0.694707000	0.042994000
H	4.711448000	-1.343354000	0.070640000
C	2.505245000	-1.124273000	0.054458000
C	0.664550000	2.753529000	0.281667000
C	-0.045167000	4.013795000	0.127527000
H	0.343407000	4.910375000	-0.329641000
C	-1.291483000	3.812373000	0.631521000
H	-2.097144000	4.529053000	0.675728000
C	-1.326329000	2.431896000	1.109273000
C	0.664550000	-2.753530000	-0.281666000
C	-0.045168000	-4.013795000	-0.127524000
H	0.343406000	-4.910374000	0.329646000
C	-1.291484000	-3.812373000	-0.631518000
H	-2.097145000	-4.529052000	-0.675723000
C	-1.326330000	-2.431897000	-1.109272000
C	1.965249000	2.461101000	-0.083222000
C	2.881603000	3.548479000	-0.517866000
C	3.571783000	3.458581000	-1.736366000
C	4.416928000	4.483345000	-2.149449000
H	4.930370000	4.405344000	-3.1011131000
C	3.077481000	4.683209000	0.282881000
C	3.933682000	5.701559000	-0.126896000
H	4.081640000	6.567040000	0.509084000
C	4.602158000	5.606957000	-1.345352000
H	5.266194000	6.401897000	-1.665473000
C	1.965249000	-2.461101000	0.083221000
C	2.881603000	-3.548479000	0.517866000
C	3.077480000	-4.683211000	-0.282880000
C	3.933681000	-5.701560000	0.126898000
H	4.081637000	-6.567042000	-0.509080000
C	4.602159000	-5.606956000	1.345353000
H	5.266195000	-6.401896000	1.665474000
C	4.416931000	-4.483342000	2.149448000
H	4.930375000	-4.405340000	3.101129000
C	3.571785000	-3.458578000	1.736365000

(2e) B3LYP/BS-I energy = -1632.53149058 a.u.			
N	0.145529000	-1.326304000	0.070732000
H	0.094693000	-0.332945000	0.278288000
N	1.704010000	0.802131000	0.828666000
N	-1.883871000	0.402289000	-0.904709000
C	1.340148000	-1.960086000	-0.128436000
C	1.043452000	-3.315688000	-0.392444000
H	1.769274000	-4.080230000	-0.616258000
C	-0.338305000	-3.467597000	-0.310942000
H	-0.903734000	-4.371710000	-0.468995000
C	-0.895234000	-2.198048000	-0.042904000
C	2.758147000	0.029217000	0.321566000
C	3.984355000	0.806535000	0.372764000
H	4.960971000	0.470050000	0.061076000
C	3.646237000	2.016698000	0.891235000
H	4.305574000	2.850044000	1.078035000
C	2.214418000	1.961152000	1.180153000
C	-2.711759000	-0.533323000	-0.270361000
C	-4.020484000	0.063482000	-0.040652000
H	-4.852775000	-0.403933000	0.462304000
C	-3.951731000	1.326963000	-0.535017000
H	-4.733645000	2.071332000	-0.527966000
C	-2.604170000	1.482723000	-1.087146000
C	2.606247000	-1.280981000	-0.084083000
C	3.805867000	-2.063698000	-0.511378000
C	4.436206000	-1.790283000	-1.730602000
C	5.554248000	-2.520514000	-2.127578000
H	6.030412000	-2.299164000	-3.076186000
C	4.315211000	-3.084440000	0.300310000
C	5.435327000	-3.810535000	-0.096591000
H	5.824251000	-4.591996000	0.546625000
C	6.057115000	-3.531448000	-1.311970000
C	-2.285117000	-1.808064000	0.045201000
C	-3.252505000	-2.852945000	0.463715000
C	-4.431684000	-3.078026000	-0.263525000
C	-5.336482000	-4.057569000	0.135323000
H	-6.237086000	-4.224457000	-0.444802000
C	-5.082456000	-4.826942000	1.268611000
C	-3.912338000	-4.617631000	1.997040000

(3a) B3LYP/BS-I energy = -2533.61541229 a.u.			
N	-2.725029000	-0.000092000	-0.000089000
H	-1.710290000	-0.000039000	-0.000067000
N	-0.766779000	1.994082000	0.027880000
N	-0.766593000	-1.994105000	-0.027915000
C	-3.498756000	1.000515000	0.509613000
C	-4.845833000	0.615109000	0.323179000
H	-5.704767000	1.197300000	0.613947000
C	-4.845758000	-0.615484000	-0.323484000
H	-5.704621000	-1.197753000	-0.614303000
C	-3.498634000	-1.000769000	-0.509835000
C	-1.676280000	2.648552000	0.867935000
C	-1.055685000	3.846326000	1.403816000
H	-1.502041000	4.539701000	2.098932000
C	0.186599000	3.906356000	0.859500000
H	0.917061000	4.681928000	1.011644000
C	0.321718000	2.729273000	-0.001670000
C	-1.676001000	-2.648671000	-0.867997000
C	-1.055303000	-3.846440000	-1.403772000
H	-1.501576000	-4.539879000	-2.098876000
C	0.186945000	-3.906375000	-0.859364000
H	0.917453000	-4.681922000	-1.011408000
C	0.321942000	-2.729235000	0.001750000
C	-2.976172000	2.222910000	1.058534000
C	-3.930730000	3.063455000	1.834365000
C	-4.587669000	2.537645000	2.956514000
C	-5.472563000	3.320655000	3.691346000
H	-5.960385000	2.903338000	4.565089000
C	-4.199147000	4.386558000	1.457500000
C	-5.094486000	5.164450000	2.187123000
H	-5.297123000	6.183256000	1.876416000
C	-5.730417000	4.635767000	3.307974000
H	-6.424661000	5.243104000	3.877703000
C	-2.975912000	-2.223132000	-1.058693000
C	-3.930358000	-3.063778000	-1.834555000
C	-4.198718000	-4.386880000	-1.457644000
C	-5.093951000	-5.164865000	-2.187298000
H	-5.296547000	-6.183669000	-1.876555000
C	-5.729832000	-4.636279000	-3.308222000
H	-6.423994000	-5.243688000	-3.877974000
C	-5.472034000	-3.321168000	-3.691640000
H	-5.959817000	-2.903926000	-4.565439000
C	-4.587247000	-2.538065000	-2.956779000
C	1.507376000	-2.392020000	0.936427000
C	1.507236000	2.392170000	-0.936274000
C	2.292808000	-1.145159000	0.407738000
C	1.601684000	0.000086000	0.000107000
H	0.525487000	0.000050000	0.000116000
C	2.292729000	1.145361000	-0.407560000
C	3.687437000	1.125512000	-0.437314000
C	4.412317000	0.000189000	0.000124000
C	3.687512000	-1.125225000	0.437463000
H	-4.386147000	1.517110000	3.260078000
H	-3.713982000	4.796150000	0.579815000
H	-3.713593000	-4.796397000	-0.579904000
H	-4.385769000	-1.517531000	-3.260376000
N	5.797820000	0.000282000	0.000269000
C	6.527736000	-1.178943000	0.427409000
H	7.595635000	-0.998713000	0.312008000

(3b) B3LYP/BS-I energy = -2514.16860656 a.u.			
N	2.572406000	-0.380787000	-0.034333000
H	1.569482000	-0.225589000	-0.026626000
N	0.319297000	-2.036656000	0.041683000
N	0.951058000	1.903952000	-0.028282000
C	3.186115000	-1.494817000	0.459160000
C	4.574446000	-1.325137000	0.256289000
H	5.334333000	-2.037432000	0.532634000
C	4.760149000	-0.104774000	-0.382331000
H	5.696121000	0.338081000	-0.680634000
C	3.488480000	0.489912000	-0.546655000
C	1.132883000	-2.833491000	0.856699000
C	0.344940000	-3.923649000	1.401301000
H	0.693355000	-4.685026000	2.081119000
C	-0.903611000	-3.783916000	0.885744000
H	-1.745075000	-4.434889000	1.050385000
C	-0.870872000	-2.593106000	0.034885000
C	1.955792000	2.419702000	-0.857645000
C	1.548792000	3.723585000	-1.348561000
H	2.105757000	4.352318000	-2.025021000
C	0.340646000	3.980894000	-0.786224000
H	-0.243538000	4.877350000	-0.901118000
C	0.007597000	2.815698000	0.037002000
C	2.488055000	-2.621181000	1.016205000
C	3.314277000	-3.608053000	1.767193000
C	4.055552000	-3.203424000	2.886709000
C	4.822093000	-4.121162000	3.598222000
H	5.377266000	-3.795125000	4.470578000
C	3.376282000	-4.950094000	1.368544000
C	4.154415000	-5.864217000	2.074482000
H	4.198733000	-6.896872000	1.747080000
C	4.875974000	-5.453790000	3.192967000
H	5.478728000	-6.166661000	3.744210000
C	3.165251000	1.789390000	-1.070820000
C	4.240423000	2.478098000	-1.839796000
C	4.743206000	3.718676000	-1.424851000
C	5.751626000	4.352548000	-2.146309000
H	6.135374000	5.307910000	-1.806346000
C	6.268406000	3.760738000	-3.296433000
H	7.051050000	4.256274000	-3.859717000
C	5.776950000	2.526158000	-3.717656000
H	6.171265000	2.060865000	-4.614049000
C	4.778168000	1.885127000	-2.991124000
C	-1.223013000	2.656241000	0.961434000
C	-2.000867000	-2.086471000	-0.890193000
C	-2.196133000	1.576076000	0.382240000
C	-1.704261000	0.307089000	0.030498000
H	-0.649642000	0.109200000	0.121124000
C	-2.552774000	-0.698446000	-0.428103000
C	-3.922368000	-0.422498000	-0.568526000
C	-4.422238000	0.819558000	-0.193376000
C	-3.564625000	1.808440000	0.296251000
H	4.012505000	-2.168831000	3.206117000
H	2.824553000	-5.268749000	0.492327000
H	4.351109000	4.175357000	-0.524081000
H	4.396362000	0.926654000	-3.322649000
C	-6.675712000	0.214126000	-0.734551000
H	-7.649257000	0.699742000	-0.685069000
H	-6.469519000	-0.074982000	-1.771393000
H	-6.685772000	-0.683627000	-0.106545000
H	-4.011765000	2.744084000	0.596294000
H	-4.585955000	-1.176565000	-0.960327000
C	-1.934242000	4.034706000	1.071435000
C	-1.996579000	4.754545000	2.267064000
C	-2.537905000	4.608763000	-0.060413000
C	-2.627839000	5.998731000	2.332298000
H	-1.552767000	4.348825000	3.165298000
C	-3.167187000	5.846660000	-0.000036000
H	-2.524704000	4.073475000	-1.002215000
C	-3.214922000	6.552434000	1.201961000
H	-2.657502000	6.529474000	3.277598000
H	-3.625467000	6.257880000	-0.892874000
H	-3.707237000	7.517150000	1.252876000
C	-0.754689000	2.194895000	2.368684000
C	0.476317000	2.605866000	2.894814000
C	-1.591916000	1.430281000	3.187453000
C	0.859044000	2.257652000	4.187376000
H	1.148487000	3.201902000	2.292094000
C	-1.211348000	1.079599000	4.481778000
H	-2.552933000	1.101020000	2.814267000
C	0.017920000	1.488986000	4.988537000
H	1.820951000	2.586394000	4.565912000
H	-1.880048000	0.480789000	5.090552000
H	0.318292000	1.212073000	5.993045000
C	-3.154921000	-3.128477000	-0.863786000
C	-3.535637000	-3.873505000	-1.981208000
C	-3.868085000	-3.335110000	0.329280000
C	-4.578980000	-4.800783000	-1.910719000
H	-3.022635000	-3.735165000	-2.922810000
C	-4.904157000	-4.258298000	0.404634000
H	-3.611106000	-2.756493000	1.208917000
C	-5.265752000	-5.001015000	-0.720290000
H	-4.849780000	-5.363588000	-2.797376000
H	-5.432168000	-4.396354000	1.341984000
H	-6.074624000	-5.721035000	-0.665475000
C	-1.419915000	-1.957971000	-2.326037000
C	-0.537846000	-2.930525000	-2.818214000
C	-1.791443000	-0.920791000	-3.184823000
C	-0.049032000	-2.869200000	-4.118725000
H	-0.227246000	-3.746988000	-2.177712000
C	-1.300708000	-0.854987000	-4.489489000
H	-2.462499000	-0.146980000	-2.837343000
C	-0.428009000	-1.827348000	-4.964016000
H	0.633985000	-3.635036000	-4.470195000
H	-1.601631000	-0.033340000	-5.130363000
H	-0.043259000	-1.774346000	-5.976469000
O	-5.741025000	1.173458000	-0.262857000

(3c) B3LYP/BS-I energy =-2736.75581774 a.u.			H	3.782445000	4.829538000	-0.563292000	
N	2.831042000	0.035398000	-0.023005000	H	3.889853000	-4.743706000	0.534210000
H	1.816675000	0.026079000	-0.009700000	H	4.547182000	-1.467063000	3.222129000
N	0.842821000	1.996035000	-0.041936000	H	-4.122378000	-2.001854000	-0.820774000
N	0.890440000	-1.974773000	0.043544000	H	-4.162581000	1.943379000	0.784383000
C	3.587416000	1.042807000	-0.544942000	C	-5.762875000	0.006599000	-0.114476000
C	4.940986000	0.671614000	-0.376538000	F	-6.188577000	0.631841000	-1.241212000
H	5.789782000	1.261948000	-0.680209000	F	-6.308357000	-1.229141000	-0.130568000
C	4.962404000	-0.557361000	0.272376000	F	-6.318419000	0.673133000	0.923582000
H	5.831037000	-1.130164000	0.552605000	C	-2.313605000	-3.661402000	-0.941616000
C	3.621871000	-0.955792000	0.478444000	C	-2.510477000	-4.433164000	-2.088350000
C	1.743161000	2.673169000	-0.875325000	C	-2.998886000	-4.042555000	0.224286000
C	1.116623000	3.884522000	-1.370783000	C	-3.349872000	-5.549750000	-2.072442000
H	1.555048000	4.596346000	-2.052005000	H	-2.012748000	-4.167868000	-3.010592000
C	-0.116617000	3.934637000	-0.804337000	C	-3.835186000	-5.152285000	0.244015000
H	-0.847230000	4.716000000	-0.921880000	H	-2.883804000	-3.455391000	1.128032000
C	-0.241713000	2.735222000	0.023935000	C	-4.014320000	-5.916331000	-0.909262000
C	1.821825000	-2.622257000	0.866162000	H	-3.482024000	-6.127349000	-2.980666000
C	1.229458000	-3.836927000	1.394726000	H	-4.352311000	-5.417032000	1.159693000
H	1.696029000	-4.529104000	2.077501000	H	-4.668652000	-6.780699000	-0.897895000
C	-0.015777000	-3.917791000	0.858753000	C	-0.837765000	-2.126207000	-2.341236000
H	-0.730271000	-4.709120000	1.006364000	C	0.270635000	-2.822937000	-2.840870000
C	-0.181341000	-2.734604000	0.014361000	C	-1.482762000	-1.227364000	-3.195495000
C	3.045810000	2.262260000	-1.080808000	C	0.719260000	-2.624626000	-4.142820000
C	3.986621000	3.121309000	-1.853568000	H	0.790950000	-3.530192000	-2.208049000
C	4.629438000	2.617848000	-2.993847000	C	-1.034060000	-1.024746000	-4.500601000
C	5.501640000	3.417336000	-3.726131000	H	-2.343389000	-0.671776000	-2.847529000
H	5.978449000	3.018082000	-4.614203000	C	0.069978000	-1.720250000	-4.981010000
C	4.256290000	4.437707000	-1.455168000	H	1.581426000	-3.176863000	-4.500716000
C	5.139595000	5.231559000	-2.182207000	H	-1.551753000	-0.316043000	-5.137598000
H	5.343923000	6.244874000	-1.855296000	H	0.422183000	-1.560097000	-5.993946000
C	5.761095000	4.725717000	-3.321529000	C	-2.364699000	3.603261000	1.060310000
H	6.445629000	5.345675000	-3.889303000	C	-2.553143000	4.321420000	2.243115000
C	3.120183000	-2.182634000	1.036318000	C	-3.071364000	4.029717000	-0.077157000
C	4.096628000	-3.013787000	1.794914000	C	-3.404390000	5.427925000	2.289679000
C	4.379573000	-4.330828000	1.407815000	H	-2.038712000	4.021890000	3.145331000
C	5.295839000	-5.098415000	2.122178000	C	-3.919749000	5.129849000	-0.034793000
H	5.509853000	-6.112498000	1.803953000	H	-2.964737000	3.486097000	-1.008587000
C	5.937677000	-4.565535000	3.237641000	C	-4.089913000	5.839168000	1.154050000
H	6.647876000	-5.165175000	3.795625000	H	-3.528679000	5.962700000	3.2224832000
C	5.665222000	-3.256342000	3.630931000	H	-4.452798000	5.429503000	-0.930355000
H	6.157731000	-2.836068000	4.500542000	H	-4.753075000	6.696056000	1.191042000
C	4.759794000	-2.483073000	2.911009000	C	-0.846106000	2.038254000	2.373185000
C	-1.377346000	-2.420001000	-0.913629000	C	0.273527000	2.714393000	2.875048000
C	-1.414040000	2.376100000	0.966949000	C	-1.483416000	1.118608000	3.211309000
C	-2.170003000	-1.172927000	-0.407139000	C	0.741454000	2.474998000	4.163480000
C	-1.505599000	-0.018486000	0.020693000	H	0.787543000	3.437442000	2.255417000
H	-0.427740000	-0.015291000	0.041700000	C	-1.015902000	0.875296000	4.502517000
C	-2.192944000	1.133370000	0.427529000	H	-2.354134000	0.580455000	2.860569000
C	-3.588144000	1.101685000	0.428305000	C	0.100182000	1.550163000	4.985109000
C	-4.262861000	-0.026420000	-0.029905000	H	1.612258000	3.011947000	4.523713000
C	-3.567136000	-1.149481000	-0.460219000	H	-1.528169000	0.151897000	5.127277000
H	4.426977000	1.602416000	-3.313590000	H	0.467365000	1.358518000	5.987199000

(3d) B3LYP/BS-I energy = -2859.23788875 a.u.			
N	-2.593081000	-0.000240000	0.000053000
H	-1.578551000	-0.000120000	0.000032000
N	-0.630002000	1.987766000	0.039174000
N	-0.629459000	-1.987862000	-0.039227000
C	-3.366938000	0.999567000	0.510948000
C	-4.714131000	0.614311000	0.324102000
H	-5.573045000	1.196094000	0.615596000
C	-4.713989000	-0.615318000	-0.323912000
H	-5.572770000	-1.197313000	-0.615377000
C	-3.366707000	-1.000239000	-0.510816000
C	-1.544962000	2.648834000	0.869045000
C	-0.933779000	3.859613000	1.385073000
H	-1.385480000	4.560358000	2.069127000
C	0.306279000	3.924167000	0.835329000
H	1.030154000	4.708893000	0.971261000
C	0.450020000	2.734991000	-0.005097000
C	-1.544350000	-2.649090000	-0.869052000
C	-0.932963000	-3.859738000	-1.385139000
H	-1.384577000	-4.560566000	-2.069166000
C	0.307131000	-3.924079000	-0.835454000
H	1.031126000	-4.708688000	-0.971417000
C	0.450716000	-2.734874000	0.004959000
C	-2.845399000	2.223115000	1.057563000
C	-3.803600000	3.067598000	1.824773000
C	-4.457048000	2.549469000	2.952434000
C	-5.345325000	3.335516000	3.679891000
H	-5.830341000	2.924832000	4.558262000
C	-4.078907000	4.385190000	1.434090000
C	-4.978084000	5.165645000	2.156167000
H	-5.186414000	6.180037000	1.835139000
C	-5.610252000	4.645154000	3.282954000
H	-6.307180000	5.254722000	3.846902000
C	-2.844896000	-2.223653000	-1.057476000
C	-3.802946000	-3.068349000	-1.824638000
C	-4.077916000	-4.386013000	-1.433960000
C	-4.976958000	-5.166666000	-2.155989000
H	-5.185028000	-6.181113000	-1.834964000
C	-5.609326000	-4.646305000	-3.282724000
H	-6.306149000	-5.256026000	-3.846635000
C	-5.344732000	-3.336598000	-3.679657000
H	-5.829904000	-2.926013000	-4.557988000
C	-4.456590000	-2.550355000	-2.952247000
C	1.635140000	-2.397717000	0.940546000
C	1.634480000	2.398020000	-0.940695000
C	2.419701000	-1.151526000	0.415585000
C	1.741520000	0.000155000	-0.000087000
H	0.664042000	-0.000037000	-0.000177000
C	2.419362000	1.152077000	-0.415639000
C	3.818016000	1.129998000	-0.443495000
C	4.487743000	0.000658000	0.000170000
C	3.818343000	-1.128928000	0.443711000
			Cl
			6.254902000
			0.000986000
			0.000354000

(3e) B3LYP/BS-I energy = -2399.61405162 a.u.			
N	0.274442000	2.342972000	-0.055290000
H	0.271403000	1.331234000	-0.155057000
N	2.003871000	0.179593000	0.089554000
N	-1.936851000	0.566636000	-0.017949000
C	1.298605000	3.023922000	0.540045000
C	0.941012000	4.390950000	0.539928000
H	1.530944000	5.189682000	0.958045000
C	-0.290706000	4.501738000	-0.094841000
H	-0.859194000	5.402114000	-0.260955000
C	-0.710658000	3.199203000	-0.446297000
C	2.806438000	1.067413000	0.818630000
C	4.058182000	0.416846000	1.154735000
H	4.878322000	0.860727000	1.696999000
C	3.999038000	-0.825153000	0.609728000
H	4.772886000	-1.573246000	0.622503000
C	2.695634000	-0.929694000	-0.048522000
C	-2.491678000	1.526346000	-0.874608000
C	-3.723386000	1.007204000	-1.443279000
H	-4.355017000	1.506029000	-2.161177000
C	-3.903989000	-0.222318000	-0.897616000
H	-4.733506000	-0.886835000	-1.068899000
C	-2.766121000	-0.450689000	-0.002402000
C	2.493438000	2.395614000	1.023609000
C	3.458723000	3.262913000	1.765842000
C	3.627538000	3.105734000	3.146265000
C	4.527342000	3.908309000	3.844100000
H	4.645056000	3.777633000	4.913949000
C	4.208291000	4.238893000	1.098064000
C	5.111898000	5.035682000	1.796560000
H	5.693804000	5.780366000	1.265053000
C	5.272285000	4.874019000	3.171381000
H	5.974755000	5.496258000	3.714211000
C	-1.963913000	2.791898000	-1.029266000
C	-2.715242000	3.836976000	-1.776434000
C	-4.038485000	4.158816000	-1.442032000
C	-4.729604000	5.141496000	-2.145916000
H	-5.748833000	5.384480000	-1.867355000
C	-4.113145000	5.814100000	-3.198418000
H	-4.652902000	6.576918000	-3.748123000
C	-2.796842000	5.505631000	-3.538158000
H	-2.311517000	6.022939000	-4.358128000
C	-2.100182000	4.533388000	-2.827910000
C	-2.565036000	-1.646996000	0.956545000
C	2.206836000	-2.102499000	-0.930466000
C	-1.377833000	-2.547641000	0.487055000
C	-0.178302000	-1.981753000	0.040826000
H	-0.096124000	-0.908096000	-0.004820000
C	0.917645000	-2.765653000	-0.344660000
C	0.782609000	-4.157252000	-0.292762000
H	1.583939000	-4.801568000	-0.623782000
C	-0.387612000	-4.734395000	0.187761000
H	-0.468023000	-5.814564000	0.246349000
C	-1.455919000	-3.941940000	0.586922000
H	-2.348816000	-4.416678000	0.968301000
C	3.346805000	-3.154751000	-1.015081000
C	3.982294000	-3.488296000	-2.212351000
C	3.769129000	-3.814718000	0.151289000

## APPENDIX -III

---

**Table A1.** Xyz-Coordinates of optimized geometry of compound 2 viz., free base *m*-BPDM,  
R"=Ph

N	2.088903000	-1.030720000	-0.130280000	H	7.964015000	-1.698071000	2.274973000
N	2.047281000	1.626698000	0.102154000	C	8.141832000	0.435510000	2.123920000
N	-1.001179000	1.467733000	0.322658000	H	0.349126000	8.478876000	-2.513584000
C	-0.997398000	-3.552769000	1.342154000	H	9.152881000	0.458184000	2.473048000
H	-0.459479000	-4.472646000	1.447267000	C	-4.427926000	-0.087815000	-0.003473000
C	-2.043791000	-3.243855000	2.219181000	C	-5.636764000	-0.520293000	0.556245000
H	-2.308936000	-3.927406000	2.998193000	C	-4.328553000	0.114514000	-1.387263000
C	-2.743672000	-2.036876000	2.075677000	C	-6.747416000	-0.749588000	-0.266774000
H	-3.537008000	-1.797607000	2.752670000	H	-5.711845000	-0.675189000	1.612307000
C	-2.409477000	-1.142650000	1.045918000	C	-5.439436000	-0.114792000	-2.210352000
C	-1.369414000	-1.452104000	0.172883000	H	-3.404789000	0.444312000	-1.815512000
H	-1.112127000	-0.775314000	-0.615178000	C	-6.649216000	-0.546336000	-1.650015000
C	-0.657967000	-2.649307000	0.329251000	H	-7.670765000	-1.079696000	0.160916000
C	-3.208220000	0.166688000	0.900490000	H	-5.363988000	0.039891000	-3.266379000
C	-2.358507000	1.299991000	0.266950000	H	-7.498146000	-0.720361000	-2.278332000
C	-3.008487000	2.444389000	-0.535593000	C	-3.676213000	0.612584000	2.298270000
H	-4.050577000	2.536828000	-0.760344000	C	-4.880396000	1.315433000	2.440502000
C	-2.053585000	3.304154000	-0.898005000	C	-2.900476000	0.316253000	3.427468000
H	-2.191520000	4.207245000	-1.454954000	C	-5.308975000	1.721806000	3.711436000
C	-0.728980000	2.761382000	-0.368213000	H	-5.472503000	1.541551000	1.578265000
C	0.498067000	3.443155000	-0.534995000	C	-3.329162000	0.723236000	4.698272000
C	1.754690000	2.903334000	-0.208272000	H	-1.980878000	-0.220760000	3.319774000
C	2.940200000	3.649202000	-0.158150000	C	-4.533623000	1.425420000	4.840355000
H	3.042583000	4.693527000	-0.366651000	H	-6.228171000	2.258262000	3.819835000
C	3.956263000	2.780851000	0.217026000	H	-2.736843000	0.497762000	5.560188000
H	4.986446000	3.028951000	0.367181000	H	-4.861342000	1.735166000	5.810694000
C	3.373445000	1.521235000	0.355409000	C	0.207481000	-2.263043000	-1.983099000
C	4.040667000	0.340150000	0.700804000	C	-1.116053000	-2.114723000	-2.419134000
C	3.355658000	-0.865801000	0.567985000	C	1.263674000	-1.801669000	-2.780530000
C	3.747521000	-2.235610000	1.086435000	C	-1.383685000	-1.501982000	-3.650598000
H	4.629287000	-2.489733000	1.637022000	H	-1.922188000	-2.469294000	-1.811446000
C	2.751379000	-3.067966000	0.713722000	C	0.995934000	-1.189437000	-4.012392000
H	2.704496000	-4.114264000	0.933765000	H	2.274585000	-1.916766000	-2.449316000
C	1.776809000	-2.338679000	-0.020549000	C	-0.327892000	-1.037920000	-4.446446000
C	0.500949000	-2.932938000	-0.627294000	H	-2.394223000	-1.388553000	-3.982866000
C	0.456228000	4.873312000	-1.103894000	H	1.802222000	-0.837559000	-4.621592000
C	1.647437000	5.587352000	-1.291351000	H	-0.532514000	-0.567795000	-5.385524000
H	2.586271000	5.136459000	-1.043908000	C	0.674896000	-4.449132000	-0.835150000
C	-0.772534000	5.460756000	-1.433319000	C	1.943195000	-4.980599000	-1.106895000
H	-1.681455000	4.913254000	-1.294373000	C	-0.436616000	-5.297533000	-0.750163000
C	1.608664000	6.891975000	-1.802589000	C	2.099417000	-6.361094000	-1.291327000
H	2.517663000	7.437956000	-1.945495000	H	2.792121000	-4.332913000	-1.173288000
C	-0.811248000	6.765182000	-1.943707000	C	-0.280806000	-6.677634000	-0.933989000
H	-1.749619000	7.214371000	-2.193785000	H	-1.404428000	-4.891094000	-0.544252000
C	0.379013000	7.481566000	-2.126500000	C	0.987327000	-7.209695000	-1.203442000
C	5.493735000	0.373916000	1.208179000	H	3.067214000	-6.767383000	-1.499037000
C	6.167086000	1.597580000	1.321840000	H	-1.130203000	-7.325085000	-0.868386000
H	5.670210000	2.508090000	1.058969000	H	1.106774000	-8.263816000	-1.341866000
C	6.143390000	-0.818368000	1.554322000	H	1.389214000	0.874127000	0.139443000
H	5.629052000	-1.752193000	1.468955000				
C	7.491959000	1.628592000	1.778486000				
H	8.007152000	2.562917000	1.863219000				
C	7.467440000	-0.787680000	2.011568000				

**Table A2.** Xyz-Coordinates of optimized geometry of ZnCl-*m*-BPDM (compound 3)

Zn	0.615804000	-0.150276000	-0.256954000	C	7.129936000	1.172508000	-2.283409000
Cl	1.013569000	-0.289136000	-3.399207000	H	7.630919000	0.681683000	-3.114410000
N	1.365430000	1.745882000	-0.103366000	C	7.125857000	2.814404000	-0.487961000
N	2.384903000	-0.988834000	0.112051000	H	7.630475000	3.587822000	0.086488000
N	-0.458280000	-1.841648000	0.164462000	C	7.789172000	2.185019000	-1.559483000
C	-1.575856000	2.588438000	-1.995226000	H	3.128582000	-7.775053000	3.387670000
H	-1.225294000	3.569691000	-2.299714000	H	8.803046000	2.476423000	-1.823499000
C	-2.121612000	1.717008000	-2.946614000	C	-4.118622000	-1.075295000	0.108598000
H	-2.220253000	2.041459000	-3.979441000	C	-5.237725000	-0.474360000	-0.516820000
C	-2.516529000	0.412815000	-2.589769000	C	-4.158340000	-1.256070000	1.505490000
H	-2.920024000	-0.247973000	-3.348005000	C	-6.364291000	-0.087364000	0.224370000
C	-2.368752000	-0.030575000	-1.264142000	H	-5.224308000	-0.299153000	-1.589527000
C	-1.859481000	0.877846000	-0.305292000	C	-5.286317000	-0.864708000	2.254549000
H	-1.853089000	0.579384000	0.737768000	H	-3.312264000	-1.699004000	2.020239000
C	-1.462734000	2.183437000	-0.645817000	C	-6.396881000	-0.283441000	1.620247000
C	-2.863059000	-1.408335000	-0.759215000	H	-7.211458000	0.369172000	-0.282441000
C	-1.791081000	-2.167609000	0.046273000	H	-5.290057000	-1.015722000	3.331687000
C	-2.038960000	-3.451967000	0.617935000	H	-7.267879000	0.016604000	2.198123000
H	-2.992890000	-3.958870000	0.623167000	C	-3.197930000	-2.391301000	-1.928492000
C	-0.821894000	-3.941186000	1.078171000	C	-4.408707000	-3.110010000	-1.997895000
H	-0.639065000	-4.902034000	1.535264000	C	-2.202391000	-2.666730000	-2.896299000
C	0.184028000	-2.952065000	0.795563000	C	-4.630886000	-4.057939000	-3.016548000
C	1.579026000	-3.146991000	1.013302000	H	-5.185124000	-2.943877000	-1.258821000
C	2.615440000	-2.239648000	0.657476000	C	-2.422382000	-3.606481000	-3.914531000
C	4.047600000	-2.417608000	0.804241000	H	-1.245452000	-2.155765000	-2.850955000
H	4.533131000	-3.280119000	1.236681000	C	-3.642693000	-4.308628000	-3.983497000
C	4.656518000	-1.273448000	0.310913000	H	-5.573813000	-4.599446000	-3.046781000
H	5.714222000	-1.054934000	0.283585000	H	-1.640898000	-3.794155000	-4.646825000
C	3.600046000	-0.367355000	-0.102114000	H	-3.813502000	-5.040461000	-4.769516000
C	3.751784000	0.993791000	-0.511881000	C	-0.946884000	2.602724000	1.850843000
C	2.712664000	1.975170000	-0.473703000	C	-2.264498000	2.560742000	2.366307000
C	2.868016000	3.377919000	-0.728445000	C	0.117794000	2.283163000	2.718079000
H	3.770826000	3.858504000	-1.073840000	C	-2.511179000	2.199949000	3.699261000
C	1.643179000	4.000064000	-0.446341000	H	-3.102801000	2.819278000	1.724092000
H	1.418121000	5.051215000	-0.530545000	C	-0.126234000	1.928479000	4.060680000
C	0.743044000	2.978155000	-0.045221000	H	1.138986000	2.302889000	2.354066000
C	-0.730793000	3.088407000	0.380521000	C	-1.439361000	1.882577000	4.558313000
C	2.000163000	-4.432377000	1.665686000	H	-3.534052000	2.171838000	4.067414000
C	2.755641000	-5.391890000	0.953138000	H	0.712264000	1.688596000	4.710614000
H	3.012070000	-5.202834000	-0.086160000	H	-1.626573000	1.608613000	5.593932000
C	1.658897000	-4.702345000	3.011369000	C	-1.232649000	4.563038000	0.379361000
H	1.086689000	-3.967667000	3.572365000	C	-0.527903000	5.526006000	1.140752000
C	3.155826000	-6.592441000	1.568361000	C	-2.444323000	4.961457000	-0.222964000
H	3.727423000	-7.323438000	1.001275000	C	-0.991731000	6.845051000	1.258547000
C	2.067605000	-5.897383000	3.630772000	H	0.376828000	5.235931000	1.667088000
H	1.804068000	-6.083400000	4.669370000	C	-2.916412000	6.283492000	-0.104789000
C	2.816053000	-6.849071000	2.910788000	H	-3.038297000	4.246030000	-0.781429000
C	5.138292000	1.428137000	-0.872543000	C	-2.189895000	7.236269000	0.628797000
C	5.821170000	0.792235000	-1.937352000	H	-0.426674000	7.562204000	1.849536000
H	5.313335000	0.016185000	-2.503645000	H	-3.853796000	6.561049000	-0.581652000
C	5.812325000	2.442821000	-0.150681000	H	-2.553663000	8.256888000	0.720498000
H	5.314512000	2.919268000	0.689430000				

**Table A3.** Xyz-Coordinates of optimized geometry of CdCl-*m*-BPDM (compound 4)

Cl	-0.470190000	-1.860379000	-1.284123000	C	7.393069000	1.781234000	1.815315000
N	2.084622000	-0.990208000	-0.189130000	H	7.870416000	2.727879000	1.967948000
N	1.970733000	1.722280000	-0.039364000	C	7.450431000	-0.644167000	1.896429000
N	-1.062208000	1.548587000	0.222426000	H	7.976676000	-1.555491000	2.109734000
C	-0.827362000	-3.246149000	1.849427000	C	8.077422000	0.589670000	2.097329000
H	-0.265720000	-4.132288000	2.047952000	H	0.202054000	8.653489000	-2.456018000
C	-1.806742000	-2.812126000	2.762628000	H	9.083135000	0.630473000	2.465915000
H	-1.978761000	-3.364770000	3.660763000	C	-4.406199000	-0.170953000	0.143284000
C	-2.566017000	-1.658832000	2.496406000	C	-5.581622000	-0.570590000	0.781086000
H	-3.310283000	-1.332680000	3.193712000	C	-4.313348000	-0.192423000	-1.252986000
C	-2.345055000	-0.936745000	1.317561000	C	-6.668019000	-1.018811000	0.019793000
C	-1.351406000	-1.336139000	0.441605000	H	-5.651121000	-0.533452000	1.847556000
H	-1.165358000	-0.745281000	-0.434471000	C	-5.397334000	-0.644324000	-2.018202000
C	-0.589630000	-2.508101000	0.681815000	H	-3.414920000	0.136240000	-1.736359000
C	-3.208392000	0.291850000	0.979284000	C	-6.572954000	-1.059883000	-1.380223000
C	-2.407378000	1.348906000	0.181441000	H	-7.564195000	-1.330599000	0.507239000
C	-3.077114000	2.372522000	-0.755867000	H	-5.322912000	-0.673966000	-3.085883000
H	-4.106673000	2.387510000	-1.026343000	H	-7.400575000	-1.411936000	-1.960937000
C	-2.150871000	3.248265000	-1.154338000	C	-3.702949000	0.944878000	2.285509000
H	-2.302020000	4.096213000	-1.785075000	C	-4.939798000	1.608269000	2.309584000
C	-0.833494000	2.813297000	-0.523826000	C	-2.921454000	0.881077000	3.448929000
C	0.369516000	3.544049000	-0.614793000	C	-5.399989000	2.190883000	3.496607000
C	1.626419000	3.027416000	-0.200452000	H	-5.533658000	1.671237000	1.416061000
C	2.752612000	3.810781000	0.097216000	C	-3.387565000	1.464137000	4.634336000
H	2.819407000	4.872806000	0.047336000	H	-1.970524000	0.388926000	3.430439000
C	3.769535000	2.953654000	0.471449000	C	-4.626653000	2.120166000	4.662403000
H	4.752331000	3.239641000	0.778324000	H	-6.343694000	2.692548000	3.510664000
C	3.268210000	1.647861000	0.368628000	H	-2.795359000	1.410391000	5.523395000
C	3.986456000	0.455628000	0.637358000	H	-4.982574000	2.567256000	5.572867000
C	3.361959000	-0.769808000	0.463803000	C	0.042079000	-2.387373000	-1.748289000
C	3.853696000	-2.120023000	0.938049000	C	-1.319731000	-2.293495000	-2.046116000
H	4.784063000	-2.337368000	1.412843000	C	0.999389000	-1.996136000	-2.691864000
C	2.865273000	-2.983824000	0.660171000	C	-1.732891000	-1.814092000	-3.292256000
H	2.868592000	-4.023747000	0.889803000	H	-2.044970000	-2.591431000	-1.319771000
C	1.809651000	-2.294219000	0.020437000	C	0.591653000	-1.512521000	-3.942679000
C	0.478939000	-2.919621000	-0.373397000	H	2.040559000	-2.063653000	-2.455663000
C	0.308349000	4.987902000	-1.160039000	C	-0.775633000	-1.423102000	-4.237214000
C	1.482192000	5.751680000	-1.230143000	H	-2.776765000	-1.746816000	-3.519786000
H	2.415155000	5.323757000	-0.931957000	H	1.322583000	-1.208752000	-4.669486000
C	-0.911234000	5.556429000	-1.582664000	H	-1.089759000	-1.053794000	-5.185508000
H	-1.811261000	4.981314000	-1.551171000	C	0.626391000	-4.450881000	-0.441957000
C	1.442107000	7.078411000	-1.691288000	C	1.856568000	-5.018980000	-0.791207000
H	2.341390000	7.652778000	-1.725676000	C	-0.471370000	-5.273256000	-0.151367000
C	-0.946752000	6.883531000	-2.047051000	C	1.990173000	-6.411494000	-0.862197000
H	-1.879118000	7.317135000	-2.359999000	H	2.692841000	-4.387344000	-1.006384000
C	0.230009000	7.643875000	-2.101956000	C	-0.337913000	-6.667384000	-0.216949000
C	5.441524000	0.501201000	1.142535000	H	-1.411773000	-4.837845000	0.118875000
C	6.080090000	1.735242000	1.329266000	C	0.893517000	-7.235055000	-0.573693000
H	5.566279000	2.642428000	1.095186000	H	2.930423000	-6.846418000	-1.136593000
C	6.134532000	-0.688862000	1.413434000	H	-1.172458000	-7.296101000	0.005293000
H	5.660938000	-1.631201000	1.246469000	H	0.996750000	-8.298484000	-0.625350000
				Cd	0.737140000	0.054845000	-0.470083000

**Table A4.** Xyz-Coordinates of optimized geometry of free base *m*-BPDM R"=H

N	-0.091613000	-0.880787000	-0.053972000	C	4.118756000	-4.192690000	-1.733424000
H	-0.031041000	0.123183000	-0.196057000	H	4.009916000	-4.758731000	-2.651693000
N	-1.733652000	1.261663000	-0.785320000	C	3.195780000	-3.199624000	-1.422416000
N	1.941854000	0.889303000	0.911655000	C	2.159658000	3.203564000	1.748383000
C	-1.284948000	-1.544371000	0.048237000	C	-1.543869000	3.568570000	-1.686365000
C	-0.980573000	-2.906402000	0.262048000	C	1.332194000	4.064191000	0.800467000
H	-1.706293000	-3.690241000	0.403660000	C	0.300123000	3.481377000	0.063529000
C	0.403836000	-3.035547000	0.251530000	H	0.119319000	2.421895000	0.163693000
H	0.974047000	-3.938831000	0.394414000	C	-0.491910000	4.230576000	-0.802729000
C	0.955540000	-1.748196000	0.072708000	C	-0.253829000	5.604946000	-0.911245000
C	-2.771737000	0.401800000	-0.398800000	H	-0.862922000	6.208887000	-1.576659000
C	-4.043344000	1.100549000	-0.505670000	C	0.767971000	6.200794000	-0.177390000
H	-5.013262000	0.684806000	-0.281377000	H	0.946988000	7.266722000	-0.269152000
C	-3.748394000	2.353053000	-0.941845000	C	1.565225000	5.434143000	0.671519000
H	-4.434560000	3.162776000	-1.145845000	H	2.364454000	5.904678000	1.235369000
C	-2.300951000	2.400991000	-1.112559000	H	2.989395000	3.795213000	2.143337000
C	2.787348000	-0.100203000	0.392390000	H	1.532096000	2.917620000	2.599641000
C	4.141637000	0.428851000	0.282947000	H	-1.040038000	3.213379000	-2.595039000
H	4.996910000	-0.094921000	-0.114078000	H	-2.262241000	4.325669000	-2.010851000
C	4.082786000	1.707901000	0.736749000	H	-4.053793000	-0.933244000	2.224092000
H	4.888820000	2.425174000	0.801797000	H	-3.728158000	-2.803935000	-1.619293000
C	2.696858000	1.939674000	1.130868000	H	4.494527000	-2.161779000	1.535466000
C	-2.572913000	-0.914744000	-0.044387000	H	2.373903000	-2.993218000	-2.097602000
C	-3.758708000	-1.773197000	0.268106000				
C	-4.414538000	-1.652544000	1.497936000				
C	-5.517940000	-2.450898000	1.791551000				
H	-6.016016000	-2.347153000	2.749009000				
C	-4.226674000	-2.709020000	-0.661326000				
C	-5.331730000	-3.504348000	-0.367175000				
H	-5.688497000	-4.219893000	-1.099566000				
C	-5.979184000	-3.378373000	0.860216000				
H	-6.838687000	-3.998427000	1.088486000				
C	2.349337000	-1.369201000	0.074642000				
C	3.328864000	-2.440619000	-0.249537000				
C	4.398794000	-2.721382000	0.613052000				
C	5.314086000	-3.724589000	0.306133000				
H	6.128936000	-3.935189000	0.989619000				
C	5.180024000	-4.459527000	-0.869541000				
H	5.894640000	-5.238705000	-1.109540000				

**Table A5.** Xyz-Coordinates of optimized geometry of free base *m*-BPDM R"=CH<sub>3</sub>

N	0.145528000	-1.326304000	0.070732000	H	-3.709418000	-5.210748000	2.881634000
H	0.094693000	-0.332945000	0.278288000	C	-3.001371000	-3.647296000	1.594078000
N	1.704011000	0.802130000	0.828666000	C	-2.060148000	2.702139000	-1.826350000
N	-1.883871000	0.402290000	-0.904709000	C	1.388187000	3.039509000	1.879769000
C	1.340146000	-1.960087000	-0.128436000	C	-1.079713000	2.233452000	-2.930873000
C	1.043449000	-3.315689000	-0.392444000	H	-0.656949000	3.101849000	-3.442987000
H	1.769271000	-4.080231000	-0.616258000	H	-1.600752000	1.611768000	-3.664538000
C	-0.338308000	-3.467597000	-0.310942000	H	-0.268390000	1.643521000	-2.507929000
H	-0.903737000	-4.371709000	-0.468995000	C	-3.226895000	3.451850000	-2.499804000
C	-0.895236000	-2.198047000	-0.042904000	H	-2.852647000	4.248039000	-3.147025000
C	2.758147000	0.029215000	0.321566000	H	-3.907151000	3.901016000	-1.772614000
C	3.984356000	0.806532000	0.372764000	H	-3.801736000	2.763867000	-3.124300000
H	4.960971000	0.470046000	0.061076000	C	0.488659000	2.360370000	2.946580000
C	3.646239000	2.016695000	0.891235000	H	-0.116930000	3.115121000	3.455112000
H	4.305576000	2.850041000	1.078035000	H	1.101955000	1.843323000	3.690281000
C	2.214420000	1.961150000	1.180153000	H	-0.176703000	1.630500000	2.488216000
C	-2.711759000	-0.533321000	-0.270361000	C	2.334616000	4.014922000	2.607044000
C	-4.020484000	0.063485000	-0.040652000	H	1.767279000	4.711788000	3.227267000
H	-4.852775000	-0.403929000	0.462304000	H	2.942336000	4.598755000	1.911950000
C	-3.951730000	1.326966000	-0.535017000	H	3.006971000	3.462645000	3.267715000
H	-4.733643000	2.071336000	-0.527966000	C	-1.276525000	3.606607000	-0.845129000
C	-2.604169000	1.482725000	-1.087146000	C	-0.337080000	3.024699000	0.009489000
C	2.606246000	-1.280983000	-0.084083000	H	-0.224357000	1.951479000	-0.004917000
C	3.805865000	-2.063701000	-0.511378000	C	0.461044000	3.771971000	0.878975000
C	4.436205000	-1.790286000	-1.730602000	C	0.315047000	5.163255000	0.868576000
C	5.554246000	-2.520518000	-2.127578000	H	0.910904000	5.791027000	1.517849000
H	6.030410000	-2.299169000	-3.076186000	C	-0.615384000	5.763605000	0.024082000
C	4.315209000	-3.084443000	0.300310000	H	-0.722581000	6.843271000	0.028901000
C	5.435324000	-3.810539000	-0.096591000	C	-1.412639000	4.998213000	-0.823002000
H	5.824247000	-4.592001000	0.546625000	H	-2.127494000	5.498079000	-1.463693000
C	6.057112000	-3.531453000	-1.311970000	H	-2.095892000	-3.484822000	2.166397000
C	-2.285118000	-1.808062000	0.045201000	H	-4.620453000	-2.495031000	-1.156489000
C	-3.252507000	-2.852942000	0.463715000	H	3.838489000	-3.297858000	1.250197000
C	-4.431686000	-3.078022000	-0.263525000	H	4.041618000	-1.008257000	-2.368929000
C	-5.336485000	-4.057565000	0.135323000	H	-5.788730000	-5.588451000	1.579636000
H	-6.237089000	-4.224452000	-0.444802000	H	6.928163000	-4.098123000	-1.621010000
C	-5.082460000	-4.826938000	1.268611000				
C	-3.912342000	-4.617628000	1.997040000				

**Table A6.** Xyz-Coordinates of optimized geometry of syn conformer of Zn(II) *m*-BPDM, R"=H

Zn	-0.000029000	1.005914000	0.671233000	C	2.500675000	3.726387000	0.279551000
Cl	0.000102000	1.575729000	2.959972000	C	-3.531516000	-2.341409000	-0.206064000
N	2.062658000	1.217187000	0.101061000	C	-4.387325000	-2.383763000	-1.329934000
N	0.000066000	-0.946021000	0.071006000	H	-4.273048000	-1.642787000	-2.116946000
N	-2.062768000	1.216940000	0.101204000	C	-3.674259000	-3.323805000	0.800285000
C	1.221467000	4.416062000	-1.829628000	H	-3.023076000	-3.296600000	1.670173000
H	2.162163000	4.534913000	-2.363668000	C	-5.366228000	-3.387717000	-1.445628000
C	-0.000357000	4.612652000	-2.501083000	H	-6.010216000	-3.413749000	-2.321314000
H	-0.000374000	4.902517000	-3.549413000	C	-4.664338000	-4.316868000	0.692545000
C	-1.222168000	4.415991000	-1.829611000	H	-4.772520000	-5.056329000	1.482177000
H	-2.162876000	4.534816000	-2.363636000	C	-5.511592000	-4.354800000	-0.432429000
C	-1.225976000	4.055320000	-0.467390000	C	3.531817000	-2.341007000	-0.206103000
C	-0.000321000	3.913661000	0.206018000	C	4.387549000	-2.383491000	-1.330025000
H	-0.000309000	3.689274000	1.271542000	H	4.273144000	-1.642680000	-2.117172000
C	1.225310000	4.055413000	-0.467393000	C	3.674696000	-3.323231000	0.800400000
C	-2.501277000	3.726121000	0.279576000	H	3.023571000	-3.295925000	1.670326000
C	-2.906677000	2.273260000	0.168884000	C	5.366519000	-3.387393000	-1.445615000
C	-4.289619000	1.847453000	0.162090000	H	6.010442000	-3.413533000	-2.321345000
H	-5.143447000	2.508943000	0.218971000	C	4.664849000	-4.316231000	0.692766000
C	-4.284025000	0.471105000	0.085364000	H	4.773144000	-5.055548000	1.482517000
H	-5.136436000	-0.191341000	0.079053000	C	5.512031000	-4.354288000	-0.432259000
C	-2.892992000	0.047950000	0.029067000	H	-6.272007000	-5.127257000	-0.518387000
C	-2.473995000	-1.280913000	-0.082329000	H	6.272494000	-5.126704000	-0.518142000
C	-1.113946000	-1.743382000	-0.124075000	H	-2.376468000	3.962575000	1.346963000
C	-0.693827000	-3.085180000	-0.447036000	H	-3.340499000	4.333547000	-0.080976000
H	-1.348595000	-3.912954000	-0.674141000	H	2.375785000	3.962654000	1.346971000
C	0.694252000	-3.085088000	-0.447013000	H	3.339742000	4.334088000	-0.080901000
H	1.349135000	-3.912786000	-0.674058000				
C	1.114191000	-1.743226000	-0.124064000				
C	2.474208000	-1.280593000	-0.082445000				
C	2.893041000	0.048329000	0.028810000				
C	4.284018000	0.471700000	0.085064000				
H	5.136531000	-0.190611000	0.078725000				
C	4.289409000	1.848048000	0.161791000				
H	5.143146000	2.509662000	0.218584000				
C	2.906409000	2.273647000	0.168696000				

**Table A7.** Xyz-Coordinates of optimized geometry of anti-conformer of Zn(II) *m*-BPDM,  
R"=H

Zn	-0.151724000	1.020451000	0.229132000	C	3.904223000	-1.829343000	-0.194916000
Cl	-0.720873000	1.485312000	2.449219000	C	4.857891000	-1.767091000	0.846675000
N	-2.013050000	0.759112000	-0.840040000	H	4.700511000	-1.080213000	1.674144000
N	0.204256000	-0.973556000	-0.092422000	C	4.107056000	-2.744050000	-1.253543000
N	1.898969000	1.472341000	-0.125891000	H	3.381585000	-2.797524000	-2.061199000
C	-2.281145000	4.591268000	0.123407000	C	5.989577000	-2.602661000	0.830483000
H	-3.361789000	4.705928000	0.173194000	H	6.707682000	-2.551660000	1.645224000
C	-1.462014000	5.211615000	1.081048000	C	5.247537000	-3.566876000	-1.278097000
H	-1.907619000	5.815854000	1.867032000	H	5.396909000	-4.255242000	-2.106390000
C	-0.070527000	5.018766000	1.052490000	C	6.191282000	-3.501903000	-0.234194000
H	0.552269000	5.462897000	1.825540000	C	-3.107460000	-2.825133000	0.098227000
C	0.519985000	4.228246000	0.048290000	C	-3.192826000	-3.389655000	1.391841000
C	-0.307566000	3.637095000	-0.926989000	H	-2.603640000	-2.964086000	2.199992000
H	0.141091000	3.073514000	-1.744271000	C	-3.881751000	-3.381700000	-0.944734000
C	-1.706351000	3.791786000	-0.883607000	H	-3.804579000	-2.968962000	-1.947337000
C	2.020390000	4.039333000	0.008454000	C	-4.051597000	-4.475199000	1.640191000
C	2.568170000	2.646552000	-0.203570000	H	-4.119365000	-4.888134000	2.643603000
C	3.980750000	2.430328000	-0.434152000	C	-4.727949000	-4.478574000	-0.698814000
H	4.718636000	3.212841000	-0.551830000	H	-5.309945000	-4.903043000	-1.513353000
C	4.178660000	1.065913000	-0.461090000	C	-4.819929000	-5.025760000	0.595468000
H	5.107867000	0.539279000	-0.619302000	H	7.068830000	-4.143781000	-0.249583000
C	2.885646000	0.435664000	-0.252434000	H	-5.478343000	-5.869678000	0.786937000
C	2.686629000	-0.949117000	-0.166435000	H	2.456200000	4.677809000	-0.777430000
C	1.423483000	-1.619382000	-0.049813000	H	2.450933000	4.407948000	0.951665000
C	1.207244000	-3.041109000	0.099968000	H	-2.053808000	2.904604000	-2.817486000
H	1.978182000	-3.793229000	0.175640000	H	-3.510164000	3.544587000	-2.055313000
C	-0.166874000	-3.238265000	0.132129000				
H	-0.692830000	-4.177619000	0.217465000				
C	-0.779871000	-1.936520000	-0.002960000				
C	-2.185328000	-1.666095000	-0.143686000				
C	-2.735753000	-0.443222000	-0.544336000				
C	-4.143425000	-0.209332000	-0.827171000				
H	-4.938730000	-0.920401000	-0.661179000				
C	-4.250212000	1.069453000	-1.338753000				
H	-5.142804000	1.580092000	-1.673852000				
C	-2.917899000	1.632670000	-1.336285000				
C	-2.573671000	3.012147000	-1.853775000				

**Table A8.** Xyz-Coordinates of optimized geometry of syn conformer of Cd(II) *m*-BPDM, R"=H

Cd	0.000026000	-1.114864000	0.770678000	H	4.724723000	5.132524000	1.542078000
Cl	0.000287000	-1.922903000	3.146761000	C	5.470977000	4.488897000	-0.390061000
N	2.152703000	-1.153173000	0.008769000	H	6.217503000	5.276392000	-0.459718000
N	0.000013000	1.016558000	0.092392000	C	5.339082000	3.543785000	-1.425572000
N	-2.152713000	-1.153174000	0.008830000	H	5.979308000	3.602242000	-2.302454000
C	-1.221448000	-4.050964000	-2.086092000	C	4.378612000	2.519989000	-1.330977000
H	-2.160743000	-4.079240000	-2.634786000	H	4.274505000	1.796527000	-2.135389000
C	-0.000165000	-4.152334000	-2.777626000	C	-3.527034000	2.435649000	-0.206178000
H	-0.000251000	-4.284904000	-3.857131000	C	-4.378536000	2.519981000	-1.331068000
C	1.221223000	-4.050965000	-2.086281000	H	-4.274289000	1.796591000	-2.135526000
H	2.160438000	-4.079247000	-2.635111000	C	-5.339045000	3.543733000	-1.425702000
C	1.231812000	-3.893940000	-0.685334000	H	-5.979165000	3.602227000	-2.302659000
C	2.531229000	-3.651281000	0.070209000	C	-5.471118000	4.488759000	-0.390135000
C	2.994086000	-2.207030000	0.005260000	H	-6.217678000	5.276218000	-0.459824000
C	4.374044000	-1.767541000	-0.028824000	C	-4.627875000	4.409608000	0.735729000
H	5.239159000	-2.416920000	-0.029188000	H	-4.725142000	5.132267000	1.542151000
C	4.351638000	-0.385133000	-0.044743000	C	-3.655241000	3.397545000	0.821995000
H	5.200393000	0.282357000	-0.050662000	H	-3.005792000	3.339976000	1.691636000
C	2.952660000	0.028386000	-0.039931000	H	0.000131000	-3.823868000	1.094630000
C	2.490164000	1.351635000	-0.099924000	H	2.402988000	-3.923677000	1.128409000
C	1.118051000	1.805250000	-0.117579000	H	3.337666000	-4.283322000	-0.321958000
C	0.693718000	3.146979000	-0.455163000	H	-2.402681000	-3.923509000	1.128800000
H	1.345989000	3.972656000	-0.697053000	H	-3.337589000	-4.283440000	-0.321350000
C	-0.693745000	3.146969000	-0.455139000				
H	-1.346022000	3.972642000	-0.697016000				
C	-1.118076000	1.805232000	-0.117563000				
C	-2.490178000	1.351617000	-0.099876000				
C	-2.952680000	0.028358000	-0.039860000				
C	-4.351643000	-0.385176000	-0.044704000				
H	-5.200417000	0.282290000	-0.050686000				
C	-4.374031000	-1.767594000	-0.028593000				
H	-5.239147000	-2.416972000	-0.028866000				
C	-2.994082000	-2.207062000	0.005495000				
C	-2.531135000	-3.651279000	0.070585000				
C	-1.231826000	-3.893942000	-0.685146000				
C	0.000047000	-3.867732000	0.005129000				
C	3.526991000	2.435694000	-0.206177000				
C	3.655012000	3.397679000	0.821933000				
H	3.005450000	3.340151000	1.691495000				
C	4.627597000	4.409792000	0.735704000				

**Table A9.** Xyz-Coordinates of optimized geometry of *anti*-conformer of Cd(II) *m*-BPDM,  
R"=H

Cd	-0.000012000	-1.147718000	0.336686000	C	-4.616919000	4.519497000	-0.839293000
Cl	-0.000128000	-1.590452000	2.792912000	H	-4.670020000	5.336266000	-1.555093000
N	-2.131020000	-1.085634000	-0.543897000	C	-5.549688000	4.441145000	0.213752000
N	0.000025000	1.054689000	-0.213345000	H	-6.320905000	5.200512000	0.318559000
N	2.131018000	-1.085704000	-0.543833000	C	-5.475791000	3.374871000	1.130474000
C	1.219387000	-4.741994000	0.618242000	H	-6.186047000	3.309983000	1.951033000
H	2.157876000	-5.025409000	1.088501000	C	-4.482830000	2.388152000	0.989647000
C	-0.000114000	-5.133495000	1.197280000	H	-4.423658000	1.569032000	1.701489000
H	-0.000149000	-5.719909000	2.111757000	C	3.538689000	2.464047000	-0.059667000
C	-1.219570000	-4.741949000	0.618177000	C	4.482938000	2.388042000	0.989618000
H	-2.158094000	-5.025329000	1.088386000	H	4.423773000	1.568920000	1.701456000
C	-1.232958000	-3.960336000	-0.555014000	C	5.475916000	3.374745000	1.130423000
C	-2.542651000	-3.517983000	-1.181070000	H	6.186193000	3.309842000	1.950962000
C	-2.953809000	-2.079529000	-0.934195000	C	5.549804000	4.441023000	0.213705000
C	-4.301822000	-1.591507000	-1.143994000	H	6.321036000	5.200378000	0.318496000
H	-5.141832000	-2.190415000	-1.469889000	C	4.617008000	4.519397000	-0.839314000
C	-4.284280000	-0.241222000	-0.852793000	H	4.670101000	5.336170000	-1.555110000
H	-5.108158000	0.454063000	-0.917164000	C	3.612552000	3.543668000	-0.969331000
C	-2.919071000	0.106445000	-0.480662000	H	2.896349000	3.606650000	-1.784490000
C	-2.477096000	1.408141000	-0.195166000	H	0.000011000	-3.026393000	-2.072135000
C	-1.115569000	1.855558000	-0.044917000	H	-2.497339000	-3.662864000	-2.272821000
C	-0.693408000	3.203979000	0.273382000	H	-3.359557000	-4.161586000	-0.829770000
H	-1.345104000	4.037628000	0.487432000	H	2.497364000	-3.663010000	-2.272686000
C	0.693515000	3.203964000	0.273368000	H	3.359477000	-4.161687000	-0.829559000
H	1.345235000	4.037598000	0.487409000				
C	1.115641000	1.855527000	-0.044910000				
C	2.477155000	1.408071000	-0.195148000				
C	2.919097000	0.106360000	-0.480622000				
C	4.284300000	-0.241347000	-0.852735000				
H	5.108195000	0.453917000	-0.917117000				
C	4.301811000	-1.591638000	-1.143913000				
H	5.141808000	-2.190571000	-1.469793000				
C	2.953787000	-2.079626000	-0.934103000				
C	2.542610000	-3.518082000	-1.180939000				
C	1.232867000	-3.960381000	-0.554948000				
C	-0.000023000	-3.587401000	-1.137714000				
C	-3.538607000	2.464136000	-0.059662000				
C	-3.612481000	3.543753000	-0.969332000				
H	-2.896301000	3.606719000	-1.784511000				

**Table A10.** Xyz-Coordinates of optimized geometry of *syn* conformer of Zn(II) *m*-BPDM, R"=CH<sub>3</sub>

Zn	-0.000033000	-0.638799000	0.498225000	H	3.423550000	-3.602514000	2.058001000
Cl	-0.000093000	-1.024938000	2.834736000	H	2.090464000	-4.726980000	1.718440000
N	-2.095498000	-0.834452000	-0.014977000	H	1.760626000	-3.017674000	2.122227000
N	0.000133000	1.318215000	-0.105755000	C	-2.437185000	-3.692262000	1.588841000
N	2.095311000	-0.834777000	-0.014578000	H	-1.761621000	-3.017000000	2.122207000
C	-1.219778000	-3.665203000	-2.103453000	H	-2.091335000	-4.726356000	1.718525000
H	-2.149236000	-3.685111000	-2.664414000	H	-3.424505000	-3.601907000	2.057806000
C	-0.000337000	-3.736279000	-2.796165000	C	-3.661601000	-4.272799000	-0.523536000
H	-0.000330000	-3.825639000	-3.880173000	H	-4.569977000	-4.229871000	0.087942000
C	1.219099000	-3.665385000	-2.103426000	H	-3.308919000	-5.310804000	-0.524478000
H	2.148563000	-3.685448000	-2.664370000	H	-3.935933000	-4.004119000	-1.549409000
C	1.232148000	-3.549368000	-0.697043000	C	3.532406000	2.745341000	-0.145327000
C	-0.000352000	-3.507952000	-0.016566000	C	3.741456000	3.532422000	-1.299608000
H	-0.000354000	-3.455331000	1.064249000	H	3.137092000	3.355283000	-2.185762000
C	-1.232846000	-3.549184000	-0.697070000	C	4.327618000	2.980237000	0.998447000
C	2.553425000	-3.353802000	0.067775000	H	4.163502000	2.386034000	1.893750000
C	2.957545000	-1.883442000	-0.047294000	C	4.735967000	4.527491000	-1.314012000
C	4.330065000	-1.427378000	-0.150913000	H	4.894535000	5.117491000	-2.213504000
H	5.201616000	-2.061502000	-0.209742000	C	5.311808000	3.986055000	0.988802000
C	4.296154000	-0.051121000	-0.178296000	H	5.909654000	4.162061000	1.879696000
H	5.132205000	0.626112000	-0.269252000	C	5.522198000	4.760418000	-0.168453000
C	2.901277000	0.349091000	-0.091774000	C	-3.531848000	2.745997000	-0.145537000
C	2.471837000	1.678242000	-0.123225000	C	-3.740511000	3.533475000	-1.299621000
C	1.113706000	2.140480000	-0.136627000	H	-3.136002000	3.356492000	-2.185707000
C	0.694102000	3.520234000	-0.169480000	C	-4.327274000	2.980710000	0.998138000
H	1.348789000	4.378419000	-0.175313000	H	-4.163435000	2.386238000	1.893313000
C	-0.693365000	3.520376000	-0.169585000	C	-4.734847000	4.528715000	-1.313949000
H	-1.347867000	4.378703000	-0.175475000	H	-4.893120000	5.118999000	-2.213306000
C	-1.113258000	2.140704000	-0.136782000	C	-5.311280000	3.986704000	0.988579000
C	-2.471486000	1.678707000	-0.123499000	H	-5.909283000	4.162558000	1.879397000
C	-2.901179000	0.349613000	-0.092120000	C	-5.521289000	4.761443000	-0.168495000
C	-4.296139000	-0.050300000	-0.178804000	H	6.286197000	5.534076000	-0.177588000
H	-5.132032000	0.627113000	-0.269865000	H	-6.285148000	5.535239000	-0.177567000
C	-4.330386000	-1.426547000	-0.151173000				
H	-5.202086000	-2.060471000	-0.209934000				
C	-2.957974000	-1.882920000	-0.047577000				
C	-2.554133000	-3.353339000	0.067673000				
C	3.660798000	-4.273383000	-0.523434000				
H	3.307856000	-5.311302000	-0.524744000				
H	4.569041000	-4.230859000	0.088270000				
H	3.935455000	-4.004492000	-1.549164000				
C	2.436294000	-3.692862000	1.588899000				

**Table A11.** Xyz-Coordinates of optimized geometry of *anti*-conformer of Zn(II) *m*-BPDM, R"=CH<sub>3</sub>.

Zn	-0.086463000	-0.634512000	0.426007000	H	-5.096978000	-3.158829000	-0.596959000
Cl	0.274262000	-1.100897000	2.694602000	H	-4.067246000	-4.572695000	-0.294362000
N	1.733925000	-1.074253000	-0.657521000	H	-3.642010000	-3.425741000	-1.580662000
N	0.290973000	1.337489000	0.029359000	C	0.687879000	-2.800351000	-3.004963000
N	-2.163194000	-0.367818000	0.036121000	H	0.149200000	-1.865023000	-2.824958000
C	0.746007000	-4.563709000	0.451863000	H	-0.011429000	-3.544042000	-3.408329000
H	1.735263000	-5.009785000	0.473221000	H	1.448467000	-2.594510000	-3.767760000
C	-0.132173000	-4.802138000	1.516780000	C	2.234889000	-4.565521000	-2.130544000
H	0.181625000	-5.435202000	2.342891000	H	2.921915000	-4.294246000	-2.941378000
C	-1.395897000	-4.190808000	1.553438000	H	1.582940000	-5.369166000	-2.492436000
H	-2.029568000	-4.353803000	2.416794000	H	2.834372000	-4.963532000	-1.305695000
C	-1.807988000	-3.348129000	0.504623000	C	-2.855304000	3.412530000	-0.405339000
C	-0.922438000	-3.141749000	-0.577263000	C	-3.040852000	4.315576000	0.664835000
H	-1.258855000	-2.533171000	-1.410325000	H	-2.597900000	4.096268000	1.633029000
C	0.360774000	-3.722817000	-0.615300000	C	-3.439523000	3.703547000	-1.657723000
C	-3.204358000	-2.709689000	0.468364000	H	-3.290902000	3.019079000	-2.489228000
C	-3.213136000	-1.226456000	0.080445000	C	-3.807120000	5.482383000	0.488365000
C	-4.459709000	-0.520797000	-0.159624000	H	-3.951231000	6.162762000	1.324135000
H	-5.443236000	-0.967311000	-0.178899000	C	-4.195171000	4.877099000	-1.837512000
C	-4.151508000	0.811230000	-0.317647000	H	-4.632488000	5.092558000	-2.809491000
H	-4.837661000	1.628781000	-0.480684000	C	-4.384803000	5.768764000	-0.764101000
C	-2.710398000	0.941343000	-0.193998000	C	4.038191000	1.895247000	0.225773000
C	-2.032435000	2.167295000	-0.212794000	C	4.255567000	2.513335000	1.479586000
C	-0.620363000	2.367834000	-0.073096000	H	3.509612000	2.406783000	2.262880000
C	0.085321000	3.629833000	-0.099816000	C	5.015725000	2.037622000	-0.785476000
H	-0.367450000	4.605265000	-0.197972000	H	4.843835000	1.592701000	-1.762064000
C	1.439157000	3.335317000	-0.002511000	C	5.436881000	3.235693000	1.723300000
H	2.264970000	4.031437000	-0.013397000	H	5.597755000	3.690101000	2.697763000
C	1.550631000	1.894854000	0.055881000	C	6.189573000	2.775122000	-0.546080000
C	2.769509000	1.131487000	-0.006361000	H	6.927008000	2.885470000	-1.337537000
C	2.842627000	-0.224960000	-0.346077000	C	6.407250000	3.371570000	0.710866000
C	4.065835000	-0.972999000	-0.586215000	H	-4.972824000	6.673022000	-0.901429000
H	5.065794000	-0.612792000	-0.395833000	H	7.317085000	3.936987000	0.897724000
C	3.700797000	-2.200730000	-1.105474000				
H	4.357742000	-2.998526000	-1.418190000				
C	2.252768000	-2.225521000	-1.146456000				
C	1.375311000	-3.342933000	-1.715068000				
C	-3.913598000	-2.794777000	1.856738000				
H	-4.087129000	-3.840520000	2.137789000				
H	-4.888727000	-2.298381000	1.819683000				
H	-3.311527000	-2.312651000	2.634805000				
C	-4.059735000	-3.511702000	-0.570964000				

**Table A12.** Xyz-Coordinates of optimized geometry of *syn* conformer of Cd(II) *m*-BPDM,  
R"=CH<sub>3</sub>

Cd	-0.000114000	-0.760372000	0.650660000	H	4.579356000	-4.213879000	-0.150661000
Cl	0.000234000	-1.268738000	3.120976000	H	3.889416000	-3.952331000	-1.760529000
N	2.188162000	-0.793461000	-0.030659000	C	-2.480028000	-3.691731000	1.423644000
N	0.000121000	1.361266000	-0.084318000	H	-1.817254000	-3.033615000	1.993922000
N	-2.188344000	-0.793207000	-0.030531000	H	-2.124152000	-4.726119000	1.520969000
C	-1.219197000	-3.358479000	-2.246409000	H	-3.472784000	-3.630788000	1.885446000
H	-2.148292000	-3.292208000	-2.804912000	C	-3.649215000	-4.232054000	-0.728882000
C	-0.000439000	-3.347869000	-2.942689000	H	-4.580006000	-4.213282000	-0.149972000
H	-0.000504000	-3.298696000	-4.029158000	H	-3.277948000	-5.263500000	-0.733503000
C	1.218401000	-3.358627000	-2.246558000	H	-3.890215000	-3.952100000	-1.759966000
H	2.147439000	-3.292513000	-2.805172000	C	3.532893000	2.806743000	-0.154244000
C	1.237874000	-3.421964000	-0.836690000	C	4.409732000	2.988037000	0.938996000
C	2.584733000	-3.299659000	-0.082871000	H	4.315361000	2.345835000	1.810799000
C	3.038385000	-1.835745000	-0.163398000	C	5.383943000	4.003209000	0.912579000
C	4.397912000	-1.364465000	-0.352174000	H	6.043382000	4.138049000	1.766401000
H	5.269370000	-1.985505000	-0.498552000	C	5.505332000	4.839462000	-0.213805000
C	4.350448000	0.016034000	-0.328185000	H	6.262019000	5.619997000	-0.236755000
H	5.174553000	0.701086000	-0.462255000	C	4.639559000	4.659242000	-1.310621000
C	2.958629000	0.402278000	-0.130514000	H	4.729596000	5.296675000	-2.186911000
C	2.487824000	1.724287000	-0.115346000	C	3.654009000	3.656270000	-1.277080000
C	1.118220000	2.178819000	-0.082416000	H	2.988197000	3.520505000	-2.125503000
C	0.693721000	3.562259000	-0.051418000	C	-3.532449000	2.807247000	-0.154238000
H	1.344221000	4.422979000	-0.016853000	C	-3.653495000	3.656614000	-1.277196000
C	-0.693250000	3.562337000	-0.051355000	H	-2.987788000	3.520582000	-2.125658000
H	-1.343656000	4.423128000	-0.016766000	C	-4.638852000	4.659778000	-1.310810000
C	-1.117908000	2.178947000	-0.082373000	H	-4.728844000	5.297080000	-2.187199000
C	-2.487563000	1.724607000	-0.115252000	C	-5.504482000	4.840351000	-0.213942000
C	-2.958595000	0.402664000	-0.130391000	H	-6.261018000	5.621031000	-0.236947000
C	-4.350451000	0.016658000	-0.328252000	C	-5.383138000	4.004273000	0.912580000
H	-5.174435000	0.701832000	-0.462425000	H	-6.042459000	4.139403000	1.766447000
C	-4.398179000	-1.363845000	-0.352041000	C	-4.409123000	2.988917000	0.939074000
H	-5.269744000	-1.984733000	-0.498441000	H	-4.314778000	2.346862000	1.810988000
C	-3.038761000	-1.835353000	-0.163234000	H	-0.000220000	-3.591091000	0.925520000
C	-2.585269000	-3.299306000	-0.082574000				
C	-1.238518000	-3.421835000	-0.836540000				
C	-0.000280000	-3.484075000	-0.153704000				
C	2.479593000	-3.692299000	1.423282000				
H	1.816805000	-3.034307000	1.993691000				
H	3.472359000	-3.631352000	1.885068000				
H	2.123793000	-4.726726000	1.520476000				
C	3.648496000	-4.232436000	-0.729467000				
H	3.277104000	-5.263836000	-0.734213000				

**Table A13.** Xyz-Coordinates of optimized geometry of *anti*-conformer of Cd(II) *m*-BPDM,  
R"=CH<sub>3</sub>

Cd	0.099873000	-0.733347000	0.576690000	H	-3.191101000	-4.556460000	-2.478559000
Cl	-0.196936000	-1.012774000	3.040419000	H	-3.013170000	-4.916687000	-0.756506000
N	-1.873570000	-1.095949000	-0.572353000	C	3.876521000	-3.433450000	-1.279371000
N	-0.290487000	1.381599000	-0.144697000	H	3.266735000	-3.266361000	-2.174145000
N	2.265696000	-0.322145000	-0.085201000	H	3.905383000	-4.511783000	-1.081429000
C	1.603713000	-3.989784000	1.432816000	H	4.897165000	-3.099100000	-1.497559000
H	2.348541000	-4.105228000	2.210565000	C	4.270291000	-2.911918000	1.159780000
C	0.325467000	-4.539773000	1.634741000	H	5.255262000	-2.496615000	0.922376000
H	0.111049000	-5.068305000	2.559414000	H	4.399059000	-3.982979000	1.358961000
C	-0.685892000	-4.372128000	0.680695000	H	3.909329000	-2.422184000	2.071324000
H	-1.673240000	-4.774879000	0.881858000	C	-4.048666000	1.999993000	0.092413000
C	-0.434701000	-3.658133000	-0.514093000	C	-4.922240000	1.669593000	1.153988000
C	-1.574341000	-3.416544000	-1.531359000	H	-4.656473000	0.860848000	1.829614000
C	-2.420305000	-2.219483000	-1.084634000	C	-6.110270000	2.396221000	1.353742000
C	-3.849959000	-2.056232000	-1.270513000	H	-6.764453000	2.139390000	2.183238000
H	-4.528521000	-2.795903000	-1.669683000	C	-6.450556000	3.450635000	0.484667000
C	-4.162994000	-0.776124000	-0.849770000	H	-7.371701000	4.008454000	0.635547000
H	-5.131768000	-0.298387000	-0.869382000	C	-5.590035000	3.779017000	-0.581569000
C	-2.921053000	-0.141316000	-0.430510000	H	-5.848832000	4.586641000	-1.262129000
C	-2.781761000	1.217406000	-0.100335000	C	-4.393359000	3.065073000	-0.771029000
C	-1.543609000	1.945425000	0.020950000	H	-3.735696000	3.318182000	-1.598533000
C	-1.398119000	3.363512000	0.278341000	C	2.873823000	3.474176000	-0.309184000
H	-2.200052000	4.056328000	0.484261000	C	2.613632000	4.436250000	-1.313083000
C	-0.040469000	3.646439000	0.226520000	H	1.823082000	4.253529000	-2.036026000
H	0.431958000	4.604503000	0.384498000	C	3.382767000	5.610380000	-1.395351000
C	0.640584000	2.396755000	-0.044530000	H	3.180541000	6.332567000	-2.182601000
C	2.059123000	2.215371000	-0.220719000	C	4.409453000	5.852489000	-0.461284000
C	2.756394000	0.999565000	-0.333610000	H	4.997781000	6.765121000	-0.519487000
C	4.145982000	0.884421000	-0.750578000	C	4.666869000	4.906736000	0.549837000
H	4.779841000	1.709438000	-1.039998000	H	5.450365000	5.089130000	1.281202000
C	4.469620000	-0.456584000	-0.747955000	C	3.911045000	3.722545000	0.619885000
H	5.419160000	-0.897441000	-1.016337000	H	4.105748000	2.998173000	1.406175000
C	3.287722000	-1.178250000	-0.308671000	H	1.086481000	-2.596986000	-1.626268000
C	3.291226000	-2.687915000	-0.033761000				
C	1.892752000	-3.269859000	0.257726000				
C	0.859602000	-3.123714000	-0.704683000				
C	-1.026673000	-3.071683000	-2.953207000				
H	-0.473845000	-2.126726000	-2.961910000				
H	-1.863012000	-2.965944000	-3.654090000				
H	-0.371410000	-3.873602000	-3.317335000				
C	-2.459486000	-4.686114000	-1.672564000				
H	-1.834244000	-5.551460000	-1.921965000				

**Table A14.** Xyz-Coordinates of optimized geometry of *syn* conformer of Zn(II) *m*-BPDM, R"=Ph.

Zn	-0.509937000	-0.476794000	0.460905000	H	-1.239578000	-8.311400000	0.178753000
Cl	-0.562657000	0.033746000	2.761422000	C	-2.363107000	-7.760899000	-1.592469000
N	0.677311000	-2.125197000	-0.135609000	H	-8.671346000	1.694862000	2.279881000
N	-2.224145000	-1.438685000	-0.084114000	H	-2.634390000	-8.783591000	-1.843113000
N	-1.426225000	1.414153000	-0.112972000	C	1.260594000	3.839338000	0.226225000
C	2.727725000	-0.195292000	-2.362661000	C	2.514421000	4.353477000	-0.183432000
H	3.293668000	-1.043650000	-2.735562000	C	0.926947000	3.906918000	1.593718000
C	2.192477000	0.731605000	-3.261777000	C	3.390881000	4.947712000	0.737111000
H	2.366722000	0.612854000	-4.328571000	H	2.812294000	4.272258000	-1.226227000
C	1.422756000	1.817340000	-2.800577000	C	1.806535000	4.499970000	2.521209000
H	1.035239000	2.529762000	-3.517870000	H	-0.000596000	3.477463000	1.957127000
C	1.169733000	1.972539000	-1.426893000	C	3.036459000	5.031258000	2.099508000
C	1.740071000	1.040341000	-0.527197000	H	4.347333000	5.337950000	0.396293000
H	1.615929000	1.197973000	0.541351000	H	1.530033000	4.527436000	3.572240000
C	2.531025000	-0.031747000	-0.971405000	H	3.713993000	5.488413000	2.816952000
C	0.350069000	3.150736000	-0.833476000	C	-0.128081000	4.148487000	-1.943740000
C	-0.973120000	2.679102000	-0.206298000	C	0.233747000	5.510059000	-1.976780000
C	-1.979968000	3.634824000	0.238311000	C	-1.040752000	3.681994000	-2.922764000
H	-1.853329000	4.707596000	0.242950000	C	-0.274541000	6.372000000	-2.970252000
C	-3.095131000	2.913213000	0.581852000	H	0.901712000	5.915397000	-1.225844000
H	-4.044969000	3.291380000	0.929570000	C	-1.547039000	4.535202000	-3.914125000
C	-2.788448000	1.508410000	0.352248000	H	-1.370545000	2.646044000	-2.896117000
C	-3.710556000	0.472521000	0.469121000	C	-1.161326000	5.890581000	-3.947579000
C	-3.470982000	-0.916895000	0.172950000	H	0.021586000	7.418584000	-2.970654000
C	-4.456152000	-1.971320000	0.122408000	H	-2.245345000	4.147290000	-4.652105000
H	-5.513872000	-1.856117000	0.306189000	H	-1.553951000	6.556584000	-4.712265000
C	-3.776562000	-3.140932000	-0.192150000	C	3.050921000	-0.711817000	1.494779000
H	-4.193793000	-4.131303000	-0.296654000	C	3.738033000	0.468445000	1.860911000
C	-2.377878000	-2.795470000	-0.313956000	C	2.558703000	-1.546038000	2.515651000
C	-1.291152000	-3.681994000	-0.588075000	C	3.913750000	0.809912000	3.209545000
C	0.077960000	-3.351158000	-0.559696000	H	4.150272000	1.117944000	1.092431000
C	1.132046000	-4.233717000	-1.011062000	C	2.744302000	-1.212363000	3.869341000
H	0.984982000	-5.218592000	-1.428224000	H	2.007076000	-2.447235000	2.266876000
C	2.332339000	-3.566261000	-0.849395000	C	3.422139000	-0.035077000	4.224093000
H	3.315296000	-3.921797000	-1.112104000	H	4.433528000	1.729900000	3.466968000
C	2.025760000	-2.277301000	-0.283551000	H	2.335732000	-1.860008000	4.640669000
C	3.024339000	-1.138329000	-0.002160000	H	3.554714000	0.228248000	5.270891000
C	-5.090929000	0.819116000	0.955935000	C	4.501654000	-1.572576000	-0.271448000
C	-6.187772000	0.868311000	0.068700000	C	5.014014000	-2.723496000	0.373440000
H	-6.032689000	0.669543000	-0.989114000	C	5.407375000	-0.772410000	-0.999082000
C	-5.299068000	1.085827000	2.327351000	C	6.364399000	-3.086262000	0.257418000
H	-4.457135000	1.037591000	3.013375000	H	4.361274000	-3.326123000	0.998684000
C	-7.473390000	1.188564000	0.543556000	C	6.765209000	-1.128684000	-1.114533000
H	-8.309004000	1.233513000	-0.150917000	H	5.068088000	0.141913000	-1.473720000
C	-6.586961000	1.396387000	2.802239000	C	7.251954000	-2.292055000	-0.495252000
H	-6.735958000	1.594381000	3.860898000	H	6.726242000	-3.977105000	0.765721000
C	-7.677353000	1.451077000	1.912425000	H	7.438656000	-0.490320000	-1.682187000
C	-1.656125000	-5.094523000	-0.939404000	H	8.300330000	-2.567150000	-0.582702000
C	-2.458809000	-5.369672000	-2.070945000				
H	-2.796488000	-4.549415000	-2.698917000				
C	-1.216643000	-6.172867000	-0.136947000				
H	-0.614631000	-5.970507000	0.744916000				
C	-2.800004000	-6.693278000	-2.401078000				
H	-3.404520000	-6.889241000	-3.283310000				
C	-1.574471000	-7.495016000	-0.456390000				

**Table A15.** Xyz-Coordinates of optimized geometry of *anti*-conformer of Zn(II) *m*-BPDM, R"=Ph.

Zn	-0.582511000	0.345292000	-0.676091000	H	-7.601327000	0.999260000	-3.060625000
Cl	-0.732059000	0.484456000	-3.027733000	C	-7.543119000	-1.345273000	-0.568470000
N	-1.696160000	-1.412192000	-0.144133000	H	-8.193414000	-2.040202000	-0.042701000
N	-2.122852000	1.428100000	0.094910000	C	-8.059960000	-0.535150000	-1.597925000
N	0.851862000	1.687635000	0.109810000	H	-1.446182000	8.149430000	3.471858000
C	1.147348000	-2.955767000	-1.938949000	H	-9.108386000	-0.608348000	-1.877012000
H	0.620657000	-3.854319000	-2.245656000	C	4.294446000	0.254697000	0.137608000
C	1.939029000	-2.265116000	-2.865294000	C	5.362849000	-0.445397000	-0.471363000
H	2.036928000	-2.645604000	-3.878599000	C	4.281223000	0.352880000	1.543680000
C	2.574322000	-1.061762000	-2.514323000	C	6.394350000	-1.005863000	0.296989000
H	3.158931000	-0.532013000	-3.257633000	H	5.383530000	-0.561781000	-1.551608000
C	2.407173000	-0.526333000	-1.225858000	C	5.313504000	-0.210895000	2.319189000
C	1.645964000	-1.256861000	-0.286654000	H	3.466075000	0.862134000	2.048615000
H	1.582782000	-0.893636000	0.733152000	C	6.378145000	-0.888789000	1.701859000
C	1.018259000	-2.470841000	-0.619214000	H	7.205139000	-1.536831000	-0.196592000
C	3.119670000	0.763915000	-0.752735000	H	5.278684000	-0.120066000	3.402484000
C	2.203403000	1.727290000	0.022783000	H	7.175769000	-1.323442000	2.299735000
C	2.722452000	2.940724000	0.625613000	C	3.603464000	1.662358000	-1.939340000
H	3.765524000	3.218009000	0.661332000	C	4.882532000	2.257585000	-1.963164000
C	1.642893000	3.663756000	1.075389000	C	2.683271000	2.003129000	-2.959826000
H	1.656105000	4.633833000	1.548964000	C	5.247469000	3.144730000	-2.993627000
C	0.444085000	2.902705000	0.762073000	H	5.603381000	2.036341000	-1.182649000
C	-0.859915000	3.355972000	1.003027000	C	3.047713000	2.887530000	-3.987815000
C	-2.081155000	2.680826000	0.665000000	H	1.677041000	1.589139000	-2.958121000
C	-3.432861000	3.145141000	0.890346000	C	4.333798000	3.462353000	-4.014374000
H	-3.712155000	4.082120000	1.348794000	H	6.241235000	3.587231000	-2.992583000
C	-4.283477000	2.150140000	0.422743000	H	2.322221000	3.128836000	-4.760748000
H	-5.363540000	2.145831000	0.445541000	H	4.614272000	4.148883000	-4.809948000
C	-3.445454000	1.073308000	-0.055922000	C	0.316122000	-2.697877000	1.854202000
C	-3.880588000	-0.222513000	-0.510153000	C	1.585108000	-2.974303000	2.417272000
C	-3.060519000	-1.359607000	-0.563541000	C	-0.657091000	-2.094271000	2.675427000
C	-3.472873000	-2.706796000	-0.911034000	C	1.873467000	-2.656764000	3.752561000
H	-4.432718000	-2.982273000	-1.321821000	H	2.352240000	-3.445228000	1.808199000
C	-2.414381000	-3.549790000	-0.620346000	C	-0.373636000	-1.781999000	4.020846000
H	-2.377997000	-4.619936000	-0.749368000	H	-1.632778000	-1.847255000	2.274114000
C	-1.342083000	-2.719828000	-0.113713000	C	0.889975000	-2.060411000	4.567771000
C	0.048769000	-3.155795000	0.381821000	H	2.858418000	-2.879002000	4.156536000
C	-1.014318000	4.687067000	1.686552000	H	-1.143173000	-1.318085000	4.633908000
C	-1.525652000	5.798503000	0.980051000	H	1.106565000	-1.819463000	5.605960000
H	-1.790704000	5.690184000	-0.068594000	C	0.186382000	-4.707184000	0.431632000
C	-0.664649000	4.840742000	3.046447000	C	-0.776852000	-5.457927000	1.147239000
H	-0.281125000	3.986787000	3.599202000	C	1.312150000	-5.392905000	-0.070098000
C	-1.673058000	7.043154000	1.619177000	C	-0.644104000	-6.844686000	1.316299000
H	-2.055654000	7.893286000	1.059647000	H	-1.624913000	-4.951307000	1.600078000
C	-0.825392000	6.082195000	3.689244000	C	1.452747000	-6.783991000	0.100102000
H	-0.559684000	6.183927000	4.738723000	H	2.093680000	-4.849221000	-0.589431000
C	-1.326870000	7.188628000	2.976908000	C	0.472486000	-7.520787000	0.786028000
C	-5.326664000	-0.347890000	-0.874197000	H	-1.402138000	-7.393825000	1.870116000
C	-5.858930000	0.475860000	-1.894858000	H	2.331454000	-7.285146000	-0.299577000
H	-5.204391000	1.171695000	-2.412721000				
C	-6.185051000	-1.257325000	-0.213410000				
H	-5.794322000	-1.872625000	0.592604000				
C	-7.211932000	0.373536000	-2.261455000				

**Table A16.** Xyz-Coordinates of optimized geometry of *syn* conformer of Cd(II) *m*-BPDM, R"=Ph.

Cd	-0.184604000	0.524512000	0.499141000	H	-8.492481000	3.636921000	0.683146000
Cl	-0.305916000	0.284299000	2.989164000	C	-6.727086000	2.815328000	1.639644000
N	1.779491000	1.383830000	-0.250442000	H	-7.139780000	2.874357000	2.643850000
N	-1.099942000	2.430672000	-0.230536000	C	-5.428817000	2.306002000	1.449479000
N	-2.130735000	-0.449159000	-0.214985000	H	-4.839878000	1.976959000	2.302045000
C	-0.045696000	-2.544419000	-2.608072000	H	0.792743000	-1.876674000	0.620014000
H	-0.809911000	-3.004675000	-3.218869000	C	3.255510000	-1.212417000	1.231304000
C	1.133496000	-2.100139000	-3.224468000	C	3.064657000	-2.577541000	1.547753000
H	1.247961000	-2.206414000	-4.300693000	C	3.565253000	-0.328706000	2.286260000
C	2.170383000	-1.535482000	-2.473664000	C	3.170149000	-3.039576000	2.869178000
H	3.071484000	-1.230469000	-2.986726000	H	2.823073000	-3.287510000	0.761858000
C	2.061766000	-1.410162000	-1.071961000	C	3.674200000	-0.787833000	3.610506000
C	3.222406000	-0.726850000	-0.251300000	H	3.707770000	0.728911000	2.091188000
C	2.999742000	0.804327000	-0.274931000	C	3.479745000	-2.146183000	3.910951000
C	4.038240000	1.818069000	-0.270616000	H	2.997076000	-4.091392000	3.082543000
H	5.100508000	1.628555000	-0.270366000	H	3.890266000	-0.078376000	4.405253000
C	3.406214000	3.045579000	-0.284250000	H	3.549500000	-2.499554000	4.936846000
H	3.871892000	4.019634000	-0.308172000	C	4.604597000	-1.046933000	-0.930373000
C	1.973806000	2.798494000	-0.275442000	C	5.457055000	-2.064185000	-0.448548000
C	0.988737000	3.798868000	-0.340041000	C	5.029571000	-0.341026000	-2.084407000
C	-0.439500000	3.638786000	-0.358166000	C	6.673119000	-2.368268000	-1.090296000
C	-1.416912000	4.706056000	-0.440366000	H	5.194403000	-2.616777000	0.444663000
H	-1.196155000	5.758771000	-0.535342000	C	6.241869000	-0.638651000	-2.727672000
C	-2.669163000	4.115953000	-0.350756000	H	4.419743000	0.464805000	-2.482765000
H	-3.628741000	4.611121000	-0.363967000	C	7.074745000	-1.660801000	-2.235729000
C	-2.454148000	2.689417000	-0.218567000	H	7.305662000	-3.155103000	-0.685622000
C	-3.480565000	1.692170000	-0.038918000	H	6.532932000	-0.071064000	-3.608675000
C	-3.334334000	0.301283000	-0.008981000	H	8.015493000	-1.893431000	-2.728963000
C	-4.4247444000	-0.649329000	0.167128000	C	-1.100172000	-3.641812000	0.834204000
H	-5.458493000	-0.386730000	0.337326000	C	-0.136171000	-4.678397000	0.788197000
C	-3.890081000	-1.913485000	0.056419000	C	-1.651121000	-3.302262000	2.085083000
H	-4.409564000	-2.858704000	0.112570000	C	0.235833000	-5.376017000	1.947020000
C	-2.465930000	-1.751839000	-0.203513000	H	0.329769000	-4.933233000	-0.160957000
C	-1.507589000	-2.928816000	-0.488878000	C	-1.273882000	-3.994898000	3.252240000
C	-0.206053000	-2.432971000	-1.214417000	H	-2.355139000	-2.482281000	2.172585000
C	0.860810000	-1.862919000	-0.466341000	C	-0.339972000	-5.041577000	3.189609000
C	1.479720000	5.222709000	-0.385155000	H	0.971155000	-6.175297000	1.881834000
C	2.006081000	5.831626000	0.775132000	H	-1.699412000	-3.697287000	4.206925000
H	2.052969000	5.265464000	1.701962000	H	-0.051002000	-5.575735000	4.091777000
C	2.451418000	7.166236000	0.739933000	C	-2.332389000	-3.896217000	-1.414165000
H	2.846884000	7.625277000	1.642775000	C	-2.459567000	-5.280362000	-1.177605000
C	2.385089000	7.904297000	-0.457629000	C	-3.026521000	-3.357873000	-2.527882000
H	2.732817000	8.934186000	-0.485377000	C	-3.227414000	-6.099622000	-2.030458000
C	1.864286000	7.300617000	-1.618861000	H	-1.981368000	-5.734111000	-0.318663000
H	1.812265000	7.861594000	-2.548925000	C	-3.790801000	-4.168292000	-3.380687000
C	1.407743000	5.969967000	-1.580988000	H	-2.985166000	-2.288823000	-2.720846000
H	1.006105000	5.506877000	-2.478918000	C	-3.892816000	-5.552742000	-3.139738000
C	-4.876517000	2.227735000	0.152606000	H	-3.307139000	-7.162996000	-1.816372000
C	-5.640710000	2.665698000	-0.950045000	H	-4.309806000	-3.719450000	-4.224438000
H	-5.221570000	2.604985000	-1.951552000	H	-4.486657000	-6.185056000	-3.795436000
C	-6.941883000	3.168140000	-0.759963000				
H	-7.523849000	3.495517000	-1.618263000				
C	-7.488436000	3.246265000	0.535856000				

**Table A17.** Xyz-Coordinates of optimized geometry of *anti*-conformer of Cd(II) *m*-BPDM, R"=Ph.

Cd	0.407086000	0.440075000	-0.965765000	H	-0.280806000	8.863208000	2.275476000
Cl	0.223856000	0.611505000	-3.454813000	C	-0.287616000	6.783022000	2.891291000
N	1.985924000	-1.036071000	-0.143598000	H	-0.415196000	7.008194000	3.947456000
N	1.752426000	1.966188000	-0.008643000	C	-0.200228000	5.442990000	2.469360000
N	-1.270653000	1.615747000	0.111786000	H	-0.255299000	4.637888000	3.198007000
C	-2.686386000	-1.654853000	-2.118611000	H	-1.079273000	-1.118206000	0.835536000
H	-3.513999000	-1.296111000	-2.718120000	C	0.311739000	-3.132570000	1.796860000
C	-1.936914000	-2.746814000	-2.569324000	C	-0.993322000	-3.462135000	2.232529000
H	-2.189995000	-3.218434000	-3.515160000	C	1.273749000	-2.815926000	2.780036000
C	-0.861568000	-3.240920000	-1.817706000	C	-1.328059000	-3.466960000	3.596788000
H	-0.324063000	-4.102228000	-2.188796000	H	-1.759726000	-3.708574000	1.503117000
C	-0.510596000	-2.649080000	-0.587316000	C	0.943690000	-2.821899000	4.148522000
C	0.675671000	-3.204462000	0.276985000	H	2.286602000	-2.557773000	2.489321000
C	1.959240000	-2.374188000	0.044384000	C	-0.358482000	-3.148067000	4.566554000
C	3.308634000	-2.903181000	0.126244000	H	-2.343496000	-3.715296000	3.895744000
H	3.568434000	-3.938135000	0.285390000	H	1.704824000	-2.568734000	4.883073000
C	4.171824000	-1.840609000	-0.047784000	H	-0.614152000	-3.150118000	5.623561000
H	5.250862000	-1.870920000	-0.059605000	C	0.976162000	-4.690014000	-0.120304000
C	3.360672000	-0.642145000	-0.176857000	C	0.550306000	-5.784973000	0.660252000
C	3.872449000	0.666343000	-0.198467000	C	1.676199000	-4.974884000	-1.319423000
C	3.130969000	1.888630000	-0.058928000	C	0.809721000	-7.111370000	0.261301000
C	3.694756000	3.191580000	0.230307000	H	0.026538000	-5.618646000	1.593809000
H	4.747686000	3.428346000	0.272217000	C	1.937265000	-6.294166000	-1.721877000
C	2.629166000	4.041142000	0.490369000	H	2.030646000	-4.159000000	-1.943882000
H	2.675591000	5.081828000	0.775084000	C	1.502481000	-7.376197000	-0.931823000
C	1.420025000	3.256580000	0.342756000	H	0.471782000	-7.932392000	0.889539000
C	0.083728000	3.702118000	0.642216000	H	2.477787000	-6.474090000	-2.648192000
C	-1.097591000	2.955325000	0.595416000	H	1.704215000	-8.399726000	-1.238598000
C	-2.400279000	3.440764000	1.035661000	C	-4.112898000	-0.650889000	0.795706000
H	-2.594267000	4.424735000	1.435631000	C	-5.011803000	-1.679909000	0.426888000
C	-3.306292000	2.425832000	0.840299000	C	-3.921726000	-0.397209000	2.169047000
H	-4.368184000	2.439044000	1.036834000	C	-5.712808000	-2.412847000	1.396523000
C	-2.575631000	1.314213000	0.246783000	H	-5.157655000	-1.916711000	-0.623531000
C	-3.293227000	0.076658000	-0.312692000	C	-4.621605000	-1.132513000	3.146143000
C	-2.363702000	-1.024342000	-0.900674000	H	-3.223887000	0.369809000	2.490483000
C	-1.275279000	-1.534963000	-0.148871000	C	-5.524478000	-2.140131000	2.767049000
C	5.366901000	0.829970000	-0.280194000	H	-6.400419000	-3.196041000	1.085642000
C	6.206284000	0.502309000	0.806998000	H	-4.455456000	-0.915628000	4.198849000
H	5.768067000	0.121918000	1.726295000	H	-6.067967000	-2.705678000	3.520359000
C	7.598635000	0.684450000	0.713709000	C	-4.200109000	0.723890000	-1.415084000
H	8.232468000	0.435251000	1.561413000	C	-5.585504000	0.919197000	-1.241493000
C	8.169125000	1.188566000	-0.471080000	C	-3.585410000	1.252211000	-2.576855000
H	9.245369000	1.324871000	-0.545009000	C	-6.345802000	1.599979000	-2.212367000
C	7.336749000	1.518962000	-1.558327000	H	-6.082891000	0.546495000	-0.351916000
H	7.767937000	1.908322000	-2.477313000	C	-4.342694000	1.930155000	-3.544475000
C	5.943377000	1.349777000	-1.460603000	H	-2.514810000	1.140022000	-2.735719000
H	5.302533000	1.608200000	-2.299830000	C	-5.730170000	2.106613000	-3.370207000
C	-0.027990000	5.132961000	1.103055000	H	-7.414047000	1.735239000	-2.058028000
C	0.058208000	6.184653000	0.164925000	H	-3.846152000	2.321314000	-4.428900000
H	0.190540000	5.952707000	-0.888921000	H	-6.316276000	2.633780000	-4.119418000
C	-0.038527000	7.524135000	0.585678000				
H	0.019908000	8.324186000	-0.148299000				
C	-0.209919000	7.828000000	1.950396000				